Physiological Effects of Prolonged Sitting and Local Pressure Application in the UH-60 Black Hawk Helicopter

by

Kenneth Eric Games

A dissertation submitted to the Graduate Faculty of
Auburn University
in partial fulfillment of the
requirements for the Degree of
Doctor of Philosophy

Auburn, Alabama
May 4, 2013

Keywords: prolonged sitting, military medicine, tissue compression,
aviators, perceived discomfort

Approved by

JoEllen Sefton, Chair, Associate Professor of Kinesiology
Joni Lakin, Assistant Professor of Educational Foundations, Leadership, and Technology
John Quindry, Associate Professor of Kinesiology
Wendi Weimar, Associate Professor of Kinesiology

Abstract

Advances in flight technologies and the demand for long range flight have increased mission lengths for United States Army UH-60 Black Hawk aviators. Prolonged mission times have increased reports of pilots discomfort and symptoms of parathesia thought to be due to Black Hawk seat design and areas of locally high pressure. Discomfort created by the seat system decreases situational awareness putting our aviators and support crew at risk of injury. Therefore, the purpose of this study was to examine the effects of prolonged restricted sitting and local pressure application in a Black Hawk helicopter on discomfort, sensory function, vascular, and neurological measures in the lower extremity. Project one tested the effects of four hours of restricted sitting on discomfort, sensory, and vascular function in the lower extremity. The results demonstrated that during four hours of restricted sitting, subjective discomfort increases, lower extremity sensory function is diminished along the S1 dermatome, and skin temperature decreases. This suggests that prolonged sitting in a Black Hawk helicopter aviator seat does create increases in discomfort, potentially through a peripheral nervous or vascular system mechanism. Project two examined the effects of local pressure application location on measures of discomfort, sensory function, and vascular function in the lower extremity. The results revealed that local pressure application increases discomfort regardless of location or magnitude. Pressure applied to the posterior thigh at a magnitude of 44 kilopascals created the greatest increases in discomfort. Skin temperature increased suggesting decreased venous return from the extremity during the test period. Project three examined the effects pressure application to the ischial tuberosity or posterior thigh on discomfort, sensory, vascular, and neurological

function in the lower extremity compared to a control condition. Mean peak-to-peak Hoffmann reflex amplitude significantly decreased, discomfort increased, skin temperature increased, and sensory function along the S1 dermatome decreased. The results suggest areas of locally high pressure created during prolonged sitting in the Black Hawk helicopter may create the discomfort and temporary parathesia by altered S1 nerve root function and decreased venous return.

Acknowledgments

Completing a dissertation is truly a community experience. Without the support, mentorship, love, and guidance of a community of individuals, this dissertation would not have come to fruition. To my parents, Bruce and Vicki Games, I want to thank you for always encouraging me and instilling in me that with integrity, hustle, and honesty I can excel in any aspect of my life. Without the two of you, this dream would not have been possible. To my sisters, Rebecca and Colleen, and my brother, Ross, thank you for pushing me to be a better person every day and for your understanding for all the missed holidays, birthdays, and family dinners.

To Dr. JoEllen Sefton, thank you for being the best advisor a doctoral student could hope for. You led by example and trusted me with more responsibility than I could have imagined. Through this, you pushed my limits; mentored me through calm and turbulent waters; and taught me to relax every once in a while. What you have taught me goes beyond facts and figures and will endure for a lifetime. To Dr. Wendi Weimar, thank you for your biomechanics expertise during the completion of my dissertation and for demonstrating that learning difficult material doesn't have to be painful and can even be fun. To Dr. John Quindry, thank you for your physiological expertise for this dissertation and teaching me how you present information is just as important the information you are presenting. To Dr. Joni Lakin, thank you for your statistical guidance throughout the dissertation and through this, demonstrating that the best way to answer my question isn't always the most complicated. I would also like to thank my outside reader, Dr.

James Witte, for his insight and evaluation of the dissertation which improved the dissertation. I'd like to thank my lab colleagues, Valerie Lee, Paras Goel, and Dr. Roger Kollock. Without your early mornings, late nights, and weekends this project would not have been successful. I'd also like to thank all of the master's students in the Warrior Athletic Training Program from 2011-2013. Every one of you helped make this dissertation a success through pilot work, allowing me to practice techniques, and with your suggestions on how to best approach challenges I had while planning for data collection. I'd also like to thank the numerous undergraduate students who volunteered their time to assist with data collection, particularly; Jordan Keeley, Whitney Gentry, Sonam Sayania, Joo Oh, Andrew Hackney, Luke McGee, Dallas Hair, Edward Fabery, and Moon Oh.

This project would not have been possible without the financial and technical support of the team at the United States Army Aeromedical Research Laboratory at Fort Rucker. Thank you for the opportunity to improve the lives of those who serve us. I would also like to thank Dr. Mary Rudisill and the Department of Kinesiology for the graduate teaching assistantships which added in funding my graduate education. I would also like to thank Nicholas Madsen from the Industrial and Graphic Design Department at Auburn. Your creativity and knowledge helped transform a vision into an invaluable tool required for the successful completion of this project.

Finally, I would like to thank my beautiful fiancée, Gina Hinel, for your love and support throughout our journey together. It hasn't always been easy, but we've both made it and are stronger now than ever before. If it was easy, everyone would do it.

Table of Contents

List of Tables

List of Figures

Chapter I

Introduction

Aircraft seat discomfort has been an issue in military populations since World War II.[1] Pilots first reported this problem, termed "butt flutter," during long reconnaissance missions.[1] Since World War II millions of dollars have been invested to examine and improve persistent problems with aircraft seating.[1,2] Seat discomfort remains a top concern even in the most advanced United States Military aircraft such as the B-2 Combat Bomber.[1,3] Common complaints during missions include buttock and lumbar soreness, numbness and tingling in the extremities, and overall fatigue.[3] Rotary-winged aviators may be at a higher risk of injury or discomfort due to the industrial vibration produced by the rotors.[4,5] As many as 82% of aviators report some sort of discomfort during flight;[4] with as much as 22% of these complaints associated with buttock, pelvis, and leg pain.[6]

Rotary-winged aircraft such as the UH-60 Blackhawk have much shorter flight times (2.3 hours)[7] compared to long range bombers like the B-2 Combat Bombers with in-air refueling (40 hours).[3] Highly modified variants of the UH-60 Blackhawk, known as the MH-60, have the capability of in-air refueling.[8] These variants are only operated by members of the Army's Special Operations Aviation Regiment.[8] The typical mission length might explain why much of the research involving prolonged restricted seating in aircraft has focused on fixed-wing aircraft.[1,3,9] However, in recent years increased operations and the utilization of "hot-refueling" have increased flight times for U.S. Army rotary-winged aviators.[10] Hot-refueling is refueling an

aircraft with the engines and rotors still operational.[10] Since the engines are engaged, the aviator must remain seated and secured in the cockpit of the aircraft. Hot-refueling has increased the typical mission length to approximately 8 or more hours. Reports from soldiers include symptoms of numbness, tingling, and pain in the buttocks and lower extremity. These symptoms decrease focus on the mission and may increase mental fatigue and decrease mission success. The prevalence of seat discomfort during prolonged restricted sitting in military aircraft has led to investigations focused on decreasing seat discomfort.[3,9,11-15] Much of the aircraft specific research focuses on measures of seat interface pressure[3,11,15] and vibration mitigation.[12-14] Little work has examined the physiological changes associated with prolonged restricted sitting and local pressure application;[3] moreover physiological changes during recovery from local pressure application remains uninvestigated.

The advances in flight technology and refueling options, paired with the limited knowledgebase of the physiological changes associated with prolonged sitting warrant investigation. Additionally, one hypothesis regarding the discomfort associated with prolonged sitting suggests that this discomfort may be the result of localized areas of high pressure. Therefore, the purpose of this project was three-fold: (1) to investigate the effects of prolonged restricted sitting in a rotary-winged aircraft aviator seat (UH-60 Black Hawk) on perceived discomfort, sensibility, superficial skin temperature, and limb oxygenation in the lower leg; (2) to investigate the effects of local pressure application to the lower extremity on perceived discomfort, sensibility, and physiological function in the lower leg; and (3) to investigate perceived discomfort, sensibility, and physiological function in the lower extremity during recovery from local compression. By addressing these questions, we were able to better understand the changes associated with prolonged sitting in Black Hawk helicopters and offer

insight into the onset and recovery of the local pressure hypothesis during prolonged restricted sitting.

Experimental and Statistical Hypotheses

Project 1

1. In project 1, we expected the data from the four subjective discomfort scales (Category Partitioning Scale, McGill Pain Questionnaire, visual analog scale, and present pain intensity score) to significantly increase across the entire 240 minute data collection period.
2. We anticipated that the sensory measures utilized to measure pressure sensitivity in this study (Semmes-Weinstein monofilament test) would increase (indicating poorer pressure sensitivity) across the entire testing period. Additionally, we expected that the measure of receptive field sensitivity (two-point discrimination test) would result in increased inter-point distance across time, indicating decreases in receptive field sensitivity.
3. We expected the measures of lower extremity arterial oxygen saturation (measured with pulse oximetry) to remain unchanged throughout the 240 minute prolonged restricted sitting protocol. Conversely we expected both lateral and anterior superficial skin temperatures in the lower extremity to decrease significantly across the 240 minute data collection.

Project 2

1. In project 2, we expected a significant 3-way interaction with all subjective questionnaire measures including: the Category Partitioning Scale, the McGill Pain Questionnaire, the visual analog scale, and the present pain intensity scale. We anticipated that follow-up tests would reveal that the Category Partitioning Scale scores would increase following 10 minutes of local pressure application to the ischial tuberosity and middle of the posterior thigh at both 36 and 44 kilopascals of pressure. Follow-up tests for the McGill Pain Questionnaire, visual analog scale, and present pain intensity scales would reveal that after 10 minutes of local pressure application to the ischial tuberosity and middle of posterior thigh at both 36 and 44 kilopascals of pressure.
2. The two sensory measures (Semmes-Weinstein monofilament test and two-point discrimination test) would reveal significant 3-way time x location x pressure magnitude interaction effect. Follow-up tests would reveal that the Semmes-Weinstein monofilament test would increase at the great toe, third metatarsal, and fifth metatarsal following 10 minutes of 44 kilopascals of pressure applied to the posterior thigh, but no 36 kilopascals of pressure applied to the posterior thigh. We expected no difference between 36 and 44 kilopascals of pressure at the ischial tuberosity. Follow-up tests for the two-point discrimination test would reveal increases in inter-point distances at the great toe when pressure was applied at 36 or 44 kilopascals to the posterior thigh, but not at the ischial tuberosity. We expected no significant differences among any locations, time points, or magnitudes for two-point discrimination tests scores taken from the medial or lateral malleoli.

3. For measures of lower extremity oxygen saturation and superficial skin temperature we expected a significant 3-way interaction effect for superficial skin temperature, but no significant interaction or main effects for lower extremity oxygen saturation. We expected no significant change in lower extremity arterial oxygen saturation at any time point, application location, or application magnitude. We expected both lateral and anterior lower leg superficial skin temperature to decrease follow 10 minutes of local pressure application applied to the middle of the posterior thigh at both 36 and 44 kilopascals of pressure, but no significant differences when pressures were applied to the ischial tuberosity.

Project 3

1. In project 3, we expected a significant 2-way location x time interaction effect for the four subject discomfort questionnaires (Category Partitioning Scale, McGill Pain Questionnaire, visual analog scale, and present pain intensity scale). Follow-up tests were expected to reveal that all four questionnaire scores would significantly increase during the 10 minutes of local pressure application and return near baseline levels (non-significant difference) by the 10 minute follow-up measure.
2. We anticipated a significant 2-way interaction effect for the Semmes-Weinstein monofilament test and the two-point discrimination test at the great toe with follow-up tests revealing a significant increase in scores during the 10 minute local pressure application period at the posterior thigh and returning to baseline levels during the 10 minute follow-up period. We did not expect any significant interaction or main effects for the Semmes-Weinstein monofilament test at the third metatarsal or fifth

metatarsal. Additionally, we did not expect significant interaction or main effects of local pressure application in two-point discrimination scores at the medial and lateral malleoli.

3. We predicted no statistically significant interaction or main effects for lower extremity arterial oxygen saturation across any of the conditions or time points. We expected a significant 2-way interaction effect for both lateral and anterior superficial lower leg temperatures. Follow-up tests were anticipated to reveal a significant decrease in lateral and anterior skin temperature during the 10 minutes of local pressure application to the middle of the posterior thigh. Additionally, we expected these levels to return to baseline and be non-significant at the 10 minute post-pressure application time point.
4. The mean amplitudes of the soleus Hoffmann reflex were predicted to demonstrate a significant 2-way interaction with follow-up tests revealing a statistically significant increase in amplitude during the 10 minute pressure application period and amplitudes returning near baseline during the 10 minute follow-up time period. For mean sural sensory nerve conduction velocity, we expected no significant 2-way interaction or main effects as a result of local pressure application.

Assumptions

1. United States Army UH-60 Black Hawk helicopter pilots experience symptoms of parathesia as a result of prolonged flight. With improved flight technologies (e.g. fuel, aircraft materials) and refueling options (e.g. in-air refueling), flight times have increased and human factors are becoming the limiting factors for Black Hawk flight.

2. All United States Black Hawk helicopters utilize a standard, rigid pilot's cockpit seat.

3. Symptoms of parathesia in prolonged sitting may be created by compression soft tissue structures within the human body (e.g. nervous tissue, vascular tissue).

4. Relief of the symptoms of parathesia in prolonged sitting may be relieved by removing compression on soft tissue structures within the human body.

5. Men comprise the vast majority of the UH-60 Black Hawk pilots in the United States Army.

Limitations

1. Participants were civilian volunteers at a large university in the Southeast United States. This may not be representative of the aviators flying Black Hawk helicopters in the United States Army.

2. Participants did not wear normal flight gear while collecting data.

3. Participants were not exposed to helicopter rotor vibration during the protocols.

4. Participants sat in an unpadded, Black Hawk helicopter seat. Black Hawk helicopter aviators usually utilize some form of seat pad during flight.

Delimitations

1. Participants had similar demographic and anthropometric measures as United States Army Black Hawk helicopter aviators.

2. Participants were wearing shorts and t-shirts in order to obtain access to necessary anatomical areas for data collection.

3. Data were not collected in an environment with helicopter rotor vibration.

4. Participants sat in a standard, unpadded Black Hawk pilot's seat to have a common denominator regardless of pads used in flight. The United States Army has multiple variations of Black Hawk helicopter seat padding.

Chapter II

Review of Literature

Introduction

Approximately 82% of rotary-winged aviators report some pain as result of sitting during missions.[4] Symptoms range from general fatigue to numbness and tingling in the extremity.[3] The flight of rotary-winged aircraft such as the UH-60 Blackhawk is much lower (2.3 hours)[7] compared to long range bombers like the B-2 Combat Bombers with in-air refueling (40 hours).[3] Variants of the UH-60 do have the capability of in-air refueling, but these variants are only utilized by the Army's Special Operations Aviation Regiment. However, increased operations in the past decade led to the utilization of "hot-refueling" (refueling the aircraft while the engine is operational) across all Army rotary-winged aircraft. During hot refueling aviators must remain seated and secured to the seat. This change increased mission times and total time seated in aircraft for U.S. Army rotary-winged aviators.[10] The prevalence of aviator discomfort during prolonged sitting in military aircraft has led to investigations examining the cause of this discomfort in military aircraft.[3,9,11-15] While much of the aircraft specific research focuses on measures of seat interface pressure[3,11,15] and vibration mitigation,[12-14] little work[3] examines physiological changes associated with prolonged restricted sitting and local pressure application. Understanding the physiological changes connected to prolonged sitting may yield insight into the potential mechanisms for the reported discomfort and temporary parathesia seen in military aircraft. Therefore, this literature review examines the scope of the problems associated with

prolonged restricted sitting; current literature examining prolonged restricted sitting and local pressure application; relevant anatomy related to symptoms commonly reported with prolonged sitting; current measures utilized to quantify discomfort; and potential physiological measures to enhance the current understanding of the changes associated with prolonged restricted sitting and local pressure application.

Scope of Problem

Problems with seat design and discomfort have been present in military aircraft since the 1940's.[1] The first incidences of discomfort were reported by American aviators during reconnaissance missions in Europe during World War II.[1] Extensive time and money has been invested into solving the problem,[2] however thus far investigations have yielded little in way of solutions.[1] Evidence of the lack of the continuing problem can be seen in the B-2 Combat Bomber in which seat discomfort remains a top concern and is the limiting factor of flight time.[1,3] Complaints related to seat discomfort range from buttock and lumbar soreness to numbness and tingling in the extremities.[3] Rotary-winged aviators may be at a higher risk of injury or discomfort due to the mechanical vibration produced by the helicopter rotors;[4,5] however, research in this area yields conflicting results. An examination of diagnosed low back complaints in fixed- and rotary-winged aircrew members found that rotary-winged aviators below the age of forty had lower odds ratios for diagnosed low back pathology compared to fixed-winged aircrew members (Odds Ratio: 1.36 and 3.69 compared to 2.96 and 3.81 respectfully).[5] The Odds Ratio is an effect size measure of the size of an effect between two variables: the higher the odds ratio, the larger the effect between variables. In other words,

rotary-winged pilots were diagnosed with low back pathologies over 100% more often than fixed-winged aircrew members. However for aviators over the age of forty, rotary-winged aviators had a much higher odds ratio for diagnosed low back problems compared to their fixed-winged counterparts (8.73 compared to 1.18).[5] When these age groups were pooled, no significant differences in odds ratios were present between the rotary-winged aircrew members and the fixed-winged aircrew members.[5] This difference may be due to the cumulative effects of flight time and mechanical vibration across the career of older rotary-winged aviators. Another study of 732 rotary- and fixed-winged aircrew members found rotary-winged aviators had a significantly higher risk for bony cervical spine injuries compared to fixed-winged aviators; this difference was not present in the lumbar spine.[16] Pain during prolonged sitting in military aircraft is a significant problem. Between 12%[4] and 22%[6] of reported pain is localized to the buttock, pelvis, and upper leg.[4,6] Reducing seat discomfort is a critical component needed to decrease injury and increase combat effectiveness in today's rotary-winged aviators.

Relevant Neurovascular Anatomy and Physiology of the Lower Extremity

Structure of the Neuron and Synapse

The neuron is the smallest functional unit of the nervous system, exhibiting a wide structural variety which is directly related to neuron function.[17-19] Despite this variation, all neurons share some distinct anatomical components (Figure 1): the dendrites, the cell body (soma), and the axon.[17-19] Each of these components is structurally and functionally unique. The dendrites are a network of branches arising from the cell body[19] which serve as the target for synaptic input from other neurons.[17] The cell body houses the nucleus and other organelles vital

to neuron function.[19] The cell body also serves as the base for an extensive cytoskeletal network which extends into the dendrites and axon of the neuron[19] through axoplasmic transport.[20] Axoplasmic transport is also the mechanism by which mitochondria, vesicles, lipids, and other cellular products move from the soma to the axon terminal.[20] The axon originates from a specialized portion of the cell body known as axon hillock.[19] It extends away from the cell body and serves the primary function of transmitting electrical signals (action potentials) to the end of the axon.[17-19] The axon terminates at the axon terminal where it creates a connection (synapse) with another neuron or a muscle.[17-19]

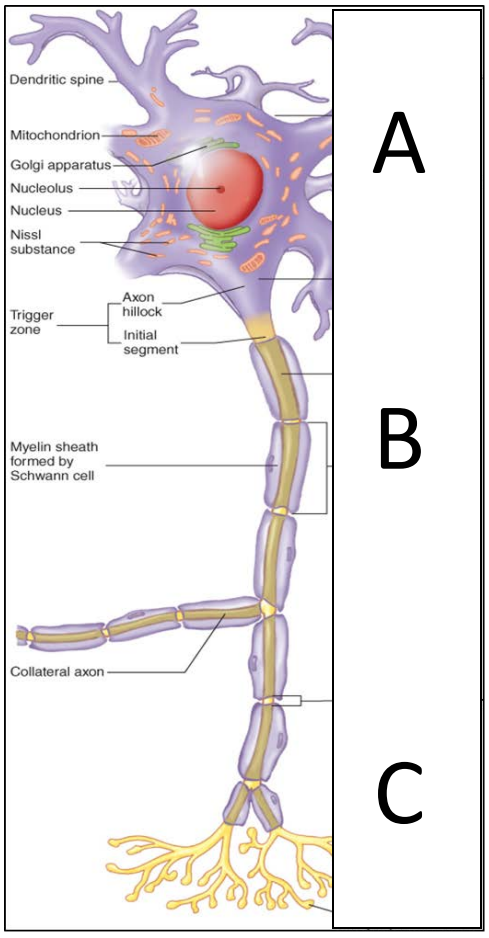

Figure 1. Structure of a neuron. A: Soma; B: Axon; C: Dendrites. Borrowed from Powers and Howley.[21]

The presynaptic terminal of an axon meets a postsynaptic terminal on any cell at the synaptic cleft of a synapse.[18,19,22] The synaptic cleft is the space between the presynaptic and postsynaptic terminal.[18] The cleft is typically between 200-300 Angstroms wide.[18] There are two types of synapses: chemical and electrical. Chemical synapses are by far the most common type of synapse[19] with electrical synapses only occurring the central nervous system.[18] The presynaptic terminal of a chemical synapse contains many vesicles filled with neurotransmitter.[18,23] The membrane of the presynaptic terminal contains voltage-sensitive calcium channels which open when depolarized allowing calcium to diffuse into the cell.[18,19] The postsynaptic terminal membrane is lined with ligand-gated neurotransmitter receptors.[18] The ligand-gated channels are composed of a binding component and an ionophore component.[18] The binding components of the receptor bind to the neurotransmitter released from the presynaptic terminal into the synaptic cleft;[19] the ionophore component is an ion channel that allows specific ions to pass through the receptor.[18] The structure of the synapse plays an integral role in its function as the primary mechanism for cell to cell communication in the nervous system.

The Action Potential

The nervous system transmits and receives information in the form of electrical signals called action potentials.[18] Hodgkin and Huxley determined that these potentials are a result of sodium ion influx and potassium ion efflux across a nerve membrane.[23,24] The flow of these ions are spontaneously reversed, restoring the resting membrane potential and preparing the membrane for the next action potential.[25] Sodium and potassium leak channels and voltage-

gated channels are located on the nerve fiber membrane.[18] The leak channels are responsible for the resting membrane potential. The voltage-gated sodium and potassium channels are primarily responsible for the influx of sodium and the efflux of potassium via diffusion down their concentration gradients, producing membrane depolarization.[18]

An action potential is composed of three stages: the resting stage, the depolarization stage, and the repolarization stage. In the resting stage the electrical potential across the membrane is stable at approximately -90 millivolts.[18,19,26] Depolarization occurs when the membrane becomes permeable to sodium ions.[18,19] The membrane is quickly depolarized, neutralizing the membrane potential.[18] Voltage-gated sodium channels then open, permitting sodium ions to diffuse down its concentration gradient into the cell,[27] while voltage-gated potassium channels begin to open allowing some potassium ions to diffuse down its concentration gradient and out of the cell.[18,28] The third stage of an action potential is the repolarization phase. Beginning soon after the membrane becomes highly permeable to sodium ions, the voltage-gated sodium channels close, stopping the diffusion of sodium into the cell.[18] The potassium channels open fully and potassium diffuses to the outside which re-establishes the normal negative membrane potential.[18] This cycle occurs anytime a stimulus is applied to a nervous tissue membrane as long as the stimulus is sufficient to reach threshold.[18]

Action potentials are initiated when a stimulus excites the membrane.[18] An action potential will not occur unless this initial stimulus is of great enough magnitude to initiate the positive feedback cycle.[29] The initial stimulus needs to be sufficient to create a sudden rise in membrane potential of approximately 25 millivolts to cause the sudden development of an action potential. If any event causes the resting membrane potential to rise above -90 millivolts, the rising voltage from the disturbance itself causes more voltage-gated sodium channels to open.[18]

This causes additional voltage-gated sodium channels to open. Once the feedback is strong enough, all of the voltage-gated sodium channels will become activated, allowing sodium to diffuse into the membrane. The threshold for action potential generation is approximately -65 millivolts.[18]

Action potentials spread or propagate in all directions away from the stimuli[18] when local depolarization at the origin of the stimulus begins to depolarize the segment of membrane directly adjacent to the area local depolarization.[30] The local depolarization opens adjacent voltage-gated sodium channels which allow sodium ions to diffuse into the membrane, propagating the action potential to the next segment of the membrane.[18] This cycle continues along the entire length of the membrane.

Synaptic Transmission

Neurons must communicate with one another in order to function as a system. This communication occurs through synaptic transmission.[22] In chemical synapses, electrical nerve impulses cause neurotransmitters to be released across the synaptic cleft onto postsynaptic receptors. The process of synaptic transmission is summarized below:[19,22]

1. An action potential travels down the axon to depolarize the axon terminal
2. The depolarization of the membrane causes voltage-gated calcium channel to open
3. An influx of calcium ions occurs through the opening of calcium channels
4. Calcium triggers the vesicles containing the neurotransmitter to bind with the presynaptic membrane, releasing the contents into the synaptic cleft via exocytosis

5. The neurotransmitter crosses the synaptic cleft and is bound to receptors on the postsynaptic membrane

6. The binding of the neurotransmitter to receptor causes ion channels to open, allowing ions to diffuse in or out of the postsynaptic membrane

7. The diffusion of ions across the membrane causes excitatory or inhibitory postsynaptic potentials which change the excitability of the postsynaptic membrane

8. The vesicle containing the neurotransmitter is reabsorbed by the presynaptic terminal and some neurotransmitter is recycled

Gross Anatomy of Lower Extremity Nerves

The sciatic nerve is the major nerve of interest in the lower extremity (Figure 2). It arises from the terminal branch of the sacral plexus and exits the pelvis at the sciatic notch, below the piriformis muscle.[31] Branches of the sciatic nerve innervate nearly all of the skin of the lower extremity and the muscles of the posterior thigh and lower leg.[31] The sciatic nerve innervates the biceps femoris, semitendinosus, semimembranosus, and the adductor magnus muscles before it splits into two divisions in the lower third of the posterior thigh known as the internal and external popliteal nerves.[31] The internal popliteal nerve continues along the posterior aspect of the thigh through the popliteal space where it supplies sensory function to the knee joint and innervates the medial and lateral heads of the gastrocnemius, the plantaris, the soleus, and the popliteus muscles prior to becoming the posterior tibial nerve.[31] The external popliteal nerve or peroneal nerve branches laterally and distally to the sciatic nerve to the fibular head.[31] The

external popliteal nerve primarily supplies sensory innervations to the posterior lateral aspect of the lower leg and some sensory innervation to the lateral aspect of the knee.[31] Divisions of the external popliteal nerve includes the anterior tibial nerve and the musculocutaneous nerve, which supplies sensory and motor function to the anterior and lateral aspects of the lower leg and foot respectively.[31] Disruption of the sciatic nerve can impact the function of all divisions and branches of the nerve distal to the area of insult.

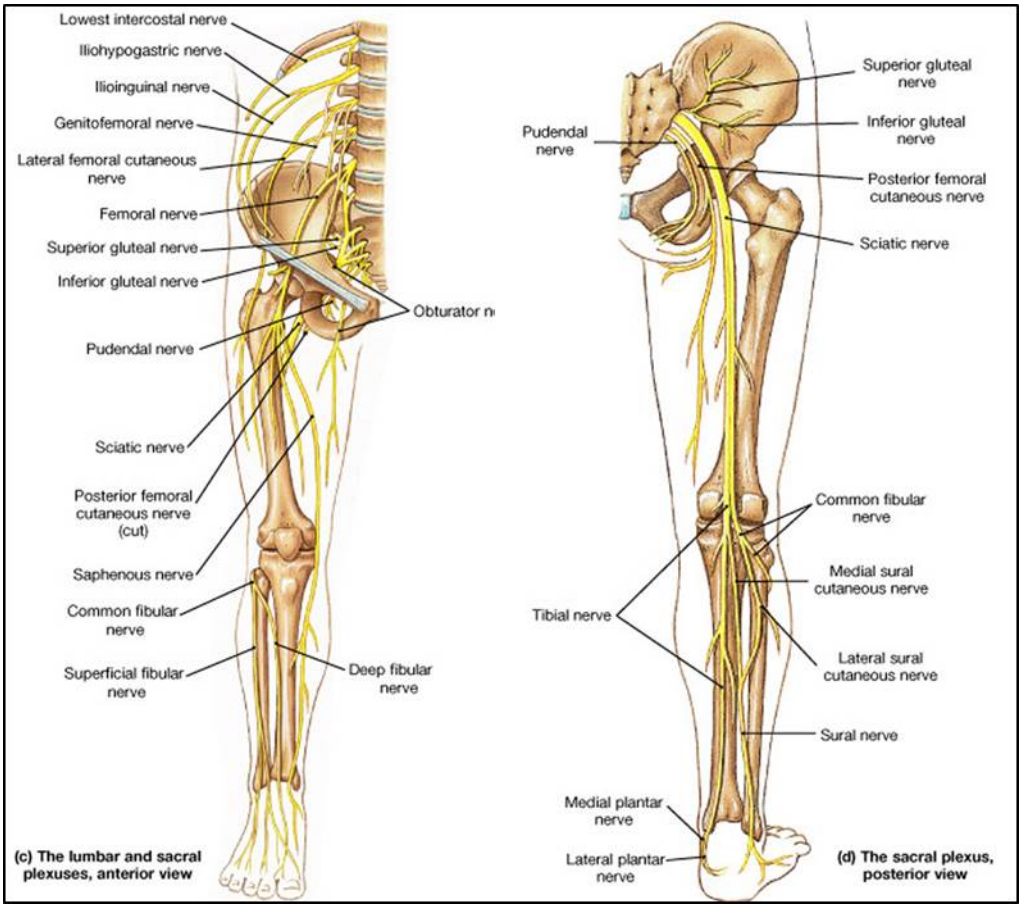

Figure 2. Lower extremity nerve distribution. Anterior structures are presented on the left and posterior structures are presented on the right. Borrowed from Martini and Bartholomew.[32]

Blood Vessels

Blood vessels enable the flow of blood and other nutrients from one area of the body to another.[33,34] Blood vessel walls are composed of several layers of smooth muscle, elastic connective tissue, and fibrous connective tissue.[34,35] The inner most lining of the blood vessel is a thin layer of endothelial cells.[34] Surrounding the endothelium are several layers of connective tissue and smooth muscle.[34] The composition of the layers of the blood vessels depend on its function.[35] Arteries, which function is to transport blood and nutrients away from the heart, have a high composition of smooth muscle and elastic tissue, while capillaries which function to diffuse oxygen and nutrients are composed of a thin layer (0.5 micrometers) of endothelial cells.[35] Veins which act to return blood to the heart from the periphery have nearly equal compositions of elastic tissue, smooth muscle, and fibrous tissue.[35] These structural differences contribute to the function of specific vessels. For example, vessels in the venous system are highly distensible and therefore able to store large quantities of blood, making it available when it is required.[33]

Regulation of Blood Flow

Blood flow in the vessels determines flow to tissues and ensures adequate perfusion based on the tissues needs.[36] Blood flow can be regulated locally, with humoral input, and with nervous system input.[36,37] Local regulation of blood flow can be explained by the vasodilator theory:[36] The greater the metabolic rate or the lower the availability of oxygen or other nutrient, the greater the formation and release of vasodilator substances from the tissue cells which increase blood flow.[38] The vasodilator theory is supported by a body of research which suggests

one of several vasodilator substances such as nitric oxide[39-43] or adenosine[44-48] are released during conditions of hypoxia or periods of increased metabolic demand.[38] Humoral control of blood flow is regulated by substances secreted or absorbed into the body fluids.[36] Humoral agents acting on the vascular tissue are typically divided into two groups: vasoconstrictor agents and vasodilator agents.[36] Vasoconstrictor agents reduce the diameter of the blood vessel and decrease local blood flow to tissues.[36] Examples of these agents include norepinephrine,[49] angiotensin II,[50] and antidiuretic hormone.[51] Vasodilator agents such as bradykinin[52] and histamine[53] increase the diameter of the blood vessels and increase the local blood flow to tissue.[36] Neuronal regulation of blood flow produces more global effects such as the redistribution of blood flow throughout the body.[37] The autonomic nervous system primarily controls blood flow with sympathetic output of norepinephrine onto α-adrenergic receptors.[54] In periods of high sympathetic output such as exercise, vasoconstriction occurs in the non-exercising muscle;[37] while vasodilation stimuli produce vasodilation in exercising muscle.[54] This example highlights one of the many interactions among the three control mechanisms of blood flow regulation in the blood vessels, and it underscores the importance of these interactions.

Gross Anatomy of Lower Extremity Vasculature

Understanding the function and distribution of the vascular tissues through the lower extremity is important in understanding how the structures could be influenced during local pressure application or prolonged restricted sitting. The femoral artery and its branches supply most of the arterial blood to the lower extremity.[31] The femoral artery originates (Figure 3) just

distal to the inguinal ligament as a direct continuation of the external iliac artery.[31] The artery continues as a single trunk from the inguinal ligament to the distal border of the popliteus muscle while changing its overall orientation from the anterior-medial aspect of the upper leg to the posterior aspect of the upper leg near the adductor magnus muscle.[31] The proximal half of the vessel is called the femoral artery, while the distal end of the vessel is known as the popliteal artery.[31] The vessel divides into the anterior and posterior tibial arteries at the popliteal space.[31] The anterior tibial artery bifurcates from the popliteal artery and continues to the anterior portion of the lower leg extending just distal to the anterior of the ankle mortis where it becomes the dorsalis pedis artery.[31] The posterior tibial artery extends distally and posterior-medially to the medial aspect of the tibia.[31] The artery continues distally and runs posterior to medial malleolus and branches to the internal and external plantar arteries.[31] These vascular structures supply the lower extremity with nutrient-rich blood and any obstruction will affect the flow of blood and nutrients to points distal.

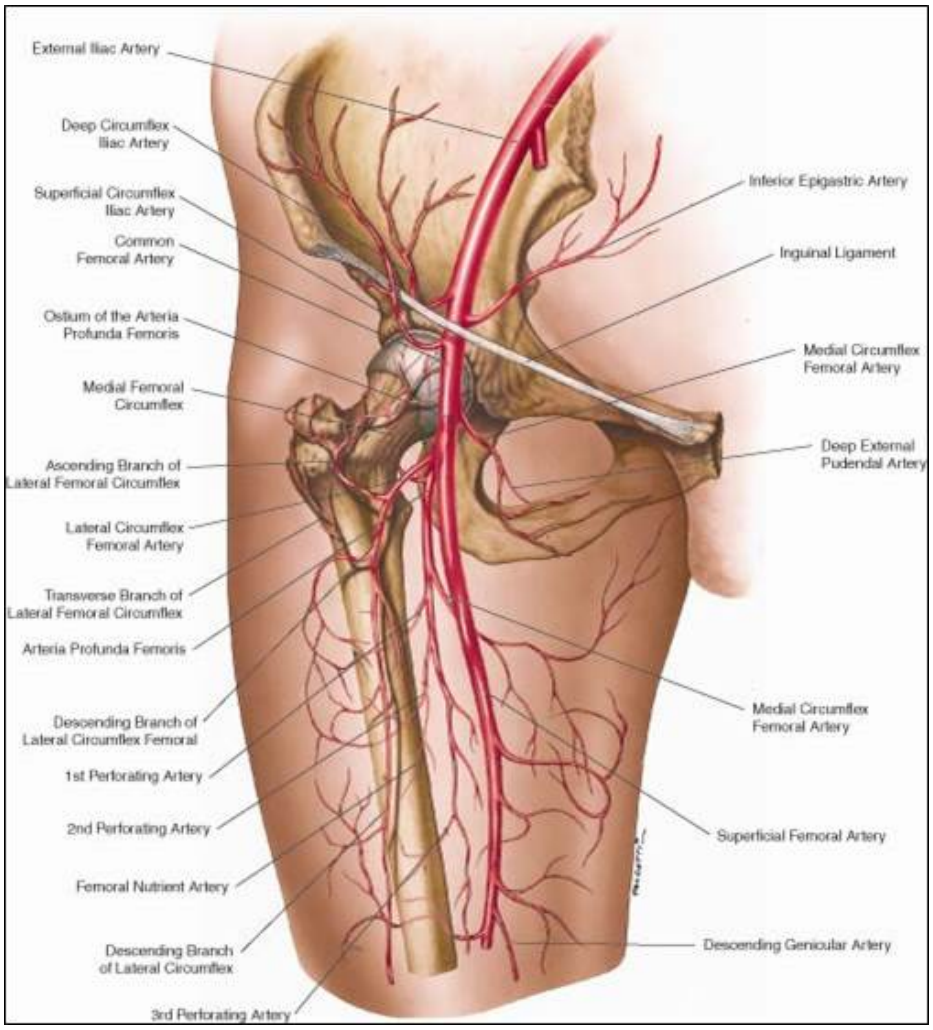

Figure 3. Anterior view of the femoral artery Borrowed from Uflacker.[55]

A system of veins returns blood to the heart from the periphery (Figure 4). Two major veins serve as the main conduits for blood to travel from the lower extremity to the heart.[31] The internal saphenous vein starts on the dorsal aspect of the foot and travels medially in front of the medial malleolus.[31] The internal saphenous continues to travel proximally, along the medial aspect of the lower and upper leg until it terminates and converges with the femoral vein.[31] The external saphenous vein originates on the lateral dorsal surface of the foot and continues posteriorly behind the lateral malleolus.[31] The external saphenous vein continues proximally

along the posterior lower leg before traveling deep near the inferior aspect of the popliteal space.[31] The external saphenous vein terminates with its convergence to the internal saphenous vein in the proximal third of the upper leg.[31] While the external and internal saphenous veins are the major tributaries by which blood returns from the periphery, many collaterals converge into the internal and external saphenous veins to return blood back to the heart.[31]

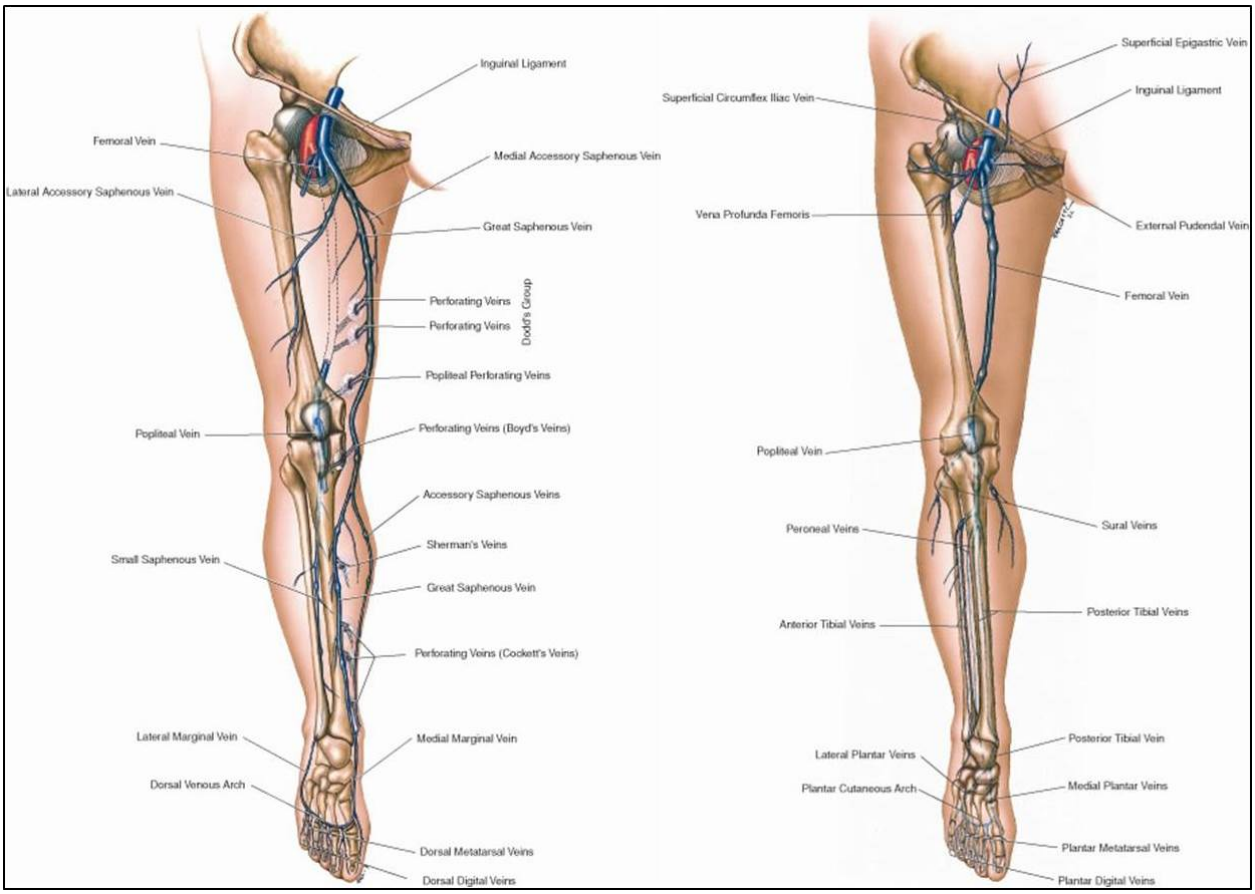

Figure 4. Lower extremity venous system. Superficial branches shown on the left and deep branches shown on the right. Borrowed from Uflacker.[55]

Aircrew Focused Research

Investigations into the physiological and reported discomfort changes which occur as a result of prolonged restricted sitting are limited despite decades of reported issues.[1] The

approach investigations have taken is summarized by Cohen,[1] "…the method for ascertaining seating pressure issues has remained, unfortunately, the same: simply ask aircrew where it hurts and hope some cushion changes work." Most of the current seating research in rotary-winged aircraft focuses on vibration attenuation.[11-14,56] Alterations to seat design and cushion materials have demonstrated an ability to attenuate the vibration experienced by pilots.[11-14,56] Cushions constructed of enhanced foam or air bladders significantly dampened the vibration signatures of AH-64 Apache aircraft and increased comfort on a thirteen point questionnaire in aviators.[11]

Pressure mapping systems have been used extensively in populations, such as individuals restricted to wheelchairs;[57-64] however, few studies have examined pressure changes in aircraft seating.[1,3,65] An introductory study utilizing United States Air Force B-2 pilots found that a high density foam cushion decreased peak pressure and increased pressure distribution area when compared to a traditional seat cushion.[1] The small sample size likely limited the application of these findings to the broader Military.[1] Other findings examining prolonged sitting in gliders found that participants began fidgeting (often a sign of discomfort) approximately 40 minutes into a 90 minute flight simulation.[15] A strong correlation (r = 0.954) between pressure-lowering fidgeting amplitude and mean peak pressure was found.[15] Fidgeting was determined to be any pressure reducing maneuver (i.e., shifting weight). No association was found between mean peak pressure measurements and body mass index, however the participants were considered to be slightly overweight (body mass index = 26.7 $kg \cdot m^{-2}$).[15] Previous research indicates that individuals with lower body mass indices experience higher sitting interface pressures due to smaller contact areas.[64] No significant association between peak pressure amplitudes and discomfort scores has been identified in research using sitting times of up to 8 hours.[3] The authors did identify a trend between peak pressure and subject discomfort in an evaluation of

four seat cushions for ejection seats, however this trend was not significant and further interpretation of the data is not warranted.[3] Dynamic seat cushions (i.e., those with inflating and deflating air bladders) elicited the highest peak pressures, but were not rated the most uncomfortable.[3] These conflicting seat interface research in aircraft suggest that there may be other parameters beyond interface pressure which contributes to the reported parathesia and discomfort in Black Hawk pilots. Other possible parameters could include blood flow and muscle oxygenation.

Measures of lower extremity oxygen saturation changes as a result of prolonged sitting have produced interesting results. During an eight hour bout of prolonged sitting, oxygen saturation in the lateral gastrocnemius muscle decreased by 4%-12% from baseline. However, this decrease was not statistically significant suggesting that prolonged sitting does not alter lower extremity muscle oxygenation.[3] A significant decrease in tissue oxygenation of 5%-18% below baseline measures was found in males.[3] No significant difference was present in females, with mean oxygen saturation increasing four hours into testing of one passive foam cushion.[3] Anthropometric differences between males and females appear to contribute to observed sex specific differences. Male volunteers, on average, were 41.4 pounds heavier and 3.87 inches taller than the female volunteers in the study.[3] Male volunteers also experience higher average interface pressures than female volunteers regardless of seat cushion time and greater contact area with the seat cushions.[3] Another contributor may be in the methodology used to measure oxygen saturation. Muscle oxygenation was measured with near-infrared spectroscopy measured at the lateral gasctrocnemius muscle. Total hemoglobin levels and tissue deoxyhemoglobin levels were not assessed in this investigation nor were the data normalized through an arterial occlusion protocol. Without normalization of the data, interpretation of the results is very

difficult. Additionally, total hemoglobin, tissue oxyhemoglobin, and tissue deoxyhemoglobin levels interact closely with one another and are typically recorded and interpreted together.[66] Further investigations into the changes in blood flow as a result of prolong sitting need to be completed.

The use of subjective questionnaires is another method which has commonly been utilized for the qualitative assessment of seat discomfort. In a series of investigations examining seat discomfort across four[3] and eight[3,9] hour sitting periods, results revealed a significant increase in buttocks discomfort.[3,9] Means of buttocks discomfort ranged from 0-3.5 on a 10 point scale. The discomfort scale ranged from 0-10 with zero indicating "no discomfort" and ten indicating "unbearable discomfort." Scores in the range of 3-4 indicated "moderate discomfort." Subjective scores of overall physical condition were also collected and ranged from 10 (Great) to 0 (Bad).[3,9] Ratings for both men and women decreased significantly from scores of 9.5-8.25 to 8-7.5 across the 8 hour prolonged sitting bout suggesting that prolonged sitting not only increases local discomfort, but also decreases overall physical condition. Overall physical condition refers to a portion of the subjective discomfort questionnaire which asked questions regarding the participant's whole body discomfort.[3] The ratings were collected from both military and civilian populations,[3,9] which suggest that ratings of perceived comfort do not differ between civilian and military populations. However, further investigation is necessary to understand if the similarity in discomfort ratings hold true under other circumstances such as in rotary-winged aircraft or during military training exercises.

Wheelchair Focused Research

Research involving the effects of prolonged sitting in individuals confined to a wheelchair focuses primarily on pressure ulcers. Excessive pressure applied to the skin over a bony prominence for a prolonged period of time is the most important extrinsic factor in the development of pressure ulcers.[67] As a result, most investigations have focused on interface pressure levels,[57,59,60,63,64,67] and cushions designed to mitigate the high levels of interface pressures.[58,61,62,68] A randomized, multicenter clinical trial found that patients who developed sitting induced pressure ulcers had significantly higher peak interface pressures (115 ± 45 mmHg; mean ± SD) compared to patients who did not develop these pressure sores (78 ± 22 mmHg; mean ± SD).[67] The areas in which pressure ulcers are likely to develop are under bony prominences in the lower extremity such as the ischial tuberosities, sacrum, trochanters, popliteal fossae, and heels.[69] Previous research indicates that the ischial tuberosities and sacrum also experience higher interface pressures in aviators.[1] Other possible influences on seat interface pressure in wheelchair sitting includes body composition[64] and wheelchair propulsion.[60] Body composition is inversely related peak interface pressure.[64] Individuals with higher body composition have a greater contact area with the wheelchair and according to the formula for pressure (pressure = force / contact area); a greater contact area will decrease the mean peak-pressure experienced on the sitting surface of the buttocks.[64] A study of seat interface pressure during propulsion found that interface pressure did not differ among five levels of propulsion speed. The authors indicate this outcome may be due to limitations in the pressure mapping device and suggest the system was not sensitive enough to measure changes in total pressure magnitude during propulsion.[64] Understanding how interface pressures contribute to pressure sores is critical in wheelchair bound populations. Understanding how physiologic function is

modified as a result of prolonged sitting and local pressure application is equally important in understanding the mechanism by which prolonged sitting induces symptoms of parathesia.

Blood flow has been used to evaluate the physiological effects of prolonged sitting in wheelchair populations. Examination of skin blood flow on the sitting surface of the buttocks can be examined with Photoplethysmography:[70,71] An optical measurement device used to non-invasively measure mircovascular blood flow.[72] The investigators report decreased skin blood flow in a geriatric population compared to a control group of young, healthy men during a five minute protocol.[70,71] However, no inferential statistics were presented and the descriptive statistics were insufficient to perform a secondary analysis of effect size. Other investigations examined blood flow on the sitting surfaces of the buttocks by measuring oxygen tension.[73,74] Oxygen tension is a non-invasive measure of oxygen saturation which provides insight into the oxygen levels within capillary beds.[75] The results indicate that a shear force applied to the skin decreased oxygen tension significantly more than in application of a normal (perpendicular) force alone. In a military aircraft, shear stresses likely result from body movement during combat operations or combat drills. This additional shear stress could contribute to the frequency and severity of symptoms reported by military aviators.

Physiologic Approaches

Examining the physiologic approaches to the effects of local pressure on various tissues can be beneficial to understanding the mechanisms by which seat discomfort arises. Studies examining the effects of local pressure application on nervous tissue function is an example of how understanding changes to isolated tissues aids in our understanding during applied

situations, such as prolonged sitting. Both acute[76-79] and chronic[80-82] compression have negative impacts on nerve function. Nerve conduction velocity appears to be the most commonly utilized tool when testing changes due to nerve compression.[76-79] Nerve conduction velocity measures the speed at which segments of nervous tissue propagate electrical signals.[83] As little as 11 minutes of local compression decreases nerve conduction velocity.[76] The decrease in nerve conduction velocity alters the rate at which tissues receive signals from the central nervous system (brain and spinal cord) potentially resulting in decreased control and performance. Other studies also found that skin sensibility is decreased 15 minutes into a compression protocol, and nerve conduction velocity begins to significantly decrease 45 minutes after the onset of local compression.[78] Research examining isolated nerve samples suggest that unmylenated fibers are more resistive to focal compression than mylenated nerves.[76] This is of note because the composition of large mixed nerves, such as the sciatic nerve, are highly mylenated.[31] During recovery unmylenated nerves regain normal conduction velocity faster than mylenated nerves,[76] and the rate of recovery in mylenated nerves may depend on the duration of local pressure application.[82] Von Frey response latency (a measure associated with sensory responses in mylenated nerves) was greater following 6 months of compression compared to 1 month of compression during an examination of prolonged compression to the sciatic nerve.[82] This response latency remained increased for the 6 month compression whereas the 1 month compression demonstrated evidence of partial recovery.[82] Interestingly, histological examinations indicate that prolonged compression to the sciatic nerve does not affect the downstream neuromuscular junctions on the soleus muscle.[81] Schwann cell production was increased at the site of compression, possibly as an adaptation to the mechanical stimuli.[80] Studies examining local compression on nerve function in humans are limited,[78,84,85] but support

that local compression alters nerve function. Investigations in the lower[78] and upper[84] extremity demonstrate that nerve compression increases nerve latency, indicating that action potentials travel at a slower rate when compression is applied between the stimulation site and the recording site. Others have examined the neurological effects of local compression using the soleus Hoffmann reflex. The Hoffmann reflex is an electrically induced reflex analogous to the stretch reflex and is a measure of α-motoneuron pool excitability.[86] An examination of soleus Hoffmann reflex suggests that during local compression, Hoffmann reflex amplitudes significantly increase compared to baseline.[85] Interpretation of the Hoffmann reflex data must be done in context, as an increase in amplitude may be beneficial or deleterious.[86] The literature suggests that local nerve compression impairs nerve function both in isolated nerve specimens and in intact humans; however, little research has investigated the effects of nerve compression on the downstream function on nervous tissue. Future work should examine function distal to the compression site to examine if local compression has whole limb effects.

Current Methods of Assessing Seating

Seat comfort and reported discomfort occurring as a result of prolonged sitting are well studied. Current methods utilized to measure seat comfort and seat pressure distributions include examining: seat interface pressures,[1,57,59-62,64,67,87-91] changes in skin blood flow at the site of compression,[70,71,73,92] magnitudes of shear stress present during sitting,[68,93] subjective perception of comfort,[89,94,95] electromyography,[96,97] and other biomechanical assessments.[95,98]

Seat Interface Pressure

Measurements of seat interface pressure are the most common of all the methods found in the current literature. The systems utilized to measure seat interface pressures range from purpose built sitting surfaces[58,70,71,87,99] to commercially available seat pressure mapping systems.[1,59,64,67,89,100] In commercially available systems, the measurement pad consists of a flexible array of capacitance sensors[1,64] which are sensitive to changes in electrical capacitance.[64] When a force is applied to an individual sensor the capacitance changes in proportion to the magnitude of the force.[1] Pressure data is the typical output for these systems and is calculated by dividing the force measured by the known area of the individual sensor.[100] The frequent use of pressure mapping systems in seating research may be due to their portability and ease of use; however, several limitations should be considered. Seat interface pressure measurement systems which utilize the array of electronic matrices can yield inaccurate results if any part of the flexible array is not directly in contact with the seating surface.[100] In first generation seat pressure monitoring systems this was a significant problem, especially if the seat surface was not flat, because measurement systems were relatively thick (larger than 2 millimeters) and inflexible.[100] Improvements in sensor technology have decreased this limitation,[100] however, care should still be taken to ensure proper contact between the pad and the sitting surface. Other limitations such as an inability to measure shear forces and diminished performance during prolong sitting make quantitative assessments of seat interface pressure difficult. Future research should examine if pressure mapping systems are a reliable quantitative measure of seat pressure and if sitting time influences the data.

Shear Stress Measures

Shear stress measurements are less common in the literature, likely because shear forces are more difficult to measure.[93] Shear stress sensors utilize changes in capacitance to quantify shear stresses similar to pressure mapping systems.[93] Previous research utilizing shear stress sensors have yielded conflicting results. A series of studies examining the influence of shear stress on skin blood flow suggests shearing forces were less likely to reduce blood flow compared to increased pressure.[70,71,99] Others[73] found that shear stress decreased skin blood flow under the sacrum in a sitting condition. Animal work supports the hypothesis that shear stress is a contributing factor in the development decubitus ulcers, thought to be a result of local ischemia.[101,102] Improved methods of assessing shear stress in prolonged sitting and local pressure application conditions needs further examination to help understand the role of shear stress in seating discomfort and ulcer formation.

Blood Flow Measures

Changes to local blood flow at locations of high interface pressure and shear stress has been examined using photoplethsmography[70,71] and transcutaneous oxygen sensors.[73] Photoplethsmography functions by emitting a specific wavelength of light through the surface of the skin. A photoreceptor receives the incoming light after the light reflects off red blood cells. The reflection and refraction of the light is used to calculate blood flow volume in arterial capillaries.[70] Transcutaneous oxygen sensors measure the partial pressure of oxygen under the transcutaneous oxygen electrode.[74] Both methods provide insight into the changes in skin blood flow and oxygenation. In order to measure changes during prolonged sitting purpose built

sensors are required to measure the changes under the ischial tuberosities and participants must wear minimal clothing on the buttocks during testing.[70,71,73] These techniques that accurately provide insight on the influence of prolonged sitting and local pressure application on blood flow changes in the lower extremity are expensive and invasive.

Other Assessment Methods

Other methods have been used to investigate the changes associated with prolonged sitting include electromyography,[96,97] subjective discomfort scales,[89,94,95] and biomechanical assessments.[95,98] Electromyography measures the electrical activity of a skeletal muscle which is linked with the mechanical activity of the muscle.[96] Electromyography has been used to investigate erector spinae muscle fatigue in civilian helicopter pilot seats[96] and in office chairs with and without lumbar support.[97] Results have added insight to seating discomfort associated with low back pain, but has not been utilized to examine the electrical activity of the lumbar musculature during prolonged sitting situations. Examination of the lumbar spine muscles during prolonged sitting may improve understanding of the postural changes which may occur during prolonged restricted sitting. Future research could utilize electromyography to examine the relationship between lumbar spine muscle activity and perceived discomfort during prolonged sitting conditions.

Perceived discomfort scales have been used to assess seating comfort in wheelchairs[94] and automobiles.[89] These scales are varied and range from asking general questions about the overall comfort of the seat[94] to specific questionnaires which divide the body into several regions and asked participants to rate discomfort at each location independently.[89,95] Perceived

discomfort data is often combined with other methods such as interface pressure[89] or motion analysis.[95] Utilizing subject discomfort scales adds valuable insight into the participants' perceptions of discomfort since much of the research within prolonged sitting aims to decrease the perception of discomfort.

Research has also attempted to provide solutions to the problem of discomfort associated with seating by performing various biomechanical assessments of the seat[98] and the seat-subject system.[95] Researchers found that pilot seating in five different civil aircraft did not meet the minimum aviation requirements when pilot anthropometry (i.e. height, weight, and body length measures) was considered.[98] The work examining the biomechanical variables associated with seat design highlights the importance between seat design and user anthropometry. Previous work in the wheelchair population has demonstrated the relationship between participant anthropometry and seat interface pressure,[64,90] but has yet to be thoroughly investigated in the military population.

Potential Methods of Assessing Seating

Previous methods used to examine factors influencing seat discomfort have yielded valuable insights into the onset, duration, and intensity of prolonged sitting and local pressure application. There are also many additional techniques that may assist in our understanding of the changes which occur during and as a result of prolonged restricted sitting and local pressure application. Some of these potential measures include the Hoffmann reflex, nerve conduction velocity, dynamic infrared thermography, pulse oximetry, two-point discrimination, the

Semmes-Weinstein Monofilament test, the Category Partitioning Scale, and the Short-Form McGill Pain Questionnaire.

Neurological Measures

Hoffmann Reflex

The Hoffmann reflex (H-reflex) is an electrically induced reflex analogous to the stretch reflex.[86] The H-reflex is a non-invasive measure of α-motoneuron pool excitability used in applied human physiology, human movement, and sports medicine research. The H-reflex is useful in examining α-motoneuron pool excitability in musculoskeletal injury,[103-114] pain conditions,[115] fatigued conditions,[116,117] during therapeutic modality and exercise,[118-125] and exercise training conditions.[126-131]

In theory every muscle is capable of producing an H-reflex. However, in order to elicit the reflex the mixed nerve and muscle of interest must be accessible.[132] H-reflex measures are commonly recorded in the soleus,[104,105,109,112,113,120,133] peroneal,[103,106,108,134,135] quadriceps,[107,110,114,115]and flexor carpi radialis[136-142] muscles. Nerve stimulation and electromyography (EMG) are required in order to collection H-reflex data.[143] The electrical nerve stimulation is applied percutaneously to a peripheral mixed nerve[144] at a stimulation duration of approximately one millisecond.[145] The stimulation initiates a nerve impulse along the afferent and efferent portions of the mixed nerve.[146] The efferent signal travels directly to the muscle, eliciting a muscle contraction recorded by the EMG.[146] This contraction is known as the muscle response or M-wave.[86] The afferent nerve impulse travels towards the spinal cord and synapses at the α-motoneuron.[143] If the nerve impulse is of sufficient strength, neurotransmitters

will be released from the pre-synaptic neuron, travel across the synaptic cleft, and cause local depolarization of the post-synaptic terminal.[86] If the local depolarization is large enough, the depolarization will spread, creating an action potential along the efferent α-motoneuron.[86] The nerve impulse will continue to travel away from the spinal cord along an efferent pathway to the neuromuscular junction where it will synapse with the motor end plate.[146] This creates a muscle response which is recorded by EMG. This muscle response is the H-reflex.[143]

The H-reflex is a useful, non-invasive measure of segmental spinal reflex activity and has shown high intersession[147-153] and intrasession[141,151,152] reliability in both weight-bearing[148] and non-weight bearing positions.[151] Although the H-reflex is an objective, reliable measure of α-motoneuron pool excitability[143] there are limitations which must be considered during planning and interpretation of the H-reflex results. Since the H-reflex is electrically induced above the muscle spindle, the input from the muscle spindle is neglected.[86] Additionally, although there is a monosynaptic connection between the Ib-afferent neuron and α-motoneuron in the spinal cord there are also many inputs which influence motor output,[148] such as supraspinal[154] and pre-synaptic inputs.[148] Despite its limitations, the H-reflex provides a non-invasive, feasible, objective, and reliable measure of α-motoneuron pool excitability and spinal reflex modulation which can be used to monitor the influence of external perturbations on the body and track changes associated with prolong sitting and local pressure application.

Nerve Conduction Velocity

Nerve conduction velocity (NCV) is a common clinical method for detecting changes in the neurological function of a nervous system segment.[155] There are three common types of

nerve conduction velocity tests: motor nerve,[156] sensory nerve,[120] and mixed nerve conduction velocities.[83] NCV is determined from the amount of time required for an electrical impulse to travel the length of nervous tissue (latency) and the length of the nerve segment of interest.[157] NCV is calculated by dividing the length of the nerve segment of interest by latency.[158] Clinical NCV tests are commonly completed on the major nerves of both the upper[159-170] and lower extremities[171-176] and are used to identify pathological conditions such as radiculopathies,[177] neuropathies,[178] and compression injuries.[179] Normative values have been established for many nerves in healthy individuals and are dependent on age and height.[83] Axon diameter, axon myelination, and axon temperature are also important in determining NCV.[180-182] The larger the axon diameter, or more myelinated the axon, the faster the action potential can be propagated.[180,182] Higher temperatures result in faster nerve conduction velocities and lower temperatures result in slower nerve conduction velocities.[183]

Nerve conduction velocity studies at the superficial peroneal nerve,[184,185] sural nerve,[184,185] and medial plantar nerve[184] are reliable measures of nerve conduction velocity in the lower extremity when performed correctly. Many of the limitations with nerve conduction velocity studies are due to inconsistencies in testing conditions.[186-188] Inconsistencies in skin temperature, stimulus intensity, surface distance, and electrode placement lead to variability in nerve conduction velocities and amplitudes.[186-188] A specific concern in the examination of local compression is the potential that the compression itself could increase the variability of the measure. Research examining pathological conditions which may disrupt nerve conduction studies found that NCV demonstrated good reproducibility, although no studies have examined the effects of compression on the reliability and variability of nerve conduction studies.[189-191] Nerve conduction velocity studies could provide insight regarding peripheral nerve function

distal to external pressure application as they have been used to examine intrinsic sources of compression on nerve conduction parameters in the past. Many of the limitations associated with nerve conduction velocity studies can be overcome with controlled, consistent procedures designed to diminish intersession variability in recording parameters.

Two-Point Discrimination

The two-point discrimination test is a clinical tool utilized to examine the sensibility and the innervation density within a receptive field on the skin.[192,193] Two-point discrimination measures the ability to distinguish static or dynamic dull pressure application from two sources at multiple inter-source distances.[194,195] The smaller the inter-source distance, the smaller the receptive field on the patch of skin of interest.[192] The inability to discriminate between two pressure sources indicates that the points are within the same receptive field or that the receptive field sensibility has been diminished.[192,194,196] Two-point discrimination is used extensively to examine the post-operative sensation redevelopment progress.[197,198] The measure has also been utilized to examine changes in sensibility as a result of cryotherapy,[199,200] thermotherapy,[199] vibration stimuli,[201] and orthopedic injury.[202] Typically, two-point discrimination data are collected from the hands[193-196,200,203-205] and feet;[199,201,202,204,206] but has also been collected at the ankle,[199,202] trunk,[192] and forearm.[207] Research suggests that the two-point discrimination test may not be a reliable measure in asymptomatic individuals.[193,194,206] The decreased reliability of the measure is most prevalent with between-subject testing.[205,206] It does provide an opportunity to non-invasively examine the receptive field and is still considered a useful clinical tool to monitor sensibility changes if caution is used in interpreting findings across subjects.[205,206]

Measuring changes to the receptive field non-invasively and quickly is important because it adds insight to the clinical manifestations of compression induced parathesia under extrinsic nerve compression conditions. The two-point discrimination test is compact, portable, and easy to use without access to an external power source. These characteristics are valuable when one considers that challenges of collecting field data in rotary-winged aircraft in remote testing locations, lacking external power sources, under dusty, wet, or cold conditions. The two-point discrimination test may be preferred over more sophisticated techniques in these circumstances.

Semmes-Weinstein Monofilaments

The Semmes-Weinstein Monofilament test is a clinical evaluation tool used to examine a patient's sensitivity to a point pressure stimulus.[208] In other words; it measures the skin's sensitivity to low level pressure application. The monofilament test typically comprised of several single Nylon fibers[209] of varying thickness.[210] The thickness of the Nylon fiber depends on the "buckling force" desired.[211] Each monofilament thickness is designed to buckle when a specific level of force is applied.[211] The levels of force before buckling range from 0.4 grams to 300 grams.[212]

The Semmes-Weinstein Monofilament test is a common, non-invasive clinical tool used during a neurological exam in the upper[208,213,214] and lower extremities.[208-210,215-218] The monofilament test is typically conducted on the hands and feet to monitor conditions such as diabetic peripheral neuropathy,[209] lumbosacral radiculopathy,[218] and following nerve repair surgeries.[213,214] In the lower extremity the best locations for testing are the plantar aspect of the great toe, the plantar aspect of the third metatarsal, and the plantar aspect of the fifth

metatarsal.[209] The test is conducted by touching the desired location with the monofilament tip until the monofilament begins to buckle.[211] The monofilament is held in place for 1.5 seconds and the examiner instructs the participant to respond "Yes" if he/she feels the monofilament against the skin.[212]

The Semmes-Weinstein Monofilament test demonstrates good intra-rater reliability at five locations on the feet,[210] but poor inter-rater reliability over the same five locations.[210] Along with the limitation of poor inter-rater reliability, calibration of the device is difficult.[211] The manufacturer calibrates the monofilaments during the manufacturing process,[212] however no work has examined if bends or kinks in the Nylon fiber affect the performance of the device. These limitations can be overcome by utilizing a single Semmes-Weinstein Monofilament rater during the entire data collection and by ensuring that the monofilament is protected when not in use to reduce the likelihood of damaging the equipment. In summary, the Semmes-Weinstein Monofilament test is an easy to obtain and non-invasive measure that has reasonable reliability when used properly. It has the potential to provide insight into the sensory changes which may occur during local compression application.

Vascular Measures

Dynamic Infrared Thermography

Dynamic infrared thermography (DIRT) is a tool that first became available for non-military use in 1958.[219] It uses specialized sensors to measure the electromagnetic radiation emitted from the body[220] to create a map of temperature distribution across a surface (thermogram).[219] Recent developments in high resolution thermal imaging have increased the

thermal and spatial resolution of thermograms.[221] Improvements in device design have decreased the size of most thermal imagers, increasing unit mobility.[222] These advances have increased the utility of infrared thermography as an emerging medical imaging device to detect injuries and illnesses.

The human body is homeothermic, meaning that it can generate and self-regulate temperatures essential for survival[219] by radiating heat from the skin's surface. Infrared thermography systems detect the radiate heat leaving the surface of the body[220] and create a color-coded image of the temperatures across the surface of the target.[220] These images are then analyzed to provide insight on physiological events influencing the surface temperature.

DIRT is currently used to examine changes in surface temperature in a variety of disease and injury states including: inflammatory arthritis,[223] osteoarthritis,[224] and pneuomthorax.[225] DIRT has also been used to examine peripheral circulation changes as a result of industrial exposure to vibration in the hands;[226] changes in physiological function as a result of non-pharmacological treatments such as massage;[227-230] and to assess physiological changes in exercise[231-233] and therapeutic intervention studies.[120,234,235]

DIRT has good inter-examiner and inter-session reliability in measuring temperatures in the lower extremity,[236] and high reproducibility in the upper extremity.[237] Recent work[238] demonstrates that skin temperature changes measured by infrared thermography compares well with radiography in the evaluation of the severity of knee osteoarthritis. An important difference between radiography and DIRT is that radiography evaluates structural changes of tissue while infrared thermography measures physiological changes. Normative infrared thermography data for various body regions is unavailable, however, research to create normative data at several

body locations is currently underway.[239] Current protocols suggest that the use of medical thermography should compare the affected side of the body to the unaffected side.[219] In intervention studies, pre- and post-measures of the same region are typically collected.[120,228,235]

Limitations in this technique include the lack of normative data which makes between subject analysis difficult.[239] Another limitation of DIRT is that the thermal environment which data is collected must be controlled, both intra-session and inter-session.[240] Recommendations suggest the temperature not vary more than 1 °C during a single session and remain between 19 °C and 23 °C for all data collection.[240] Additionally, the wide variety and quality of infrared thermography detection systems creates difficulties for standard assessment of thermograms or comparisons between units.[240] Finally, in order to accurately measure superficial skin temperature requires the skin to remain uncovered throughout testing. For military seating studies, this means that pilots or participants would not be able to wear the traditional Army Combat Uniform or ACU.

DIRT can use temperature to evaluate the skin's surface circulation. The portability of DIRT and non-invasive data collection makes it ideal to monitor surface temperature changes which may be difficult to access with other methods. In the evaluation of prolonged sitting and local pressure application, DIRT is well-suited to evaluate temperature if access to the lower extremity is limited due to the physical structure of the chair.

Pulse Oximetry

Pulse oximetry is a non-invasive tool used to measure arterial blood oxygenation.[241,242] Although the components of the equipment were available and tested in the late 1940's, it was

not until the 1980's that pulse oximetry became widely available for clinical use.[242] Pulse oximetry works by utilizing spectral analysis,[242] the examination of the components of a solution based on the solution's light absorption properties.[241-243] The pulse oximeter unit emits two wavelengths of light, one red and one infrared.[242,244,245] The light travels through the capillary bed of a finger, toe, or earlobe and then is recorded by a photo detector on the other side of the tissue of interest.[245] Oxygenated hemoglobin absorbs more infrared light and is more transparent to red light than deoxygenated hemoglobin.[245] The unit then utilizes the data to calculate the percentage of oxygenated hemoglobin present in the capillary bed.[246] The unit typically displays results in percent oxygen saturation (SpO_2).[245]

Pulse oximetry is regularly used in hospital and athletic health care settings to assess blood oxygen saturation.[245,247] In human movement studies, pulse oximetry has been utilized to track oxygen desaturation in participants following sprint activities,[248] maximal cycling activities,[249] and swimming.[250] Pulse oximetry is a reliable measure of blood oxygen saturation for oxygen saturations between 70 and 100%,[241] below 70% the reliability of pulse oximetry is significantly decreased.[251] Therefore, its use in intensive exercise studies or other hypoxic conditions is not recommended.[251] In addition to its limitation for use in hypoxic conditions, pulse oximetry may be limited in situations in which relatively high levels of carbon monoxide are present,[252] intravenous administration of drugs containing dyes occurs,[253] when nail polish is covering the fingernail of the digit used for investigation,[254] or in conditions in which motion artifact may be present.[255] An additional limitation for seating studies is that the feet are required to be exposed during testing. This requires that participants not wear flight approved boots or shoes during testing which could alter the overall seating experience. In an examination of prolonged restricted sitting and local pressure application these limitations can be mitigated with

proper design. Pulse oximetry provides the opportunity to investigate whole-limb changes in oxygen saturation to local pressure application and prolonged restricted sitting. The compact size, portability, and ease of use make it an ideal measure to investigate oxygen saturation changes occurring in the lower extremity.

Subjective Discomfort Scales

Category Partitioning Scale

The Category-Partitioning Scale is utilized to examine the perception of local pressure intensity levels and discomfort,[256,257] a logical choice to examine seat comfort in human factors research.[258] It consists of a vertical scale starting at zero and is divided into five categories: "very slight," "slight," "medium," "severe," and "very severe."[257,258] Each category is further divided into 10 scale points for a total range of 0 – 50, with numbers above fifty provided to avoid the ceiling effect in the case of extreme pain or discomfort.[257] Participants are given instructions to rate their discomfort in one of the five categories, they then "fine tune" their discomfort rating using the numerical scale points.[257] Only the numerical value is reported.

The Category-Partitioning Scale demonstrates high test-retest reliability, low intersession change, and high intra- and inter-individual reliability.[257] In an examination of six seat pressure and discomfort rating scales, the Category-Partitioning Scale demonstrated the highest validity and reliability of the six scales.[257] This suggests that the measure is appropriate in the examination of the local pressure application and prolonged sitting. A potential limitation to this scale is that participants may have difficulty distinguishing discomfort near the edges of each category. For example, the differences between a score of 10 in the slight discomfort category

and a score of 1 in the discomfort category. The Category-Partitioning Scale is a measure that is currently being utilized to report seating pressure and discomfort perception in consumer vehicle studies (i.e., passenger cars). Applying this measure to military aircraft seating provides the opportunity to compare ratings of discomfort and pressure across both the military and civilian settings.

Short-Form McGill Pain Questionnaire

The McGill Pain Questionnaire is a widely utilized subjective pain questionnaire.[259] It provides information on the sensory, affective, and evaluative aspects of pain.[259] However, this questionnaire may not be useful in all situations because completion time is typically 5-10 minutes.[259,260] The Short-Form McGill Pain Questionnaire (MPQ) was developed in response to the need to collect subject pain information in a shorter period of time.[260] The MPQ is a 17-point questionnaire originally designed to evaluate labor, menstrual, headache, dental, cancer, arthritis, and musculoskeletal pain.[260] Since its development it has also successfully been used to evaluate joint pain,[261,262] nerve pain,[263] and therapeutic intervention effectiveness.[264,265] The questionnaire consists of eleven sensory dimension descriptors (throbbing, shooting, stabbing, sharp, cramping, gnawing, hot-burning, aching, heavy, tender, and splitting) and four affective dimension descriptors (tiring-exhausting, sickening, fearful, punishing-cruel).[260] Each descriptor is ranked on an intensity scale of 0 = none, 1 = mild, 2 = moderate, and 3 = severe.[260] Additionally one visual analogue scale and one Present Pain Intensity question are presented to provide overall intensity scores.[260] Scoring of the MPQ is completed by summing the reported scores of the sensory and affective descriptors to obtain a composite score.[260] Sensory and affective

descriptors can also be evaluated separately by summing only the descriptors in the respective domains.[260] The visual analogue scale and Present Pain Intensity questions are evaluated separately. The total distance (in centimeters) from 0 is measured and recorded for the visual analogue scale, the single Present Pain Intensity serves as the pain intensity score.[260] In total, five measurements are obtained from the SFMPQ: total score, sensory domain score, affective domain score, visual analog scale distance, and Present Pain Intensity score.[260] The MPQ correlates well with the scores reported in the Long-Form McGill Pain Questionnaire.[260] It has high intraclass correlation for total, sensory, affective, and visual analogue scale measures (0.96, 0.95, 0.88, and 0.89, respectively), but a lower intra-class correlation for Present Pain Intensity scores (0.75).[266] The MPQ demonstrates high overall reliability and should be considered an appropriate measure of pain and discomfort during prolonged restricted sitting and local pressure application.

Conclusion

Prolonged restricted sitting is a significant problem in military populations.[1] Investigations into prolonged restricted sitting have enhanced our understanding of reported symptoms and interface pressures typically experienced. Despite these investigations, prolonged restrict sitting still poses a problem to today's aviators. Future investigations are needed to examine physiological changes which occur as a result of prolonged restricted sitting and to investigate potential aggravating factors such as tissue compression magnitude; tissue compression duration; mechanical vibration; posture; and aviator anthropometry; on the development of symptoms associated with prolonged sitting. Through physiological

examinations of the symptoms associated with prolonged sitting and local compression, metrics could be developed to serve as a method of evaluating seat comfort beyond subjective questionnaires and seat interface pressures. Additionally, these physiologic examinations could be utilized to guide the development of new seat designs to better serve the aviators and other military personnel who are regularly exposed to long durations of restricted sitting.

Chapter III

Methods

This project was composed of three projects. Project 1 (Figure 5) had the aim of determining the effects of prolonged restricted sitting on perceived discomfort, lower extremity sensibility, and lower extremity total limb blood oxygen saturation. Project 2's (Figure 6) aim was to determine the effects of two local pressure application magnitudes on perceived discomfort, lower extremity sensibility, and lower extremity total limb oxygen saturation at two lower extremity application sites. Project 3 (Figure 7) had the aim of determining the effects of one local pressure application magnitude at two lower extremity application sites on perceived discomfort, lower extremity sensibility, soleus α-motoneuron pool excitability, sural sensory nerve conduction velocity, superficial skin temperature, and lower extremity total limb oxygen saturation.

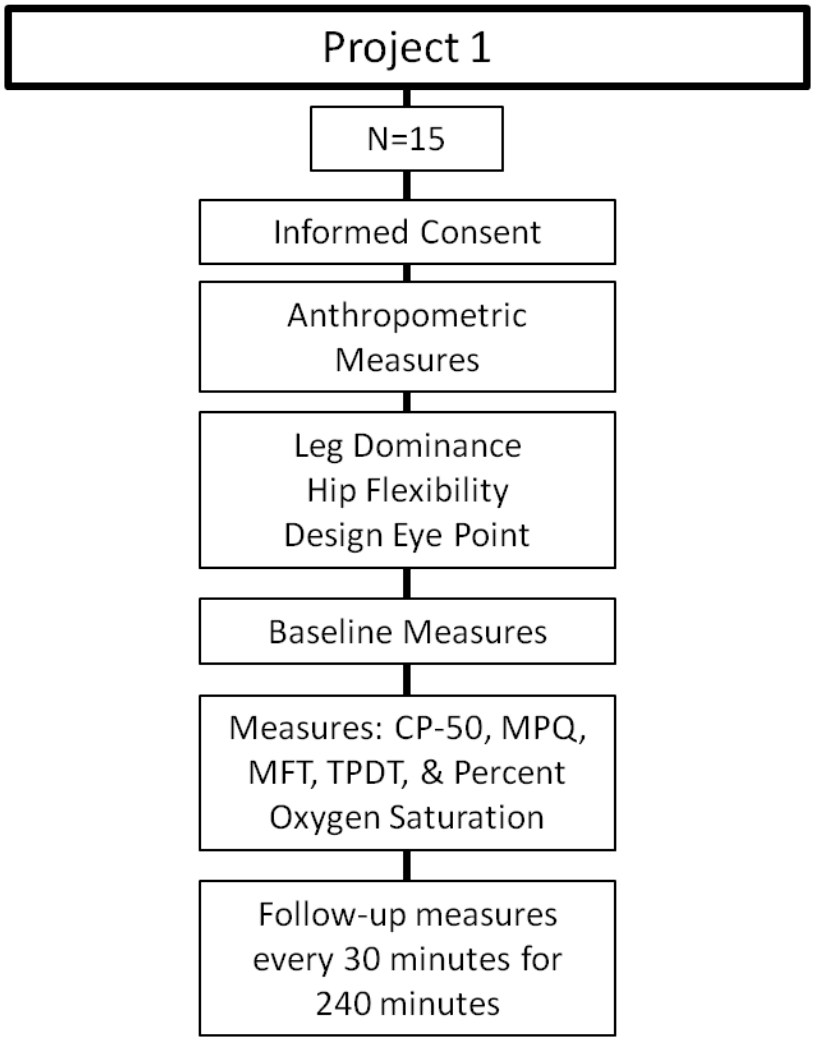

Figure 5. Project one summary.

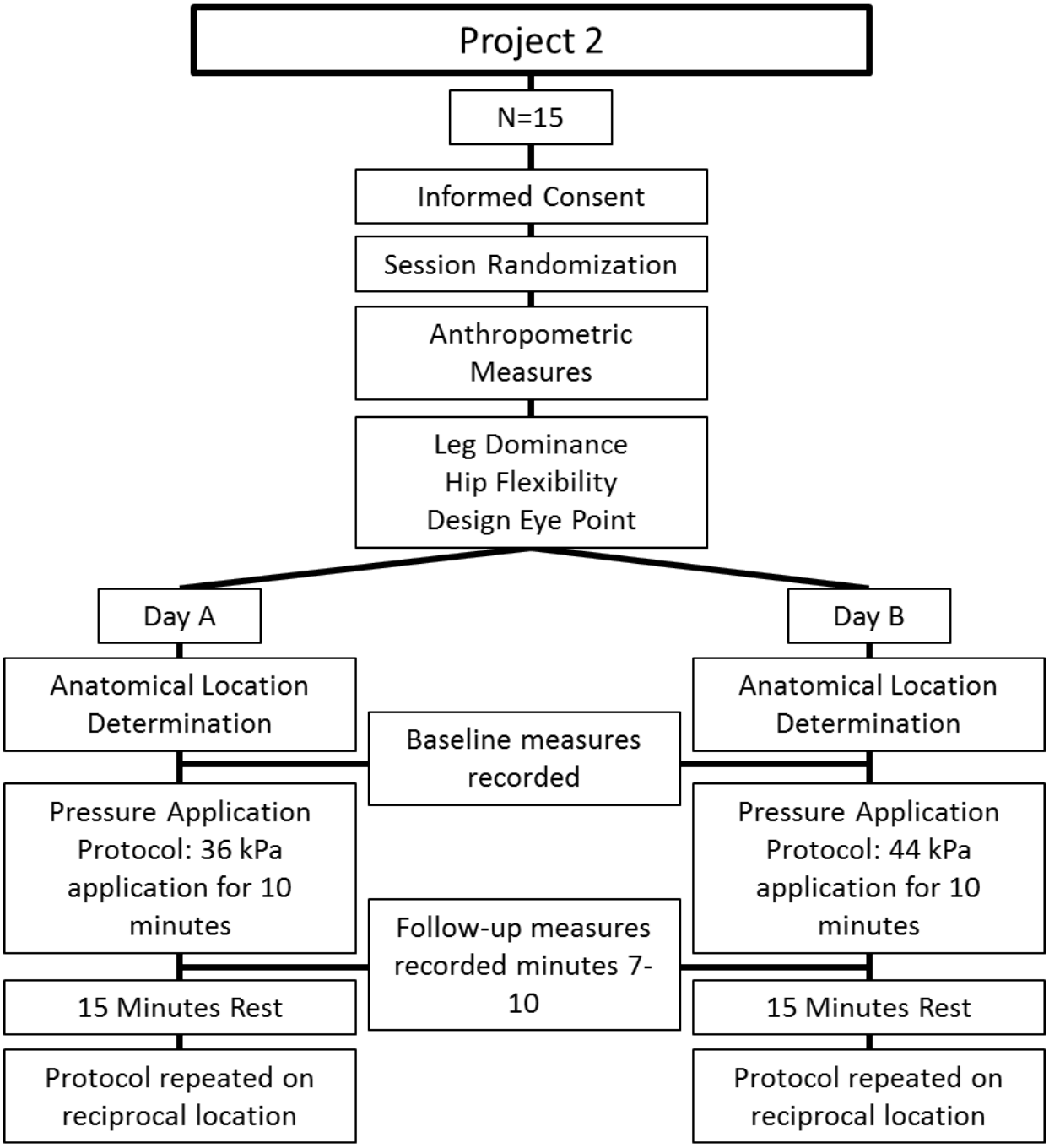

Figure 6. Project two summary.

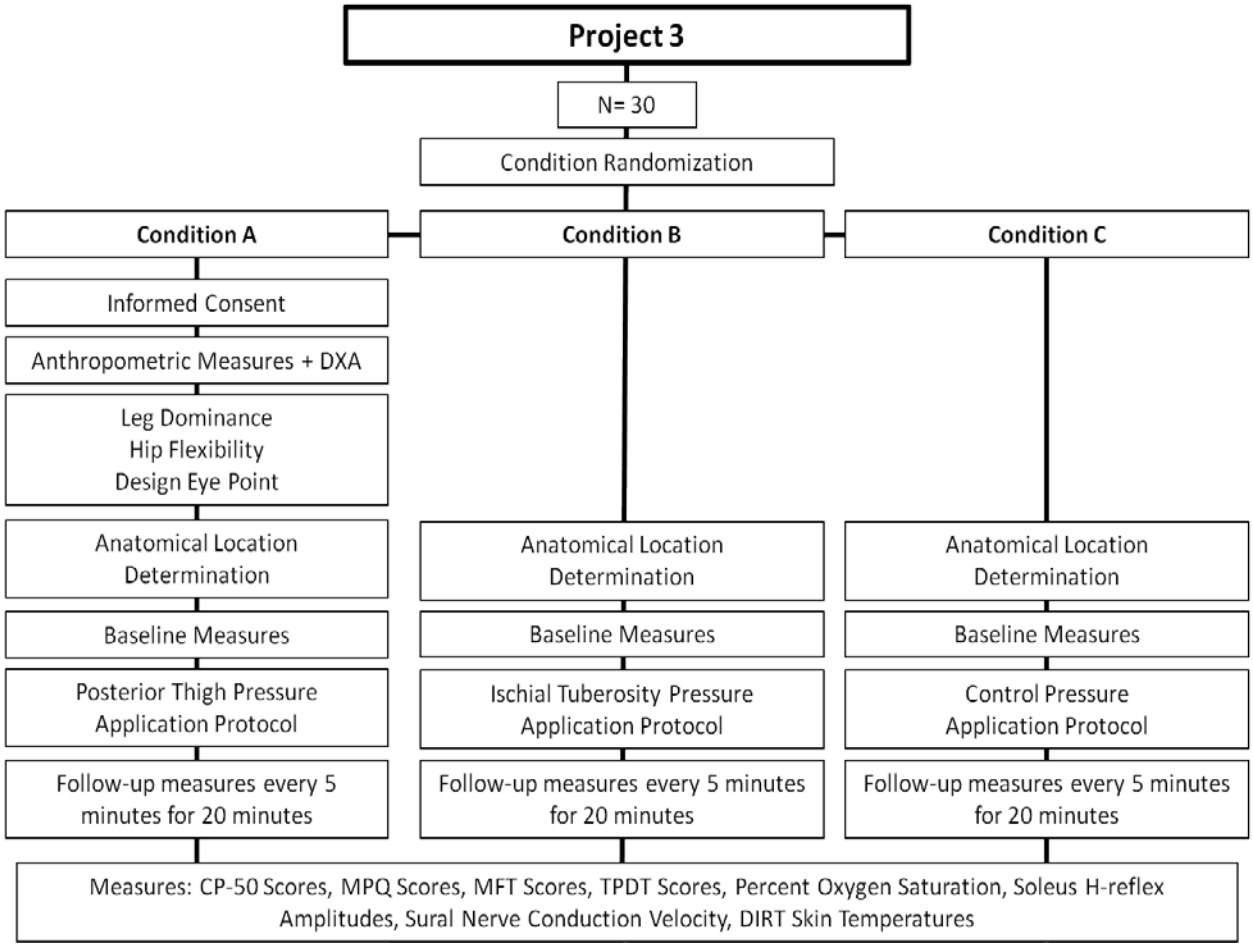

Figure 7. Project three summary.

Measures

Perceived Discomfort

Category Partitioning Scale (CP-50)

Perceived discomfort during prolonged restricted sitting and local pressure application was measured using the Category Partitioning Scale (CP-50).[257] The CP-50 scale is a reliable measure of perceived pressure intensity and discomfort ratings[257] and is used as a standard for measuring discomfort while sitting.[258] The scale (Figure 8) is arranged vertically, has a starting

point of zero, and has 5 categories: very slight, slight, medium, severe, and very severe discomfort. Each of the 5 categories is further divided into 10 scale points. Points above 50 are provided to avoid the ceiling effect on ratings of extreme intensity. The scale achieves this through a two-step method in which participants first verbally name a category to which the stimulus "belongs" and then they fine tune the category using the numerical subdivisions. For example, if a participant feels a discomfort or pressure level is high and almost very high, the category high pressure comprises numbers 31-40. Due to the tendency towards very high pressure, fine tuning may result in choosing a number close to the upper category boundary such as 38 or 39.

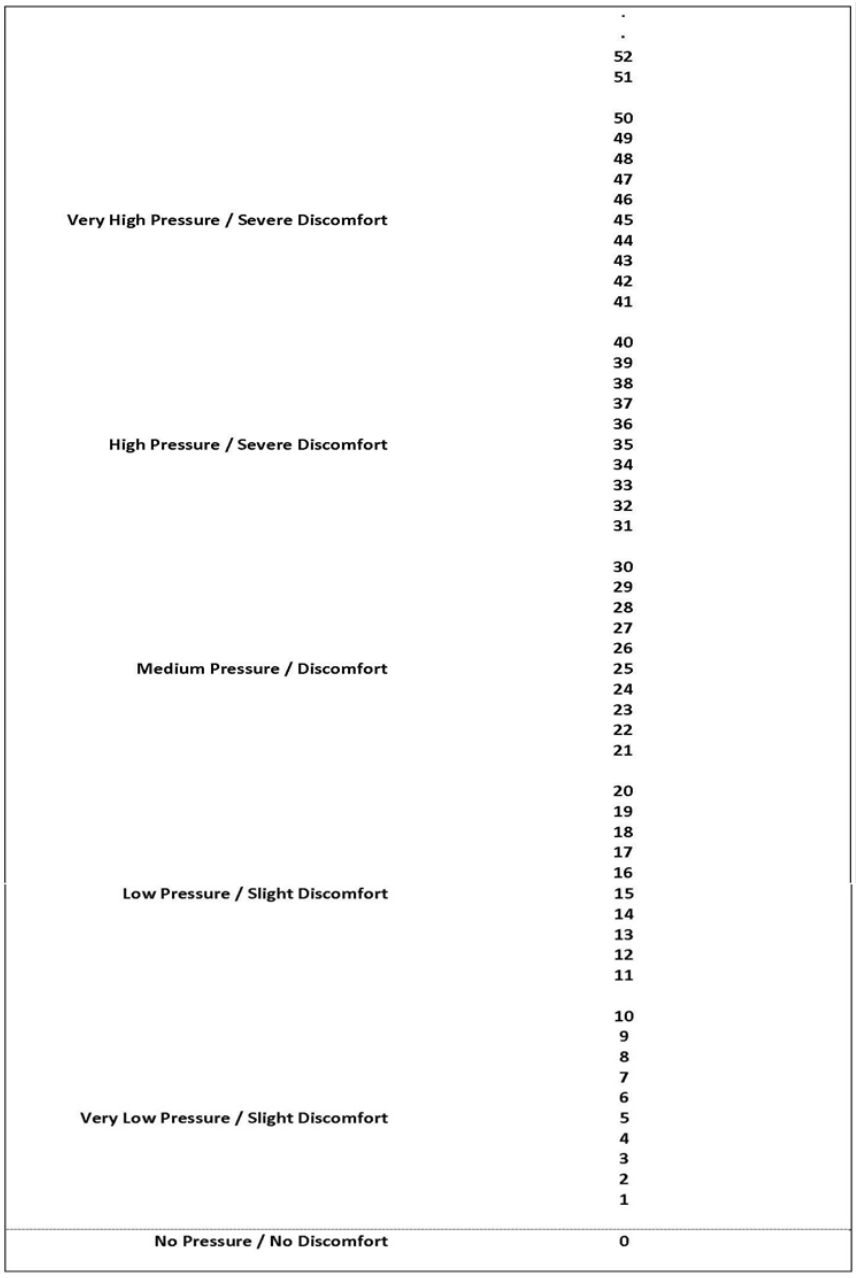

Figure 8. Category Partitioning Scale

Short-Form McGill Pain Questionnaire (MPQ)

The Short-Form McGill Pain Questionnaire (MPQ) is a 17-point questionnaire which evaluates sensory, affective, and current pain intensities.[260] The MPQ demonstrates high overall

reliability[260,266] and has been used to evaluate joint pain,[261,262] nerve pain,[263] and therapeutic intervention effectiveness.[264,265] The questionnaire (Figure 9) consists of eleven sensory dimension descriptors (throbbing, shooting, stabbing, sharp, cramping, gnawing, hot-burning, aching, heavy, tender, and splitting) and four affective dimension descriptors (tiring-exhausting, sickening, fearful, punishing-cruel).[260] Each descriptor is ranked on an intensity scale of 0 = none, 1 = mild, 2 = moderate, and 3 = severe.[260] One visual analogue scale and one present pain intensity question are presented to indicate overall discomfort intensity.[260]

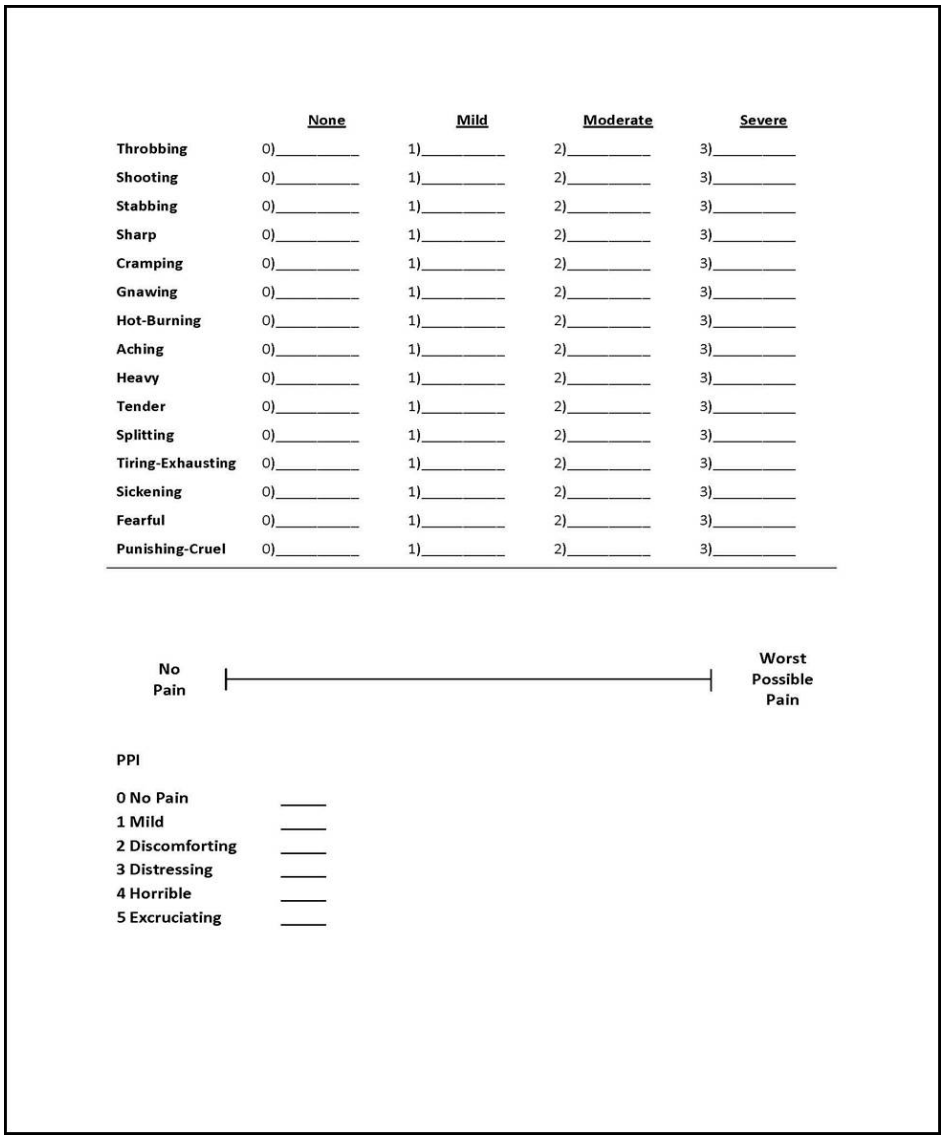

	None	Mild	Moderate	Severe
Throbbing	0)_____	1)_____	2)_____	3)_____
Shooting	0)_____	1)_____	2)_____	3)_____
Stabbing	0)_____	1)_____	2)_____	3)_____
Sharp	0)_____	1)_____	2)_____	3)_____
Cramping	0)_____	1)_____	2)_____	3)_____
Gnawing	0)_____	1)_____	2)_____	3)_____
Hot-Burning	0)_____	1)_____	2)_____	3)_____
Aching	0)_____	1)_____	2)_____	3)_____
Heavy	0)_____	1)_____	2)_____	3)_____
Tender	0)_____	1)_____	2)_____	3)_____
Splitting	0)_____	1)_____	2)_____	3)_____
Tiring-Exhausting	0)_____	1)_____	2)_____	3)_____
Sickening	0)_____	1)_____	2)_____	3)_____
Fearful	0)_____	1)_____	2)_____	3)_____
Punishing-Cruel	0)_____	1)_____	2)_____	3)_____

Figure 9. Short-Form McGill Pain Questionnaire. Adapted from Melzack.[260]

Lower Extremity Sensibility

Semmes-Weinstein Monofilament Test (MFT)

The Semmes-Weinstein Monofilament Test (MFT) (Touch-Test Sensory Evaluator, North Coast Medical Inc., Morgan Hill, CA, USA) is a clinical evaluation tool used to examine a patients sensitivity to a point pressure stimulus.[208] The MFT is comprised of several single

Nylon fibers[209] of varying thickness.[210] Each monofilament thickness is designed to buckle when a specific level of force is applied.[211] The exam was performed with a trained investigator placing the monofilament on the test location until the monofilament begins to buckle.[211] The monofilament was held in place for 1.5 seconds and the examiner instructed the participant to respond "Yes" if the participant felt the monofilament against the skin.[212] The testing sites utilized in this study were the plantar aspect of the great toe, the plantar aspect of the third metatarsal, and the plantar aspect of the fifth metatarsal (Figure 10).[209]

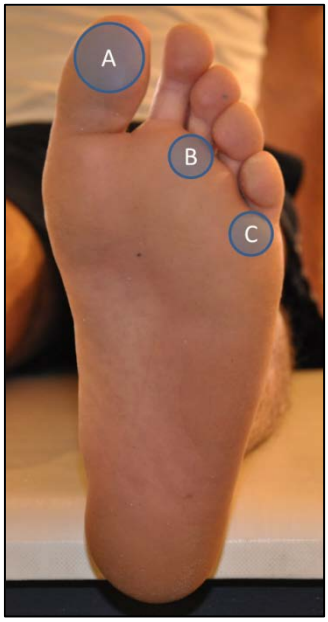

Figure 10. Semmes-Weinstein Monofilament Test locations. A: Great toe; B: Third metatarsal; C: Fifth metatarsal.

Two-Point Discrimination Test (TPDT)

The two-point discrimination test (TPDT) (Disk-Criminator, North Coast Medical Inc., Morgan Hill, CA, USA) is a clinical tool utilized to examine the sensibility and the innervation density within a receptive field on the skin.[192,193] This test measured the ability to distinguish

static dull pressure application from two sources at various distances.[194,195] The smaller the distance, the smaller the receptive field on the patch of skin of interest.[192] The inability to discriminate between two pressure sources indicates that the points are within the same receptive field or that the receptive field sensibility has been diminished.[192,194,196] It has also been utilized to examine changes in sensibility as a result of cryotherapy,[199,200] thermotherapy,[199] vibration stimuli,[201] and orthopedic injury.[202] TPDT scores are extensively collected from the hands[193-196,200,203-205] and feet,[199,201,202,204,206] and testing locations for these examinations occurred at the medial malleolus, lateral malleolus, and plantar of the great toe (Figure 11).[208]

Figure 11. Two-point discrimination test locations. A: Medial malleolus; B: Great toe; C: Lateral malleolus.

Neurological Measures

Hoffmann Reflex (H-reflex)

The Hoffmann Reflex (H-reflex) is a non-invasive measure of α-motoneuron pool excitability. The H-reflex has been used to examine α-motoneuron pool excitability in musculoskeletal injury,[103-114] pain conditions,[115] fatigued conditions,[116,117] during and after therapeutic modality application,[118-125] and during or after exercise training conditions.[126-131]

The functionally dominant leg soleus muscle was chosen for assessment due to its location in the lower leg, importance in operating the pedals during flight, and ease of access in a seated position (Figure 12). The electrode sites for the soleus H-reflex were shaven to remove excess hair, gently abraded to remove dead skin, and cleaned with isopropyl alcohol to improve surface electromyography signals recorded from the muscles of interest.[133] Electrode placement was completed using protocols as previously described (Figure 13).[120,125,133] Disposable adhesive silver/silver chloride (Ag/AgCl) electrodes (EL503, Biopac Systems Inc., Goleta, CA, USA) were placed on the soleus muscle 2 centimeters distal to the belly of the gastrocnemius muscle with an inter-electrode distance of 2 centimeters. A ground electrode (EL 503, Biopac Systems Inc., Goleta, CA, USA) was placed on the ipsilateral medial malleolus. A stimulating electrode (EL 254, Biopac Systems Inc., Goleta, CA, USA) was placed over the posterior tibial nerve in the popliteal fossa of the posterior knee. An 8 centimeter, round dispersal pad was placed above the patella on the ipsilateral quadriceps muscles. A series of 1.0 millisecond square wave stimuli were delivered via transcutaneous stimulation (STMISOC, Biopac Systems Inc., Goleta, CA, USA) at 10 to 20 second intervals while increasing stimulus intensity by 0.2 volts until the soleus maximum H-reflex (H_{max}) and maximum M-wave (M_{max}) were found for each

participant. The test stimulus was normalized to 25 percent of soleus M_{max}.[267] Electromyographic (EMG) data was collected and the signal amplified using an EMG amplifier (EMG100C, Biopac Systems Inc., Goleta, CA, USA). The raw signal was differentially amplified (gain, 1000; common mode rejection ratio, 110dB; input impedance, 1000MΩ; signal noise, 0.2) and digitally converted at 2000Hz.[112] The data were analyzed using AcqKnowledge Software (Biopac Systems Inc., Version 4.0, Goleta, CA, USA). Seven repetitions were completed and averaged for each time point data is collected.[112] During the local pressure application protocols the electrodes, stimulator, and leads all remained in place on the participant and be connected to the data acquisition system.

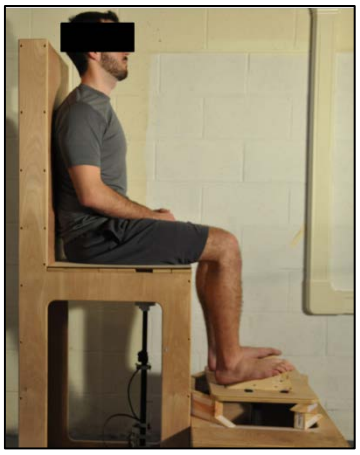

Figure 12. Seated testing position.

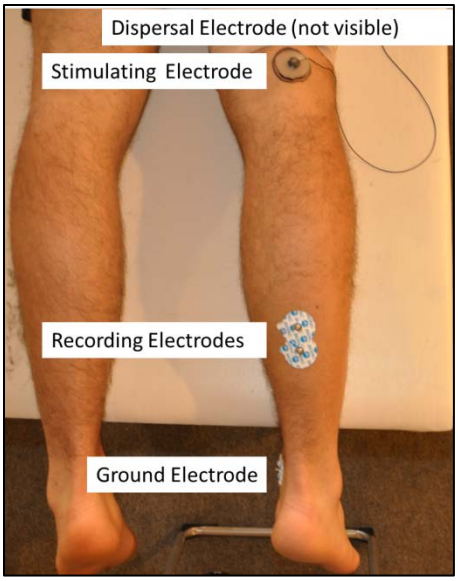

Figure 13. Soleus Hoffmann reflex electrode placement.

Sural Sensory Nerve Conduction Velocity (NCV)

Nerve conduction velocity (NCV) is a clinical and research method for detecting changes in the function of a segment of nerve tissue.[155] NCV is comprised of two components: the amount of time required for an electrical impulse to travel the length of nervous tissue (latency) and the length of the nerve segment of interest.[157] NCV is calculated by dividing the length of the nerve segment of interest by latency.[158] NCV tests are commonly completed in the major nerves of both the upper[159-170] and lower extremities.[171-176]

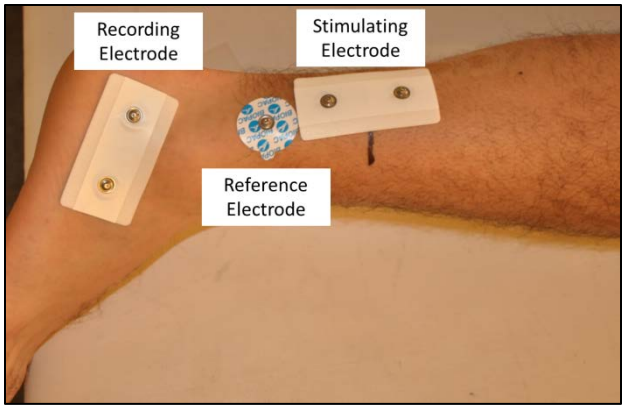

Figure 14. Sural sensory nerve conduction velocity electrode placement.

The functionally dominant leg sural sensory nerve was chosen to collect NCV data because of the role of peripheral nerves in determining correct foot position in helicopters, its easy access in a seated position, and its downstream anatomical location to the local compression sites (Figure 14). The electrode sites were shaven to remove excess hair, gently abraded with fine grit sandpaper to remove dead skin, and cleaned with isopropyl alcohol to improve surface electromyography signals recorded from the sural nerve. Disposable adhesive foam paired electrodes (EL500, Biopac Systems Inc., Goleta, CA, USA) were placed one centimeter posterior and one centimeter inferior to the lateral malleolus and served as the active recording electrodes.[182] A stimulating electrode (EL500, Biopac Systems Inc., Goleta, CA, USA) was placed 14 centimeters from the center of the active recording electrodes. A reference electrode (EL 503, Biopac Systems Inc., Goleta, CA, USA) was placed between the stimulating and recording electrodes.[182] The signal was differentially amplified (gain, 2000; low pass filter, 5kHz; high pass filter, 10Hz; sampling rate, 10,000Hz; input impedance, 1000MΩ; signal noise, 0.2) and digitally converted at 2000Hz. Rectangular electrical pulses 0.1 milliseconds in duration were delivered once every three seconds via transcutaneous stimulation (STMISOC,

Biopac Systems Inc., Goleta, CA, USA) at an intensity sufficient to obtain a sensory response.[182] Five stimulations were delivered at each time point during the local compression protocol. The peak negative potential was measured from the end of the stimulation artifact.[182] The latencies were averaged to obtain the mean sural nerve latency. The sural sensory nerve latency (milliseconds) were converted to NCV (meters/seconds) by taking the stimulating electrode - recording electrode distance (14 centimeters) and dividing it by the sural sensory nerve latency (in milliseconds) The NCV was then standardized by converting centimeters into meters and milliseconds into seconds.

Vascular Measures

Dynamic Infrared Thermography (DIRT)

Dynamic Infrared Thermography (DIRT) uses specialized sensors to measure the electromagnetic radiation emitted from the body[220] to create a map of temperature distribution across a surface, called a thermogram.[219] Recent developments in high resolution thermal imaging have increased the thermal and spatial resolution of the thermograms,[221] and have allowed for the development of portable units.[222] DIRT has been utilized to examine microvascular changes after massage,[227-230] exercise studies,[231-233] and other therapeutic intervention studies.[120,234,235]

Figure 15. Analysis areas for dynamic infrared thermography. A: Anterior ankle; B: Lateral ankle.

A digital infrared camera (FLIR T420, FLIR Systems Inc., Wilsonville, OR, USA) was used to measure non-contact, superficial temperature changes (°C) in the functional dominant lower leg. Anterior and lateral images (Figure 15) were taken at every time point during Project 1, 2, and 3. Ambient room temperature was maintained for all participants. Average temperature values for regions of interest at the anterior and lateral ankle were measured using the Glamorgan Protocol.[268] The anterior ankle region of interest was comprised of the width of the ankle with upper and lower edges at the tip of the medial malleolus and the tip of the navicular bone, respectively.[268] The lateral ankle region of interest included the entire anterior to posterior thickness at the level of the lateral malleolus.[268] The regions of interests were measured and analyzed using FLIR ExaminIR Software (FLIR Systems Inc., Boston, MA, USA).

Pulse Oximetry

Pulse oximetry is a non-invasive tool used to measure arterial blood oxygenation.[241,242] The oximeter unit emits two wavelengths of light, one red and one infrared.[242,244,245] Light travels through the capillary bed of the tissue of interest and is recorded by a photo detector on the other side of the tissue.[245] Oxygenated hemoglobin absorbs more infrared light and is more transparent to red light than deoxygenated hemoglobin.[245] The unit calculates the percentage of oxygenated hemoglobin present in the capillary bed and results are presented in percent oxygen saturation ($Sp0_2$).[245,246]

The pulse oximeter (Nonin Onyx Vantage 9590, Nonin Medical Inc., Plymouth, MN, USA) was secured to the great toe of the functional dominant leg (Figure 16). Percent oxygen saturation was recorded utilizing the spot check method.[245] The spot check method involves applying and removing the pulse oximeter following a short evaluation period (5-10 seconds). This is the common method utilized in ambulatory settings when continuous monitoring may not be feasible or practical. The spot check method was used instead of a continuous measure because access to the great toe is required for other measures. Following the collection of sensibility measures at each data collection time point in all protocols, the pulse oximeter was placed on the great toe, secured with friction, and SpO_2 (%) were recorded following a five second analysis period. The pulse oximeter was removed after every data collection period to accommodate the sensibility measures.

Figure 16. Pulse oximetry test location.

Project 1

Experimental Design

This study utilized a 1 x 9 repeated measures crossover design. The independent variable was time with 9 levels (time = 0, 30, 60, 90, 120, 150, 180, 210, and 240 minutes). The dependent variables were Category Partitioning Scale scores, McGill Pain Questionnaire (descriptor, visual analog scale, and present pain intensity) scores, Semmes-Weinstein monofilament test (great toe, third metatarsal, and fifth metatarsal) scores, two-point discrimination (great toe, medial malleolus, and lateral malleolus) scores, dynamic infrared thermography (lateral lower leg and anterior lower leg) mean temperatures, and pulse oximetry (percent oxygen saturation) levels.

Participants

Sixteen healthy male participants ages 19-30 were recruited for this study. One participant withdrew from the study prior to any data collection, leaving 15 participants for analysis. Participants who participated in Project 1 also participated in Project 2. Participants wore comfortable athletic shorts, tennis shoes, and a t-shirt to the data collection session. Exclusion criteria included a current or two year history of cardiovascular, neurological, or metabolic disease; a current or two year history of surgery or fracture in the lumbar spine or lower extremity; a current history of low back pain or lower extremity injury; or current use of prescription or non-prescription pain relievers. Participants were screened for these exclusion criteria via an 18-point health questionnaire. Participants must also have met minimal body segment lengths measures and minimum/maximum weights required to obtain flight status in the United States Army (Table 1). Prior to all data collection participants provided written informed consent to the experimental protocol approved by the Auburn University Institutional Review Board.

Table 1. United States Army anthropometric minimums required for flight status.

Body Measure	Men
Total Arm Reach, cm	≥ 164.0
Crotch Height, cm	≥ 75.0
Sitting Height, cm	< 102.0
Minimum Weight, kg	45.3
Maximum Weight, kg	107.9

Cognitive Task

During the prolonged restricted sitting protocol in Project 1, a common cognitive task was utilized to diminish participants focusing on discomfort between data collection time points.[3] The task was comprised of a helicopter flight simulation (Take On Helicopters, Bohemia Interactive Inc., Prague, Czech Republic) controlled by a joystick (Logitech Extreme 3D Pro, Logitech Inc., Fremont, CA, USA) and displayed onto a 55 inch light emitting diode television monitor (Samsung ME55A, Samsung America Inc., Ridgefield Park, NJ, USA). Participants completed task "missions" created by the software and selected by the investigator (Figure 17). Mission order remained the same for each participant, however time spent on each mission was not controlled as participants worked through the missions at their own pace. This protocol was similar to others[3,9] examining prolonged restricted sitting.

Figure 17. Flight simulator cognitive task.

Experimental Procedures

Participants reported to the Neuromechanics Research Laboratory for all testing procedures. Following completion of the informed consent, participants were screened for exclusion criteria and had their height, weight, and body segment lengths measured and recorded. Functional leg dominance, hip flexibility, and Design Eye Point knee sitting angle were then be determined and recorded.

Functional Leg Dominance

Functional leg dominance was determined by three functional tests: ball kick test, step up test, and balance recovery test.[269,270] Three trials of each test were completed. The leg used by the participant in 2 out of the 3 trials was identified as the dominant leg for the test. The balance recovery test was only used if functional leg dominance had not been determined by the step up test and the ball kick test.

For the ball kick test, the participant was asked to kick a standard kick ball (8.5" Poly-PG Ball, School Specialty Sportime, Appleton, WI, USA) at a target on the wall 5 meters from the participant at a moderate intensity with maximal accuracy.[269,270] The leg used to kick the ball was identified as the dominant leg for the trial. Successfully kicking the ball near the target was not a criterion for this test.[269,270] During the step up test, the participant was asked to step up onto a 20 centimeter high step.[269,270] The leg used to step onto the step was determined the dominant leg for each trial. For the balance recovery test, the investigator gently nudged the subject by applying force on the spine at the midscapular level.[269,270] Prior to the push, the participant was notified that a push is about to occur. The amplitude of the force used was sufficient to create a response from the subject. The leg used to recover balance was marked as the dominant leg. The sequence of the tests was the same for all participants.

Hip Flexibility

Hip flexibility were measured for the hip extensor muscles (gluteus maximus, semitendinosus, semimembranosus, and biceps femoris),[271] hip flexor muscles (psoas major, illiacus, and rectus femoris),[271] and the external rotator muscles (piriformis, obturator externus, obturator internus, quadrates femoris, gemmelus superior, gemellus inferior, and gluteus maximus).[271] All flexibility measures were taken with a standard, manual goniometer (12.5" International Standard Goniometer, Patterson Medical Holdings Inc., Bolingbrook, IL, USA) and in accordance with standard procedures.[272,273] Reference values originally collected by Hoppenfeld[272] were used to determine normal range of motion limits. All measures took place on a firm examination table. To measure hip extensor flexibility, participants laid on their back

and were asked to relax while the investigator slowly stretched the lower extremity of the participant in a straight leg position. The stretch was applied until the first resistance was felt. A second investigator measured the hip flexion angle using a manual goniometer. To measure hip flexor flexibility, the Thomas test was used. Participants pulled one leg towards their chest and "roll" onto the examination table, relaxing the leg to be measured. The participant was asked to flatten the lower back against the table to minimize the lordotic curve. Once the position was achieved, the hip extension angle was measured. To measure hip external rotation, the participant laid prone on the examination table with one knee flexed at 90 degrees. The participant was passively moved into external rotation and pressure applied until first resistance felt. The external rotation angle was then measured. Each measure was repeated three times and averaged for each leg.

Design Eye Point Sitting Knee Angle

The Design Eye Point is the position in United States Army aircraft in which aviator vision and access to equipment is optimized.[274] The Army has developed protocols for each aircraft to find the Design Eye Point.[274] In this study the Design Eye Point for the UH-60 Black Hawk helicopter was used as a UH-60 Black Hawk pilot seat was used in Project 1. To determine the Design Eye Point, participants sat and were secured in a UH-60 mock cockpit. The seat rested on a one meter high platform to simulate the sitting height in the UH-60. A blue plastic ball placed on the floor twelve feet from the platform served as the focus point (Figure 18). Participants were asked to adjust the seat height and distance from the pedals until they could clearly see the top of the ball. Participants were asked to place their feet on the "pedals"

and the knee angle of the dominant leg was measured by an investigator with a goniometer (12.5" International Standard Goniometer, Patterson Medical Holdings Inc., Bolingbrook, IL, USA). The knee angle was measured three times and averaged to determine the Design Eye Point knee sitting angle. This angle was recreated during the testing protocols for Projects 1 and 2.

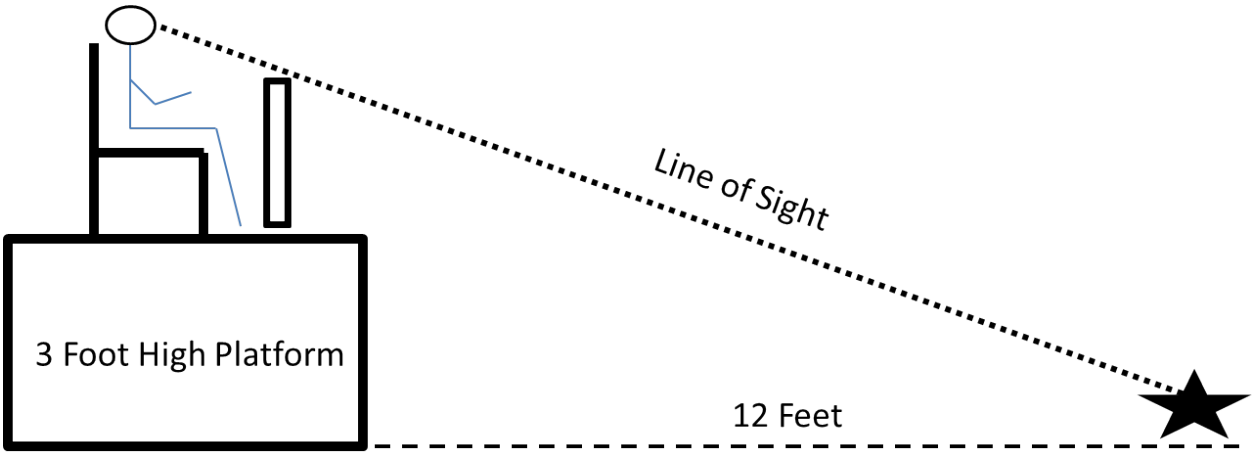

Figure 18. Design Eye-Point participant positioning.

Seat Interface Pressure

Seat interface pressure is a measure of the contact pressure between two surfaces.[275] This is assessed by placing the pressure sensors between the two surfaces of interest (e.g. a buttock and a chair). The pressure sensors produce a two- or three-dimensional image of areas of high and low interface pressures.[275] This technology has been used in previous military research examining seat interface pressure within United States Air Force aircraft seats.[3] However, the reliability of the absolute quantitative pressures has not been fully evaluated and may not be appropriate for quantitative analysis. The output in this study provided a colored pressure map

which allowed investigators to determine areas of high pressure and to confirm relative "hot spots" for Projects 2 and 3.

During Project 1, we examined seat interface pressure with a commercially available pressure mapping system (X2 Pressure Imaging System, XSENSOR Technology Inc., Calgary, Alberta, Canada). Prior to the start of the study, the pressure mapping system was calibrated using the manufacturer's calibration recommendations. Due to questions regarding the reliability of the absolute quantitative pressure recordings, the seat interface pressure data were used to monitor relative, qualitative changes in overall pressure distribution.

Prolonged Restricted Sitting Protocol

After preliminary data collection participants started the prolonged restricted sitting protocol. Prior to the start of the protocol, participants were encouraged to use the restroom to minimize ending the data collection session early. Participants sat barefoot in the UH-60 pilot seat and investigators replicated the Design Eye Point seat position and knee sitting angle from the preliminary data collection. The pressure mapping system was secured to the seat pan of the UH-60 seat prior to the participant sitting in order to record pressure seat pressure data (Figure 19). Once the participant was correctly positioned, the pressure mapping system began recording seat interface pressure data at a frequency of 1 Hertz. Baseline data collection began after a 6 minute settling period.[3] The order of data collection was as followed: Category Partitioning Scale, McGill Pain Questionnaire, dynamic infrared thermography, Semmes-Weinstein monofilament test, two-point discrimination test, and pulse oximetry. The data was collected as described above and recorded using a tablet computer (iPad2, Apple Inc., Cupertino,

CA, USA) onto custom electronic data collection sheets (Quickoffice Pro HD for iPad, Google Inc., Mountain View, CA, USA). An individual, paper McGill Pain Questionnaire was completed by the participant for each data collection time point. Data collection was repeated every 30 minutes for the entire 240 minute protocol or until a CP-50 score of 45 is reached. The limit of a CP-50 score of 45 was chosen to minimize participant exposure to high levels of discomfort. Participants did not have knowledge of this pre-determined stoppage point. Data collection order remained the same for all data collection time points and for all participants.

Figure 19. Seat interface pressure mapping system. 1: Black Hawk seat without mapping system; 2: Pressure mapping system; 3: Pilot's seat and mapping system integrated.

Statistical Analysis

Data were collected with a tablet computer (iPad2, Apple Inc., Cupertino, CA, USA), electronically transferred into a custom database (Microsoft Excel 2010, Microsoft Corp., Redmond, WA, USA), and analyzed using Statistical Package for Social Sciences version 19 (IBM SPSS Statistics 19, IBM Corp., Somers, NY, USA). Descriptive statistics (mean ± SD)

were calculated. Thirteen, 1 x 9 (treatment x time) repeated measures ANOVAs and follow-up dependent *t*-tests with Holm's sequential Bonferroni adjustments were performed. Significance levels were set *a priori* at $p \leq 0.05$.

Project 2

Experimental Design

This study utilized a 2 x 2 x 2 factorial repeated measures crossover design. The independent variables were location with two levels (ischial tuberosity and posterior thigh), pressure magnitude with two levels (36 kilopascals and 44 kilopascals), and time with two levels (pre-pressure and during pressure). The dependent variables were Category Partitioning Scale scores, McGill Pain Questionnaire (descriptor, visual analog scale, and present pain intensity) scores, Semmes-Weinstein monofilament test (great toe, third metatarsal, and fifth metatarsal) scores, two-point discrimination (great toe, medial malleolus, and lateral malleolus) scores, dynamic infrared thermography (lateral lower leg and anterior lower leg) mean temperatures, and pulse oximetry (percent oxygen saturation) levels.

Local Pressure Application Apparatus (LPAAP)

A purpose-built LPAAP was used to apply pressures of 36 kilopascals and 44 kilopascals to the ischial tuberosity and posterior thigh of participants in a seated position. The apparatus consisted of: the pressure application system (Figure 20), the seat pan (Figure 21), and the foot rest (Figure 22). The pressure application system consisted of a step motor secured to an

extendable metal rod and load cell with a custom-built, round pressure application head 25.5176 centimeters squared in area. The unit was controlled by custom-written computer software and operated through a laptop computer (Dell Latitude D430, Dell Inc., Round Rock, TX, USA). The seat was built of wood and consists of an 80.10 x 55.88 centimeter (height x width) seat back and a 50.80 x 55.88 centimeter (depth x width) seat pan. The seat pan is comprised of 14 removable slats which allow the pressure application head to apply pressure to the area of interest while still supporting the participant (Figure 23). The foot rest is a 91.44 x 50.80 x 35.56 centimeter (length x width x height) box with an adjustable crank lift to accommodate participants of different heights.

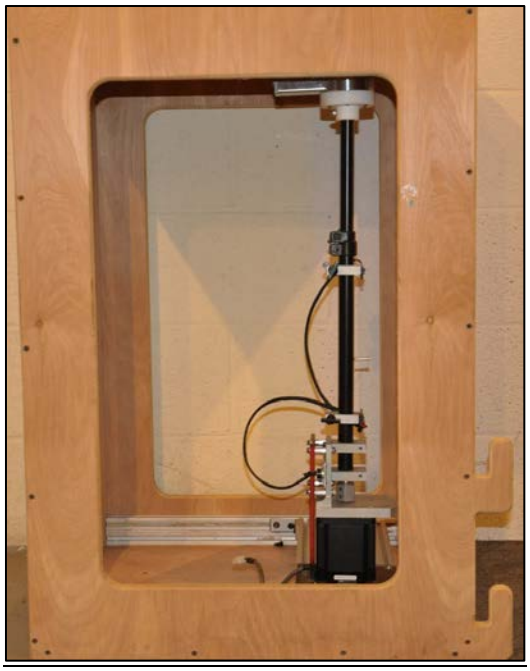

Figure 20. Pressure application mechanism under seat pan.

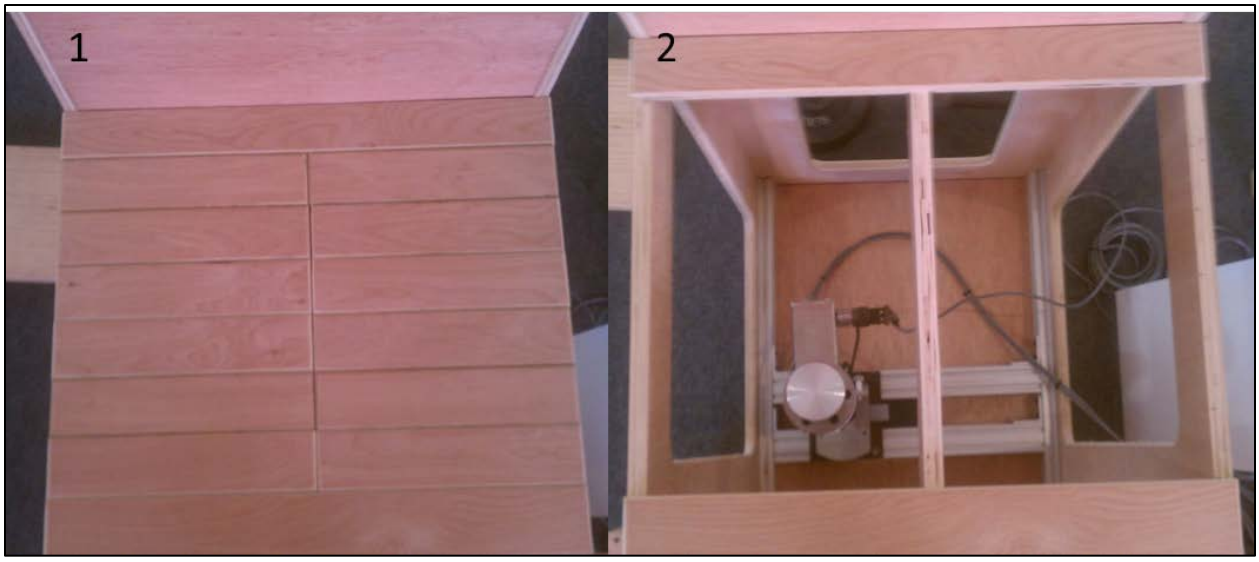

Figure 21. Seat pan of local pressure application apparatus. 1: All slats in place; 2: All slats removed.

Figure 22. Local pressure application apparatus foot rest.

Figure 23. Seat pan prepared for posterior thigh pressure application.

Determination of Anatomical Locations

Local pressure was applied to the ischial tuberosity and the mid-point of the posterior thigh on the dominant lower extremity of participants. These locations were chosen based on the underlying anatomy, results from Project 1's pressure mapping system, and previous research.[85] The ischial tuberosity was palpated and marked with adhesive tape. The mid-point of the posterior thigh was defined as the distance from the greater trochanter to the lateral epicondyle between the medial and lateral edges of the posterior thigh. The distance between the greater trochanter and the lateral epicondyle (both determined by palpation) was measured using a fabric tape measure (Medco Tape Measure, Patterson Medical Holdings Inc., Bolingbrook, IL, USA). The distance was rounded to the nearest half centimeter and using permanent marker. The distance between the medial and lateral borders of the thigh was then measured in the same manner from the permanent marker used to demarcate the mid-point of the femur along its long

axis. This point was marked with permanent marker and served as the location for posterior thigh pressure application. Prior to local pressure application, these locations were visually confirmed in the LPAAP. In the case of the ischial tuberosity, verbal confirmation from the participant was also be elicited.

Local Pressure Application Protocol for Project 2

Sessions were grouped based on pressure magnitude level and randomized using a random number generator (TI-83 Plus, Texas Instruments Inc., Dallas, TX, USA). Within each session, location order was also randomized using a random number generator. Participants reported to the Neuromechanics Research Laboratory on two separate occasions with a minimum of 24 hours between data collection sessions. Since participants were the same as in Project 1, a minimum of 24 hours between the end of Project 1 and Project 2 was required. During session one, participants had the two locations measured and marked as described above on the functionally dominant leg (determined during Project 1). Once marked, participants sat on the pressure application chair barefoot with the appropriate slats removed and pressure application head correctly positioned. The participant was asked to sit upright and as far back in the chair as possible. The foot rest was adjusted to the appropriate height and participants' knees will be positioned at the Design Eye Point sitting knee angle (determined in Project 1). Following positioning, baseline measures of Category Partitioning Scale, McGill Pain Questionnaire, dynamic infrared thermography, Semmes-Weinstein monofilament, two-point discrimination, and pulse oximetry were taken. Local pressure was applied at the specified amplitude (36 kilopascals or 44 kilopascals) for a total of minutes. During the pressure application the

magnitude of the pressure was maintained within 5% of the set value. The participant and application pressure were continuously monitored by the investigators and regular feedback was solicited to ensure the participant was not experiencing any adverse events. At seven minutes into the pressure application protocol, follow-up measures began. Starting data collection at seven minutes allowed the entire data collection to occur with local pressure applied to the location of interest. The order of measure data acquisition remained the same for each session and for each participant. Following 10 minutes of pressure application the pressure was removed and the participant was helped by a trained investigator. The participant was then given a 15 minute break and allowed to move around the laboratory. This 15 minute break allowed time for participants to recover from any numbness or tingling which may have occurred during testing and allowed time for the investigators to reposition the pressure application head to the next pressure application location. Fifteen minutes was determined to be a sufficient time to recover from possible residual effects of temporary parathesia through pilot work which found that no pilot participants reported symptoms of parathesia including numbness, tingling, loss of strength, or lose of sensation. After 15 minutes, the participant was asked to again sit in the pressure application seat. The Design Eye Point knee sitting angle and visual confirmation of pressure application were again completed. Once in position, the participant was secured and the local pressure application protocol was repeated on the untested location at the same pressure magnitude. During session two, this protocol was repeated at the remaining pressure application magnitude (36 kilopascals or 44 kilopascals).

Statistical Analysis

Data were collected with a tablet computer (iPad2, Apple Inc., Cupertino, CA, USA), electronically transferred into a custom database (Microsoft Excel 2010, Microsoft Corp., Redmond, WA, USA), and analyzed using Statistical Package for Social Sciences version 19 (IBM SPSS Statistics 19, IBM Corp., Somers, NY, USA). Descriptive statistics (mean ± SD) were calculated. Thirteen, 2 x 2 x 2 (magnitude x location x time) factorial repeated measures ANOVAs were performed. Appropriate follow-up tests were completed dependent on significant interaction and main effects. Significance levels will be set *a priori* at $p \leq 0.05$.

Project 3

Experimental Design

This study utilized a 3 x 5 factorial repeated measures design. The independent variables were location with three levels (ischial tuberosity, posterior thigh, and control) and time with five levels (pre-application, 5 minutes into-application, 10 minutes into-application, 5 minutes post-application, and 10 minutes post-application). The dependent variables were Category Partitioning Scale scores, McGill Pain Questionnaire (descriptor, visual analog scale, and present pain intensity) scores, Semmes-Weinstein monofilament test (great toe, third metatarsal, and fifth metatarsal) scores, two-point discrimination (great toe, medial malleolus, and lateral malleolus) scores, dynamic infrared thermography (lateral lower leg and anterior lower leg) mean temperatures, pulse oximetry (percent oxygen saturation) levels, soleus H-reflex (mean peak-to-peak amplitude), and sural sensory nerve conduction velocity. A pressure magnitude of 44 kilopascals was applied. Additionally, body composition data was collected utilizing dual-

energy x-ray absorptiometry (DXA) to examine the relationship between reported discomfort, sensibility, physiological measures, and body composition.

Dual-Energy X-Ray Absorptiometry (DXA)

Body composition was assessed in participants using DXA (Lunar Prodigy Advance, GE Healthcare Inc., Waukesha, WI, USA). DXA delivers very low-level x-rays through the body to determine the amount of fat mass, lean mass, and bone density in a minimally invasive manner.[276,277] Participants underwent a single DXA scan for this study. The total percent fat mass was determined and recorded with scanner specific software (enCore version 9.1, GE Healthcare Inc., Waukesha, WI, USA).

Participants

Thirty healthy male participants ages 19-30 were recruited for this study. At every data collection session, participants wore athletic shorts, tennis shoes, and a t-shirt. Exclusion criteria included a current or two year history of cardiovascular, neurological, or metabolic disease; a current or two year history of surgery or fracture in the lumbar spine or lower extremity; a current history of low back pain or lower extremity injury; or current use of prescription or non-prescription pain relievers. Participants were screened for the exclusion criteria using an 18-point health questionnaire. Participants met minimal body segment lengths measures and minimum/maximum weights required to obtain flight status in the United States Army. Prior to data collection participants completed an informed consent approved by the Auburn University

Institutional Review Board and the United States Army Medical Research and Materials Command Institutional Review Board.

Local Pressure Application Protocol for Project 3

Participants reported to the Neuromechanics Research Laboratory on three separate occasions with a minimum of 24 hours between data collection sessions. Sessions were randomized using a random number generator (TI-83 Plus, Texas Instruments Inc., Dallas, TX, USA). Functional leg dominance, height, weight, Design Eye Point knee angle, and DXA were completed as described above during the first session. Participants were exposed to the same pressure magnitude (44 kilopascals) at both locations for the pressure application sessions. During the control session participants sat in the LPAAP with no pressure applied.

Participants removed their shoes and had electrodes placed on the dominant leg as described above. With the assistance of two investigators, participants were transferred from an examination table to the LPAAP. Once seated, the anatomical locations of interest were visually confirmed and the pressure application head was adjusted accordingly. The foot rest was adjusted and feet placed on mock pedals to recreate the previously determined Design Eye Point sitting knee angle. A 15 minute rest period to diminish the influence of the investigators touching the skin on superficial skin temperature then occurred. The 15 minute rest period was necessary to dissipate any heat transferred from the investigators to the participant. It also served as adequate time to determine the maximal Hoffmann reflex amplitude, maximal muscle wave amplitude, and test stimulus of 25% maximal muscle wave amplitude. Baseline measures will then be taken. The order of data collection was Category Partitioning Scale, McGill Pain

Questionnaire, dynamic infrared thermography, H-reflex, sural sensory nerve conduction velocity, Semmes-Weinstein monofilament, two-point discrimination, and pulse oximetry. This order was chosen to maximize data collection efficiency. The order of dependent variable acquisition remained the same for all data collection time points and across all participants. The pressure application was then applied at the appropriate location for 10 minutes. Data collections were repeated at 5 minutes and 10 minutes into pressure application and 5 minutes and 10 minutes following pressure application removal. Total data collection time was 20 minutes. Following data collection participants were asked to carefully stand and step off of the LPAAP, return to the examination table, have the electrodes removed, and scheduled for the next data collection session no less than 24 hours from the start of the current session. The second pressure application session followed the same procedures at the untested location. The no pressure (control) session followed the same procedure; however no pressured was applied.

Statistical Analysis

Data were collected electronically with a tablet computer (iPad2, Apple Inc., Cupertino, CA, USA). transferred into a custom database (Microsoft Excel 2010, Microsoft Corp., Redmond, WA, USA), and analyzed using Statistical Package for Social Sciences version 19 (IBM SPSS Statistics 19, IBM Corp., Somers, NY, USA). Descriptive statistics (mean ± SD) were calculated. Fifteen, 3 x 5 (location x time) factorial repeated measures ANOVAs were performed. Appropriate follow-up tests were completed dependent on significant interaction and main effects. Significance levels were set *a priori* at $p \leq 0.05$.

Chapter IV

Effects of Prolonged Restricted Sitting in UH-60 Black Hawk Helicopters

Introduction

Seat discomfort is a major concern for today's UH-60 Black Hawk helicopter aviators. Approximately 82% of rotary-winged aviators report experiencing discomfort during flight.[4] The Black Hawk helicopter originally had a maximum flight time of 2.3 hours before the aircraft required refueling.[7] Advances in fuel and engine technology as well as the utilization of "hot-refueling" (refueling while engines are operational and rotors engaged) and in some instances, in-air refueling all have increased the total flight time and average mission length of United States Army Black Hawk Aviators. During the mid-1990's United States Army rotary-winged Aviators regularly spent six hours at their crew station within the helicopter.[11] The recent conflicts in Iraq and Afghanistan have required aviators to frequently fly multiple, long duration missions. Anecdotal reports from Iraq War Black Hawk Aviators indicate that mission lengths of eight or more hours were not unusual. Interviews with aviators flying during Operation Iraqi Freedom and Operation Enduring Freedom reveal that mission lengths of 6-12 hours are regularly required.[278] Advances in flight technology have allowed rotary-winged aircraft to operate for extended periods of time without prolonged down time, but human factors currently limit the flight time capabilities of the Black Hawk helicopter.[279] A primary limiting human factor is prolonged restricted sitting by pilots.

Investigations into prolonged restricted sitting and seat discomfort in Black Hawk helicopters are limited. The pilot's seat was designed to improve crashworthiness while allowing aviators to access and operate the aircraft effectively.[13] To date, no studies examining the effects of prolonged restricted sitting in Black Hawk helicopters have been completed; however investigations examining other rotary-winged aircraft, fixed-wing aircraft and civilian aircraft may yield insight into prolonged restricted sitting in Black Hawk helicopters.

Much of the work completed in rotary-winged aircraft has focused on vibration attenuation during flight.[12-14,280] Exposure to vibration from the rotors of the helicopter has been demonstrated to produce adverse health effects such as spine pain and spinal musculature injuries.[281,282] Experimental vibration attenuation devices within the seat systems of rotary-winged aircraft have been shown to reduce vertical vibration levels from 25%-38% and anterior-posterior vibration levels from 17% to 85% at certain points along the vibration spectrum (2Hz/rev of the rotor blades and 4Hz/rev of the rotor blades, respectively).[13,14] However, this work does not address the problems of discomfort and temporary parathesia observed as a result of prolonged restricted sitting in rotary-winged aircraft.

Several studies have addressed the symptoms of discomfort and temporary parathesia in both military[1,3,9,11] and civilian aircraft.[15] Prolonged restricted sitting in aircraft results in higher levels of reported subjective discomfort,[3,9,15] high levels of seat interface pressure,[3,9,15] and increased trapezius muscle fatigue.[3] However, many of these studies utilized fixed-wing aircraft and the results may not be transferrable to rotary-winged aircraft. A study testing alternative seat pads for United States Army AH-64 Apache helicopters found that aviator subjective discomfort is reduced with air-filled or foam-filled seat cushions compared to a standard AH-64 seat cushion.[11] While this work aids our understanding of aviator seat cushion preference, the short

testing time used (1 hour) does not address the effects of prolonged restricted sitting on symptoms of discomfort and temporary parathesia in rotary-winged aviators.

The majority of the aviator discomfort studies utilize subjective discomfort scales.[3,9,11,15] Few studies have utilized more objective measures such seat interface pressure,[3,9,15] electromyography,[3] or near infrared spectroscopy.[3] More physiological or clinical measures may add insight to our understanding of aviator discomfort and temporary parathesia during prolonged restricted sitting. The Semmes-Weinstein monofilament test and the two-point discrimination test could add insight regarding the sensory nervous systems response to prolonged restricted sitting. Superficial blood flow changes could be measured using dynamic infrared thermography and limb oxygen saturation could be measured using portable pulse oximetry. Utilizing tools and measures beyond subjective discomfort scales and interface pressures could allow for a better understanding of the negative effects reported during prolonged restricted sitting.

Advances in flight technology and refueling options, paired with our limited knowledge regarding the neurological and vascular changes associated with prolonged sitting in rotary-winged aircraft suggest that measures beyond the traditional subject questionnaires are required to understand the development of the symptoms of discomfort and temporary parathesia during rotary-winged flight. Therefore, the purpose of this investigation is to examine the effects of a four hour bout of restricted sitting in a Black Hawk helicopter pilot seat on subjective discomfort, sensibility, lower extremity blood oxygenation, and lower extremity superficial skin temperature.

Methods

Experimental Design

This study utilized a 1 x 9 repeated measures crossover design. The independent variable was time with 9 levels (time = 0, 30, 60, 90, 120, 150, 180, 210, and 240 minutes). The dependent variables were Category Partitioning Scale scores, McGill Pain Questionnaire (descriptor, visual analog scale, and present pain intensity) scores, Semmes-Weinstein monofilament test (great toe, third metatarsal, and fifth metatarsal) scores, two-point discrimination (great toe, medial malleolus, and lateral malleolus) scores, dynamic infrared thermography (lateral lower leg and anterior lower leg) mean temperatures, and pulse oximetry (percent oxygen saturation) levels.

Participants

Sixteen male volunteers responded to the solicitation (flyers and group presentations) to participate in the study. Fifteen healthy male participants (age = 23.4 ± 3.1 years) completed the study (one did not attend the data collection session and no data was collected). Participants met minimal body segments length measures and minimum/maximum weights required to obtain flight status in the United States Army (Table 2). Participants self-reported no history of cardiovascular, neurological, or metabolic disease in the past two years; no current or two year history of surgery or fracture in the lumbar spine or lower extremity; no current history of low back pain or lower extremity injury; and no current use of prescription or non-prescription pain relievers. Participants were screened via an 18-point health questionnaire administered by an

allied health profession and signed a written consent. The study was approved by the University's Institutional Review Board.

Table 2. United States Army anthropometric flight status requirements.

Body Measure	Men
Total Arm Reach, cm	≥ 164.0
Crotch Height, cm	≥ 75.0
Sitting Height, cm	< 102.0
Minimum Weight, kg	45.3
Maximum Weight, kg	107.9

Experimental Procedures

Participants reported to the laboratory one time to complete data collection. During the session, functional leg dominance was determined using three tests: the step up test, the ball kick test, and the balance recovery test.[270] Investigators then recorded the anthropometric measures of arm length, crotch height, sitting height, height, and weight from the participants to ensure all Army flight status requirements in these areas were met. Participants next had lower extremity flexibility measures of hip flexion, hip extension, and hip external rotation collected along with sit-and-reach scores.

For all data collection, participants sat and were secured to an unpadded UH-60 Black Hawk helicopter pilot's seat (Armored Crashworthy UH-60A, Ara Inc., Industry, CA, USA). The seat structure was secured to a 1 meter high wooden platform equipped with wooden foot pedals, a cyclic joystick, and 0.85 meter dashboard screen to replicate a UH-60 Black Hawk cockpit. To reproduce pilot sitting postures in the UH-60 helicopter, Design Eye Point knee sitting angles were collected using a goniometer (12.5" International Standard Goniometer, Patterson Medical Holdings Inc., Bolingbrook, IL, USA) and recorded using standard United States Army Design Eye Point procedures.[274] The Design Eye Point is a position in which aviators vision and access to equipment are optimized.[274] This position is created by positioning the seat at a location in which the aviator can see an object placed on the ground 12-15 feet in front of the aircraft (Figure 24).[274] This knee angle was recreated by passively moving the participants' knees prior to the start of data collection and following each data collection time point. Data was collected at baseline and every 30 minutes for 240 minutes (4 hours) or until a Category Partitioning Score of 45 was reached (to minimize participants' exposures to painful stimuli). Participants had no knowledge of this cut-off. Between each time point, participants completed the cognitive task of flying a helicopter using a flight simulator.

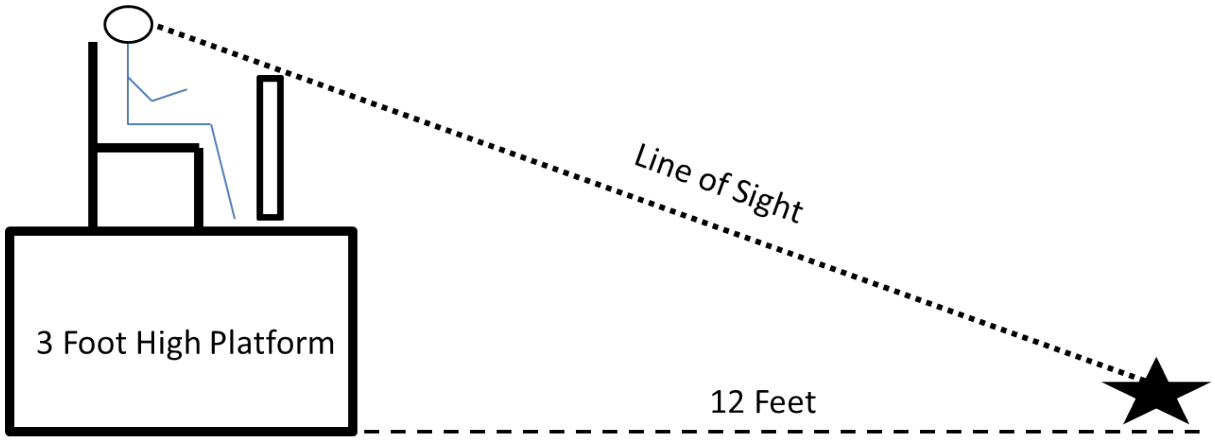

Figure 24. Design Eye Point participant positioning.

Cognitive Task

A common cognitive task was utilized to minimize the participants focus on the discomfort between data collection time points.[3] During the task participants controlled a helicopter flight simulation computer program comprised of helicopter flight simulation software (Take On Helicopters, Bohemia Interactive Inc., Prague, Czech Republic) controlled by a joystick (Logitech Extreme 3D Pro, Logitech Inc., Fremont, CA, USA) and displayed onto a 55 inch light emitting diode television monitor (Samsung ME55A, Samsung America Inc., Ridgefield Park, NJ, USA). Participants completed task "missions" created by the software. Mission order remained the same for each participant; however, time spent on each mission was not controlled and participants completed the missions at their own pace. This protocol is similar to other studies[3,9] examining prolonged restricted sitting in vehicles.

Prolonged Sitting Protocol

Participants were positioned in the UH-60 Black Hawk pilot's chair with their feet resting on wooden pedals and knees at the knee angle determined during the Design Eye Point assessment. Participants were instructed not to flex or extend their knees once positioned. Participants wore athletic shorts, a t-shirt, and no shoes or socks for the data collection in order to access measurement locations. Once positioned, the dashboard screen was also removed to allow for the measurements to be completed. Baseline data collection was initiated following a six minute sitting pressure mapping system equilibration period. The Design Eye Point sitting angle was repositioned following every data collection to eliminate knee angle changes as a result of data collection.

Discomfort Measures

Category Partitioning Scale

The Category-Partitioning Scale was utilized to examine the perception of local pressure intensity levels and discomfort.[256,257] The tool consists of a vertical scale starting at zero and is divided into five categories: "very slight," "slight," "medium," "severe," and "very severe."[257,258] Each category is further divided into 10 scale points for a total range of 0 – 50, with numbers above fifty provided to avoid the ceiling effect in the case of extreme pain or discomfort.[257] Participants were instructed to rate their discomfort in one of the five categories, then asked to "fine tune" their discomfort rating using the numerical scale points.[257] The numerical data were recorded with a tablet computer (iPad 2, Apple Inc., Cupertino, CA, USA) and entered into an electronic data collection sheet (Quickoffice Pro HD for iPad, Google Inc., Mountain View, CA, USA).

Short-Form McGill Pain Questionnaire (MPQ)

The 17-point Short-Form McGill Pain Questionnaire (MPQ) was used to evaluate the sensory, affective, and current pain intensities.[260] The questionnaire consisted of eleven sensory dimension descriptors and four affective dimension descriptors .[260] Each descriptor is ranked on an intensity scale of 0 = none, 1 = mild, 2 = moderate, and 3 = severe.[260] One 10 centimeter visual analogue scale and one Present Pain Intensity question were also presented as part of the MPQ to indicate overall discomfort intensity.[260] A paper version of the questionnaire was handed to the participant at every data collection time point and the numerical scores were then

entered into an electronic spreadsheet (Microsoft Excel 2010, Microsoft Corp., Redmond, WA, USA) for analysis.

Sensory Measures

Semmes-Weinstein Monofilament Test (MFT)

Point pressure stimuli sensitivity was evaluated using the Semmes-Weinstein Monofilament Test (MFT) (Touch-Test Sensory Evaluator, North Coast Medical Inc., Morgan Hill, CA, USA).[208] The MFT was comprised of several single Nylon fibers[209] of varying thickness.[210] The monofilament was held in place for 1.5 seconds and the examiner instructed the participant to respond "Yes" when asked if the participant felt the monofilament against the skin.[212] Locations for measurement included the plantar aspect of the great toe, the plantar aspect of the third metatarsal, and the plantar aspect of the fifth metatarsal of the dominant foot of participants.[209] The last correctly reported monofilament thickness was recorded with a tablet computer (iPad 2, Apple Inc., Cupertino, CA, USA) and entered into an electronic data collection sheet (Quickoffice Pro HD for iPad, Google Inc., Mountain View, CA, USA).

Two-Point Discrimination Test (TPDT)

Lower extremity receptive field sensitivity was measured with the two-point discrimination test (TPDT) (Disk-Criminator, North Coast Medical Inc., Morgan Hill, CA, USA).[192,193] The TPDT was comprised of dull point calipers with inter-point distances ranging from 2 to 15 millimeters.[194,195] The calipers were placed on the testing locations for 1.5 seconds

and the participant was instructed to verbally indicate if one or two points were in contact with the skin. To discourage participants from guessing the number of points, single and double pin points were interchanged randomly. Testing locations included the planar surface of the great toe, the medial malleolus, and the lateral malleolus of the dominant lower leg of participants.[208] The last correctly reported inter-point distance was recorded with a tablet computer (iPad 2, Apple Inc., Cupertino, CA, USA) and entered into an electronic data collection sheet (Quickoffice Pro HD for iPad, Google Inc., Mountain View, CA, USA).

Circulatory Measures

Dynamic Infrared Thermography (DIRT)

A digital infrared camera (FLIR T420, FLIR Systems Inc., Wilsonville, OR, USA) was used to measure non-contact, superficial temperatures (°C) in the lower leg. Anterior and lateral infrared images were taken 1 meter from the dominant leg of participants. The mean temperature of the anterior and lateral ankle was analyzed using the mean temperature function (FLIR ExaminIR, version 1.40.12.44). Average temperature values for regions of interest at the anterior and lateral ankle were measured using the Glamorgan Protocol.[268] The anterior ankle region of interest was comprised of the width of the ankle with upper and lower edges at the tip of the medial malleolus and the tip of the navicular bone, respectively.[268] The lateral ankle region of interest included the entire anterior to posterior thickness at the level of the lateral malleolus.[268]

Pulse Oximetry

A pulse oximeter (Nonin Onyx Vantage 9590, Nonin Medical Inc., Plymouth, MN, USA) was secured with friction to the great toe of the dominant leg. Percent oxygen saturation was recorded utilizing the spot check method.[245] This method was used to allow access to the great toe for other measures. Following a five second analysis period, percent blood oxygen ($\%SpO_2$) was recorded to an electronic spreadsheet (Microsoft Excel 2010, Microsoft Corp., Redmond, WA, USA). The pulse oximeter was removed following every data collection time point.

Statistical Analysis

Data was collected and electronically transferred into a custom database (Microsoft Excel 2010, Microsoft Corp., Redmond, WA, USA), and analyzed using Statistical Package for Social Sciences version 19 (IBM SPSS Statistics 19, IBM Corp., Somers, NY, USA). Descriptive statistics (mean ± SD) were calculated. Thirteen, 1 x 9 (treatment x time) repeated measures ANOVAs and follow- up dependent *t*-tests with Holm's sequential Bonferroni adjustments were performed. Significance levels were set *a priori* at $p \leq 0.05$.

Results

Descriptive statistics and confidence intervals for all measures can be found in Appendix A.

A 1 x 9 repeated measures ANOVA revealed that Category Partitioning Scale scores increased significantly among time points (Wilks' $\Lambda = 0.10$; $F_{(8,7)} = 7.89$, $P = 0.007$; $\eta_p^2 = 0.90$).

Follow-up *t*-tests indicated significant increases in CP-50 scores at eight time points: 30 minutes ($t_{(14)}$ = -5.13, P = 0.021); 60 minutes ($t_{(14)}$ = -9.46, P = 0.003); 90 minutes ($t_{(14)}$ = -13.40, P = 0.002); 120 minutes ($t_{(14)}$ = -19.33, P < 0.0001); 150 minutes ($t_{(14)}$ = -24.20, P < 0.0001); 180 minutes ($t_{(14)}$ = -28.07, P < 0.0001); 210 minutes ($t_{(14)}$ = -28.73, P < 0.0001); and 240 minutes of sitting ($t_{(14)}$ = -30.27, P < 0.0001). This suggests that perceived discomfort increases with increased time (Figure 25).

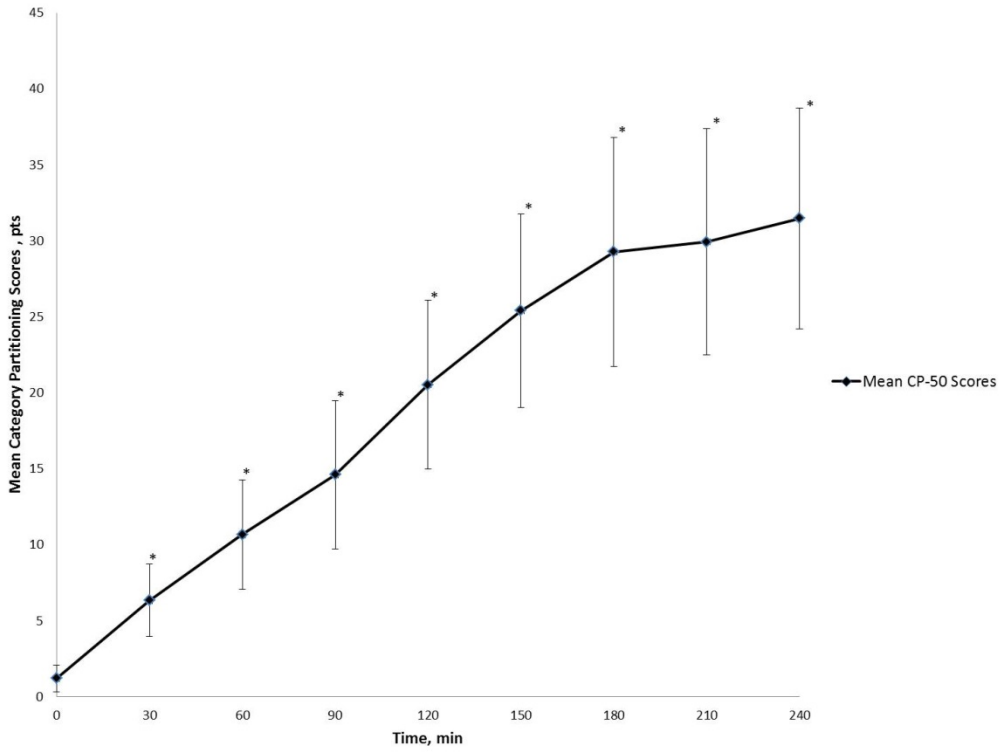

Figure 25. Category Partitioning Scale scores across the four hour testing period. CP-50: Category Partitioning Scale; pts: points; min: minutes; *= P < 0.05.

A repeated measures ANOVA indicated that the descriptor score for the McGill Pain Questionnaire was significantly greater among all time points (Wilks' Λ = 0.17; $F_{(8,7)}$ = 4.17, P = 0.038; η_p^2 = 0.83), indicating higher levels of discomfort across the 240 minute data collection. Follow-up *t*-tests revealed significant increases in descriptor scores at each of eight time points:

30 minutes ($t_{(14)}$ = -0.87, P = 0.045); 60 minutes ($t_{(14)}$ = -1.67, P = 0.003); 90 minutes ($t_{(14)}$ = -2.87, P = 0.003); 120 minutes ($t_{(14)}$ = -4.53, P < 0.0001); 150 minutes ($t_{(14)}$ = -6.00, P = 0.001); 180 minutes ($t_{(14)}$ = -7.20, P = 0.001); 210 minutes ($t_{(14)}$ = -7.27, P = 0.001); and 240 minutes of sitting ($t_{(14)}$ = -8.53, P = 0.001). The visual analog scale score for the McGill Pain Questionnaire was also significantly greater among all time points (Wilks' Λ = 0.18; $F_{(8,7)}$ = 3.97, P = 0.043; η_p^2 = 0.82), again indicating increased perceived discomfort with increased time. Follow-up *t*-tests indicated significant increases compared to baseline in visual analog scale scores at seven time points: 60 minutes ($t_{(14)}$ = -0.97, P = 0.001); 90 minutes ($t_{(14)}$ = -1.67, P = 0.004); 120 minutes ($t_{(14)}$ = -2.82, P = 0.005); 150 minutes ($t_{(14)}$ = -3.45, P = 0.004); 180 minutes ($t_{(14)}$ = -4.25, P = 0.003); 210 minutes ($t_{(14)}$ = -4.73, P = 0.005); and 240 minutes of restricted sitting ($t_{(14)}$ = -4.83, P = 0.004). The present pain intensity score for the McGill Pain Questionnaire was significantly higher among all time points (Wilks' Λ = 0.086; $F_{(8,7)}$ = 9.27, P = 0.004; η_p^2 = 0.91), suggesting that perceived discomfort increased during the 240 minute data collection period. Follow-up *t*-tests revealed significant increases compared to baseline at eight time points: 30 minutes ($t_{(14)}$ = -0.60, P = 0.015); 60 minutes ($t_{(14)}$ = -0.93, P = 0.001); 90 minutes ($t_{(14)}$ = -1.33, P < 0.0001); 120 minutes ($t_{(14)}$ = -1.60, P < 0.0001); 150 minutes ($t_{(14)}$ = -1.80, P < 0.0001); 180 minutes ($t_{(14)}$ = -2.00, P < 0.0001); 210 minutes ($t_{(14)}$ = -2.20, P < 0.0001); and 240 minutes of sitting ($t_{(14)}$ = -2.33, P < 0.0001). Figure 26 summarizes these changes.

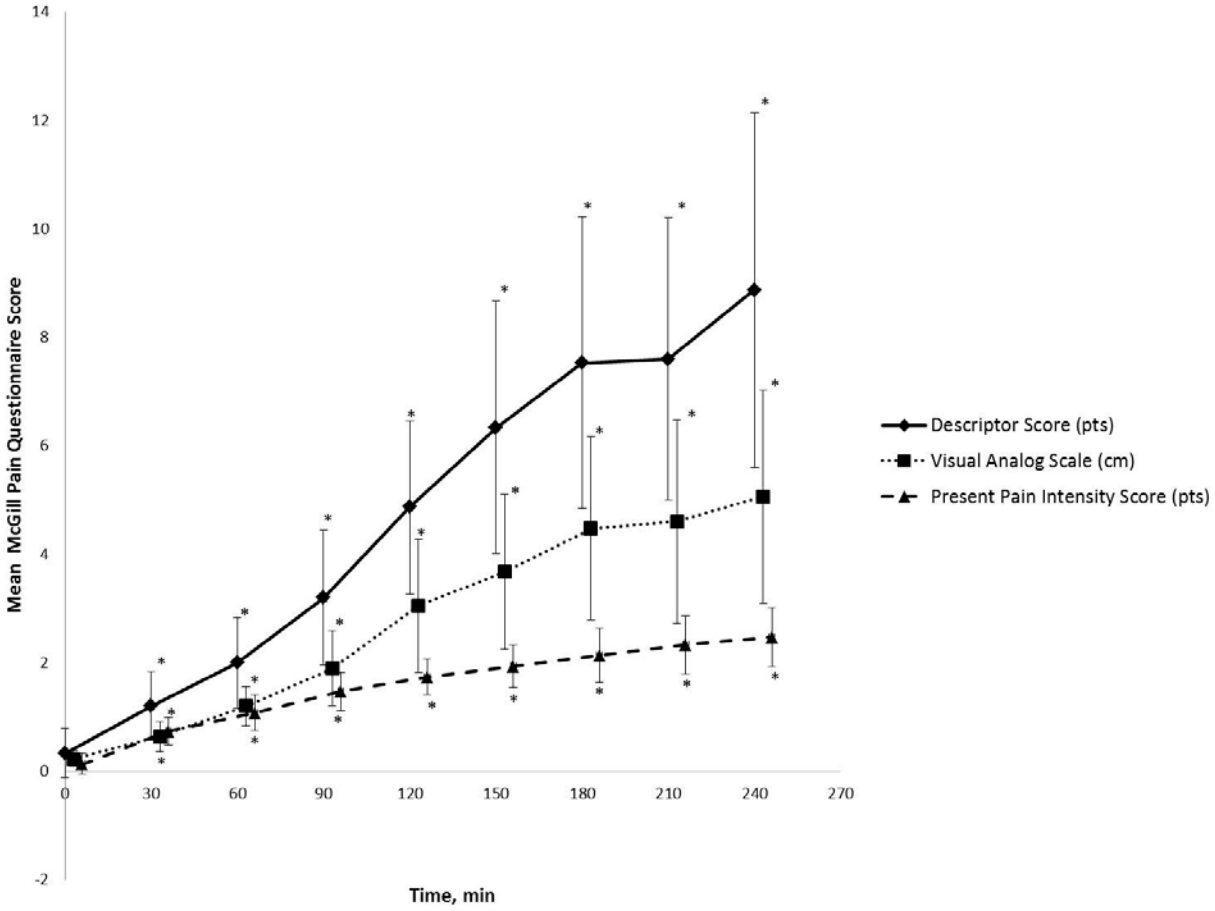

Figure 26. Short Form McGill Pain Questionnaire summary. min: minutes; pts: points; cm: centimeters; * = *P* < 0.05.

A 1 x 9 repeated measures ANOVA found no significant difference in Semmes-Weinstein monofilament test scores at the great toe across the 240 minute prolonged sitting protocol (Wilks' $\Lambda = 0.37$; $F_{(8,7)} = 1.50$, $P = 0.302$; $\eta_p^2 = 0.63$). Similarly, no significant difference in monofilament test scores at the third metatarsal (Wilks' $\Lambda = 0.37$; $F_{(8,7)} = 1.52$, $P = 0.296$; $\eta_p^2 = 0.64$) were found. However at the fifth metatarsal, monofilament test scores significantly increased across the 240 minute test period (Wilks' $\Lambda = 0.12$; $F_{(8,7)} = 6.51$, $P = 0.011$; $\eta_p^2 = 0.88$). Follow-up *t*-tests for the fifth metatarsal yielded no significant differences between any two data collection time points. These results together indicate that during 240

minutes of restricted sitting, the ability to perceive pressure at the foot is unchanged except at the fifth metatarsal. A summary of the Semmes-Weinstein monofilament test data can be found in Figure 27.

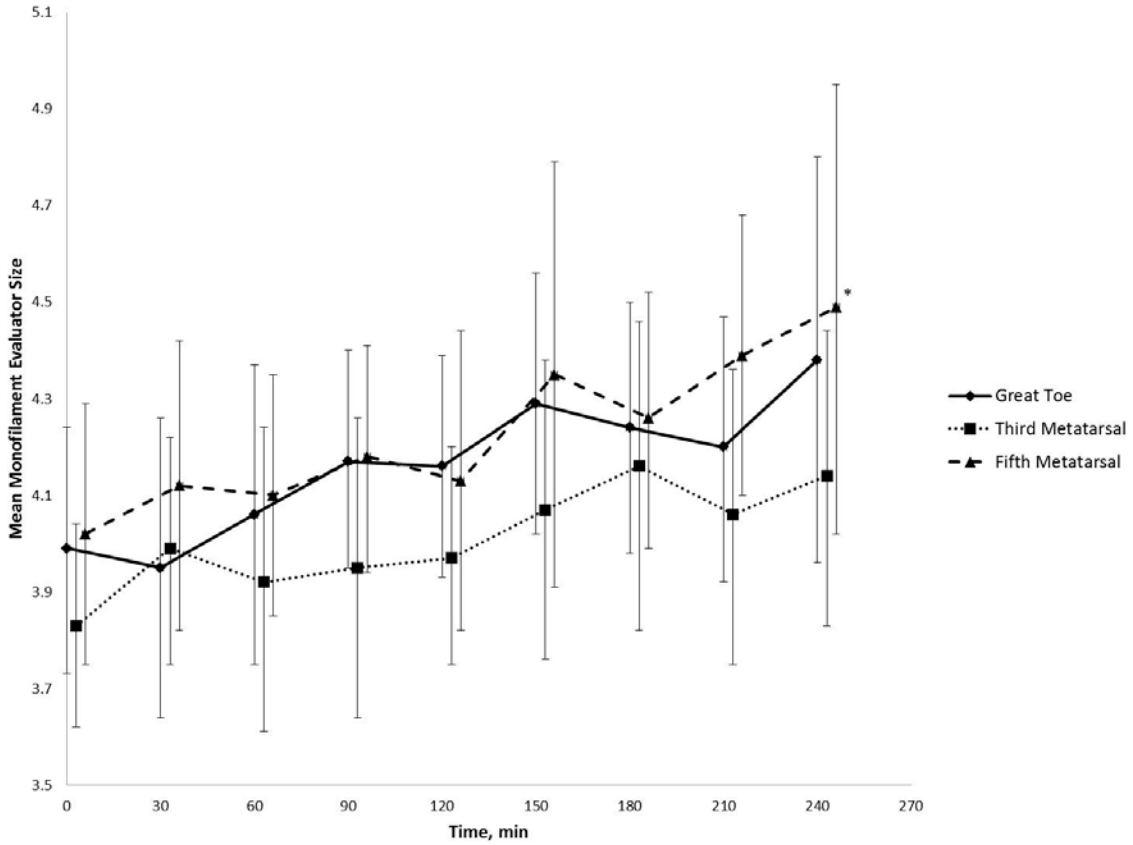

Figure 27. Semmes-Weinstein monofilament test data summary. min: minutes; *= *P* <0.05.

A 1 x 9 repeated measures ANOVA revealed that two-point discrimination test scores at the great toe were not significantly different in scores across the testing period (Wilks' $\Lambda = 0.47$; $F_{(8,7)} = 0.98$, $P = 0.519$; $\eta_p^2 = 0.53$). No significant differences among time points were found for two-point discrimination test scores at the medial malleolus (Wilks' $\Lambda = 0.60$; $F_{(4,11)} = 1.83$, $P = 0.193$; $\eta_p^2 = 0.40$) or the lateral malleolus (Wilks' $\Lambda = 0.67$; $F_{(5,10)} = 1.00$, $P = 0.465$; $\eta_p^2 = 0.33$).

Together these results suggest no changes of receptive field size occur at the foot or ankle during a 240 minute restricted sitting protocol (Figure 28).

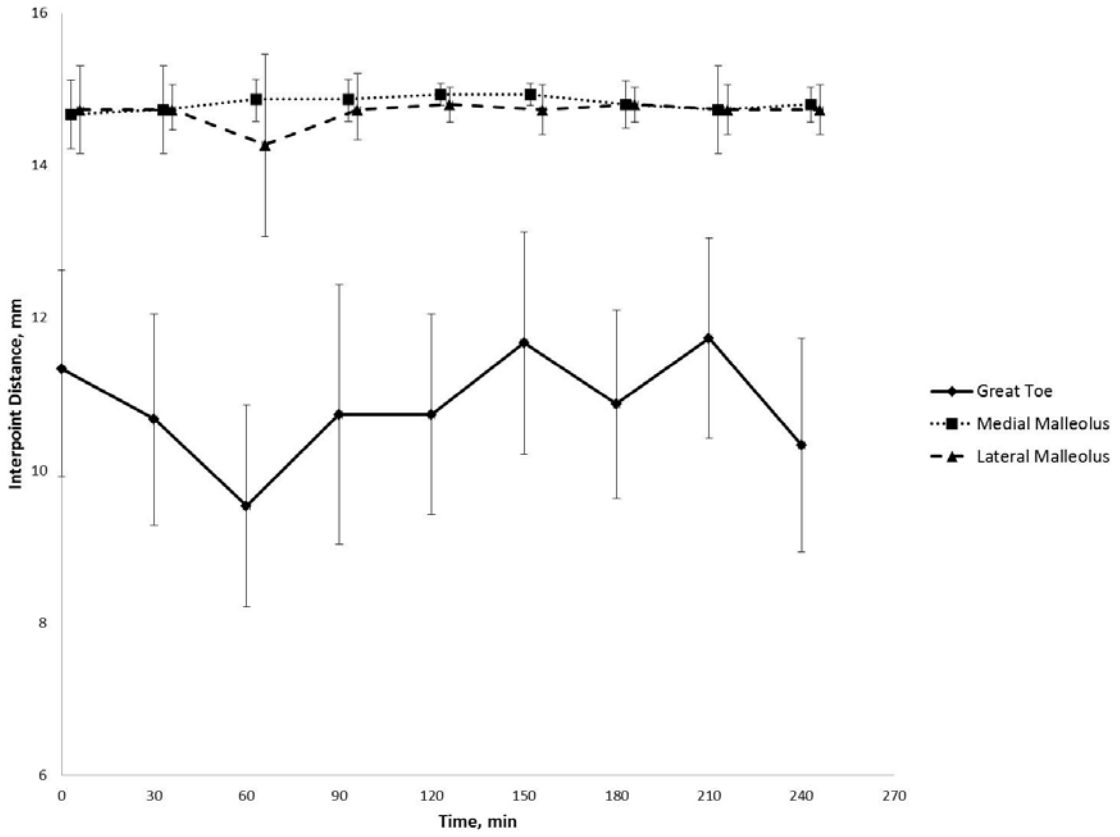

Figure 28. Two-point discrimination data summary during prolonged restricted sitting. min: minute; mm: millimeter.

A 1 x 9 repeated measures ANOVA found that percent oxygen saturation in the lower limb measured from the dominant great toe did not significantly differ across the 240 minute prolonged restricted sitting protocol (Wilks' $\Lambda = 0.21$; $F_{(8,7)} = 3.29$, $P = 0.067$; $\eta_p^2 = 0.79$) (Figure 29).

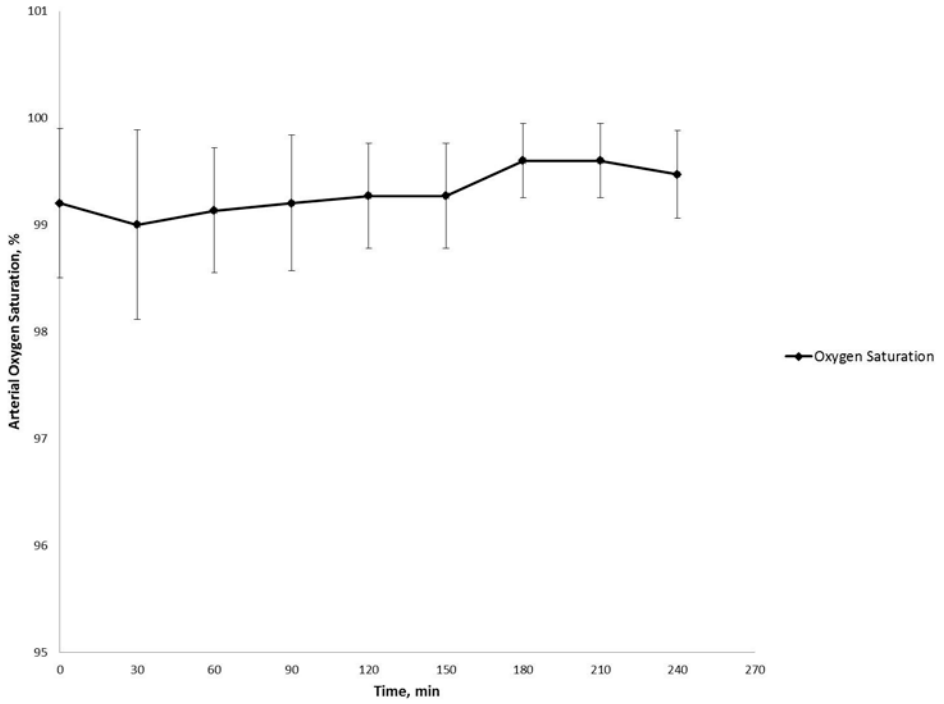

Figure 29. Percent arterial oxygen saturation. min: minute; %: percent.

Using a 1 x 9 (condition x time) repeated measures ANOVA, we found that superficial temperature on the anterior aspect of the ankle decreased significantly (Wilks' $\Lambda = 0.11$; $F_{(8,7)} = 7.01$, $P = 0.009$; $\eta_p^2 = 0.88$). Follow-up pairwise comparisons revealed significant differences at 30 minutes ($t_{(14)} = 0.78$; $P > 0.001$), 60 minutes ($t_{(14)} = 1.32$; $P > 0.001$); 90 minutes ($t_{(14)} = 1.66$; $P > 0.001$), 120 minutes ($t_{(14)} = 1.99$; $P > 0.001$), 150 minutes ($t_{(14)} = 2.24$; $P > 0.001$), 180 minutes ($t_{(14)} = 2.35$; $P > 0.001$), 210 minutes ($t_{(14)} = 2.64$; $P > 0.001$), and 240 minutes ($t_{(14)} = 2.78$; $P > 0.001$) compared to baseline. This data indicates that during a bout of prolonged restricted sitting, anterior ankle skin temperature is decreased. A 1 x 9 (condition x time) repeated measures ANOVA revealed a significant decrease in superficial skin temperature at the lateral aspect of the ankle (Wilks' $\Lambda = 0.08$; $F_{(8,7)} = 9.83$, $P = 0.003$; $\eta_p^2 = 0.91$). Follow-up pairwise comparisons yielded significant differences at 30 minutes ($t_{(14)} = 0.88$; $P > 0.001$), 60

minutes ($t_{(14)}$ = 1.31; P > 0.001), 90 minutes ($t_{(14)}$ = 1.87; P > 0.001), 120 minutes ($t_{(14)}$ = 2.18; P > 0.001), 150 minutes ($t_{(14)}$ = 2.41; P > 0.001), 180 minutes ($t_{(14)}$ = 2.54; P > 0.001), 210 minutes ($t_{(14)}$ = 2.72; P > 0.001), and 240 minutes ($t_{(14)}$ = 2.84; P > 0.001) when compared to baseline measures. This data demonstrates that during a bout of prolonged restricted sitting lateral ankle skin temperature decreases across the 4 hour data collection time period (Figure 30).

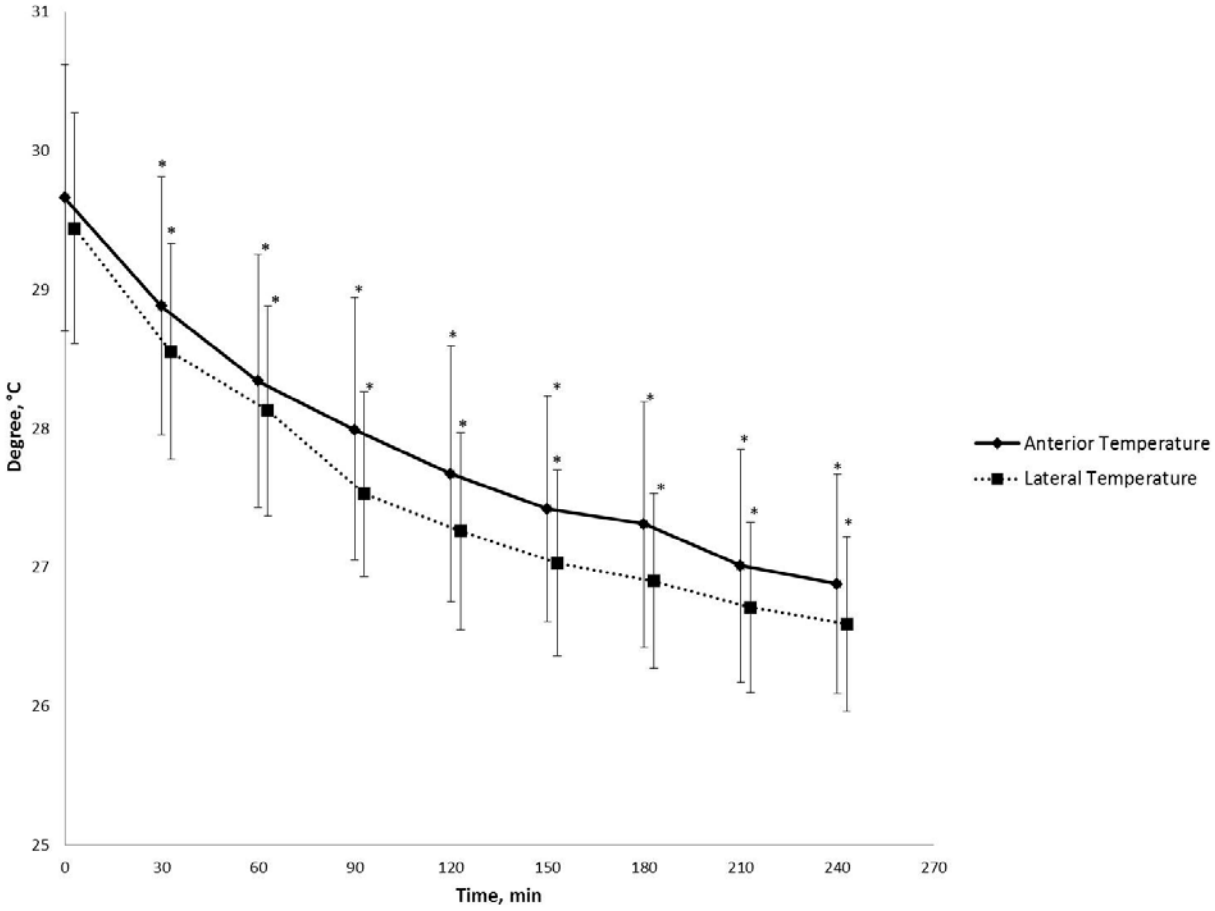

Figure 30. Anterior and lateral ankle skin temperature during prolonged restricted sitting. min: minute; C: Celsius; * = P < 0.05.

Discussion

This project examined the effects of four hours of restricted sitting in an unpadded, Black Hawk helicopter pilot's seat on subjective discomfort, sensibility, lower extremity blood oxygenation, and lower extremity superficial skin temperature. The authors hypothesized that prolonged restricted sitting would produce increases in subjective discomfort, decrements in lower extremity sensibility, and altered lower extremity vascular function.

Subjective Discomfort Measures

Our results indicate that Category Partitioning Scale scores representing subjective discomfort increased across four hours of restricted sitting. Subjective discomfort scores increased 30.27 points across the four hour time period, representing a change in the discomfort categories from "very low pressure/slight discomfort" to "high pressure/severe discomfort". Previous research in F-16 ejection seats found that an 8 hour sitting period resulted in a significant decrease in subject comfort between 1 and 2 points on a 10-point scale.[3] Other work has found similar results demonstrating a 1.5-3 point increase in discomfort on a 10-point scale.[9] Comparisons between the 10 point scale and the 52 point Category Partitioning Scale can be made if a percent change is utilized rather than raw scores. The results of the current study represent a 58% increase in discomfort across four hours. Previous work demonstrated a 20% decrease in whole-body comfort[3] and up to a 30% increase in buttocks discomfort.[9] We hypothesize that our change in discomfort is greater than previous work because we did not utilize a seat cushion during data collection. We chose to test the Black Hawk pilot's seat without a seat cushion because numerous variations of Black Hawk seat cushions exist. By

utilizing the lowest common denominator among all Black Hawk helicopter seating options (the armored, unpadded seat); we believe our results could extend beyond a specific seat cushion.

The McGill Pain Questionnaire data also support that prolonged restricted sitting in Black Hawk helicopter pilot's seats result in increased discomfort. The total descriptor score significantly increased at every time point during the four hour sitting period. Increases in visual analog scale distances and present pain intensity scores also were observed. If all three components of the McGill Pain Questionnaire are examined together we see a similar pattern of increasing discomfort across all time points for all measures. To the authors' knowledge, this was the first study to utilize the Short-Form McGill Pain Questionnaire as an outcome measure for prolonged sitting in military or civilian aircraft. Previous work has shown that the Short-Form McGill Pain Questionnaire has good test-retest reliability and responsiveness to change when utilized as an outcome measure for pain.[283] Future studies examining prolonged restricted sitting in experimental or field settings should consider utilizing the Short-Form McGill Pain Questionnaire.

Lower Extremity Sensibility

A single prolonged restricted sitting session of four hours significantly increased the Semmes-Weinstein monofilament test scores at the plantar aspect of the fifth metatarsal. Increases in monofilament scores suggest a decrease in sensitivity to point pressure applied to the area of interest. Conversely, we did not find significant changes in monofilament test scores at the plantar aspect of the great toe or at the plantar aspect of the third metatarsal. The difference between our significant results at the fifth metatarsal and non-significant results at the great toe

and third metatarsal may be explained by the separate dermatomes at the testing locations. The S1 dermatome comprises the fifth metatarsal, whereas the L5 dermatome distribution comprises both the great toe and the third metatarsal test locations.[272] Our partial eta squared value of 0.88 suggests that there is a clinical decrease in sensibility across four hours of restricted sitting at the fifth metatarsal, suggesting that prolonged sitting alters the S1 nerve root fibers of the sciatic nerve. The mean monofilament test scores for the fifth metatarsal at each time point were all above 4.0. Previous research has shown that the threshold for normal pressure sensibility is 3.61.[284] This suggests that at the fifth metatarsal the participants in this study did not have normal sensitivity to pressure. S1 nerve root impairment leads to symptoms of muscle weakness in the plantar flexors (gastrocnemius and soleus muscles) and subtalar joint evertors (peroneus longus and peroneus brevis muscles).[272] Additionally the Achilles tendon reflex would also be diminished.[272] Impairment to the S1 nerve root is a particular concern for Black Hawk helicopter pilots. Rotary-winged aircraft like the Black Hawk require full function of both legs and feet to effectively control the aircraft. The feet and legs are used to operate the anti-torque pedals which are used to counteract the torque created by the main rotors.[285] They are also used to adjust the yaw of the aircraft left or right during a hover.[285] A lowered ability to effectively operate the anti-torque pedal could increase fatigue and may result in diminished control of the aircraft during flight. It is important to note that while we suspect diminished motor performance occurred during prolonged sitting, we did not collect any measures of motor function (e.g. force output, reaction time, α-motoneuron output) of the plantar flexors during this study. Future research should expand on the hypothesis that S1 nerve root function is diminished during prolonged sitting, therefore negatively affecting S1 nerve root motor performance by examining electromyographic, reflex, and force data at the muscles innervated by the S1 myotome.

The two-point discrimination test revealed no change in receptive field sensitivity at the great toe, the medial malleolus, and the lateral malleolus across the four hour sitting protocol. We suspect no change was found because the measure may not have been sensitive enough to detect changes in receptive field sensitivity. The two-point discrimination tool utilized in this study had a maximum inter-point distance of 15 millimeters. This distance may not have been a large enough inter-point distance, particularly at the medial and lateral malleolus. We observed that very few participants were able to identify inter-point distances closer than 15 millimeters. Previous work has also identified large inter- and intra-individual variations,[206] possibly reducing the sensitivity of the measure due to the within-subjects design of this study. The non-significant results at the great toe support our previous finding that the L5 nerve root fibers may not be influenced with four hours of restricted sitting. The mean inter-point distance at the great toe is 6.6 millimeters, well within the testing capabilities of the two-point discrimination tool. In the present study, the test locations for two-point discrimination test and the Semmes-Weinstein monofilament test were not the same. This decision was made based on recommended testing locations proposed by previous work.[201,202,209] Future work should examine two-point discrimination scores at the same locations as the Semmes-Weinstein monofilament test (plantar aspects of the great toe, third metatarsal, and fifth metatarsal) to test if dermatome dependent changes occur with the two-point discrimination test and the monofilament test.

Vascular Measures

Total limb percent oxygen saturation as measured at the great toe revealed no significant changes in oxygen saturation levels across 4 hours of restricted sitting. These results are in line with previous work which found that 8 hours of restricted sitting in F-16 ejection seats did not significantly alter muscle blood flow levels.[3] The redundancy of the vascular network in the lower extremity combined with the lack of compression of the major artery while in a seated position may explain the consistency of the oxygen saturation measures.[31] The femoral artery enters the lower extremity on the anterio-medial aspect of the upper leg and remains on the medial aspect until it reaches the medial epicondyle of the femur where it moves posteriorly into the popliteal fossa.[31] Compression of the femoral artery could occur at the end of the seat pan; however, observations during sitting indicate that the femoral artery moves posterior to the popliteal space distal to the end of the seat pan. Future research could examine if any vascular structures are compressed during prolonged restricted sitting by measuring structural changes in the gross anatomy of the vascular tissue using imaging devices such as magnetic resonance imaging or ultrasound.

Dynamic infrared thermography measures of superficial skin temperature at the anterior and lateral ankle revealed decreases in anterior and lateral ankle superficial skin temperature by 2.78° C and 2.85° C, respectively. This is a relative decrease of 9.3% at the anterior ankle and a 9.6% decrease at the lateral ankle. These data demonstrated that superficial skin temperature decreases as a result of prolonged sitting. Superficial skin temperature has been identified as an indirect, non-contact measure of skin blood perfusion.[286] Previous work with dynamic infrared thermography indicates that a change in 0.5° C is clinically significant.[286] Previous work has utilized near infrared spectroscopy to examine changes in muscle oxygenation during prolonged sitting, but this work did not examine total muscle blood flow changes.[3] To our knowledge this

is the first study to measure superficial skin temperature during prolonged restricted sitting in Black Hawk helicopters. Future work should continue to utilize dynamic infrared thermography as a non-contact measure of superficial skin temperatures during prolonged sitting to provide insight on how peripheral vasculature function is altered.

Conclusions

This study found that four hours of prolonged restricted sitting results in increases in subjective discomfort in a Black Hawk helicopter pilot's seat. This supports previous work in fixed-wing aircraft. The current study also found that four hours of restricted sitting results in diminished S1 nerve root function when measured with the Semmes-Weinstein monofilament test. Finally, this study demonstrated that superficial skin temperature at the anterior and lateral ankle decreases during prolonged sitting, suggesting decreases in skin blood perfusion across time during restricted sitting. Future work should build upon these results to understand the etiology of discomfort and temporary parathesia in rotary-winged aircraft in order to develop ways to mitigate the negative effects associated with prolonged restricted sitting.

Chapter V

Effects of Local Pressure Application on Discomfort, Skin Sensitivity, Temperature, and Limb Oxygenation

Introduction

The symptoms of seat discomfort and temporary parathesia remain top concerns in today's Black Hawk aviators despite millions of dollars invested in research and development of UH-60 Black Hawk helicopter pilot's seating.[1] Approximately one-fifth of rotary-winged pilots report some level of pain, numbness or tingling in the buttocks and lower extremity during prolonged flight.[4,6] This reported discomfort extends beyond feeling pain during flight; rotary-wing pilots have also been shown to experience more low back and pelvic musculoskeletal injuries than their fixed-wing counterparts.[5] Additionally, the discomfort associated with prolonged sitting impairs mission performance.[11,287] In fact, 34% of naval helicopter pilots reported that discomfort due to prolonged restricted sitting resulted in decrease situational awareness.[287] Discomfort from prolonged restricted sitting could interfere with the attentional capacity to perform a task. Attentional capacity is the amount of attention an individual has to devote to task performance.[288] During task performance, a portion of the attentional resources are devoted to perform that task.[288,289] The more complex a task is, the more attentional resources required.[289] If there are competing tasks for attentional resources performance of the

both tasks decrease.[289] In practice, this could result in a decreased ability to perform a complex task (operating a helicopter) due to discomfort competing for a finite pool of attentional resources; resulting in loss of equipment, injury, or death.

There is also a financial cost associated with discomfort and injury resulting from the helicopter seat system. It has been calculated that the annual cost (including: medical, lost time, and training) for Naval rotary-winged aviators is $10.6 million.[290] Other studies examining the long-term costs associated with pain and injury resulting from the seat system found that the 5 year cost (including medical, lost time, and training, but excluding disability mishap costs) was $54.8 million.[287] Other estimated costs of pain and injury due to prolonged sitting suggest that each injury caused by the helicopter seat system costs $1,500 annually.[291] By understanding the symptoms of discomfort and temporary parathesia, significant improvements to the helicopter seat system can be made to help reduce the monetary costs associated with the discomfort and injury caused by prolonged restricted sitting.

Symptoms of discomfort and temporary parathesia during prolonged rotary-winged flight could develop from areas of locally high pressure compressing nervous and vascular system tissues. Studies utilizing pressure mapping systems in fixed-wing aircraft have found that areas of high pressure develop during periods of prolonged sitting.[3,9,15] However, research examining the effects of local pressure application to body surfaces in ambulatory populations remains scarce.[85] The only available study found that the soleus Hoffmann reflex mean amplitude when measured in a prone position increases with 10 minutes of local pressure applied to the posterior thigh; and that subjective discomfort increases with 10 minutes of pressure application.[85] Interpretation of this data is problematic because of the known position dependent responses of the Hoffmann reflex.[143] Applying specific amounts of local pressure while in a seated position to

sites on the sitting surfaces of the body is difficult, but could yield valuable insights into testing the hypothesis that localized high pressure creates the reported discomfort and temporary parathesia in rotary-winged aviators.

Investigations into the effects of prolonged restricted sitting have utilized primarily subjective discomfort scales[3,9,11,15] and seat interface pressure;[3,9,15] while investigations into possible etiology of the symptoms of discomfort and temporary parathesia have utilized neurological measures such as the Hoffmann reflex.[85] Bridging the gap between the measures utilized in prolonged sitting studies and local pressure studies would assist in improving current understanding of the development of discomfort in both a real world and experimental setting. Measures exist that can effectively be used in both the field setting and an experimental setting. Potential measures could include: the Semmes-Weinstein monofilament test, the two-point discrimination test, dynamic infrared thermography, and lower extremity pulse oximetry. The Semmes-Weinstein monofilament and two-point discrimination tests could enhance our understanding of how the sensory nervous system changes with local pressure application. Dynamic infrared thermography and pulse oximetry could provide insight to changes to the vascular system distal to pressure application. These four tools have been used previously to monitor changes as a result of prolonged restricted sitting in a Black Hawk.[292] By utilizing these same measures to examine a potential cause (local pressure application) of the reported discomfort and temporary parathesia, we can better understand the develop of discomfort and parathesia with the end goal of decreasing injury and increasing combat effectiveness in today's rotary-winged aviators.

Understanding the etiology of discomfort and temporary parathesia during prolonged missions in Black Hawk helicopters is critical to enhancing pilot safety and increasing mission

effectiveness. One hypothesis for the development of discomfort and temporary parathesia is that local pressure compresses the neurological and vascular structures. Therefore, the purpose of this study is to determine if 10 minutes of local pressure application at two locations on the sitting surface of the body and at two different magnitudes results in changes to subjective discomfort scores, clinical measures of sensory nervous system function, and vascular function in the lower extremity.

Methods

Experimental Design

This study utilized a 2 x 2 x 2 factorial repeated measures crossover design. The independent variables were location with two levels (ischial tuberosity and posterior thigh), pressure magnitude with two levels (36 kilopascals and 44 kilopascals), and time with two levels (pre-pressure and during pressure). The dependent variables included Category Partitioning Scale scores, McGill Pain Questionnaire (descriptor, visual analog scale, and present pain intensity) scores, Semmes-Weinstein monofilament test (great toe, third metatarsal, and fifth metatarsal) scores, two-point discrimination (great toe, medial malleolus, and lateral malleolus) scores, dynamic infrared thermography (lateral lower leg and anterior lower leg) mean temperatures, and pulse oximetry (percent oxygen saturation) levels.

Participants

Sixteen male volunteers responded to advertisements (flyers and group presentations) to participate in the study. Fifteen healthy male participants (age = 23.4 ± 3.1 years) completed the study (one did not attend the data collection session and no data was collected). Participants met minimal body segment length measures and minimum/maximum weights required to obtain flight status in the United States Army (Table 3). Participants were screened via an 18-point health questionnaire and self-reported no history of cardiovascular, neurological, or metabolic disease in the past two years; no current or two year history of surgery or fracture in the lumbar spine or lower extremity; no current history of low back pain or lower extremity injury; and no current use of prescription or non-prescription pain relievers. All participants provided signed written consent. The study was approved by the University's Institutional Review Board.

Table 3. United States Army anthropometric flight status requirements.

Body Measure	Men
Total Arm Reach, cm	≥ 164.0
Crotch Height, cm	≥ 75.0
Sitting Height, cm	< 102.0
Minimum Weight, kg	45.3
Maximum Weight, kg	107.9

Experimental Procedures

Participants reported to the laboratory two times with a minimum of 24 hours between sessions. Testing order was randomized (computerized random number generator, TI-83 Plus, Texas Instruments Inc., Dallas, TX, USA) into 2 conditions; with a pressure magnitude of 36 kilopascals (condition A) completed on one day, and a pressure magnitude of 44 kilopascals (condition B) completed on the other day. Within each condition, randomization of pressure application location order was also completed between the ischial tuberosity (location A) and the middle of posterior thigh (location B). During session one, functional leg dominance was determined using three tests: the step up test, the ball kick test, and the balance recovery test.[270] Investigators then recorded the anthropometric measures of arm length, crotch height, sitting height, height, and weight from the participants to ensure all Army flight status requirements were met. Participants next had lower extremity flexibility measures of hip flexion, hip extension, and hip external rotation collected along with sit-and-reach scores.

For all data collection, participants sat in a purpose-built pressure application seat. The seat's design allowed for local pressure to be applied only to the location of interest while still supporting the participants' body weight. To replicate sitting postures in the UH-60 helicopter, Design Eye Point knee sitting angles were collected using a goniometer (12.5" International Standard Goniometer, Patterson Medical Holdings Inc., Bolingbrook, IL, USA) and recorded using standard United States Army Design Eye Point procedures.[274] The Design Eye Point position optimizes the aviator's ability to monitor aircraft controls while also providing clear lines of sight (Figure 31). This knee angle was reproduced in the purpose-built pressure application seat by passively moving the participants' knees prior to the start of all data collection and following each data collection time point. Data were collected at baseline and

during the final 3 minutes of the pressure application protocol. During the pressure application, participants were asked to sit quietly with their head facing forward.

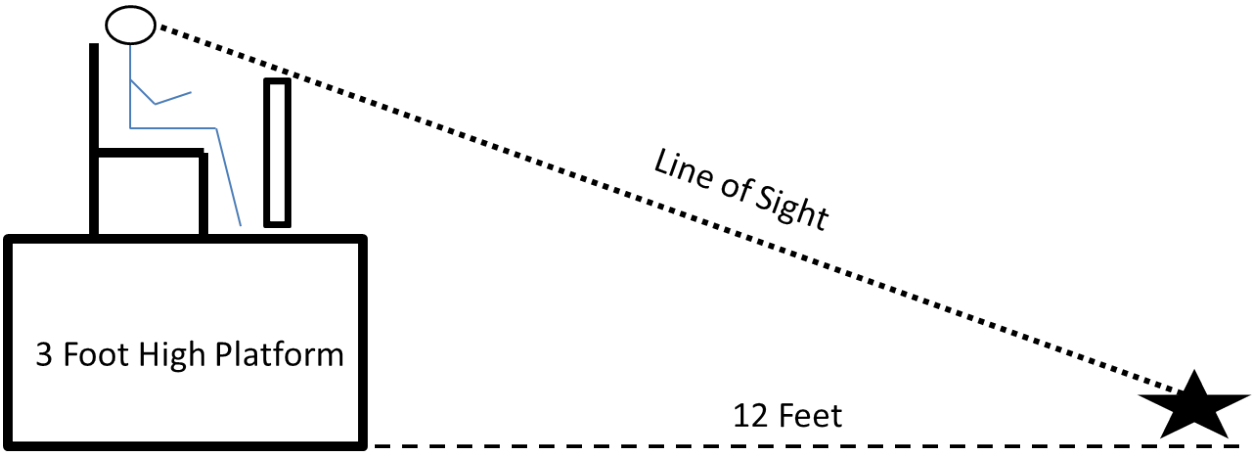

Figure 31. Design Eye Point participant positioning.

Local Pressure Application Apparatus (LPAAP)

The purpose-built LPAAP was designed to apply pressures of 36 kilopascals and 44 kilopascals to the ischial tuberosity and posterior thigh of participants in a seated position. The LPAAP system consisted of a step motor secured to an extendable metal rod and load cell with a custom-built, round pressure application head 25.5176 centimeters squared in area. The unit (Figure 32) was controlled using custom-written computer software and operated through a laptop computer (Dell Latitude D430, Dell Inc., Round Rock, TX, USA). The seat was built of wood and consisted of an 80.01 x 55.88 centimeter (height x width) seat back and a 50.80 x 55.88 centimeter (depth x width) seat pan. The seat pan was comprised of 14 removable slats which allowed the pressure application head to apply pressure to the area of interest while still supporting the participant (Figure 33). The foot rest was a 91.44 x 50.80 x 35.56 centimeter

(length x width x height) box with an adjustable crank lift to accommodate participants of different heights.

Figure 32. Local pressure application apparatus.

Figure 33. Local pressure application head integrated into seat pan.

Determination of Anatomical Locations

Local pressure was applied to the ischial tuberosity and the mid-point of the posterior thigh on the dominant lower extremity of participants. The two locations were chosen based on anatomy and previous research.[85] The ischial tuberosity was located using palpation by a trained investigator and marked with adhesive tape. The mid-point of the posterior thigh was defined as half the distance from the greater trochanter to the lateral epicondyle and halfway between the medial and lateral edges of the posterior thigh. A trained investigator measured the distance between the greater trochanter and the lateral epicondyle (both determined by palpation) using a fabric tape measure (Medco Tape Measure, Patterson Medical Holdings Inc., Bolingbrook, IL, USA). The distance was rounded to the nearest half centimeter and marked with permanent marker. The distance between the medial and lateral borders of the thigh was measured in the same manner with the permanent marker line demarcating the mid-point of the femur along its long axis. This point was marked with permanent marker and served as the location for posterior thigh pressure application. Prior to local pressure application, these locations were visually confirmed in the LPAAP. In the case of the ischial tuberosity, verbal confirmation participant was also elicited.

Local Pressure Application Protocol

Participants were asked to sit on the pressure application chair barefoot with the appropriate slats removed and pressure application head correctly positioned (Figure 34). The participant was instructed to sit upright and as far back in the chair as possible. The foot rest was adjusted to the appropriate height and participants' knees were positioned at the Design Eye

Point knee angle. Following positioning, baseline measures of Category Partitioning Scale, McGill Pain Questionnaire, dynamic infrared thermography, Semmes-Weinstein monofilament, two-point discrimination, and pulse oximetry were taken. Local pressure was applied at the specified amplitude (36 kilopascals or 44 kilopascals) for a total time of 10 minutes. During the pressure application the magnitude of the pressure was maintained to within 5% of the set value. At seven minutes into the pressure application protocol, during pressure follow-up measures were taken. During pressure follow-up measures began at 7 minutes to allow investigators to complete all data collection before the 10 minute total pressure application time expired. The order of measure data acquisition remained the same for each session and for each participant. Following 10 minutes of pressure application, the pressure magnitude was decreased to zero and the participants were given a 15 minute break. During the 15 minute break, participants were permitted to stand and walk around the laboratory. The 15 minute break allowed time for participants to recover from any numbness or tingling which may have occurred during testing and allowed for the investigators to reposition the pressure application head to the next pressure application location. The 15 minute break time period was determined from pilot work which found that following 15 minutes, no pilot participants reported symptoms of temporary parathesia. The randomization of pressure magnitude and location ensured the order effect was minimized and pressure was not applied to the same location (ischial tuberosity or posterior thigh) twice during a single data collection session. Following the 15 minute break, participants were asked to again sit in the pressure application seat. The Design Eye Point knee angle and visual confirmation of pressure application location were again completed. Once in position, the protocol was repeated on the untested location at the same pressure magnitude. During the

second session, the above protocol was repeated at the remaining pressure application magnitude (36 kilopascals or 44 kilopascals).

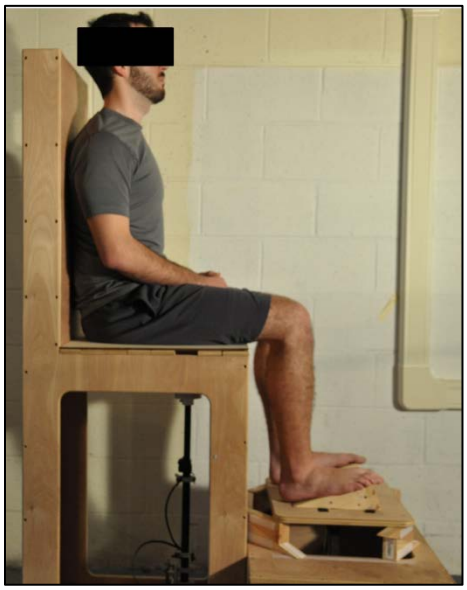

Figure 34. Correct participant positioning for local pressure application testing.

Discomfort Measures

Category Partitioning Scale

The Category-Partitioning Scale was utilized to examine local pressure intensity level and perceived discomfort.[256,257] The tool consists of a vertical scale divided into five categories: "very slight," "slight," "medium," "severe," and "very severe."[257,258] Each category is subdivided into 10 scale points, with numbers above fifty provided to avoid the ceiling effect in the case of extreme pain or discomfort.[257] Participants were asked to rate their discomfort in one of the five categories, then instructed to "fine tune" their discomfort rating using the numerical scale within each category.[257] The numerical data were recorded with a tablet computer (iPad 2, Apple Inc.,

Cupertino, CA, USA) and entered into an electronic data collection sheet (Quickoffice Pro HD for iPad, Google Inc., Mountain View, CA, USA).

Short-Form McGill Pain Questionnaire (MPQ)

The 17-point Short-Form McGill Pain Questionnaire (MPQ) evaluated the sensory, affective, and current pain intensities.[260] The questionnaire consisted of eleven sensory dimension descriptors and four affective dimension descriptors.[260] Each descriptor was ranked on an intensity scale of 0 = none, 1 = mild, 2 = moderate, and 3 = severe.[260] One 10 centimeter visual analogue scale and one Present Pain Intensity question were also presented as part of the MPQ to indicate overall discomfort intensity.[260] The questionnaire was handed to the participant at every data collection time point and the numerical scores tallied and entered into a custom spreadsheet (Microsoft Excel 2010, Microsoft Corp., Redmond, WA, USA).

Sensory Measures

Semmes-Weinstein Monofilament Test (MFT)

Point pressure stimuli sensitivity was evaluated using the Semmes-Weinstein Monofilament Test (MFT) (Touch-Test Sensory Evaluator, North Coast Medical Inc., Morgan Hill, CA, USA).[208] The MFT was comprised of several single Nylon fibers[209] of varying thickness.[210] The monofilament was held in place for 1.5 seconds and participants were instructed to respond “Yes” if they felt the monofilament against the skin.[212] Locations for measurement included the plantar aspect of the great toe, the plantar aspect of the third metatarsal, and the plantar aspect of the fifth metatarsal of the dominant foot of participants.[209]

The last correctly reported monofilament thickness was recorded with a tablet computer (iPad 2, Apple Inc., Cupertino, CA, USA) and entered into an electronic data collection sheet (Quickoffice Pro HD for iPad, Google Inc., Mountain View, CA, USA).

Two-Point Discrimination Test (TPDT)

Lower extremity receptive field sensitivity was measured with the two-point discrimination test (TPDT) (Disk-Criminator, North Coast Medical Inc., Morgan Hill, CA, USA).[192,193] The TPDT was comprised of a disk caliper with inter-point distances ranging from 2 to 15 millimeters.[194,195] The disk caliper was placed on the testing locations for 1.5 seconds and the participant was asked to verbally indicate if one or two points were in contact with the skin. To discourage participants from guessing, single and double pin points were interchanged randomly. Testing locations included the planar surface of the great toe, the medial malleolus, and the lateral malleolus of the dominant lower leg of participants.[208] The last correctly reported inter-point distance was recorded with a tablet computer (iPad 2, Apple Inc., Cupertino, CA, USA) and entered into an electronic data collection sheet (Quickoffice Pro HD for iPad, Google Inc., Mountain View, CA, USA).

Circulatory Measures

Dynamic Infrared Thermography (DIRT)

A digital infrared camera (FLIR T420, FLIR Systems Inc., Wilsonville, OR, USA) was used to measure non-contact, superficial temperatures (°C) in the lower leg. Anterior and lateral infrared images were taken 1 meter from the dominant leg of participants. The mean

temperature of the lateral and anterior ankle was analyzed using the mean temperature function (FLIR ExaminIR, version 1.40.12.44). Mean temperature values for regions of interest at the anterior and lateral ankle were measured using the Glamorgan Protocol.[268] The anterior ankle region of interest included the width of the ankle with upper and lower edges at the tip of the medial malleolus and the tip of the navicular bone, respectively.[268] The lateral ankle region of interest included the entire anterior to posterior thickness at the level of the lateral malleolus.[268]

Pulse Oximetry

A pulse oximeter (Nonin Onyx Vantage 9590, Nonin Medical Inc., Plymouth, MN, USA) was secured to the great toe of the dominant leg. Percent oxygen saturation was recorded utilizing the spot check method.[245] This method was used to allow access to the great toe for other measures. Following a five second analysis period, percent blood oxygen (%SpO_2) was recorded to a custom electronic spreadsheet (Microsoft Excel 2012, Microsoft Corp., Redmond, WA, USA). The pulse oximeter was removed following every data collection time point.

Statistical Analysis

Data were collected and electronically transferred into a custom database (Microsoft Excel 2010, Microsoft Corp., Redmond, WA, USA), and analyzed using Statistical Package for Social Sciences version 19 (IBM SPSS Statistics 19, IBM Corp., Somers, NY, USA). Descriptive statistics (mean ± SD) were calculated. Thirteen, 2 x 2 x 2 (magnitude x location x time) factorial repeated measures ANOVAs performed. Appropriate follow-up ANOVAs and

dependent *t*-tests with Holm's sequential Bonferroni adjustments were performed. Significance levels were set *a priori* at $p \leq 0.05$.

Results

Descriptive statistics and confidence intervals for all measures can be found in Appendix B.

No significant 3-way interaction was found following a 2 x 2 x 2 factorial repeated measures ANOVA for the Category Partitioning Scale scores (Wilks' $\Lambda = 0.83$; $F_{(1,14)} = 2.94$, $P = 0.108$; $\eta_p^2 = 0.17$). There were significant magnitude x time (Wilks' $\Lambda = 0.55$; $F_{(1,14)} = 11.39$, $P = 0.005$; $\eta_p^2 = 0.45$) and location x time (Wilks' $\Lambda = 0.40$; $F_{(1,14)} = 20.76$, $P < 0.0001$; $\eta_p^2 = 0.60$) two-way interactions for Category Partitioning Scale scores. Follow-up *t*-tests for the magnitude x time interaction yielded a significant effect of magnitude at the middle of the posterior thigh ($t_{(14)} = -2.82$, $P = 0.014$) and ischial tuberosity ($t_{(14)} = -2.51$, $P = 0.025$). There was also a significant effect of time at a magnitude of 36 kilopascals at the posterior thigh ($t_{(14)} = -5.51$, $P < 0.0001$) and at the ischial tuberosity ($t_{(14)} = -3.14$, $P = 0.007$); and at a magnitude of 44 kilopascals at the posterior thigh ($t_{(14)} = -7.53$, $P < 0.0001$) and at the ischial tuberosity ($t_{(14)} = -4.28$, $P = 0.001$). Follow-up *t*-tests for the location x time interaction indicated a significant difference between the posterior thigh and ischial tuberosity at the during pressure time point at 36 kilopascals ($t_{(14)} = 2.60$, $P = 0.021$) and 44 kilopascals ($t_{(14)} = 4.16$, $P = 0.001$) of pressure. These data suggests that Category Partitioning Scale scores were higher (indicating more discomfort) at the posterior thigh during both the 36 kilopascal and 44 kilopascal pressure

applications than at the ischial tuberosity during the same pressure application magnitudes (Figure 35).

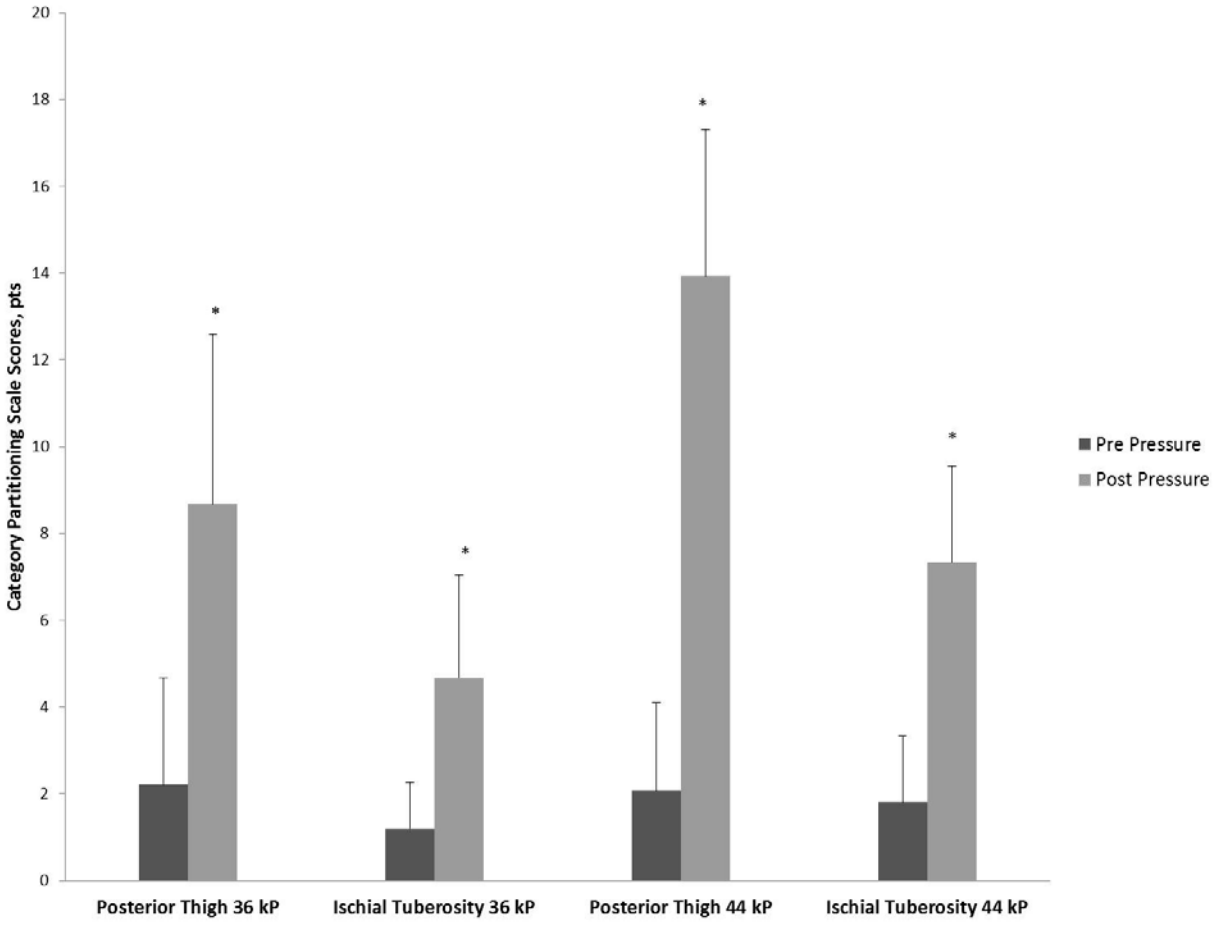

Figure 35. Category Partitioning Scale scores for project two. kP: kilopascals; pts: points; * = *P* < 0.05.

The descriptor scores for the McGill Pain Questionnaire yielded a significant location x time two-way interaction (Wilks' $\Lambda = 0.44$; $F_{(1,14)} = 17.79$, $P = 0.001$; $\eta_p^2 = 0.56$). Follow-up *t*-tests for this interaction indicated a significant effect of time with 36 kilopascals of pressure at the posterior thigh ($t_{(14)} = -3.37$, $P = 0.005$) and the ischial tuberosity ($t_{(14)} = -2.75$, $P = 0.016$); and at 44 kilopascals of pressure applied to the posterior thigh ($t_{(14)} = -6.44$, $P < 0.0001$) and the

ischial tuberosity ($t_{(14)} = -4.53$, $P < 0.0001$), indicating the MPQ scores were higher during pressure application than baseline measures regardless of pressure magnitude or application location (Figure 36). The visual analog scale scores for the McGill Pain Questionnaire yielded significant magnitude x time (Wilks' $\Lambda = 0.54$; $F_{(1,14)} = 11.58$, $P = 0.004$; $\eta_p^2 = 0.45$) and location x time (Wilks' $\Lambda = 0.55$; $F_{(1,14)} = 11.23$, $P = 0.005$; $\eta_p^2 = 0.44$) two-way interactions. Follow-up *t*-tests for the magnitude x time interaction demonstrated significant effects of time at a pressure magnitude of 36 kilopascals at the posterior thigh ($t_{(14)} = -3.66$, $P = 0.003$) and the ischial tuberosity ($t_{(14)} = -2.53$, $P < 0.024$), indicating that visual analog scale scores are higher during 36 kilopascals of pressure application compared to baseline at both the posterior thigh and ischial tuberosity. At a pressure magnitude of 44 kilopascals, a significant effect of time was also present at the posterior thigh ($t_{(14)} = -4.45$, $P = 0.001$) and the ischial tuberosity ($t_{(14)} = -3.20$, $P = 0.006$). Similarly, this indicates higher reported discomfort during the application of 44 kilopascals of pressure at both test locations. There was also a significant effect of magnitude during the pressure application time point at the posterior thigh application site ($t_{(14)} = -2.59$, $P = 0.021$), indicating that 44 kilopascals of pressure elicited higher levels of discomfort compared to the 36 kilopascal magnitude at the posterior thigh. Follow-up *t*-tests for the location x time interaction effect indicated significant effects of pressure application location at both 36 ($t_{(14)} = 2.57$, $P = 0.022$) and 44 ($t_{(14)} = 2.98$, $P = 0.01$) kilopascals of pressure at the during pressure application time point. This suggests that during both 36 and 44 kilopascals of pressure, visual analog scores were higher at the posterior thigh than the ischial tuberosity (Figure 37). The present pain intensity scores for the McGill Pain Questionnaire yielded significant magnitude x time (Wilks' $\Lambda = 0.57$; $F_{(1,14)} = 10.33$, $P = 0.006$; $\eta_p^2 = 0.43$) and location x time (Wilks' $\Lambda = 0.72$; $F_{(1,14)} = 5.56$, $P = 0.033$; $\eta_p^2 = 0.28$) two-way interaction effects. Follow-up *t*-tests

indicated a significant effect of time at both pressure magnitude and location conditions: 36 kilopascals at the posterior thigh ($t_{(14)}$ = -3.50, P = 0.004); 36 kilopascals at the ischial tuberosity ($t_{(14)}$ = -2.65, P = 0.019), indicating the pressure present pain intensity scores were higher during 36 kilopascals of pressure application at both the posterior thigh and ischial tuberosity; 44 kilopascals at the posterior thigh ($t_{(14)}$ = -5.12, P < 0.0001), suggesting that discomfort scores are higher during 44 kilopascals of pressure at the posterior thigh compared to baseline; and 44 kilopascals at the ischial tuberosity ($t_{(14)}$ = -4.00, P = 0.001), meaning that present pain intensity scores during 44 kilopascals of pressure at the ischial tuberosity are higher than baseline measures (Figure 38).

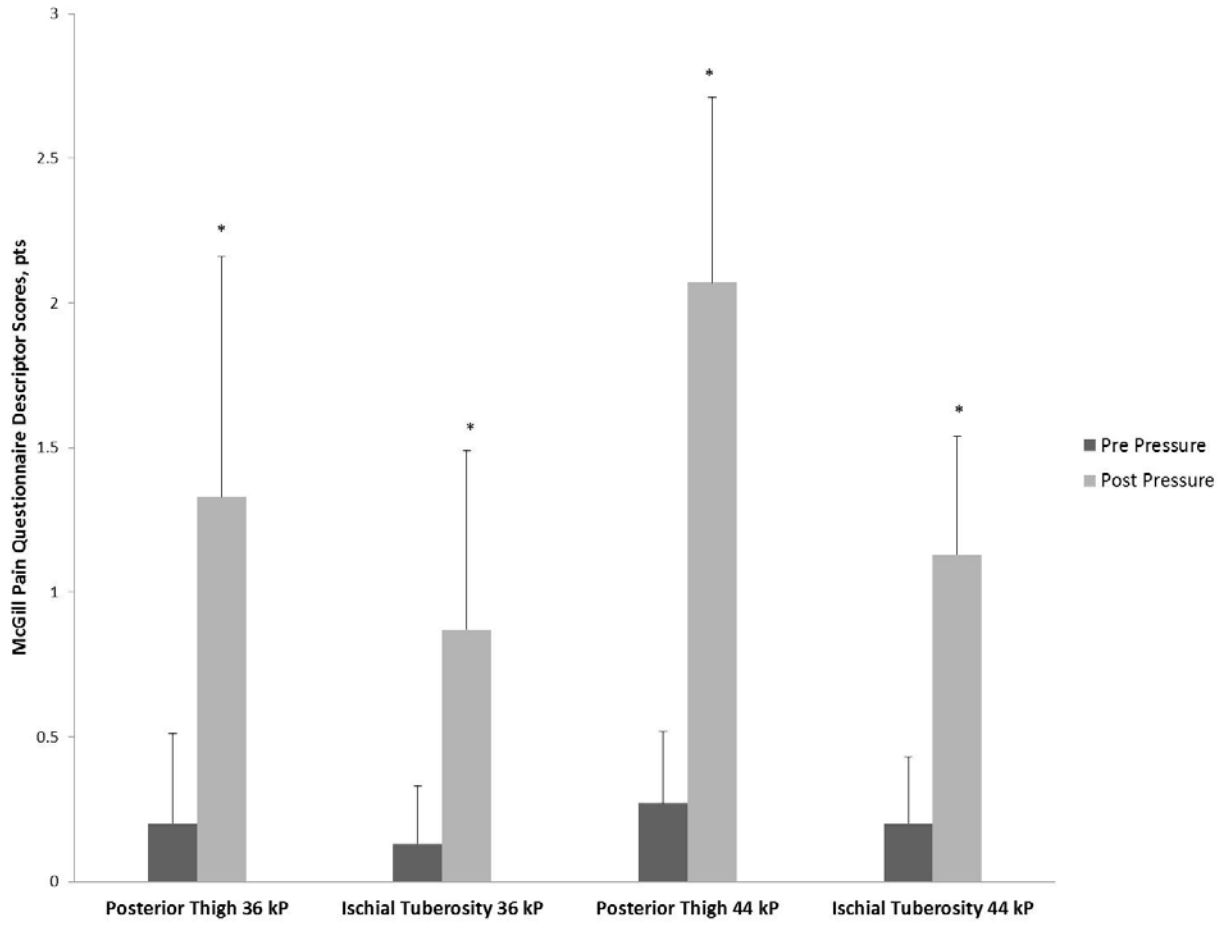

Figure 36. Short Form McGill Pain Questionnaire descriptor scores for project two. kP: kilopascals; pts: points; * = P < 0.05.

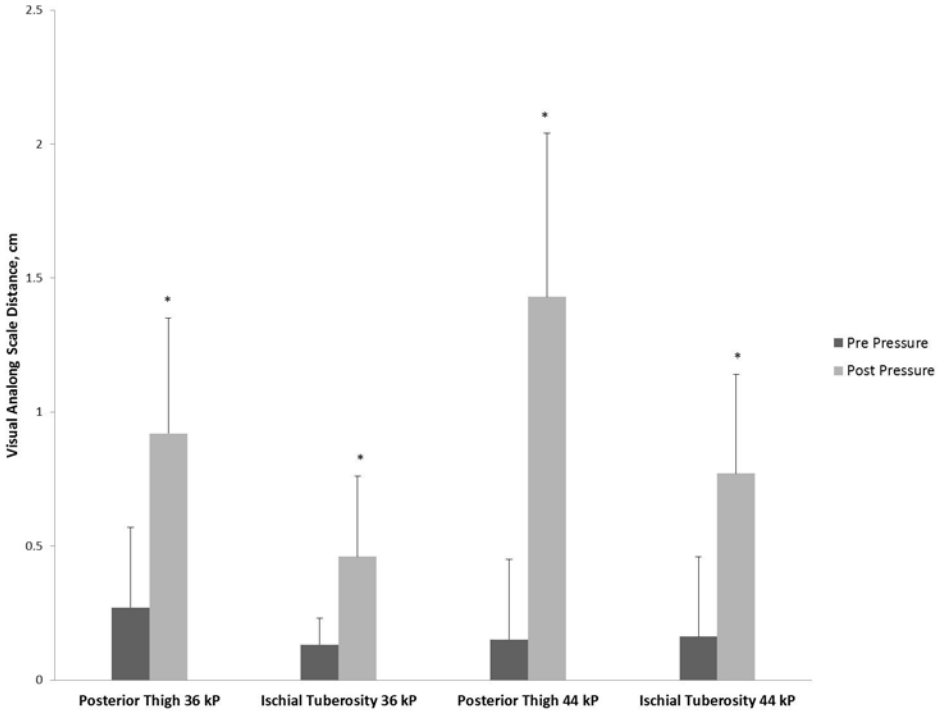

Figure 37. Visual Analog Scale scores for project two. kP: kilopascals; cm: centimeter; * = $P < 0.05$.

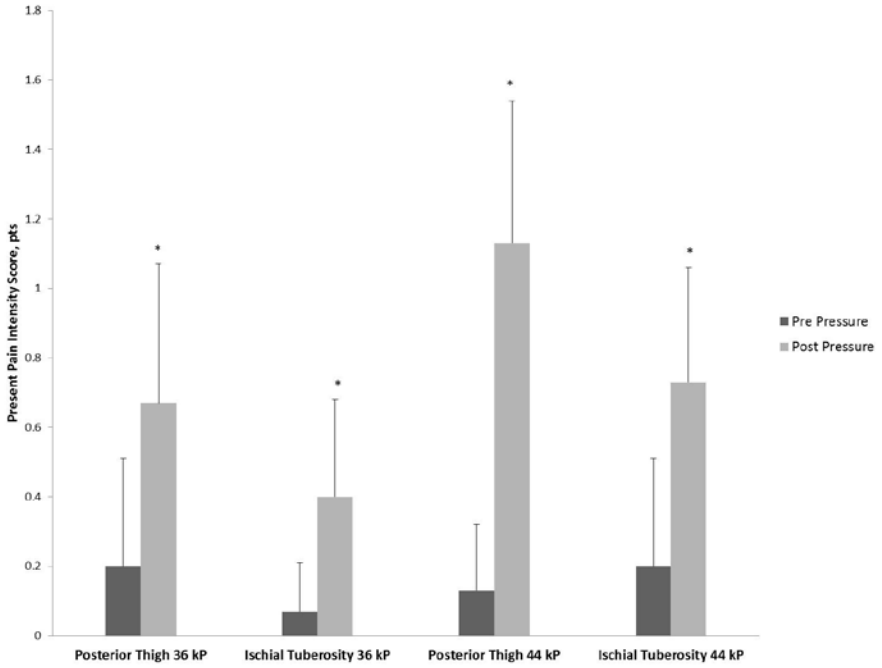

Figure 38. Present Pain Intensity scores for project two. kP: kilopascals; pts: points; * = *P* < 0.05.

Using a 2 x 2 x 2 factorial repeated measures ANVOA, the Semmes-Weinstein Monofilament Test scores at the great toe indicated no significant three-way interaction (Wilks' $\Lambda = 0.99$; $F_{(1,14)} = 0.015$, $P = 0.904$; $\eta_p^2 = 0.001$), no two-way location x time (Wilks' $\Lambda = 0.99$; $F_{(1,14)} = 0.043$, $P = 0.838$; $\eta_p^2 = 0.003$), no magnitude x time (Wilks' $\Lambda = 0.99$; $F_{(1,14)} = 0.12$, $P = 0.732$; $\eta_p^2 = 0.009$), or no magnitude x location (Wilks' $\Lambda = 0.96$; $F_{(1,14)} = 0.64$, $P = 0.438$; $\eta_p^2 = 0.044$) interactions. A significant difference for the main effect of time (Wilks' $\Lambda = 0.75$; $F_{(1,14)} = 4.78$, $P = 0.046$; $\eta_p^2 = 0.26$) was found. Follow-up *t*-tests for the main effect of time found that monofilament test scores at the great toe were significantly lower at the pre-pressure application time point than the during pressure application time point ($t_{(14)} = -0.119$, $P = 0.046$). This indicates that pressure sensitivity decreases with during pressure application regardless of pressure application location or magnitude. The Semmes-Weinstein Monofilament Test scores

at the third metatarsal revealed no significant three-way interaction (Wilks' $\Lambda = 0.92$; $F_{(1,14)} = 1.26$, $P = 0.280$; $\eta_p^2 = 0.083$); no two-way interactions: location x time (Wilks' $\Lambda = 0.80$; $F_{(1,14)} = 3.498$, $P = 0.082$; $\eta_p^2 = 0.20$), magnitude x time (Wilks' $\Lambda = 0.92$; $F_{(1,14)} = 1.23$, $P = 0.285$; $\eta_p^2 = 0.081$), magnitude x location (Wilks' $\Lambda = 0.99$; $F_{(1,14)} = .024$, $P = 0.879$; $\eta_p^2 = 0.002$); nor significant main effects of magnitude (Wilks' $\Lambda = 0.95$; $F_{(1,14)} = .792$, $P = 0.389$; $\eta_p^2 = 0.054$), location (Wilks' $\Lambda = 1.00$; $F_{(1,14)} = 0.00$, $P = 0.995$; $\eta_p^2 = 0.000$), or time (Wilks' $\Lambda = 0.94$; $F_{(1,14)} = 0.89$, $P = 0.361$; $\eta_p^2 = 0.060$). Indicating that pressure sensitivity at the third metatarsal is unchanged with local pressure application. Similar results were found for the Semmes-Weinstein Monofilament Test at the fifth metatarsal with no significant three-way interaction (Wilks' $\Lambda = 0.99$; $F_{(1,14)} = 0.015$, $P = 0.903$; $\eta_p^2 = 0.001$); two-way interactions: location x time (Wilks' $\Lambda = 0.96$; $F_{(1,14)} = 0.58$, $P = 0.458$; $\eta_p^2 = 0.040$), magnitude x time (Wilks' $\Lambda = 0.99$; $F_{(1,14)} = 0.098$, $P = 0.759$; $\eta_p^2 = 0.007$), magnitude x time (Wilks' $\Lambda = 0.91$; $F_{(1,14)} = 1.36$, $P = 0.264$; $\eta_p^2 = 0.088$); nor simple main effects: magnitude (Wilks' $\Lambda = 1.00$; $F_{(1,14)} = 0.002$, $P = 0.963$; $\eta_p^2 = 0.00$), location (Wilks' $\Lambda = 0.93$; $F_{(1,14)} = 1.09$, $P = 0.315$; $\eta_p^2 = 0.072$), time (Wilks' $\Lambda = 0.76$; $F_{(1,14)} = 4.42$, $P = 0.054$; $\eta_p^2 = 0.240$) found. This means that no changes in pressure sensitivity at the fifth metatarsal were detected regardless of the conditions or time points used in the present study (Figure 39).

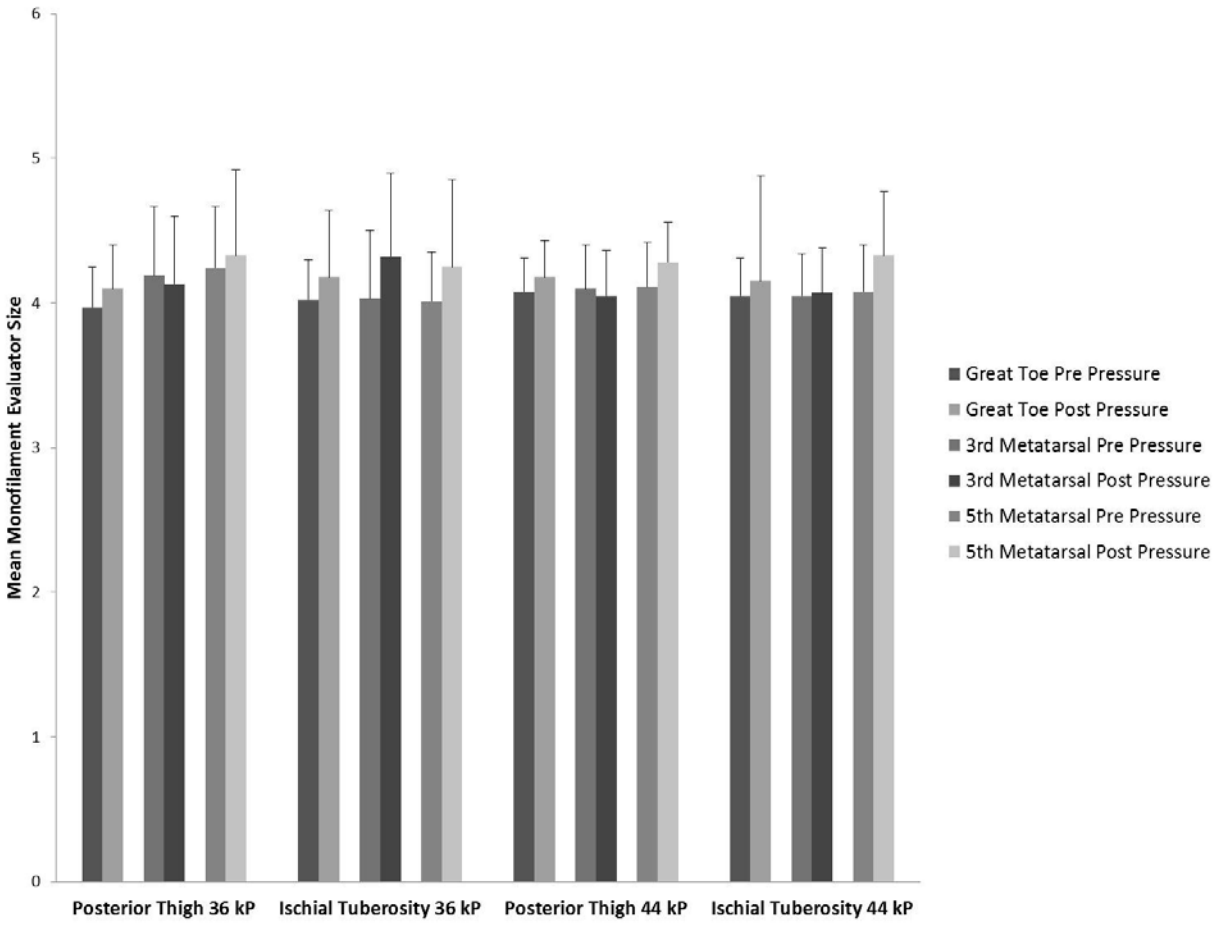

Figure 39. Semmes-Weinstein monofilament test scores for project two. kP: kilopascals.

A 2 x 2 x 2 factorial repeated measures ANOVA revealed that the two-point discrimination test scores recorded at the great toe had no significant three-way or two-way interactions: magnitude x location x time (Wilks' $\Lambda = 0.81$; $F_{(1,14)} = 3.21$, $P = 0.095$; $\eta_p^2 = 0.187$), location x time (Wilks' $\Lambda = 0.97$; $F_{(1,14)} = 0.491$, $P = 0.495$; $\eta_p^2 = 0.034$), magnitude x time (Wilks' $\Lambda = 0.99$; $F_{(1,14)} = 0.017$, $P = 0.900$; $\eta_p^2 = 0.001$), and magnitude x location (Wilks' $\Lambda = 0.96$; $F_{(1,14)} = 0.614$, $P = 0.446$; $\eta_p^2 = 0.042$). Additionally, no significant differences were found for the main effects of magnitude (Wilks' $\Lambda = 0.99$; $F_{(1,14)} = 0.063$, $P = 0.805$; $\eta_p^2 = 0.004$), location (Wilks' $\Lambda = 0.99$; $F_{(1,14)} = 0.02$, $P = 0.889$; $\eta_p^2 = 0.001$), or time (Wilks' $\Lambda = 0.95$; $F_{(1,14)}$

= 0.779, $P = 0.392$; $\eta_p^2 = 0.053$). This indicates that no change in receptive field size occurs as a result of local pressure application. No significant interaction or main effects were found for the two-point discrimination test scores at the medial malleolus: magnitude x location x time (Wilks' $\Lambda = 0.96$; $F_{(1,14)} = 0.58$, $P = 0.458$; $\eta_p^2 = 0.040$), location x time (Wilks' $\Lambda = 0.99$; $F_{(1,14)} = 0.03$, $P = 0.865$; $\eta_p^2 = 0.002$), magnitude x time (Wilks' $\Lambda = 0.78$; $F_{(1,14)} = 3.89$, $P = 0.068$; $\eta_p^2 = 0.22$), magnitude x location (Wilks' $\Lambda = 0.99$; $F_{(1,14)} = 0.062$, $P = 0.806$; $\eta_p^2 = 0.004$), magnitude (Wilks' $\Lambda = 0.99$; $F_{(1,14)} = 0.062$, $P = 0.806$; $\eta_p^2 = 0.004$), location (Wilks' $\Lambda = 0.89$; $F_{(1,14)} = 1.75$, $P = 0.207$; $\eta_p^2 = 0.11$), and time (Wilks' $\Lambda = 0.97$; $F_{(1,14)} = 0.52$, $P = 0.485$; $\eta_p^2 = 0.035$). Two-point discrimination test scores at the lateral malleolus yielded no significant three-way interaction, two-way interactions, or main effects: magnitude x location x time (Wilks' $\Lambda = 0.98$; $F_{(1,14)} = 0.223$, $P = 0.64$; $\eta_p^2 = 0.016$), location x time (Wilks' $\Lambda = 0.88$; $F_{(1,14)} = 1.88$, $P = 0.192$; $\eta_p^2 = 0.119$), magnitude x time (Wilks' $\Lambda = 0.95$; $F_{(1,14)} = 0.78$, $P = 0.389$; $\eta_p^2 = 0.053$), magnitude x location (Wilks' $\Lambda = 0.99$; $F_{(1,14)} = 0.07$, $P = 0.80$; $\eta_p^2 = 0.005$), magnitude (Wilks' $\Lambda = 0.99$; $F_{(1,14)} = 0.157$, $P = 0.698$; $\eta_p^2 = 0.011$), location (Wilks' $\Lambda = 0.99$; $F_{(1,14)} = 0.031$, $P = 0.862$; $\eta_p^2 = 0.002$), and time (Wilks' $\Lambda = 0.78$; $F_{(1,14)} = 3.91$, $P = 0.068$; $\eta_p^2 = 0.218$). Similar to the great toe, two-point discrimination scores at the medial and lateral malleoli suggest that receptive field size or sensitivity is not altered with local pressure application to the posterior thigh or ischial tuberosity (Figure 40).

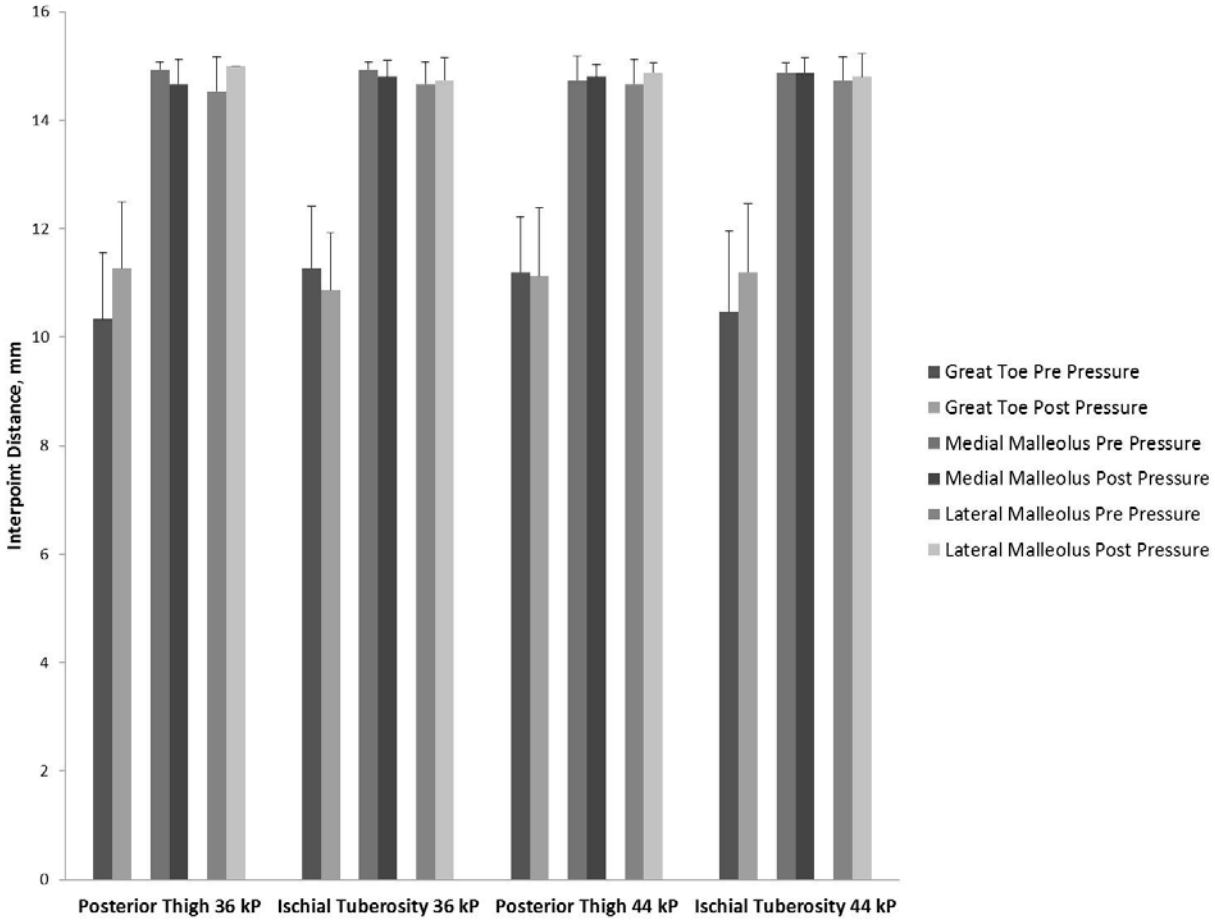

Figure 40. Two-point discrimination test scores for project two. kP: kilopascals; mm: millimeter.

Using a 2 x 2 x 2 factorial repeated measures ANOVA, percent oxygen saturation of the dominant foot great toe did not yield significant three-way or two-way interaction effects: magnitude x location x time (Wilks' $\Lambda = 0.93$; $F_{(1,14)} = 1.03$, $P = 0.327$; $\eta_p^2 = 0.069$), location x time (Wilks' $\Lambda = 0.99$; $F_{(1,14)} = 0.036$, $P = 0.852$; $\eta_p^2 = 0.003$), magnitude x time (Wilks' $\Lambda = 0.99$; $F_{(1,14)} = 0.09$, $P = 0.758$; $\eta_p^2 = 0.007$), or magnitude x location (Wilks' $\Lambda = 0.85$; $F_{(1,14)} = 2.52$, $P = 0.135$; $\eta_p^2 = 0.15$). There were also no significant main effects of magnitude (Wilks' $\Lambda = 0.94$; $F_{(1,14)} = 0.840$, $P = 0.375$; $\eta_p^2 = 0.057$), location (Wilks' $\Lambda = 0.95$; $F_{(1,14)} = 0.76$, $P = 0.40$; $\eta_p^2 = 0.051$), or time (Wilks' $\Lambda = 0.98$; $F_{(1,14)} = 0.27$, $P = 0.61$; $\eta_p^2 = 0.019$). This data suggest

that local pressure application to the posterior thigh or ischial tuberosity does not alter limb oxygen saturation when measured with pulse oximetry (Figure 41).

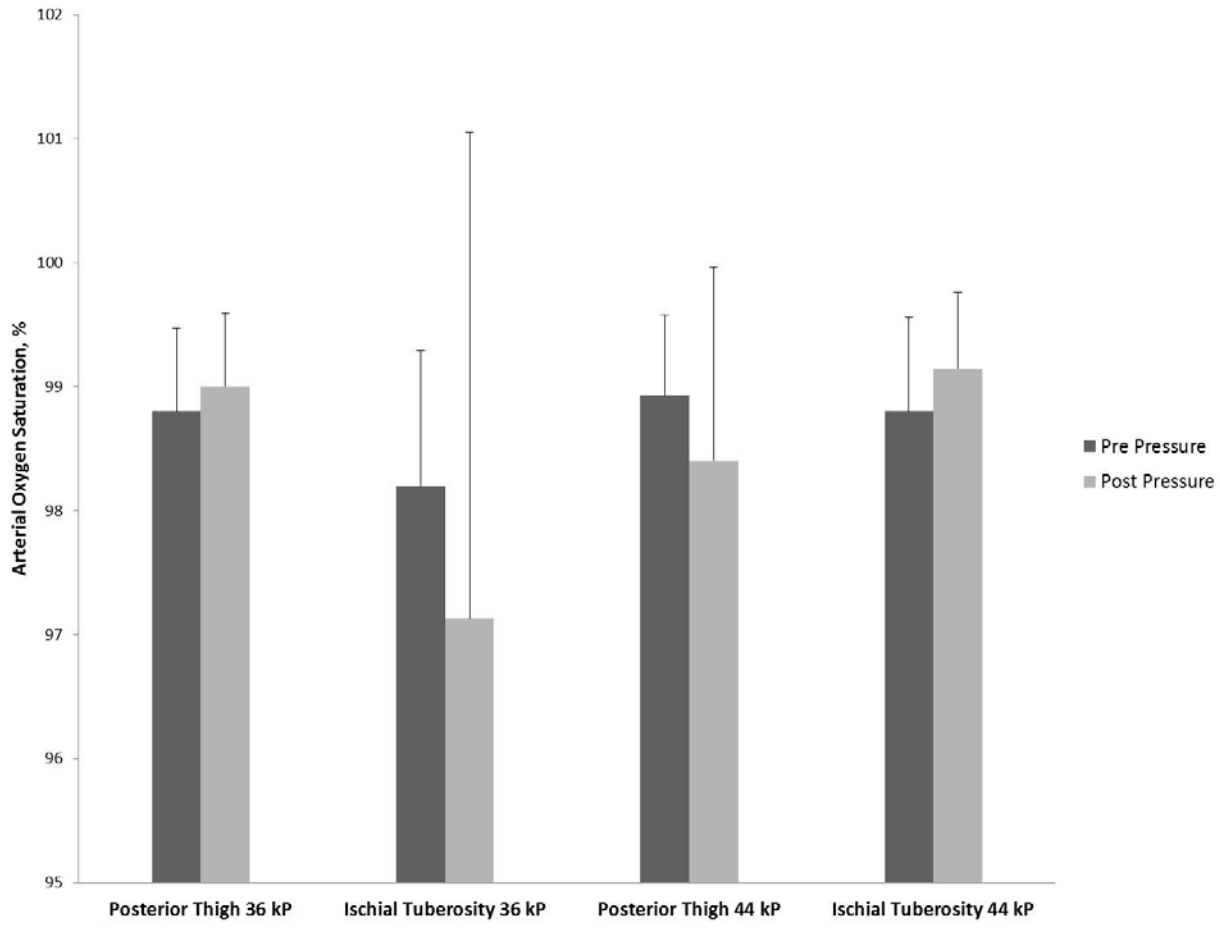

Figure 41. Percent arterial oxygen saturation for project two. kP: kilopascal; %: percent.

A 2 x 2 x 2 three-way (magnitude x location x time) repeated measures ANOVA examining anterior ankle temperatures revealed no significant three-way interaction (Wilks' Λ = 0.93; $F_{(1,14)} = 0.840$, $P = 0.343$; $\eta_p^2 = 0.064$). Additionally, no two-way interactions were found: location x time (Wilks' $\Lambda = 1.00$; $F_{(1,14)} = 0.001$, $P = 0.976$; $\eta_p^2 = 0.00$), magnitude x time (Wilks' $\Lambda = 0.96$; $F_{(1,14)} = 0.562$, $P = 0.466$; $\eta_p^2 = 0.039$), or magnitude x location (Wilks' Λ = 1.00; $F_{(1,14)} > 0.001$, $P = 0.994$; $\eta_p^2 = 0.00$). Test for main effects revealed a significant effect of

time (Wilks' $\Lambda = 0.23$; $F_{(1,14)} = 45.42$, $P > 0.001$; $\eta_p^2 = 0.76$), but not for location (Wilks' $\Lambda = 0.96$; $F_{(1,14)} = 2.14$, $P = 0.165$; $\eta_p^2 = 0.133$) or magnitude (Wilks' $\Lambda = 0.94$; $F_{(1,14)} = 0.83$, $P = 0.377$; $\eta_p^2 = 0.056$). A follow-up pairwise comparison of the two data collection time points revealed a significant increase in anterior ankle skin temperature during pressure application ($t_{(14)} = -0.61$; $P > 0.001$). These data suggest that during a 10 minute pressure application session superficial skin temperature is increased. To analyze lateral ankle skin temperatures a 2 x 2 x 2 three-way (magnitude x location x time) repeated measures ANOVA was completed and revealed no significant three-way interaction (Wilks' $\Lambda = 0.87$; $F_{(1,14)} = 1.940$, $P = 0.185$; $\eta_p^2 = 0.12$). No two-way interactions were found: location x time (Wilks' $\Lambda = 0.94$; $F_{(1,14)} = 0.79$, $P = 0.388$; $\eta_p^2 = 0.054$), magnitude x time (Wilks' $\Lambda = 0.96$; $F_{(1,14)} = 0.584$, $P = 0.457$; $\eta_p^2 = 0.04$), or magnitude x location (Wilks' $\Lambda = 0.974$; $F_{(1,14)} = 0.37$, $P = 0.55$; $\eta_p^2 = 0.026$). Additionally, no significant main effects were found for magnitude (Wilks' $\Lambda = 0.99$; $F_{(1,14)} = 0.11$, $P = 0.740$; $\eta_p^2 = 0.008$), location (Wilks' $\Lambda = 0.89$; $F_{(1,14)} = 1.66$, $P = 0.21$; $\eta_p^2 = 0.10$), or time (Wilks' $\Lambda = 0.81$; $F_{(1,14)} = 3.25$, $P = 0.093$; $\eta_p^2 = 0.18$). These data indicate that skin temperature at the lateral ankle do not change as a result of pressure application. Anterior and lateral ankle temperature data are summarized in Figure 42.

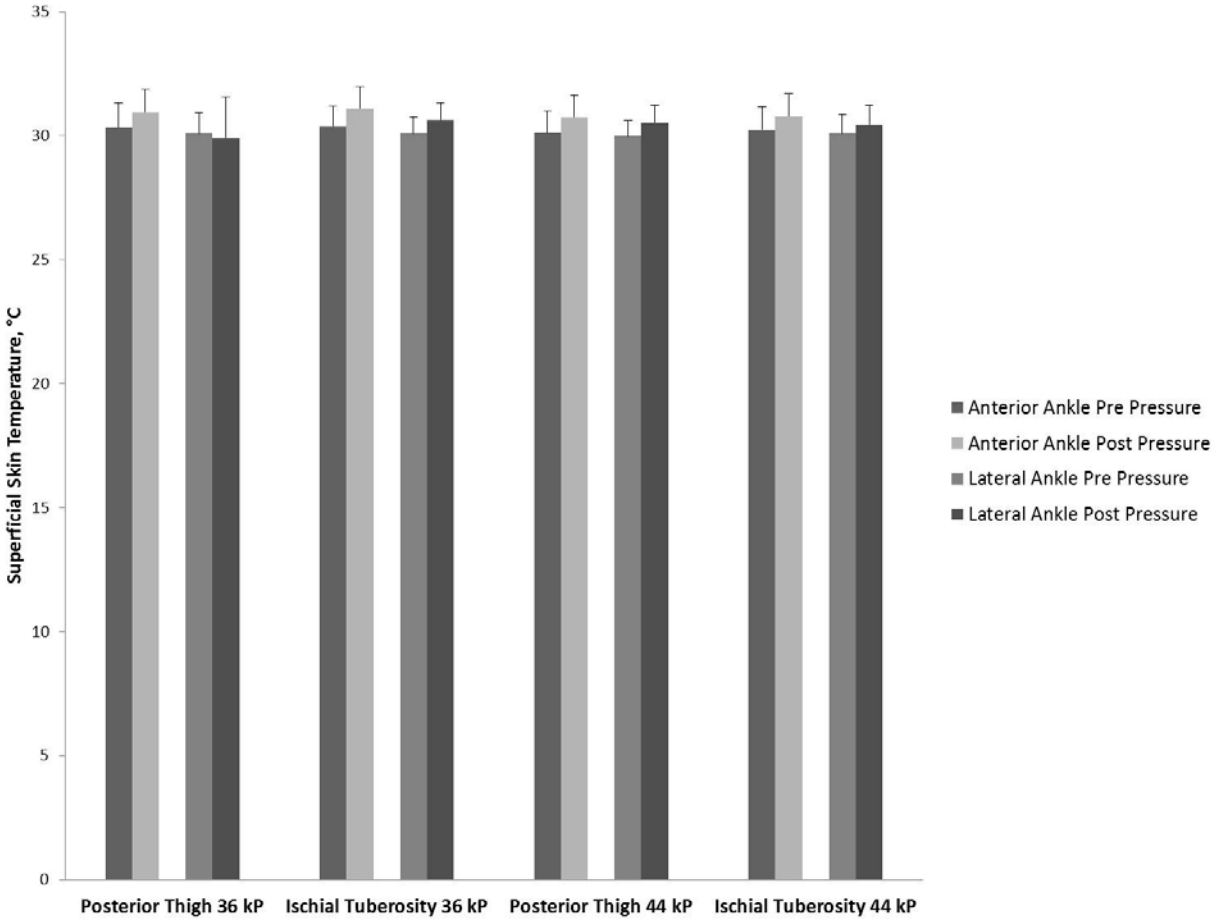

Figure 42. Anterior and lateral ankle temperatures during project two. kP: kilopascals; C: Celsius.

Discussion

This study examined the effects of local pressure application applied at two locations (ischial tuberosity and the posterior thigh) and at two pressure magnitudes (36 and 44 kilopascals) on subjective discomfort scores, lower extremity sensibility, total limb blood oxygenation levels, and superficial skin temperature. We hypothesized that the higher pressure application would elicit greater changes in measures of discomfort, sensibility, blood oxygenation, and superficial skin temperature.

Subject Discomfort

Category Partitioning Scale scores increased with all pressure application locations and magnitudes across 10 minutes of pressure application. Our data reveal that all pressure application conditions significantly increased discomfort when compared to baseline measures. Pressure applied to the posterior thigh at 36 kilopascals resulted in a statistically significant 5.5 point increase in discomfort; while pressure applied at 44 kilopascals to the posterior thigh significantly increased discomfort by 7.5 points. Similarly, pressure applied to the ischial tuberosity at a magnitude of 36 kilopascals increased discomfort by 3.1 points compared to baseline, while 44 kilopascals of pressure magnitude produced an increase of 4.2 points. The significant magnitude x time and location x time two-way interactions and associated pairwise comparisons indicated that pressure application to the posterior thigh increases discomfort more than pressure application at the ischial tuberosity. Additionally, 44 kilopascals of pressure application elicited higher levels of discomfort compared to 36 kilopascals of pressure. This supports our hypothesis that greater magnitudes at the posterior thigh would result in greater discomfort. Our hypothesis is based on the underlying anatomy at both of the pressure application sites. The ischial tuberosities are bony prominences which are designed to bear weight during sitting. Whereas, pressure application to the posterior thigh could result in compression of nervous and vascular system tissues (the sciatic nerve and femoral vein, respectively).[31] Previous work examined the effects of local pressure application on discomfort utilizing 9 minutes of local pressure applied to the posterior thigh or ischial tuberosity at a magnitude of 28 kilopascals.[85] Subject comfort was assessed using a 1-10 scale in which 10 represented “Extremely Comfortable” and 1 represented “Pain and Distress.”[85] No significant differences were found between the posterior thigh pressure application condition scores (7.00)

and the ischial tuberosity condition scores (7.80).[85] The present study found that pressure application location is an important factor in perceived discomfort. We suspect the differences between this study and previous work are a result of the higher pressure magnitudes applied to the test locations.

Subjective discomfort levels measured with the McGill Pain Questionnaire also demonstrated that local pressure application increases levels of subjective discomfort. The McGill Pain Questionnaire descriptor scores increased by 3 points at the posterior thigh and 2 points at the ischial tuberosity during 36 kilopascals of pressure application. Descriptor scores significantly increased by 6 points at the posterior thigh and 4 points at the ischial tuberosity during 44 kilopascals of pressure application. Subjective discomfort increases with pressure application when compared to the baseline as did the Category Partitioning Scale. The visual analog scale portion of the McGill Pain Questionnaire supports the hypothesis that local pressure application to the posterior thigh at higher pressure magnitude elicits greater discomfort. We found that 44 kilopascals of pressure applied to the posterior thigh resulted in a statistically significant 0.5 centimeter greater increase in reported discomfort compared to 36 kilopascals of pressure applied to the posterior thigh. The ischial tuberosity visual analog scale scores were 0.3 centimeters greater following 10 minutes of 44 kilopascal pressure application compared to 36 kilopascals of pressure application however, these were not statistically different. The third portion of the McGill Pain Questionnaire, the present pain intensity score, supports that local pressure application to the ischial tuberosity and posterior thigh results in higher levels of perceived discomfort compared to baseline measures. Present pain intensity scores increased significantly with 36 kilopascals of pressure by 0.4 points when applied to the posterior thigh and increased significantly by 0.3 points when applied to the ischial tuberosity. Likewise, present

pain intensity scores during 44 kilopascals of pressure application significantly increased by 1 point when applied to the posterior thigh and significantly increased by 0.53 points when applied to the ischial tuberosity. Together the McGill Pain Questionnaire data suggests that local pressure application at 36 and 44 kilopascals to the buttocks and posterior thigh increases subjective discomfort, and this increased discomfort may be greater when applied at the posterior thigh at 44 kilopascals of pressure although this is inconclusive. Previous seating research using pressure mapping pads found "hot spots" of high pressure located under the ischial tuberosities.[1,3,15] In this project we found that isolated local pressure application to the ischial tuberosity increases discomfort using multiple measures of subjective discomfort. This discomfort could interfere with mission success and task performance.

Sensibility Measures

The Semmes-Weinstein monofilament test results revealed that sensitivity to point pressure is diminished at the great toe during local pressure at the pressure magnitudes and locations used in this study. Semmes-Weinstein monofilament test scores at the plantar aspect of the third and the fifth metatarsals did not indicate a change in point pressure sensitivity. This was the first study to examine the effects of local pressure application on point pressure sensitivity at the foot. Previous work in our laboratory did find that the Semmes-Weinstein monofilament test scores were diminished at the plantar aspect of the fifth metatarsal during four hours of prolonged restricted sitting.[292] Our previous work did not find corresponding changes at the great toe and third metatarsal locations.[292] This finding was attributed to the different dermatomes of the foot that serve the three test locations. The great toe and the third metatarsal

test locations both are within the dermatome of the L5 nerve root, while the fifth metatarsal test location is located within the S1 nerve root dermatome. We would expect that a change in the great toe would be accompanied by changes at the third metatarsal. The differences observed in this study could be due to differences in sensitivity at each individual test location. An examination of the effect sizes found that the great toe and fifth metatarsal test locations had similar effect sizes ($\eta_p^2 = 0.25$ and $\eta_p^2 = 0.24$, respectively), whereas the effect size at the third metatarsal was much lower ($\eta_p^2 = 0.06$). This indicates that the great toe had greater changes in sensitivity than the third metatarsal test location, and although it was not statistically significant ($P = 0.54$), the great toe and fifth metatarsal had similar responses. If we further examine the mean variability across all conditions at the great toe and third metatarsal test locations we find that measures taken at the third metatarsal were more variable than measures taken at the great toes (mean standard deviation = 0.71 and mean standard deviation = 0.51, respectively). This may explain why we did not see changes to sensitivity at the third metatarsal even though the great toe and third metatarsal test locations were located in within the same L5 nerve root dermatome. The similar effect sizes suggest that the test locations had the same clinical response although we saw different statistical results with great toe sensitivity being statistically significant and fifth metatarsal sensitivity being non-significant. The low effect size of the third metatarsal test location suggests that there was a minimal clinical response. Effect sizes aid in determining the true effect of a treatment on a measure which can better guide clinical decision-making.[293] The pressure application produced similar changes at the great toe and fifth metatarsal test locations, but we cannot determine if these differences were clinically significant. Previous research has found that the threshold for normal deep pressure and sensation on the plantar surface of the foot is 3.61.[284] Since all of the baseline and test means for the great toe and

fifth metatarsal were above this threshold distinguishing between the two is difficult. Future work should determine clinically important thresholds for decreased lower extremity sensitivity utilizing the monofilament test at each of the testing locations on the foot. This would provide military medical personnel an easy method of determining sensitivity changes seen in the foot during prolonged missions. Researchers would then be able to determine if pilots are at a real risk of decreasing mission efficacy.

The two-point discrimination measure of lower extremity sensibility remained unaltered during all of the testing magnitudes, locations, and times. This suggests that the receptive fields of the foot and ankle do not change as a result of local pressure application. Previous work examining local pressure application to the posterior thigh and ischial tuberosity found that two-point discrimination scores also remained unaltered with 9 minutes of pressure application at 28 kilopascals.[85] However, comparison between previous work and the current project is difficult because detailed procedures and testing locations in previous research are unavailable.[85] Other previous work examining the effects of prolonged restricted sitting on two-point discrimination scores suggested that the two-point discrimination test was not sensitive enough to detect changes in cutaneous receptive field sensistity.[292] In the current study, it is possible that the local pressure magnitude or duration was not sufficient to elicit a response. The two-point discrimination in a valuable tool within the clinical setting to detect changes to receptive field sensitivity,[203,206] but may not be viable as an outcome measure in studies exploring symptoms of temporary parathesia in otherwise healthy adults.

Vascular Measures

We measured changes in blood oxygen saturation levels for the lower extremity using portable pulse oximetry. Our results indicate that oxygen saturation of the dominant limb of participants is not changed as a result of local pressure application to the ischial tuberosity or posterior thigh. These data suggest that local pressure application does not alter limb oxygenation levels at the levels we tested in the current study. To our knowledge, this was the first study to examine changes in limb oxygenation levels during local pressure application to the posterior thigh or ischial tuberosity. Our results are in line with previous work assessing blood oxygenation levels during sitting.[3,292] In a study of 8 hours of prolonged restricted sitting in an F-16 ejection seat no significant change in gastrocnemius muscle oxygenation levels were found when measured by near infrared thermography.[3] Another study examining the effects of 4 hours of restricted sitting in Black Hawk helicopter seats found no significant change in total limb oxygen saturation when measured with pulse oximetry.[292] These combined works suggest that that the reported discomfort and temporary parathesia in the lower extremity are not due to areas of localized high seat interface pressure altering blood oxygenation levels. However, this interpretation has limitations. None of the existing research has utilized a model in which participants actively use their legs and feet to operate the anti-torque pedals in a rotary-winged aircraft. Actively contracting muscle tissue requires nutrients and oxygen for steady, prolonged activities. Rotary-winged pilots must actively contract the lower extremity muscles during flight. If there is an occlusion of fresh blood due to areas of high pressure from prolonged sitting, it is possible that a decrease in oxygen saturation could occur. This diminished oxygen saturation could, in part, be responsible for the reported discomfort and parathesia in Black Hawk helicopter pilots during prolonged flight. Future research should test this hypothesis by

measuring oxygen saturation during a bout of prolonged restricted sitting and with local pressure application while participants complete activities similar to operating helicopter anti-torque pedals.

Superficial skin temperature measurements found that anterior ankle temperature increased during the ten minutes of pressure application at all pressure magnitudes and locations. The temperature increased by 0.61° C across the 10 minute pressure application time period and had a large effect size of 0.76. Previous work has shown that an increase of 0.5° C is clinically significant.[286] Superficial skin temperature has been shown to be a non-contact, indirect measure of skin blood perfusion.[286] These results suggest that skin blood flow is increased with local pressure application. We suspect that this increase in superficial skin blood flow was a result of decreased venous return due to decreased lower extremity muscle contractions and occlusion of the venous return from the periphery near the sitting surface of the body. The veins have a very low pressure,[294] and we suspect that the extra-venous pressure from sitting was great enough to occlude major routes of venous return such as the femoral vein. Additionally, following 3-5 minutes of inactivity the lower extremity veins are filled and serve as a reservoir for blood.[294] This would suggest that halfway through the 10 minute pressure application session, the lower extremity venous system would be filled with warm, arterial blood. The short 10 minute testing period may not have allowed for adequate heat exchange between the warmed lower leg and the ambient air resulting in the observed increase temperature at the 10 minute data collection time point. This is the first study to examine the effects of local pressure application on superficial skin temperature in a functional, seated position. We hypothesize that if we continued to measure superficial skin temperature, we would see a gradual decrease in skin temperature as time increased due to loss of heat through the heat exchange between the skin's surface and the

ambient air. Previous work has shown that with four hours of prolonged restricted sitting in a Black Hawk helicopter seat superficial skin temperature decreases significantly.[292] In this previous work, temperature was measured every 30 minutes, so no observations of the immediate effects of sitting on skin temperature are available. Future work should track the effects local pressure application and recovery from local pressure application on superficial skin temperature to better understand changes occurring at the onset of pressure application and during the recovery from pressure application.

Conclusions

Prolonged restricted sitting in rotary-winged aviators has been shown to increase discomfort and the symptoms of temporary parathesia. One hypothesis as to the cause of this reported discomfort and temporary parathesia is that areas of locally high pressure are created during prolonged sitting which in turn compresses vascular and neurological structures. We tested this hypothesis by applying two magnitudes of pressure at two locations. We found that local application increases subjective discomfort, decreases lower extremity sensitivity, and increases superficial skin temperature at the anterior ankle. These results support the hypothesis that locally high pressure creates symptoms of discomfort and parathesia. However, research examining the effects of local pressure application on physiologic and neurologic function is needed. Moreover, work must be completed to determine if the changes observed in the present study lead to decreases in performance and negatively affect mission efficacy.

Chapter VI

Effects of Local Pressure and Pressure Recovery on Subjective Discomfort, Neurological Function, and Circulatory Measures

Introduction

Prolonged restricted sitting during long missions has been a challenge for aviators since World War II.[1] Seat designs have evolved from simple wooden seats to highly advanced, armored ejection seats; however, the problem of aviator discomfort negatively affecting mission performance has persisted despite changes to seat design.[1] Several studies have attempted improve mission effectiveness by elucidating the problem of aviator discomfort during flight using seat interface pressure mapping devices[3,9,15] and subjective discomfort scales.[3,9,11,15] Together these studies demonstrate that prolonged restricted sitting in aircraft results in higher levels of reported discomfort and high peak pressures.[3,9,11,15] This research provided important information such as the onset of discomfort during prolonged restricted sitting, but did not address the etiology of the reported discomfort and temporary parathesia. The primary hypothesis for the etiology of discomfort and temporary parathesia during prolonged restricted sitting has been that areas of locally high pressure on the buttocks and posterior thigh compresses the nervous and vascular tissue, resulting in discomfort, altered sensory function, and temporary parathesia.

The local pressure hypothesis is reasonable based on the previous research with pressure mapping systems which show areas of high pressure at locations on the buttocks and posterior thigh. Additionally, physiological research examining isolated nerves demonstrates that local pressure alters the downstream nerve function.[76,78] Moreover, the negative effects of local pressure application on nerve tissue effects mylenated nerves more than unmylenated nerves.[76] The sciatic nerve is the major nerve in the lower extremity of humans and is highly mylenated.[31] This further supports the hypothesis that local areas of high pressure could create symptoms of discomfort and temporary parathesia during prolonged sitting in aircraft. However, there is limited research testing this hypothesis in the context of prolonged sitting in humans. The assessment of the influence of local pressure application on nerve conduction velocity would provide a direct measure of nerve function in a seated position.

Research demonstrates that local pressure applied to the posterior aspect of the thigh and buttocks results in increased soleus Hoffmann reflex amplitude.[85] The Hoffmann reflex is a non-invasive measure of α-motoneuron pool excitability[86] providing valuable insight on changes to the central nervous system at the level of the spinal cord. The Hoffmann reflex has been used to examine responses to musculoskeletal injury,[105,108] pain,[115] and fatigue conditions.[116,117] While the results showing an increase in soleus Hoffmann reflex amplitude are interesting, they are difficult to interpret in the context of local pressures experienced during prolonged flight because the measures were taken in a prone position. The Hoffmann reflex is dependent on position[143] and results found in one position cannot be applied to other positions. Therefore, monitoring changes to α-motoneuron pool excitability in response to local pressure application during flight should be taken from a seated position for the most accurate interpretation.

Finally, compression of vascular tissues would likely influence distal blood flow. Assessment of peripheral blood perfusion using dynamic infrared thermography would provide a non-contact surface temperature assessment suggesting changes in blood flow before, during and after localized pressure application in the seated position. Additionally, pulse oximetry would provide an assessment of total limb oxygen saturation before, during, and after pressure application in a functional position. Together, these four measures would assist in the understanding of the physiological contributors to aviator discomfort and parathesia.

It is essential to examine the effects of local pressure application in a seated position in order to test the hypothesis that local pressure application is responsible for subjective discomfort and temporary parathesia. Therefore, the purpose of the current study was to examine the effect of local pressure application to two locations on the sitting surface of the body in a functional, seated position on subjective discomfort, neurological function, and vascular function in the lower extremity. These results will help elucidate the etiology of aviator discomfort and temporary parathesia and assist decreasing aviator injury and improving combat effectiveness.

Methods

Experimental Design

This study utilized a 3 x 5 factorial repeated measures design. The independent variables included location with three levels (ischial tuberosity, posterior thigh, and control) and time with five levels (pre-application, 5 minutes into-application, 10 minutes into-application, 5 minutes post-application, and 10 minutes post-application). The dependent variables included Category

Partitioning Scale scores, McGill Pain Questionnaire (descriptor, visual analog scale, and present pain intensity) scores, Semmes-Weinstein monofilament test (great toe, third metatarsal, and fifth metatarsal) scores, two-point discrimination (great toe, medial malleolus, and lateral malleolus) scores, dynamic infrared thermography (lateral lower leg and anterior lower leg) mean temperatures, pulse oximetry (percent oxygen saturation) levels, soleus H-reflex (mean peak-to-peak amplitude), and mean sural sensory nerve conduction velocity. Body composition data was collected using dual-energy x-ray absorptiometry (DXA) to examine if differences in body composition are present between participants, and if so, does a relationship exist between reported discomfort, sensibility, physiological measures, and body composition.

Participants

Thirty male volunteers responded to the solicitation (group presentations) to participant in the study. Thirty healthy male volunteers (age = 21.7 ± 2.2 years) completed the study. Participants self-reported no cardiovascular, neurological, or metabolic disorders; no current or two year history of surgery or fracture in the lumbar spine or lower extremity; no current history of lower back pain or lower extremity; and no current use of prescription or non-prescription pain relievers. Participants were screened using an 18-point health questionnaire administered by the investigators. Participants were also screened to meet the minimal body segment length measures and minimum and maximum weights required to obtain flight status in the United States Army (Table 4). Participants were provided and signed a written consent. This study was approved by the University's Institutional Review Board and the Institutional Review Board of the United States Army Medical Research and Material Command.

Table 4. United States Army anthropometric flight status requirements.

Body Measure	Men
Total Arm Reach, cm	≥ 164.0
Crotch Height, cm	≥ 75.0
Sitting Height, cm	< 102.0
Minimum Weight, kg	45.3
Maximum Weight, kg	107.9

Experimental Procedures

Participants reported to the laboratory three times with a minimum of 24 hours between sessions. Testing order was randomized (computerized random number generator, TI-83 Plus, Texas Instruments Inc., Dallas, TX, USA) into 3 conditions; with pressure application to the middle of the posterior thigh (condition A) completed on one day; pressure application to the ischial tuberosity (condition B) completed on another day, and a control condition with no pressure application (condition C) completed on the remaining day. All pressure application conditions used a magnitude of 44 kilopascals. The pressure level was determined from the previous pressure study portion of this project. During session one, functional leg dominance was determined using three tests: the step up test, the ball kick test, and the balance recovery test.[270] Body composition was then determined using DXA.[276,277] Investigators then recorded the anthropometric measures of arm length, crotch height, sitting height, height, and weight from the participants to ensure all Army flight status requirements were met. Lower extremity

flexibility measures of hip flexion, hip extension, and hip external rotation collected along with sit-and-reach scores were then collected.

During all data collection, participants sat in a custom-built pressure application seat. The seat's design allowed for local pressure to be applied only to the location of interest while still supporting the participant's body weight (Figure 43). To reproduce sitting postures in the UH-60 helicopter, Design Eye Point knee sitting angles were evaluated, collected using a goniometer (12.5" International Standard Goniometer, Patterson Medical Holdings Inc., Bolingbrook, IL, USA), and recorded using standard United States Army Design Eye Point procedures.[274] The Design Eye Point is an aircraft specific position for aviators that optimizes field of view and equipment access within the cockpit (Figure 44).[274] This knee angle was replicated by passively moving the participants' knees prior to the start of all data collection sessions and after each data collection time point. The 44 kilopascal pressure was applied to the location of interest (middle of the posterior thigh, ischial tuberosity, or control) for a total of 10 minutes. Data was collected pre-application, 5 minutes into pressure application, 10 minutes into pressure application, 5 minutes post-application, and 10 minutes post-application. During the pressure application, participants were asked to sit quietly with their head facing forward and hands resting on their laps.

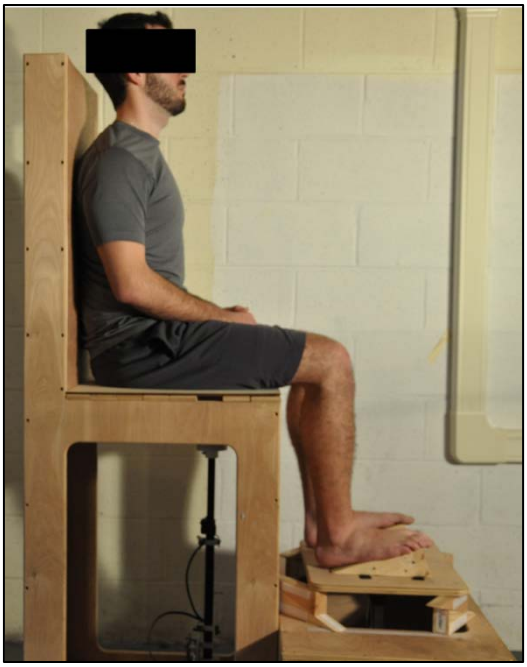

Figure 43. Participant sitting position during project three.

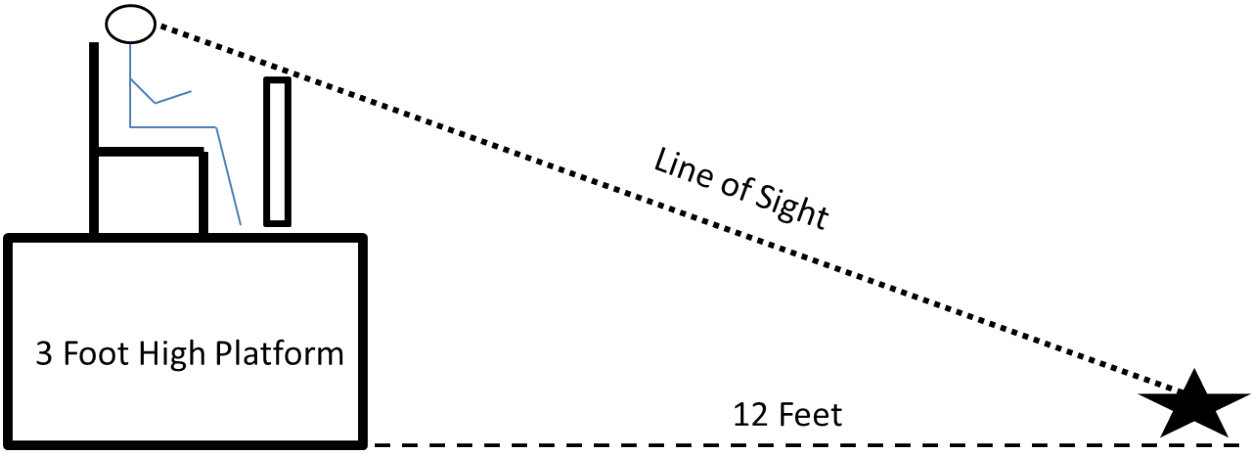

Figure 44. Design Eye Point participant sitting position.

Local Pressure Application Apparatus (LPAAP)

The purpose-built Local Pressure Application Apparatus (LPAAP) was designed to apply local pressure to location on the posterior aspect of the upper leg of participants in a seated position. The LPAAP consisted of a step motor secured to an extendable metal rod and load cell with a custom-built, round pressure application head 25.5176 centimeters squared in area. The unit was controlled using custom-written computer software and operated through a laptop computer (Dell Latitude D430, Dell Inc., Round Rock, TX, USA). The seat was built of wood and consisted of an 80.01 x 55.88 centimeter (height x width) seat back and a 50.80 x 55.88 centimeter (depth x width) seat pan. The seat pan was comprised of 14 removable slats which allowed the pressure application head access to the area of interest while supporting the body mass of the participant. The foot rest was a 91.44 x 50.80 x 35.66 centimeter (length x width x height) box with an adjustable crank lift to accommodate participants of different heights.

Determination of Anatomical Locations

Local pressure was applied to the ischial tuberosity and the mid-point of the posterior thigh on the dominant lower extremity of participants. The two locations were chosen based on the underlying anatomy and previous research.[85] The ischial tuberosity was palpated by a trained investigator and marked with adhesive tape. The mid-point of the posterior thigh was defined as half the distance from the greater trochanter to the lateral epicondyle and halfway between the medial and lateral edges of the posterior thigh. The distance between the greater trochanter and the lateral epicondyle (determined by palpation) using a tape measure (Medco Tape Measure, Patterson Medical Holdings Inc., Bolingbrook, IL, USA). The distance was rounded to the

nearest half centimeter and marked with permanent marker. The distance between the medial and lateral borders of the thigh was measured in the same manner with the permanent marker line demarcating the mid-point of the femur along its polar axis. This location was marked with permanent marker and served as the location for posterior thigh pressure application. The locations were visually confirmed in the LPAAP prior to pressure application. For the ischial tuberosity, verbal confirmation from participant was also elicited. For the control condition, the pressure application was lowered below the threshold of the seat pan and all open slats were filled to create a flat seating surface. Participants sat on the flat seating surface for all control data collection.

Local Pressure Application Protocol

Following participant preparation (e.g. application of electrodes) each day, participants were instructed to sit on the pressure application chair barefoot with the appropriate slats removed and pressure application head correctly positioned. The participant was instructed to sit upright and as far back in the chair as possible. The foot rest was adjusted to the appropriate height and participants' knees were positioned at the Design Eye Point knee angle. Following positioning, a fifteen minute rest period occurred in order to remove the influence of investigators touching the skin influencing dynamic infrared thermography results. After the rest period, baseline measures of Category Partitioning Scale, McGill Pain Questionnaire, soleus Hoffmann reflex, sural sensory nerve conduction velocity, dynamic infrared thermography, Semmes-Weinstein monofilament, two-point discrimination, and pulse oximetry were taken. Local pressure was applied at 44 kilopascals to one of the specified locations (middle of the

posterior thigh, ischial tuberosity, or control) for a total 10 minutes. During the pressure application the magnitude of the pressure was maintained to within 5% of the set value. Following 5 and 10 minutes of pressure application, follow-up measures were taken. Additional follow-up measures were collected during the recovery from local pressure application period at time points of 5 and 10 minutes post-pressure application. The time required to collect data at each time point was approximately 180-200 seconds. The order of data acquisition remained the same for each session and for each participant. Following the 20 minute protocol, participants had electrodes removed, exited the chair, and scheduled for the subsequent data collection with no less than 24 hours between data collection periods. This procedure was repeated for all three pressure location conditions.

Body Composition Measures

Dual-Energy X-Ray Absorptiometry (DXA)

Body composition was assessed using Dual-Energy X-Ray Absorptiometry (DXA) (Lunar Prodigy Advance, GE Healthcare Inc., Waukesha, WI, USA). DXA delivers very low-level x-rays through the body in order to determine the amount of fat mass, lean mass, and bone density in a minimally invasive manner.[276,277] Participants completed a single DXA scan during session one. The total percent fat mass was recorded and analyzed (enCore version 9.1, GE Healthcare Inc., Waukesha, WI, USA).

Discomfort Measures

Category Partitioning Scale

The Category-Partitioning Scale was utilized to examine the perception of local pressure intensity levels and discomfort.[256,257] The scale starts at zero and is divided into five categories: "very slight," "slight," "medium," "severe," and "very severe."[257,258] Each category is further divided into 10 scale points for a total range of 0 – 50. Numbers above fifty provided to avoid the ceiling effect in the case of extreme pain or discomfort.[257] Participants were instructed to rate their discomfort in one of the five categories, then instructed to "fine tune" their discomfort rating using the numerical scale points.[257] The numerical data provided by the participant were recorded with a tablet computer (iPad 2, Apple Inc., Cupertino, CA, USA) and entered into an electronic data collection sheet (Quickoffice Pro HD for iPad, Google Inc., Mountain View, CA, USA).

Short-Form McGill Pain Questionnaire (MPQ)

The Short-Form McGill Pain Questionnaire (MPQ) was used to evaluate perceptions of discomfort.[260] The questionnaire consisted of eleven sensory dimension descriptors and four affective dimension descriptors .[260] Each descriptor was ranked on an intensity scale with 0 = none, 1 = mild, 2 = moderate, and 3 = severe.[260] One 10 centimeter visual analogue scale and one present pain intensity question were also included as part of the MPQ to indicate overall discomfort intensity.[260] A blank questionnaire was handed to the participant at every data collection time point and the numerical scores were calculated and entered into a custom

electronic spreadsheet application (Microsoft Excel 2010, Microsoft Corp., Redmond, WA, USA) for analysis.

Neurological Measures

Hoffmann Reflex (H-reflex)

The functionally dominant leg soleus muscle was chosen for assessment due to its location in the lower leg, importance in foot function, and ease of access in a seated position. The electrode sites for the soleus H-reflex were shaven to remove excess hair, abraded, and cleaned with isopropyl alcohol.[133] Disposable adhesive silver/silver chloride (Ag/AgCl) electrodes (EL503, Biopac Systems Inc., Goleta, CA, USA) were placed on the soleus muscle 2 centimeters distal to the belly of the gastrocnemius muscle with an inter-electrode distance of 2 centimeters. A ground electrode (EL 503, Biopac Systems Inc., Goleta, CA, USA) was placed on the ipsilateral medial malleolus. A stimulating electrode (EL 254, Biopac Systems Inc., Goleta, CA, USA) was placed over the posterior tibial nerve in the popliteal fossa of the posterior knee. An 8 centimeter, round dispersal pad was placed above the patella on the ipsilateral quadriceps muscles. A series of 1.0 millisecond square wave stimuli were delivered via transcutaneous stimulation (STMISOC, Biopac Systems Inc., Goleta, CA, USA) at 10 to 20 second intervals while increasing stimulus intensity by 0.2 volts until the soleus maximum H-reflex (H_{max}) and maximum M-wave (M_{max}) are found for each participant. The test stimulus was normalized to 25 percent of soleus M_{max}. Electromyographic (EMG) data was collected and the signal amplified using an EMG amplifier (EMG100C, Biopac Systems Inc., Goleta, CA, USA). The raw signal was differentially amplified (gain, 1000; common mode rejection ratio,

110dB; input impedance, 1000MΩ; signal noise, 0.2) and digitally converted at 2000Hz.[112] The data was analyzed using AcqKnowledge Software (Biopac Systems Inc., Version 4.0, Goleta, CA, USA). Seven repetitions were completed and averaged for each time point.[112] During the local pressure application protocols the electrodes, stimulator, and leads remained in place connected to the data acquisition system. Data collection occurred during the same time of day for each session to eliminate the diurnal effects on the H-reflex.

Sural Sensory Nerve Conduction Velocity (NCV)

The dominant leg was prepared for the sural sensory NCV as described with the H-reflex. Disposable adhesive foam paired electrodes (EL500, Biopac Systems Inc., Goleta, CA, USA) were placed one centimeter posterior and one centimeter inferior to the lateral malleolus and served as the active recording electrodes.[182] A stimulating electrode (EL500, Biopac Systems Inc., Goleta, CA, USA) was placed 14 centimeters from the center of the active recording electrodes. A reference electrode (EL 503, Biopac Systems Inc., Goleta, CA, USA) was placed between the stimulating and recording electrodes.[182] The signal was differentially amplified (gain, 2000; low pass filter, 5kHz; high pass filter, 10Hz; sampling rate, 10,000Hz; input impedance, 1000MΩ; signal noise, 0.2) and digitally converted at 2000Hz. Rectangular electrical pulses 0.1 milliseconds in duration were delivered once every three seconds via transcutaneous stimulation (STMISOC, Biopac Systems Inc., Goleta, CA, USA) at an intensity sufficient to obtain a sensory response.[182] Five stimulations were delivered at each time point during the local pressure application protocol. The peak negative potential was measured from the end of the stimulation artifact.[182] The latencies were averaged to obtain mean sural nerve

latency. The sural sensory nerve latency (milliseconds) was converted to NCV (meters/seconds) by taking the stimulating electrode to recording electrode distance (14 centimeters) and dividing it by the sural sensory nerve latency (in milliseconds) The NCV was standardized by converting centimeters into meters and milliseconds into seconds.

Semmes-Weinstein Monofilament Test (MFT)

Pressure sensitivity at the foot was evaluated using the Semmes-Weinstein Monofilament Test (MFT) (Touch-Test Sensory Evaluator, North Coast Medical Inc., Morgan Hill, CA, USA).[208] The MFT was comprised of several single Nylon fibers[209] of varying thickness.[210] The monofilament was placed on the skin for 1.5 seconds and the participant was asked to respond "Yes" when asked if the participant felt the monofilament against the skin.[212] Measurement locations included the plantar aspect of the great toe, the plantar aspect of the third metatarsal, and the plantar aspect of the fifth metatarsal of the dominant foot of participants.[209] The last correctly reported monofilament thickness was recorded and used for analysis.

Two-Point Discrimination Test (TPDT)

Lower extremity receptive field sensitivity was measured with the two-point discrimination test (TPDT) (Disk-Criminator, North Coast Medical Inc., Morgan Hill, CA, USA).[192,193] The TPDT was comprised of dull point calipers with inter-point distances ranging from 2 to 15 millimeters.[194,195] The calipers were placed on the testing locations for 1.5 seconds and the participant was instructed to verbally indicate if one or two points were in contact with

the skin. To discourage participants from guessing the number of points, single and double pin points were interchanged randomly. Testing locations included the planar surface of the great toe, the medial malleolus, and the lateral malleolus of the dominant lower leg of participants.[208] The last correctly reported inter-point distance was recorded with a tablet computer (iPad 2, Apple Inc., Cupertino, CA, USA) and entered into an custom electronic data collection sheet (Quickoffice Pro HD for iPad, Google Inc., Mountain View, CA, USA).

Circulatory Measures

Dynamic Infrared Thermography (DIRT)

A digital infrared camera (FLIR T420, FLIR Systems Inc., Wilsonville, OR, USA) was used to measure non-contact, superficial temperatures (°C) in the lower leg. Anterior and lateral infrared images were taken 1 meter from the dominant leg of participants. The average temperature of the lateral and anterior ankle was analyzed using manufacturer specific analysis software (FLIR ExaminIR, version 1.40.12.44). Average temperature values for regions of interest at the anterior and lateral ankle were measured using the Glamorgan Protocol.[268] The anterior ankle region of interest was comprised of the width of the ankle with upper and lower edges at the tip of the medial malleolus and the tip of the navicular bone, respectively.[268] The lateral ankle region of interest included the entire anterior to posterior thickness at the level of the lateral malleolus.[268]

Pulse Oximetry

A pulse oximeter (Nonin Onyx Vantage 9590, Nonin Medical Inc., Plymouth, MN, USA) was attached to the great toe of the dominant leg. The spot check method was utilized to measure percent oxygen saturation during each data collection time point.[245] This method was used in order to gain access to the great toe for other measurement tools (i.e., monofilament and two-point discrimination tests). Following a five second analysis period, percent blood oxygen ($\%SpO_2$) was recorded to an electronic spreadsheet (Microsoft Excel 2010, Microsoft Corp., Redmond, WA, USA) for analysis. The pulse oximeter was removed after every data collection time point.

Statistical Analysis

Data was collected electronically via a tablet computer (iPad 2, Apple Inc., Cupertino, CA, USA) and transferred into a custom database (Microsoft Excel 2010, Microsoft Corp., Redmond, WA, USA), and analyzed using Statistical Package for Social Sciences version 19 (IBM SPSS Statistics 19, IBM Corp., Somers, NY, USA). Descriptive statistics (mean ± SD) were calculated. Fifteen, 3 x 5 (location x time) factorial repeated measures ANOVAs were performed. Appropriate follow-up ANOVAs and dependent *t*-tests with Holm's sequential Bonferroni adjustments were performed. Significance levels were set *a priori* at $p \leq 0.05$.

Results

The means, standard deviations and 95% confidence intervals of all variables are presented in Appendix C.

Influence of Body Composition

To test if body composition influenced any of the measures, we first examined if the body fat percentages of the participants differed from one another. The body fat percentage data were normally distributed (Shapiro-Wilk Statistic = 0.936; $P = 0.072$) and did not vary from the sample mean or the median when examined with a one-sample *t*-test ($t_{(29)} = 0.004$; $P = 0.997$ and $t_{(29)} = 0.67$; $P = 0.503$, respectively). Additionally, bivariate Pearson's correlations between each of the test variables at each time point and condition and body fat percentage of participants were completed and revealed no significant correlations. Many of these correlations were very low (0.01 to 0.10). It was determined that body fat percentages within our sample did not vary enough to warrant separating the data into groups based on body fat percentage. All data were analyzed as one group for subsequent analyses.

Category Partitioning Scale

A 3 x 5 (condition x time) repeated measures ANOVA was completed and a significant two-way location x time interaction was found for the Category Partitioning Scale scores (Wilks' $\Lambda = 0.44$; $F_{(8,22)} = 3.42$; $P = 0.010$; $\eta_p^2 = 0.55$). Follow-up tests for main effects revealed a significant effect of time for all conditions: with pressure applied to the posterior thigh (Wilks' Λ

= 0.36; $F_{(4,26)}$ = 11.25; $P < 0.001$; $\eta_p^2 = 0.63$); the ischial tuberosity (Wilks' $\Lambda = 0.39$; $F_{(4,26)}$ = 9.96; $P < 0.001$; $\eta_p^2 = 0.60$); and during the no pressure condition (Wilks' $\Lambda = 0.39$; $F_{(4,26)}$ = 9.90; $P < 0.001$; $\eta_p^2 = 0.60$). Follow-up dependent *t*-tests showed significant increases in Category Partitioning Scale scores at 5 minutes into pressure application on the posterior thigh ($t_{(29)} = -6.73$; $P < 0.001$); 10 minutes into pressure application ($t_{(29)} = -9.36$; $P < 0.001$); 5 minutes post-pressure application ($t_{(29)} = -8.30$; $P < 0.001$); and 10 minutes post-pressure application ($t_{(29)} = -9.50$; $P < 0.001$) compared to baseline measures. These data suggest that discomfort (as measured by the Category Partitioning Scale) increases during local pressure application to the posterior thigh and remain elevated during a 10 minute recovery period. Follow-up dependent *t*-tests also revealed significant increases in Category Partitioning Scale scores at 5 minutes into pressure application at the ischial tuberosity ($t_{(29)} = -5.06$; $P < 0.001$); 10 minutes into pressure application ($t_{(29)} = -7.13$; $P < 0.001$); 5 minutes post-pressure application ($t_{(29)} = -7.86$; $P < 0.001$); and 10 minutes post-pressure application ($t_{(29)} = -8.93$; $P < 0.001$) compared to baseline measures. Pressure application to the ischial tuberosity also increased discomfort levels during 10 minutes of pressure application and during a 10 minute recovery period following pressure application. Follow-up *t*-tests during the control condition found that sitting with no pressure application also resulted in significant increases in Category Partitioning Scale scores at the 5 minutes into pressure application time point ($t_{(29)} = -2.26$; $P < 0.001$); at the 10 minutes into pressure application time point ($t_{(29)} = -3.56$; $P < 0.001$); at the 5 minutes post-pressure application time point ($t_{(29)} = -5.66$; $P < 0.001$); and at the 10 minutes post-pressure application time point ($t_{(29)} = -7.10$; $P < 0.001$) compared to baseline measures. These data suggest that sitting in the local pressure application apparatus for 20 minutes without pressure application results in increases in discomfort (Figure 45).

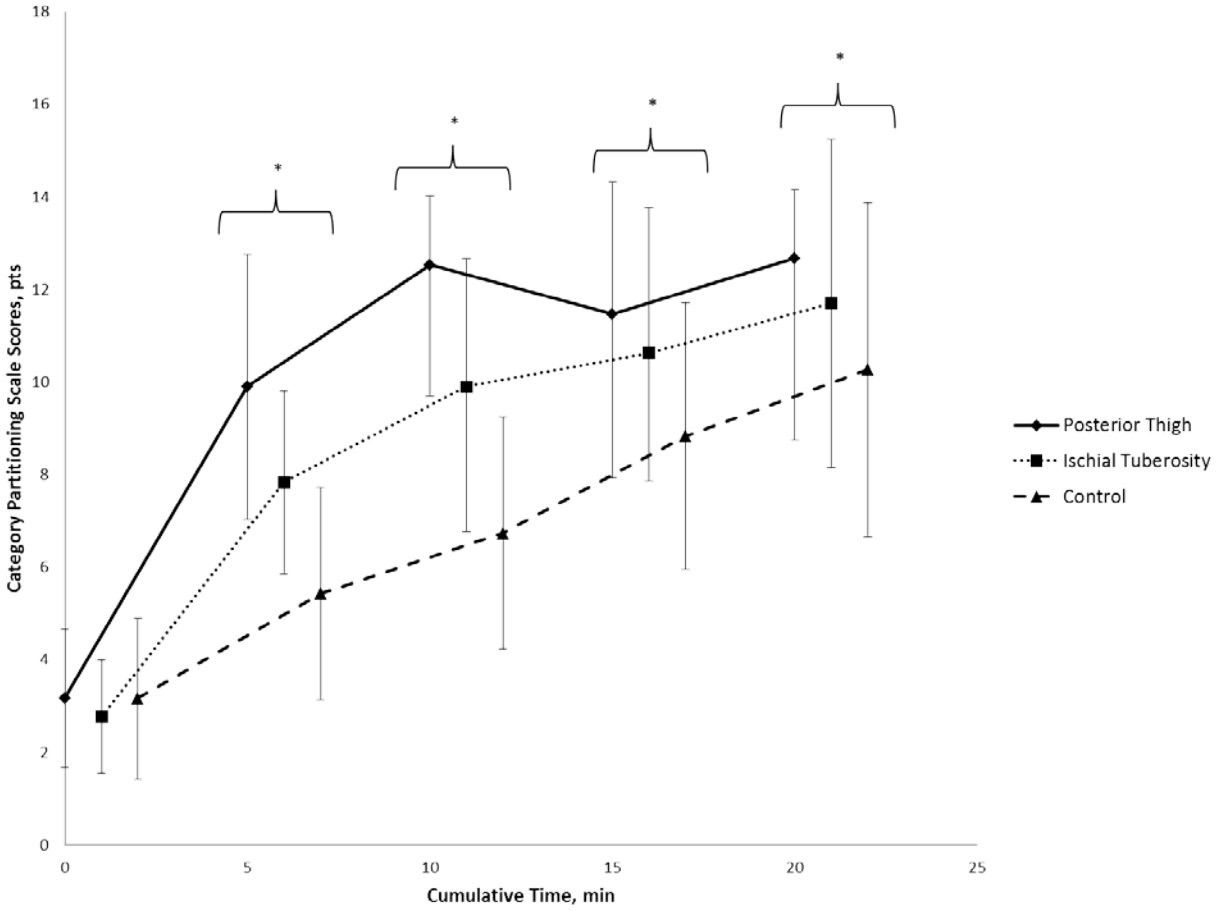

Figure 45. Category Partitioning Scale scores for project three. min: minutes; pts: points; * = *P* < 0.05.

Next, we examined differences in discomfort among the three the pressure application locations at each time point using five, 1 x 3 (time x condition) repeated measures ANOVA. During the baseline condition, no significant difference was found among the three conditions (Wilks' $\Lambda = 0.96$; $F_{(2,28)} = 0.51$; $P = 0.60$; $\eta_p^2 = 0.03$). At 5 minutes into pressure application, a significant difference among the three conditions was found (Wilks' $\Lambda = 0.68$; $F_{(2,28)} = 6.44$; $P = 0.005$; $\eta_p^2 = 0.31$). Follow-up dependent *t*-tests revealed that at 5 minutes Category Partitioning Scale scores were significantly higher (indicating more discomfort) during the posterior thigh condition than during the control condition ($t_{(29)} = -3.61$; $P = 0.001$). Likewise, at 10 minutes

into pressure application there was a significant difference among the three test conditions (Wilks' $\Lambda = 0.57$; $F_{(2,28)} = 10.42$; $P < 0.001$; $\eta_p^2 = 0.42$). Dependent *t*-tests revealed that pressure applied to the posterior thigh resulted in higher levels of discomfort than pressure applied to the ischial tuberosity ($t_{(29)} = 2.63$; $P = 0.004$) or the control condition ($t_{(29)} = 5.8$; $P < 0.001$). There was also a significant difference in Category Partitioning Scale scores between the ischial tuberosity and control conditions at the 10 minute time point ($t_{(29)} = 3.16$; $P = 0.028$). At 5 minutes post-pressure application (Wilks' $\Lambda = 0.85$; $F_{(2,28)} = 2.33$; $P = 0.11$; $\eta_p^2 = 0.14$) and 10 minutes post-pressure application (Wilks' $\Lambda = 0.88$; $F_{(2,28)} = 1.6$; $P = 0.18$; $\eta_p^2 = 0.11$) no significant differences among the three pressure application conditions were found. This indicates that after pressure application is removed, participants report similar Category Partitioning Scale scores.

McGill Pain Questionnaire

A 3 x 5 (condition x time) repeated measures ANOVA was completed and no significant two-way interaction effect was found for McGill Pain Questionnaire descriptors scores (Wilks' $\Lambda = 0.57$; $F_{(8,22)} = 2.05$; $P = 0.087$; $\eta_p^2 = 0.42$). There were significant main effects of pressure application condition (Wilks' $\Lambda = 0.79$; $F_{(2,28)} = 3.6$; $P = 0.04$; $\eta_p^2 = 0.20$) and time (Wilks' $\Lambda = 0.50$; $F_{(4,26)} = 6.27$; $P = 0.001$; $\eta_p^2 = 0.49$) on McGill Pain Questionnaire descriptor scores. Follow-up pairwise comparisons for the effect of pressure application condition on McGill Pain Questionnaire descriptor scores found a significant difference between the posterior thigh condition compared to the control condition ($t_{(29)} = 0.63$; $P = 0.011$), but no difference between the posterior thigh and ischial tuberosity conditions ($t_{(29)} = 0.16$; $P = 0.42$). No differences were

found between the ischial tuberosity and control conditions ($t_{(29)}$ = 0.47; P = 0.054). These data reveal that pressure application to the posterior thigh results in high levels of discomfort as measured by the McGill Pain Questionnaire. Follow-up pairwise comparisons for the effect of time on McGill Pain Questionnaire scores showed that there is a significant increase in discomfort 5 minutes into the pressure application ($t_{(29)}$ = -0.87; P < 0.001); 10 minutes into pressure application ($t_{(29)}$ = -1.14; P < 0.001); 5 minutes post-pressure application ($t_{(29)}$ = -1.67; P = 0.001); and 10 minutes post-pressure application ($t_{(29)}$ = -2.07; P = 0.001) compared to baseline levels of discomfort. These results suggest that discomfort increases during local pressure application and remains elevated during recovery (Figure 46).

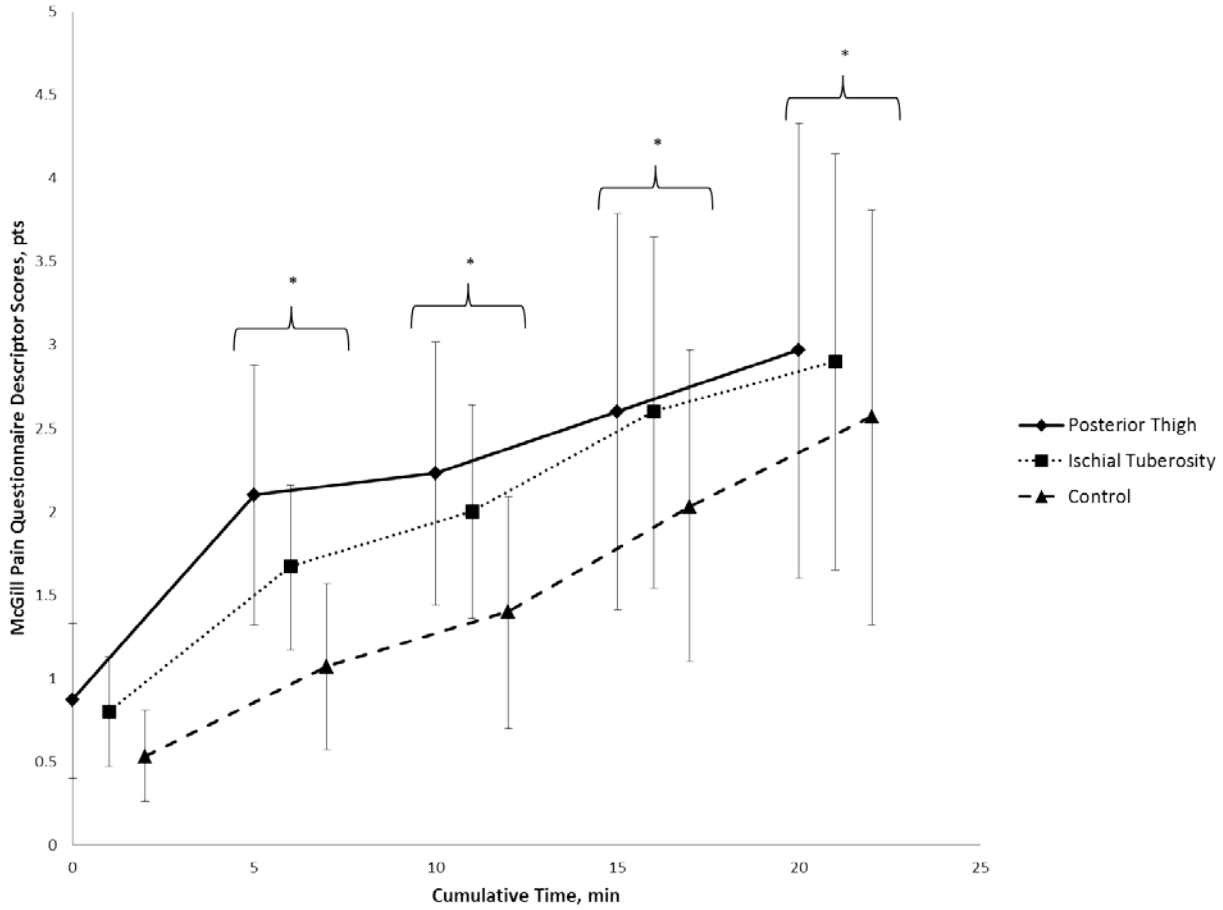

Figure 46. Short Form McGill Pain Questionnaire descriptor scores for project three. min: minute; pts: points; * = P < 0.05.

A 3 x 5 (condition x time) repeated measures ANOVA revealed a significant two-way interaction for the visual analog scale scores (Wilks' $\Lambda = 0.52$; $F_{(8,22)} = 2.45$; $P = 0.045$; $\eta_p^2 = 0.47$). Follow-up one-way repeated measures ANOVAs for effect of time revealed a significant effect of time during the posterior thigh condition (Wilks' $\Lambda = 0.31$; $F_{(4,26)} = 14.45$; $P < 0.001$; $\eta_p^2 = 0.69$); during the ischial tuberosity condition (Wilks' $\Lambda = 0.49$; $F_{(4,26)} = 6.69$; $P = 0.001$; $\eta_p^2 = 0.50$); and during the control condition (Wilks' $\Lambda = 0.46$; $F_{(4,26)} = 7.57$; $P < 0.001$; $\eta_p^2 = 0.53$). Follow-up pairwise comparisons for the posterior thigh condition revealed a significant increase in discomfort at 5 minutes into pressure application ($t_{(29)} = -0.68$; $P < 0.001$); 10 minutes into pressure application ($t_{(29)} = -0.89$; $P < 0.001$); 5 minutes post-pressure application ($t_{(29)} = -0.93$; $P < 0.001$); and 10 minutes post-pressure application ($t_{(29)} = -1.13$; $P < 0.001$) compared to baseline. These data suggest that visual analog scale scores increase during the 10 minutes of pressure application and continue to increase during the 10 minute follow-up period. Follow-up pairwise comparisons for the ischial tuberosity condition found a significant increase in visual analog scale scores at 5 minutes into pressure application ($t_{(29)} = -0.42$; $P < 0.001$); 10 minutes into pressure application ($t_{(29)} = -0.61$; $P < 0.001$); 5 minutes post-pressure application ($t_{(29)} = -0.76$; $P < 0.001$); and 10 minutes post-pressure application ($t_{(29)} = -1.02$; $P < 0.001$) when compared to baseline measures. Like the posterior thigh condition, discomfort increases during pressure application and continues to increase during the 10 minute recovery period. Follow-up tests investigating the control condition indicated that significant increases in discomfort were found at the 5 minutes into pressure application time point ($t_{(29)} = -0.33$; $P = 0.001$); the 10 minutes into pressure application time point ($t_{(29)} = -0.46$; $P < 0.001$); the 5 minutes post-pressure application time point ($t_{(29)} = -0.74$; $P < 0.001$); and the 10 minutes post-pressure application time point ($t_{(29)} = -0.81$; $P < 0.001$) compared to baseline measures. Similar to the posterior

thigh and ischial tuberosity pressure conditions, discomfort increases at every data collection time point across the 20 minute data collection period. To examine the effect of pressure application condition on visual analog scale scores we compared the three conditions at each of data collection time points. As expected there was no significant differences between the three pressure locations on scores at the baseline time point (Wilks' $\Lambda = 0.92$; $F_{(2,28)} = 1.11$; $P = 0.34$; $\eta_p^2 = 0.07$). There was a significant difference among the three conditions at the 5 minutes into pressure application time point (Wilks' $\Lambda = 0.70$; $F_{(2,28)} = 5.91$; $P = 0.007$; $\eta_p^2 = 0.29$). Follow-up pairwise analyses revealed that visual analog scale scores were significant higher at the posterior thigh compared to the ischial tuberosity ($t_{(29)} = 0.36$; $P = 0.008$) and control ($t_{(29)} = 0.50$; $P = 0.003$) conditions. There was no significant difference between the ischial tuberosity and control conditions at 5 minutes ($t_{(29)} = 0.14$; $P = 0.325$). These data suggests that discomfort scores are higher when pressure is applied to the posterior thigh than when applied to the ischial tuberosity or no pressure is applied. At 10 minutes into pressure application there was a significant difference among the three conditions (Wilks' $\Lambda = 0.72$; $F_{(2,28)} = 5.34$; $P = 0.011$; $\eta_p^2 = 0.27$). Follow-up pairwise comparisons showed significantly higher levels of discomfort during the posterior thigh condition compared to the ischial tuberosity ($t_{(29)} = 0.38$; $P = 0.004$) condition and the control condition ($t_{(29)} = 0.59$; $P = 0.01$). No difference was identified between the ischial tuberosity and control condition ($t_{(29)} = 0.21$; $P = 0.26$). Together these data indicate that at 10 minutes into pressure application discomfort during the posterior thigh condition is greater than at the ischial tuberosity and control conditions. At 5 and 10 minutes post-pressure application, no significant differences were found among the three conditions [(Wilks' $\Lambda = 0.86$; $F_{(2,28)} = 2.13$; $P = 0.137$; $\eta_p^2 = 0.13$) and (Wilks' $\Lambda = 0.81$; $F_{(2,28)} = 3.17$; $P = 0.057$; $\eta_p^2 = 0.18$),

respectively]. These data suggest that during the 10 minute recovery period, discomfort levels do not differ among the conditions (Figure 47).

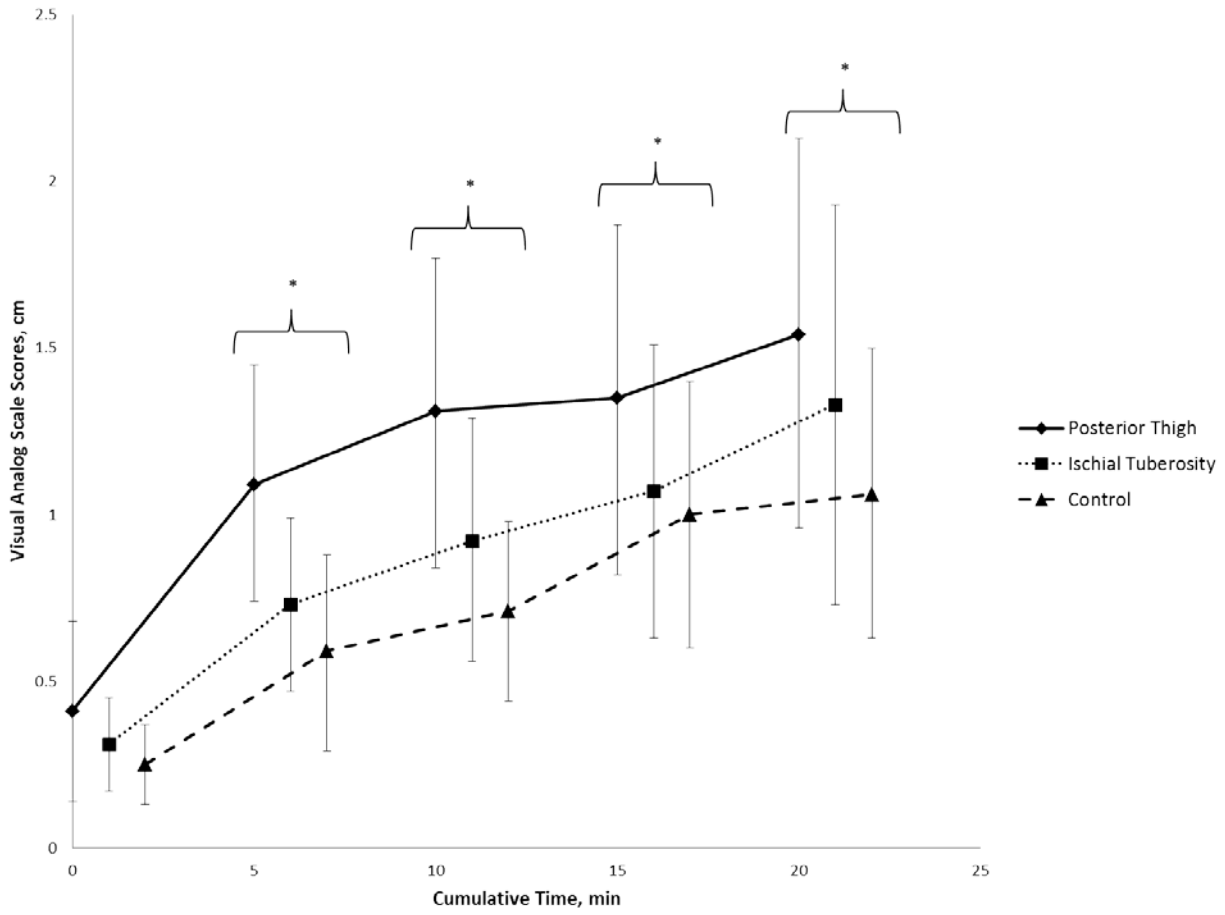

Figure 47. Visual Analog Scale scores for project three. min: minute; cm: centimeter: * = *P* < 0.05.

We completed a 3 x 5 (condition x time) repeated measures ANOVA and no significant two-way interaction was identified for the present pain intensity scores (Wilks' $\Lambda = 0.80$; $F_{(8,22)} = 0.65$; $P = 0.724$; $\eta_p^2 = 0.19$). Analyses of the simple main effects did reveal significant effects of pressure application condition (Wilks' $\Lambda = 0.78$; $F_{(2,28)} = 3.80$; $P = 0.035$; $\eta_p^2 = 0.21$) and time (Wilks' $\Lambda = 0.39$; $F_{(4,26)} = 10.15$; $P < 0.001$; $\eta_p^2 = 0.61$). Follow-up pairwise comparisons for the

main effect of condition indicated significantly higher discomfort during the posterior thigh condition compared to the control condition ($t_{(29)} = 0.24$; $P = 0.009$); however, no difference in discomfort was seen between the posterior thigh and ischial tuberosity conditions ($t_{(29)} = 0.09$; $P = 0.269$) or the ischial tuberosity and control condition ($t_{(29)} = 0.15$; $P = 0.089$). These data indicate that during the posterior thigh condition, discomfort measured by the present pain intensity scale is greater than the other conditions. Follow-up pairwise comparisons for the main effect of time found that present pain intensity scale scores increased at 5 minutes into pressure application ($t_{(29)} = -0.42$; $P < 0.001$); 10 minutes into pressure application ($t_{(29)} = -0.46$; $P < 0.001$); 5 minutes post-pressure application ($t_{(29)} = -0.55$; $P < 0.001$); and 10 minutes post-pressure application ($t_{(29)} = -0.64$; $P < 0.001$) when compared to baseline measures. These results suggest that during a 20 minute testing protocol, discomfort significantly increases at each time point (Figure 48).

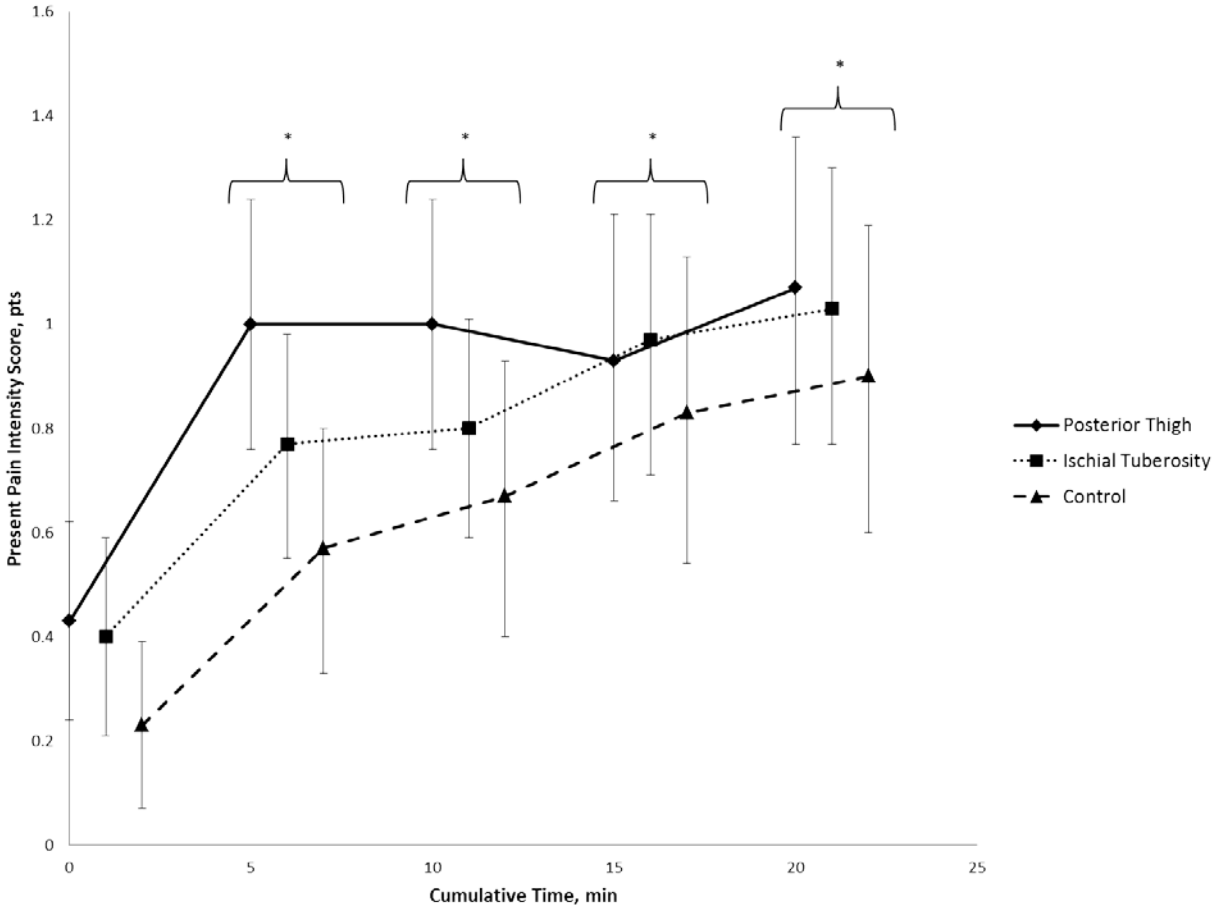

Figure 48. Present Pain Intensity scores for project three. min: minute; pts: points; * = *P* < 0.05.

Semmes-Weinstein Monofilament Test

A 3 x 5 (condition x time) repeated measures ANOVA revealed no significant two-way interaction for the Semmes-Weinstein monofilament scores collected from the great toe (Wilks' $\Lambda = 0.89$; $F_{(8,22)} = 0.32$; $P = 0.94$; $\eta_p^2 = 0.10$). Additionally, no significant simple main effects were identified for pressure application condition (Wilks' $\Lambda = 0.96$; $F_{(2,28)} = 0.55$; $P = 0.57$; $\eta_p^2 = 0.03$) or time (Wilks' $\Lambda = 0.81$; $F_{(4,26)} = 1.45$; $P = 0.246$; $\eta_p^2 = 0.18$) (Figure 49). These data suggest that local pressure application does not alter the ability to sense point pressure at the

great toe. A 3 x 5 (condition x time) repeated measures ANOVA also found no significant two-way interaction effect (Wilks' $\Lambda = 0.87$; $F_{(8,22)} = 0.39$; $P = 0.912$; $\eta_p^2 = 0.12$) or for simple main effects condition (Wilks' $\Lambda = 0.86$; $F_{(2,28)} = 2.10$; $P = 0.141$; $\eta_p^2 = 0.13$) or time (Wilks' $\Lambda = 0.76$; $F_{(4,26)} = 1.99$; $P = 0.126$; $\eta_p^2 = 0.23$) for Semmes-Weinstein monofilament scores at the third metatarsal (Figure 50). Similarly, these results suggest that local pressure does not alter sensitivity to point pressure at the third metatarsal. At the fifth metatarsal, using a 3 x 5 (condition x time) repeated measures ANOVA, no significant two-way interaction effect was identified for Semmes-Weinstein monofilament scores (Wilks' $\Lambda = 0.71$; $F_{(8,22)} = 1.12$; $P = 0.388$; $\eta_p^2 = 0.28$). A significant main effect was found for time (Wilks' $\Lambda = 0.69$; $F_{(4,26)} = 2.84$; $P = 0.045$; $\eta_p^2 = 0.30$), but not for condition (Wilks' $\Lambda = 0.92$; $F_{(2,28)} = 1.17$; $P = 0.324$; $\eta_p^2 = 0.07$). Follow-up pairwise comparisons for the significant main effect of time found that a Semmes-Weinstein monofilament test scores were significantly higher at 10 minutes into pressure application time point ($t_{(29)} = -0.14$; $P = 0.004$) compared to baseline. No other significant differences were found at the other time points. These data indicate that at 10 minutes into pressure Semmes-Weinstein monofilament scores indicate a decreased ability to detect point pressure (Figure 51).

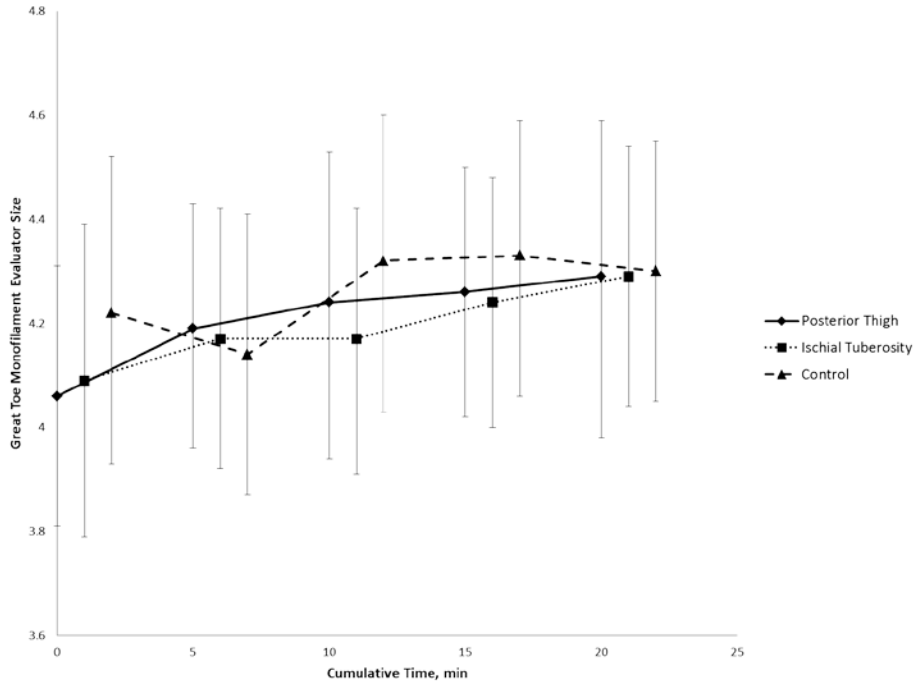

Figure 49. Semmes-Weinstein monofilament test scores at the great toe for project three. min: minute.

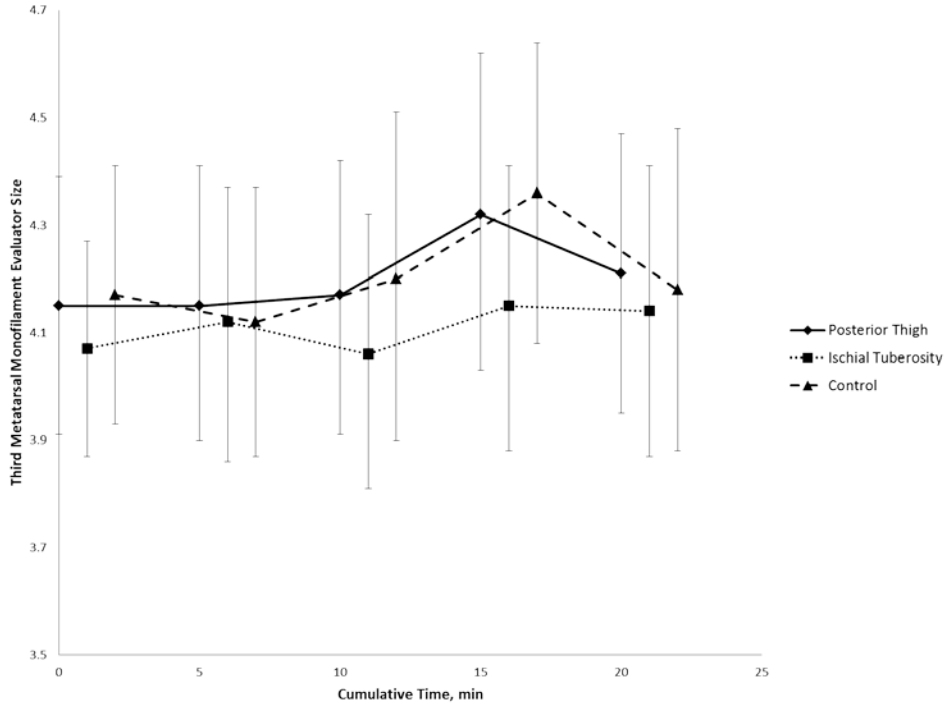

Figure 50. Semmes-Weinstein monofilament test scores at the third metatarsal for project three. min: minute.

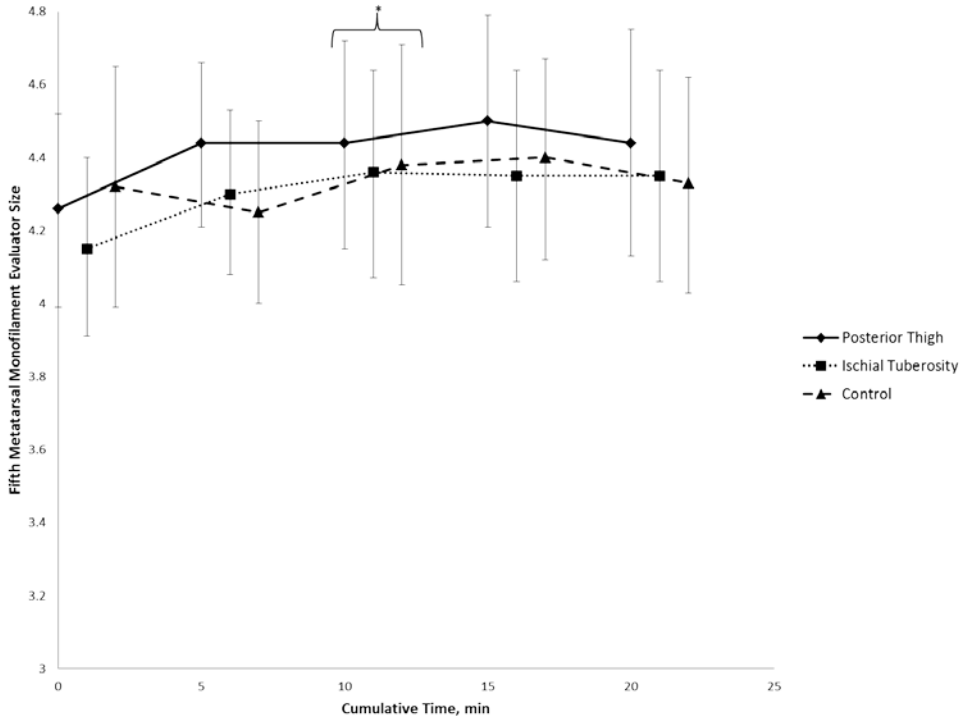

Figure 51. Semmes-Weinstein monofilament test scores at the fifth metatarsal for project three. min: minute; * = *P* < 0.05.

Two-Point Discrimination Test

A 3 x 5 (condition x time) repeated measures ANOVA was used to analyze the two-point discrimination test scores at the great toe and revealed no significant two-way interaction effect (Wilks' $\Lambda = 0.82$; $F_{(8,22)} = 0.58$; $P = 0.782$; $\eta_p^2 = 0.17$). Tests for main effects also yield non-significant results for pressure application condition (Wilks' $\Lambda = 0.95$; $F_{(2,28)} = 0.67$; $P = 0.517$; $\eta_p^2 = 0.04$) or time (Wilks' $\Lambda = 0.85$; $F_{(4,26)} = 1.14$; $P = 0.35$; $\eta_p^2 = 0.15$) (Figure 52). These data indicate that receptive field sensitivity and size is does not change as a result of location pressure application. Two-point discrimination test scores collected at the medial malleolus demonstrated no two-way interaction (Wilks' $\Lambda = 0.71$; $F_{(2,28)} = 1.09$; $P = 0.406$; $\eta_p^2 = 0.28$) when analyzed with a 3 x 5 (condition x time) repeated measure ANOVA. Additionally, no significant main

effects for pressure application condition (Wilks' $\Lambda = 0.94$; $F_{(2,28)} = 0.77$; $P = 0.470$; $\eta_p^2 = 0.05$) or time (Wilks' $\Lambda = 0.85$; $F_{(4,26)} = 1.12$; $P = 0.365$; $\eta_p^2 = 0.14$) were present (Figure 53). These results indicate that local pressure application does not alter the skin's receptive field size or sensitivity. Similarly, a 3 x 5 (condition x time) repeated measures ANOVA found that two-point discrimination test scores at the lateral malleolus did not demonstrate a significant two-way interaction effect (Wilks' $\Lambda = 0.65$; $F_{(8,22)} = 1.43$; $P = 0.239$; $\eta_p^2 = 0.34$); no significant main effect of pressure application condition (Wilks' $\Lambda = 0.98$; $F_{(2,28)} = 0.28$; $P = 0.758$; $\eta_p^2 = 0.02$); and no significant effect of time (Wilks' $\Lambda = 0.77$; $F_{(4,26)} = 1.85$; $P = 0.149$; $\eta_p^2 = 0.22$). These data suggest that receptive field size and sensitivity remain unchanged with local pressure application (Figure 54).

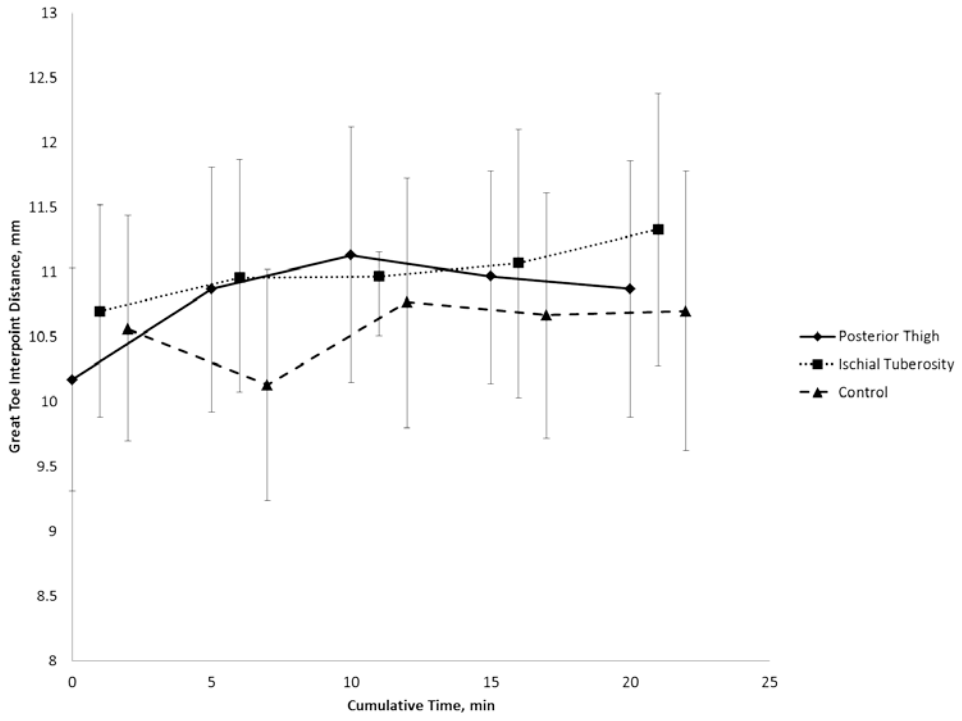

Figure 52. Two-point discrimination test scores at the great toe for project three. min: minute; mm: millimeter.

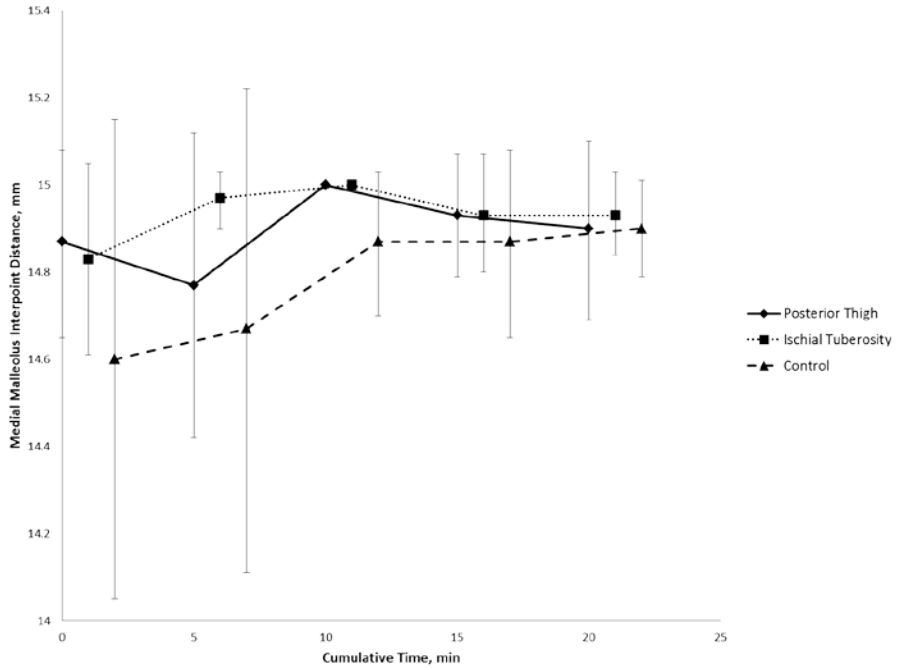

Figure 53. Two-point discrimination test scores at the medial malleolus for project three. min: minute; mm: millimeter.

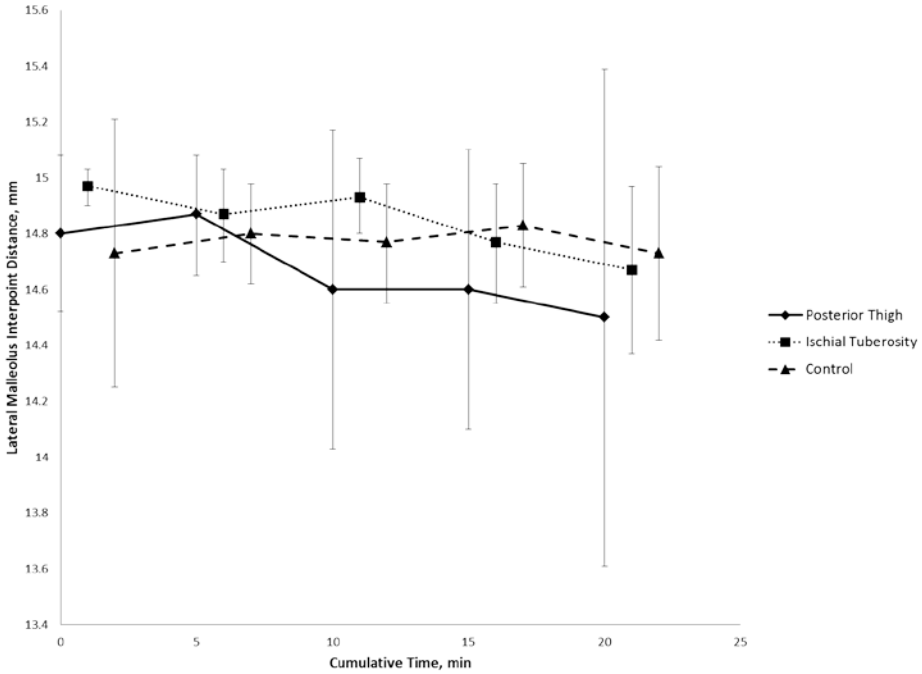

Figure 54. Two-point discrimination test scores at the lateral malleolus for project three. min: minute; mm: millimeter.

Superficial Skin Temperature

A 3 x 5 (condition x time) repeated measures ANOVA indicated no significant two-way interaction (Wilks' $\Lambda = 0.71$; $F_{(8,22)} = 1.10$, $P = 0.395$; $\eta_p^2 = 0.28$) for anterior ankle skin temperature. A significant time main effect was found (Wilks' $\Lambda = 0.20$; $F_{(4,26)} = 1.10$, $P > 0.001$; $\eta_p^2 = 0.79$), however no significant effect of location was found (Wilks' $\Lambda = 0.98$; $F_{(2,28)} = 0.29$, $P = 0.75$; $\eta_p^2 = 0.02$). Follow-up pairwise comparisons for the main effect of time revealed a significant increase in temperature at 5 minutes into pressure application ($t_{(29)} = -0.42$; $P > 0.001$) and 10 minutes in pressure application ($t_{(29)} = -0.24$; $P = 0.002$) (Figure 55). These data indicate that superficial skin temperature at the anterior ankle is increased during the first 10 minutes of the protocol. A 3 x 5 (condition x time) repeated measures ANOVA analyzing skin temperatures at the lateral ankle revealed a non-significant two-way interaction (Wilks' $\Lambda = 0.88$; $F_{(8,22)} = 0.37$, $P = 0.992$; $\eta_p^2 = 0.12$). A significant main effect of time was found (Wilks' $\Lambda = 0.17$; $F_{(4,26)} = 31.2$, $P > 0.001$; $\eta_p^2 = 0.82$), but no significant effect of location was present (Wilks' $\Lambda = 0.96$; $F_{(2,28)} = 0.45$, $P = 0.63$; $\eta_p^2 = 0.03$). Follow-up pairwise comparisons found a significant increase in lateral ankle skin temperature at 5 minutes into pressure application ($t_{(29)} = -0.44$; $P > 0.001$) and at 10 minutes into pressure application ($t_{(29)} = -0.26$; $P > 0.001$) (Figure 56). Like anterior skin temperature data, these data suggest that skin temperatures at the lateral ankle are increased during the first 10 minutes of the 20 minute protocol.

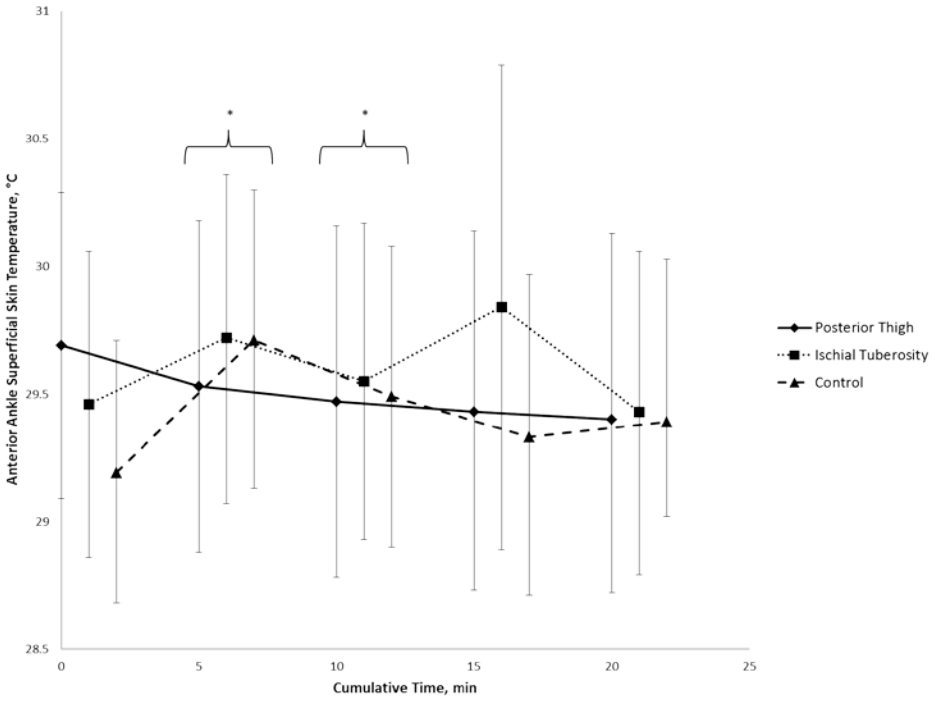

Figure 55. Anterior ankle superficial skin temperature for project three. min: minute; C: Celsius; * = *P* < 0.05.

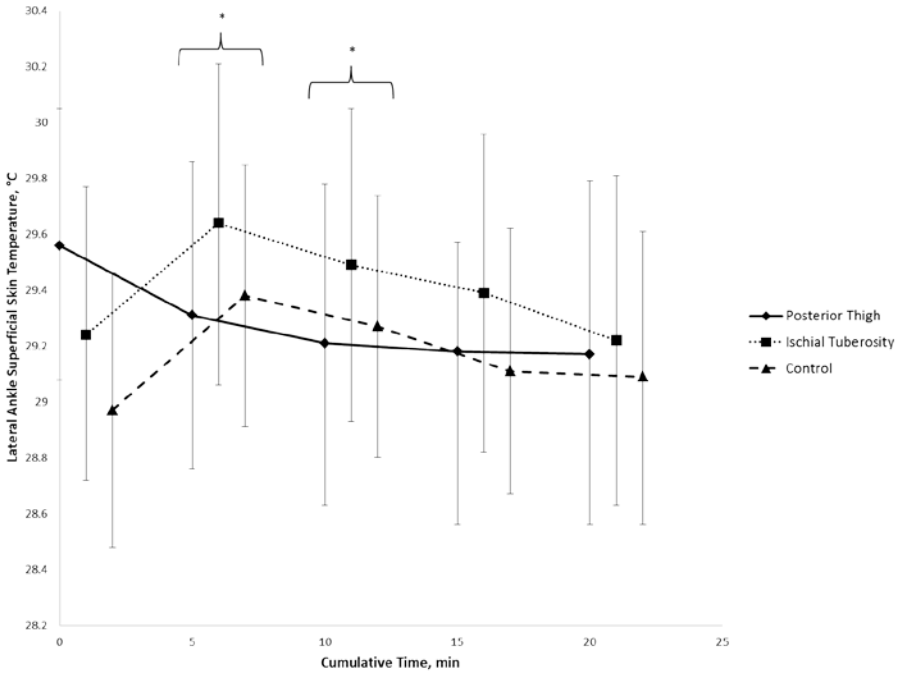

Figure 56. Lateral ankle superficial skin temperature for project three. min: minute; C: Celsius; * = *P* < 0.05.

Percent Oxygen Saturation

Percent oxygen saturation of the lower extremity measured with pulse oximetry at the great toe analyzed with a 3 x 5 (condition x time) repeated measures ANOVA revealed no significant two-way location x time interaction effect (Wilks' $\Lambda = 0.61$; $F_{(8,22)} = 1.71$; $P = 0.151$; $\eta_p^2 = 0.38$). No significant main effect of pressure application location (Wilks' $\Lambda = 0.89$; $F_{(2,28)} = 1.63$; $P = 0.213$; $\eta_p^2 = 0.10$) or time (Wilks' $\Lambda = 0.76$; $F_{(4,26)} = 1.99$; $P = 0.125$; $\eta_p^2 = 0.23$) was found. These data indicate the percent oxygen saturation is not altered during local pressure application (Figure 57).

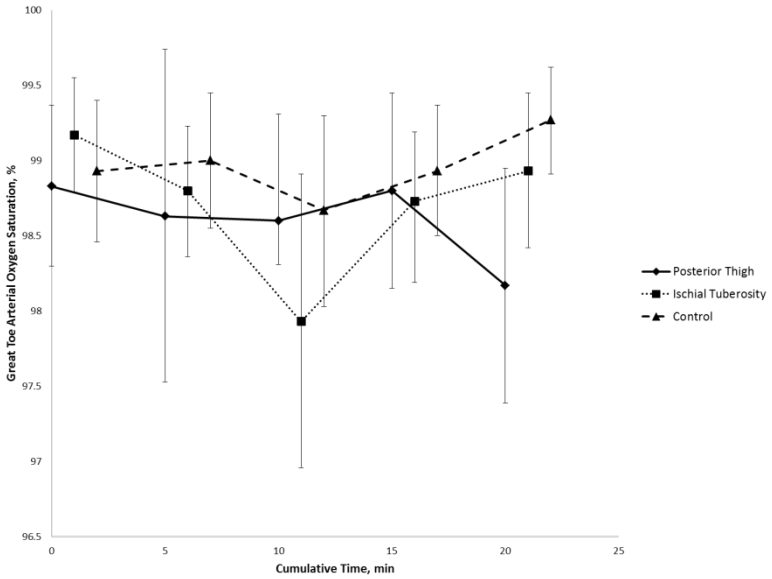

Figure 57. Percent arterial oxygen saturation for project three. min: minute; %: percent.

Soleus Hoffmann Reflex

A 3 x 5 (condition x time) repeated measures ANOVA revealed that mean peak-to-peak soleus Hoffmann reflex amplitudes demonstrated no significant two-way location x time interaction effect (Wilks' $\Lambda = 0.59$; $F_{(8,22)} = 1.90$; $P = 0.110$; $\eta_p^2 = 0.41$). However, significant

main effects were found for pressure application condition (Wilks' $\Lambda = 0.74$; $F_{(2,28)} = 4.68$; $P = 0.018$; $\eta_p^2 = 0.25$) and for time (Wilks' $\Lambda = 0.65$; $F_{(4,26)} = 3.46$; $P = 0.021$; $\eta_p^2 = 0.34$). Follow-up tests for the significant main effect of pressure application condition revealed a significant decrease in Hoffmann reflex peak-to-peak amplitude during the posterior thigh condition compared to both the ischial tuberosity condition ($t_{(29)} = -0.86$; $P = 0.007$) and the control condition ($t_{(29)} = -0.51$; $P = 0.029$). No significant difference was found between the ischial tuberosity and control condition ($t_{(29)} = 0.34$; $P = 0.218$). These data suggest that mean peak-to-peak Hoffmann reflex amplitudes are decreased during the local pressure application to the posterior thigh but not the ischial tuberosity. Follow-up pairwise comparisons for the significant main effect of time found a significant decrease in mean peak-to-peak amplitude at the 5 minutes post-pressure application time point ($t_{(29)} = 0.29$; $P = 0.028$) compared to baseline measures. These data suggest that five minutes following the removal of pressure application mean peak-to-peak soleus Hoffmann reflex amplitudes are decreased (Figure 58).

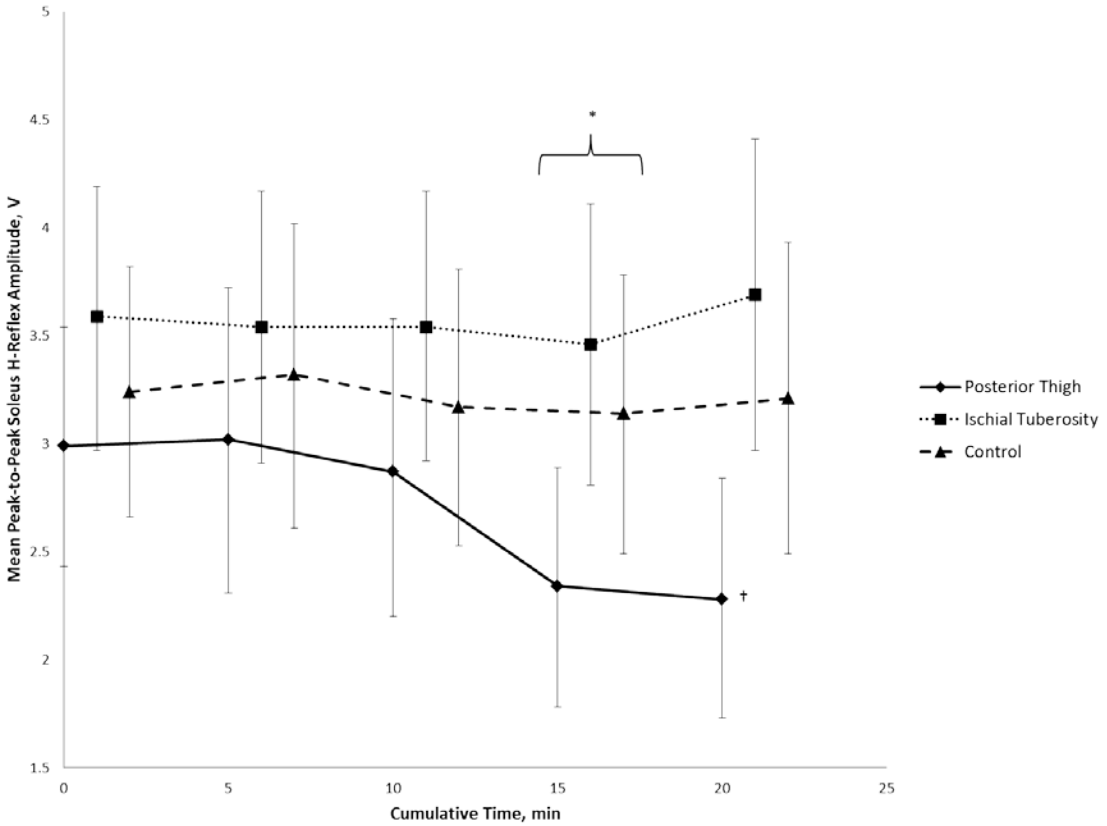

Figure 58. Soleus Hoffmann reflex mean peak-to-peak amplitudes for project three. min: minute; V: volts; * = *P* < 0.05 across time; † = *P* < 0.05 between conditions.

Sural Nerve Conduction Velocity

A 3 x 5 (condition x time) repeated measures ANOVA analysis of the sural sensory nerve conduction velocity revealed no significant two-way interaction effect (Wilks' $\Lambda = 0.64$; $F_{(8,22)} = 1.51$; $P = 0.208$; $\eta_p^2 = 0.35$). No significant main effect of pressure application condition (Wilks' $\Lambda = 0.97$; $F_{(2,28)} = 0.43$; $P = 0.651$; $\eta_p^2 = 0.03$) or time (Wilks' $\Lambda = 0.92$; $F_{(4,26)} = 0.55$; $P = 0.698$; $\eta_p^2 = 0.07$) was found. These data indicate that local pressure application does not alter mean sural sensory nerve conduction velocity (Figure 59).

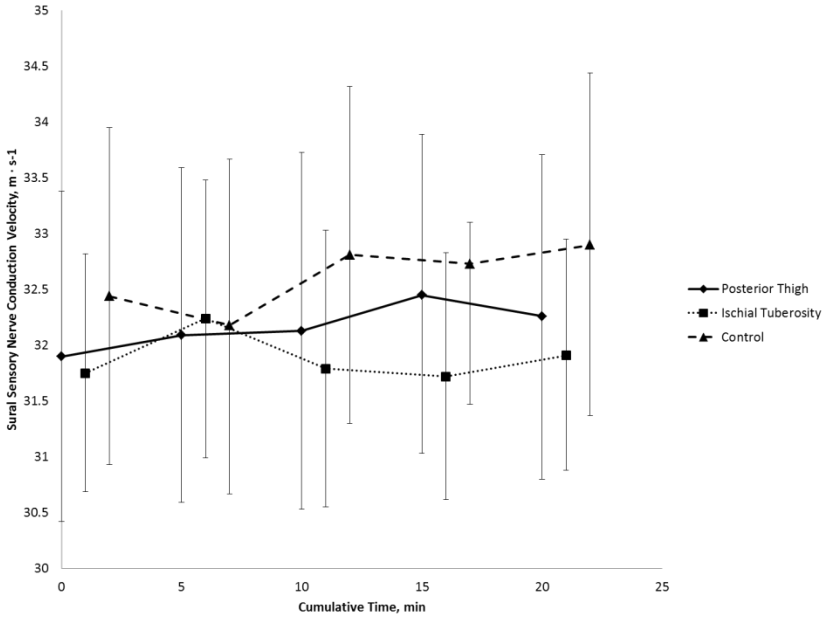

Figure 59. Sural sensory nerve conduction velocity for project three. min: minute; $m \cdot s^{-1}$: meters per second.

Discussion

This study investigated the effects of 44 kilopascals of pressure application at three locations (control, ischial tuberosity, posterior thigh) on subjective discomfort, lower extremity sensibility, vascular function, and nervous system function.

Neurological Measures

The most notable results from this study were that mean peak-to-peak Hoffmann reflex amplitudes were decreased when 44 kilopascals of pressure was applied to the posterior thigh. Peak-to-peak amplitude during posterior thigh pressure application was 0.87 volts below H-reflex amplitudes at the ischial tuberosity and 0.52 volts below H-reflex amplitudes during the

control conditions. Our results show a non-significant increase in mean amplitude from baseline to 5 minutes into pressure (2.98 volts to 3.01 volts), and a decrease at each of the remaining time points of 10 minutes into pressure, 5 minutes post-pressure, and 10 minutes post-pressure (2.86, 2.33, and 2.28 volts, respectively). This study was the first study to examine the Hoffmann reflex in a functional position when pressure was applied to the ischial tuberosity and posterior thigh. Previous research examining the effects of local pressure application on Hoffmann reflex amplitude while in the prone position produced different results.[85] Previous work found an 17% increase in H-reflex amplitude following 9 minutes of pressure application of 28 kilopascals to the posterior thigh.[85] The authors hypothesized that cutaneous stimulation during the pressure application created an increase in α-motoneuron pool excitability.[85] Other work does suggest that there may be location dependent cutaneous stimuli responses although no work has examined the effects of cutaneous stimulation at the posterior thigh on H-reflex amplitude. Work examining the effects of pressure stimuli on soleus H-reflex amplitudes during locomotion found that H-reflex amplitudes are inhibited when mechanical pressure is applied to the plantar aspect of the foot. [295] However, additional work supports more specific location dependent cutaneous stimuli changes to H-reflex amplitudes. Cutaneous stimuli at the heel resulted in significant facilitation of the soleus H-reflex while cutaneous stimulation at the third metatarsal resulted in significant inhibition of soleus H-reflex amplitudes in a study examining the effects of specific pressure application at either the plantar surface of the heel or the third metatarsal.[296] Work at other locations in the lower extremity does appear to support location dependent cutaneous stimuli changes to H-reflex output.[85] We suspect the differences between results of previous work and the current study are a result of participant position (prone vs. upright sitting), pressure application magnitude (28 kilopascals and 44 kilopascals) and H-reflex amplitude

normalization procedures (50% H_{max} vs 25% M_{max} test stimulus). Participant position and stimulation intensity have both been shown influence the H-reflex outputs.[86,143]

An inhibition of the soleus H-reflex amplitude could have significant performance implications for Black Hawk pilots. Rotary-winged pilots are required to use both hands and both feet to safely and effectively operate the aircraft. The feet operate the anti-torque pedals of the aircraft.[285] The force output at the soleus may be diminished if the pilot's experience a decrease in α-motoneuron output at the soleus muscle. A diminished ability to recruit a sufficient level of force to operate the anti-torque pedals could result in the recruitment of more motor units which may increase fatigue. Failure to effectively operate the anti-torque pedals will result in loss of control of the helicopter.[285] This loss of control could result in injury, equipment damage, or death. The results of the current project are supported by previous work in our laboratory which found that prolonged restricted sitting results in a decreased sensitivity to point pressure at the plantar aspect of the fifth metatarsal.[292] The skin of the plantar aspect of the fifth metatarsal is part of the S1 nerve root dermatome.[31] The S1 nerve root is also responsible for motor control of several lower extremity muscles including the soleus.[272] Future work should examine if soleus H-reflex amplitude is decreased during a prolonged (4-8 hour) restricted sitting bout. Additionally, research should examine the influence of diminished α-motoneuron output on the recruitment of additional motor units during prolonged task (e.g. operating anti-torque pedals).

The results for the sural nerve conduction velocity found that 44 kilopascals of local pressure application at the ischial tuberosity or posterior thigh does not change the conduction velocity compared to a control condition. This study was the first to explore the effects of proximal local pressure application (posterior thigh and ischial tuberosity) on distal peripheral

nerve conduction velocity in the lower leg (sural sensory nerve) of humans. Other work has demonstrated that acute compression to isolated nerves decreases nerve conduction velocity and alters nerve function.[76-79] However, the previous work applied focal pressure between the stimulation site and the recording site.[76-79] We hypothesize that if nerve conduction velocity is tested across the segment at which the pressure is applied (ischial tuberosity and posterior thigh), nerve conduction velocity and function would be altered, particularly at the posterior thigh location due to the path of the sciatic nerve along the posterior aspect of the thigh. Testing this hypothesis would be difficult due to methodological limitations of nerve conduction studies at the sciatic nerve, but other neurological tests like the H-reflex provide valuable information as shown in this present study.

Vascular Measures

Our results for anterior and lateral ankle skin temperatures indicate that anterior superficial skin temperature significantly increases (0.42° C) and lateral superficial skin temperature significantly increases (0.44 °C) during the first five minutes of pressure application. Superficial skin temperature at the anterior ankle begins to decrease 10 minutes after the beginning of the protocol, but is still significantly greater than baseline measures (29.52° C compared to 29.28° C). Lateral ankle superficial skin temperature also begins to decrease 10 minutes after the beginning of the protocol, but is also still significantly greater than baseline (29.35 °C compared to 29.08 °C) None of the remaining time points for either the anterior or lateral ankle were significantly different from baseline (Figure 60). The superficial skin temperature results were not dependent on pressure application location as determined by

the no location interaction effect. This suggests that the local pressure application did not alter anterior or lateral skin temperature compared to the control condition. We hypothesize that sitting on the hard surface of the pressure application device, along with a diminished muscle pump due to inactivity of the lower extremity muscles, decreased venous return which caused pooling of the blood in the lower leg. Venous pressure under normal physiology is very low.[294] It is likely that the interface pressure between the buttocks and firm surface of the local pressure application apparatus was sufficient to occlude venous return, however this was not measured. The flow into the venous system is exclusively from the arterial system. Additionally, after three to five minutes of inactivity the venous system is filled and serves as a reservoir for blood.[294] We suspect that the first five minutes of sitting resulted in an increase in temperature because the venous system was filling with warm arterial blood. After the filling was complete, heat exchange from the lower leg to the environment occurred via thermal radiation at a rate faster than which fresh, warmed arterial blood entered the venous system. Previous research within our laboratory found a similar pattern with both 44 and 36 kilopascals applied to the posterior thigh and ischial tuberosity across a 10 minute pressure application period.[292] Previous work within our laboratory examining the effects of prolonged sitting in a Black Hawk helicopter found that superficial skin temperature at the anterior and lateral ankle decreased by 2.78-2.85° C across a four hour time period.[292] During the prolonged restricted sitting study, temperature measures were only collected once every 30 minutes, thus, and changes between the 30 minute data collection periods were not analyzed. Future research should collect data more frequently in order to examine the effects of prolonged sitting in an effort to determine if there is a pattern of temperature increases followed by decreases as we observed in this study.

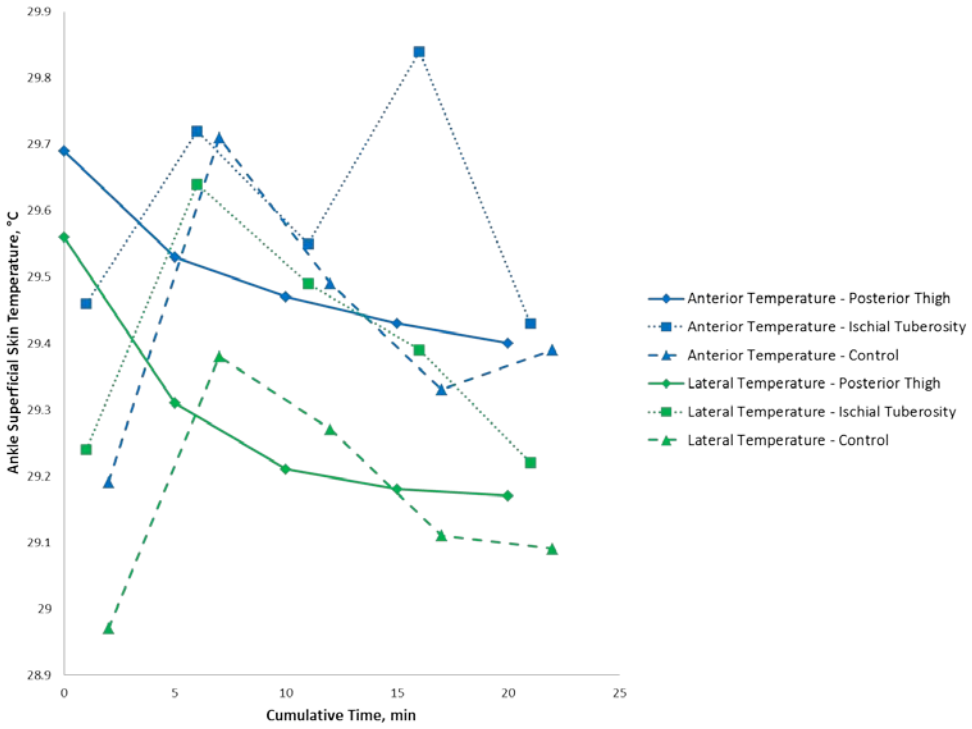

Figure 60. Combined anterior and lateral ankle superficial skin temperatures for project three. min: minute; C: Celsius.

Pulse oximetry results suggest that arterial oxygen saturation is unaltered during local pressure application to the posterior thigh or ischial tuberosity when compared to a no pressure condition. These results are in line with previous research which found local pressure application and prolonged restricted sitting do not alter arterial oxygen saturation.[292] Work examining muscle oxygenation at the medial gastrocnemius muscle during 8 hours of prolonged restricted sitting also found that muscle oxygenation levels are not significantly changed.[3] Our work, along with the work of others, suggests that the discomfort and temporary parathesia reported in rotary-winged pilots during prolonged missions is not associated with decreases in arterial or muscle oxygenation levels in the lower extremity.

Lower Extremity Sensibility

The Semmes-Weinstein monofilament test results revealed a significant increase in monofilament test scores at the fifth metatarsal. An increase in monofilament test scores signifies a decrease in sensitivity to point pressure. Data at the great toe and third metatarsal demonstrate no significant change in monofilament test scores (Figure 61). This pattern of decreased sensibility on the lateral portion of the plantar surface of the foot suggests that there may be a dermatome specific change associated with a specific spinal nerve root. The lateral foot dermatome is associated with the S1 nerve root while the great toe and third metatarsal test locations are associated with the L5 nerve root. Previous research examining the effects of prolonged sitting on Semmes-Weinstein monofilament test scores found a similar pattern of dermatome specific changes.[292] Moreover, Hoffmann reflex data collected in the present study supports our hypothesis of targeted changes associated with spinal nerve roots. The S1 nerve root supplies motor function to the lateral and posterior musculature of the lower leg.[272] A clinical test for S1 nerve root dysfunction is the Achilles tendon tap reflex.[272] A decreased reflex response suggests impairment to S1 nerve root.[272] The soleus Hoffmann reflex is an electrically induced reflex equivalent to the Achilles tendon tap reflex which bypasses the muscle spindle.[86] We found an inhibited Hoffmann reflex amplitude during location pressure application to the posterior thigh suggesting decreased α-motoneuron output at the level of S1. The present study demonstrates that the function of the dermatome and myotome of the S1 spinal nerve root is decreased during pressure application, while function the L5 spinal nerve root dermatome is not decreased. These data support a spinal level dependent response to local pressure application although we did not measure the L5 level myotome with reflex testing. Future studies should

examine the reflex response during local pressure application using a muscle innervated from the L5 level.

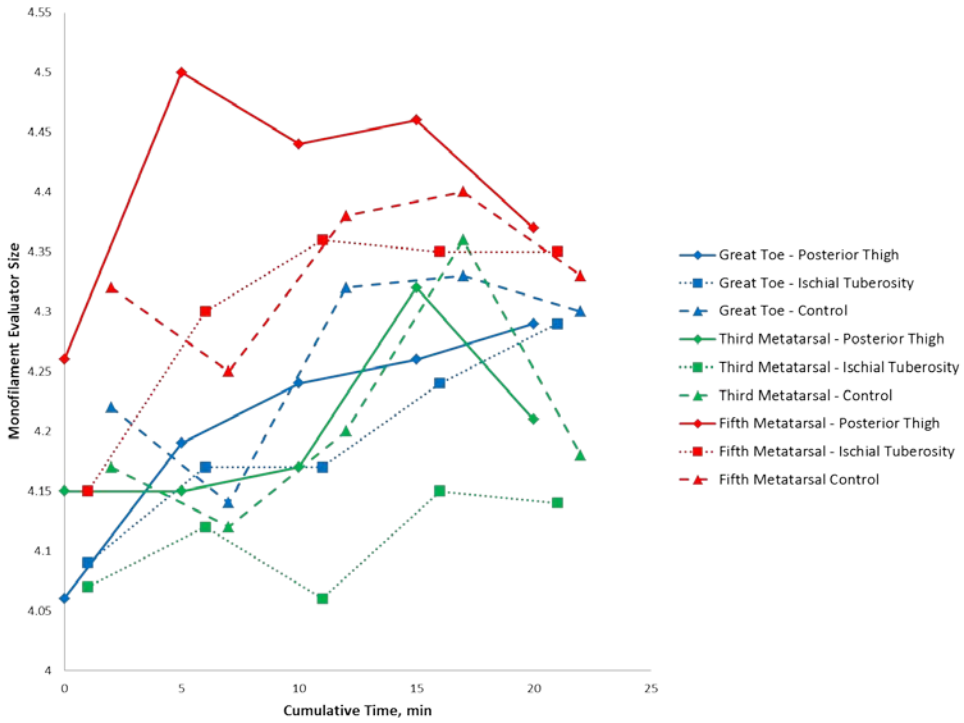

Figure 61. Combined Semmes-Weinstein monofilament test scores for project three. min: minute.

The two-point discrimination test at the great toe, medial malleolus, and lateral malleolus found no significant changes across all three conditions or across time (Figure 62). This indicates that receptive field size and sensitivity are unchanged as a result of local pressure application. Our results are similar to others which found no significant difference of two-point discrimination scores during local pressure application[85,292] or during a prolonged restricted sitting protocol.[292] While used frequently in clinical settings,[194,201,205] our results and the results of others suggest that the two-point discrimination test may not be a viable measure to examine

the effect of local pressure application or prolonged restricted sitting on lower extremity receptive field size or function. Future research should explore other means of examining the sensory nervous system which could be used in both an experimental and field setting.

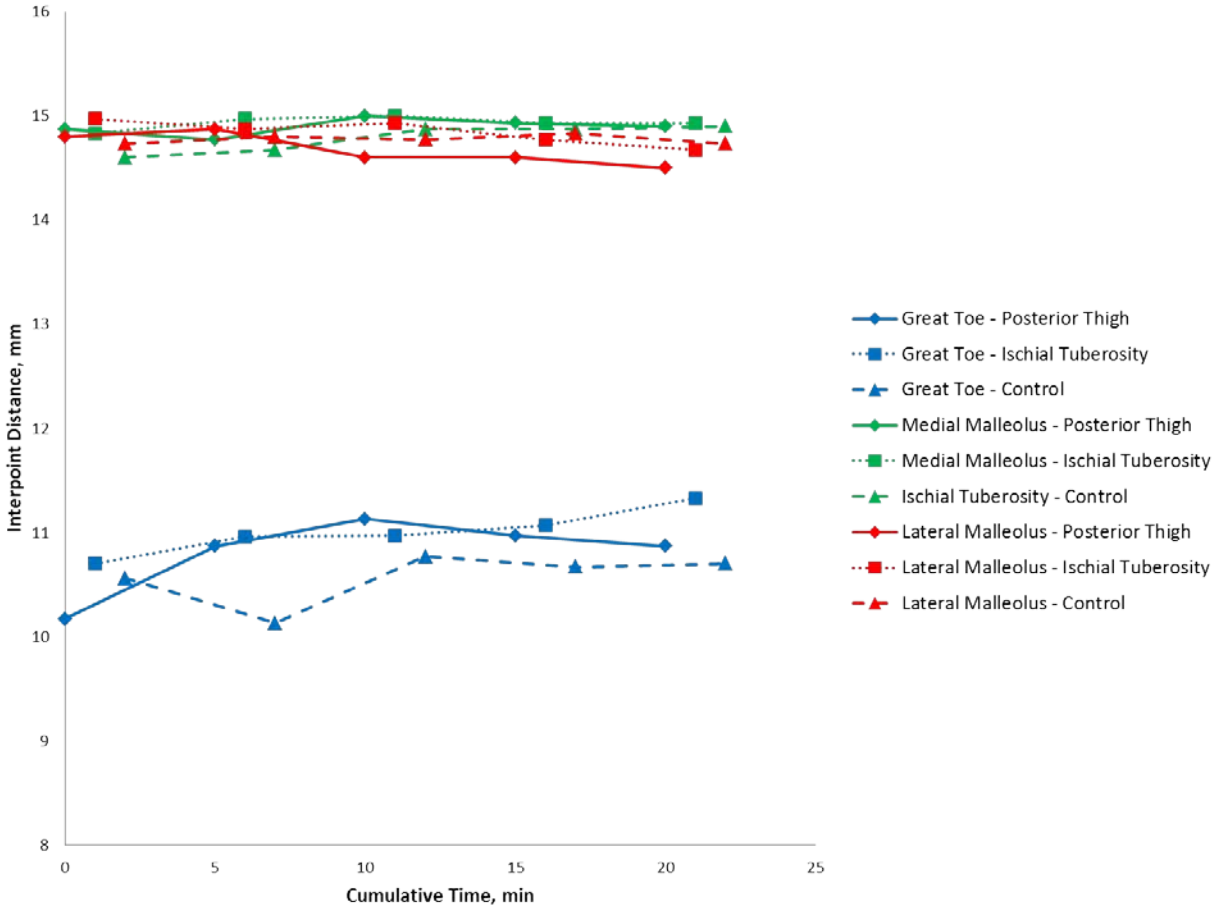

Figure 62. Combined two-point discrimination test scores for project three. min: minute; mm: millimeter.

Subjective Discomfort

Subjective discomfort as measured with the Category Partitioning Scale was increased when pressure was applied to the posterior thigh when compared to the ischial tuberosity and the control condition. The discomfort remained elevated above baseline (5 minutes post-pressure =

11.46 points and 10 minutes post-pressure = 12.66 points, compared to 3.16 points at baseline) following pressure application. The three subsections of the short form of the McGill Pain Questionnaire (descriptor scores, visual analog scale distances, and present pain intensity scores) all showed similar results (Figure 63). These results are in agreement with previous research which found that local pressure application to the posterior thigh and ischial tuberosity increased discomfort during and after application;[85,292] and also work which examined the effects of prolonged restricted sitting in rotary-winged[292] and fixed-winged aircraft.[3,9,15] While these results seem obvious they provide evidence that local pressure application creates increases in subjective discomfort similar to the increases observed during prolonged restricted sitting; supporting the hypothesis that areas of locally high pressure create discomfort during prolonged missions. Additionally, these results demonstrate areas of high pressure near the edge of the seat (close to the posterior thigh pressure application) may be more problematic than the areas of highest pressure recorded near the ischial tuberosities.[1,15] Future research should continue to examine the relationship between local pressure application discomfort, discomfort experienced during prolonged restricted sitting, and the relation of these to improved seat design.

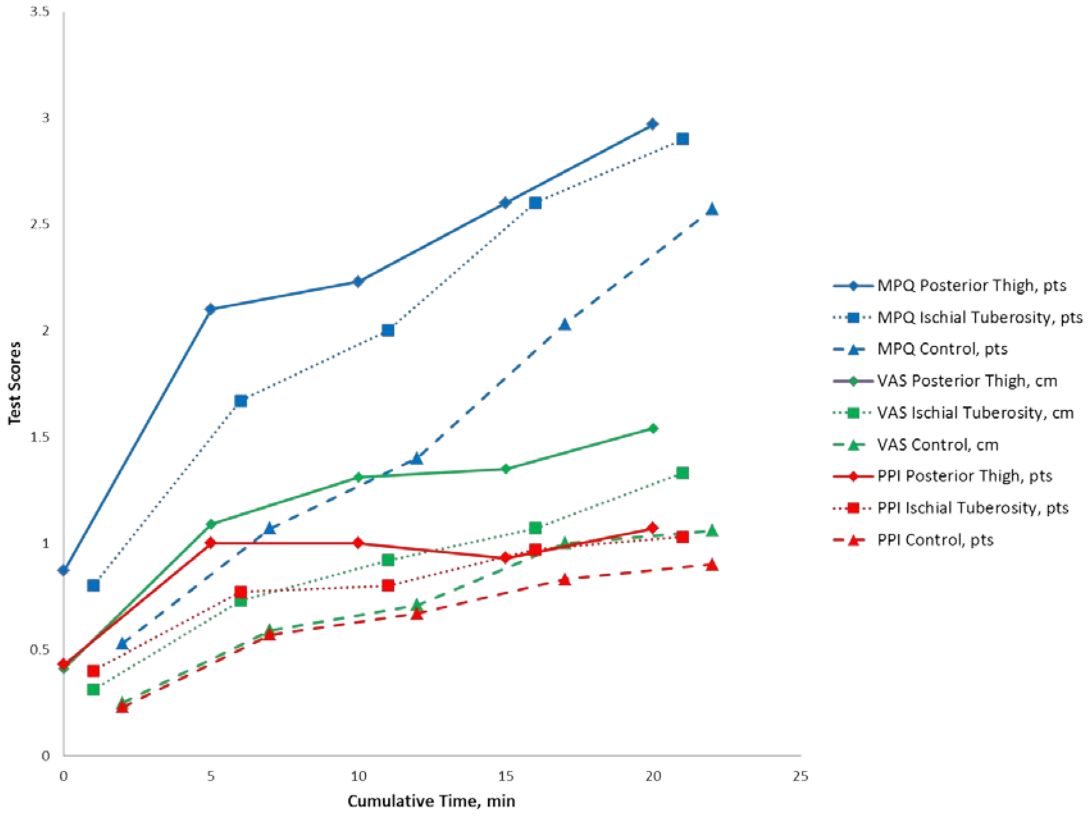

Figure 63. Combined McGill Pain Questionnaire subsections for project three. min: minute; pts: points; cm: centimeter.

Conclusion

Together these results suggest that 44 kilopascals of local pressure application decreases motoneuron pool excitability, increases superficial anterior and lateral ankle skin temperature, decreases sensitivity of the lateral aspect of the plantar surface of the foot, and increases subjective discomfort. These differences were greater when pressure was applied to the posterior thigh compared to the ischial tuberosity. We also believe that the neurological changes associated with local pressure application follow a nerve root dependent distribution, however more work needs to be completed in this area.

Chapter VII

Conclusions and Future Work

This study examined the effects of prolonged restricted sitting in a UH-60 Black Hawk helicopter pilot's seat and local pressure application to the buttocks. Three projects were developed to investigate changes to subjective discomfort, lower extremity sensibility, lower extremity vascular function, and neurological function during sitting. The data demonstrated that, as expected, a 4 hour bout of restricted sitting resulted in increased discomfort, decreased lower extremity sensibility, and decreased skin temperature at the anterior and lateral ankle. Additionally we found that local pressure application to the posterior thigh and ischial tuberosity at 36 and 44 kilopascals increased discomfort, decreased lower extremity sensibility, and increased skin temperature at the anterior and lateral ankle. These effects where more pronounced when pressure was applied at 44 kilopascals to the posterior thigh than at the other conditions. Finally, we found that 44 kilopascals of pressure applied to the posterior thigh or ischial tuberosity decreased soleus Hoffmann reflex amplitude, increased subjective discomfort, decreased lower extremity sensibility, and increased lower extremity temperature. These data indicate that pilot's seats in Black Hawk helicopters produce symptoms of discomfort which may be due to areas of locally high pressure altering neurological and vascular function. However, much work needs to be completed in order to better understand changes associated with prolonged sitting and improving seat structure to diminish the negative effects associated with prolonged sitting such as pain and temporary parathesia.

Future Work

There are multiple directions in which this current research could be expanded. These include: examining anatomical changes with imaging modalities (e.g. magnetic resonance imaging); investigating the contribution of rotor vibration and shock to discomfort during prolonged restricted sitting; and examining the effects of Warrior gear on physiologic changes and discomfort during flight. Each of these areas will aid in our understanding of how the human body changes during bouts of prolonged sitting and local pressure application in rotary-winged aircraft.

Examining the anatomical changes occurring during prolonged sitting and local pressure application is essential to understanding which tissues are affected. Results from the present study suggest which anatomical structures are altered during local pressure application and prolonged sitting based on the physiological changes observed. However, without confirmation through imaging devices such as magnetic resonance imaging and sonography no conclusions can be made. Our laboratory is currently collecting pilot data to observe anatomical changes during local pressure application using high-field (3 Tesla) magnetic resonance imaging. We plan to expand on this project by incorporating the neurological measures collected in the present study with high-field magnetic resonance imaging to directly examine the effects of local pressure application on physiologic function.

The current study did not examine the effects of rotor vibration and prolonged restricted sitting on discomfort or temporary parathesia. Ideally, data would be collected on Black Hawk pilot's during prolonged flight, however the feasibility of such studies is low. An alternative to collecting data during flight is to collect the vibration profile of the Black Hawk helicopter using

accelerometers and then transferring those data into a multi-axis ride simulator which would provide the exact ride profile found during prolonged flight in a Black Hawk in a laboratory setting. This would allow researchers to replicate the physical stresses on the body during prolonged flight while still allowing for the safe and effective collection of physiologic data.

In the present study, participants wore shorts and a t-shirt with bare feet to allow access to the lower extremity in order to collect data. In the field, Black Hawk helicopter pilots wear many pieces of equipment and clothing including: the Army Combat Uniform; protective helmets with night vision goggles; combat boots; and body armor. This adds a substantial amount of mass to the pilot, which increases the mass applied to the seat pan during flight possibly changing the onset and intensity of the discomfort and temporary parathesia. Testing participants in full flight gear will require innovative methods of data collection, but will yield invaluable insights into the effects of prolonged restricted sitting in a rotary-winged aircraft.

The end goal of any research needs to be improved aviator performance, health and wellbeing. Ultimately, improving the current seat design while maintaining or improving safety is the goal. This will require expertise from several disciplines including kinesiology, physiology, aviation medicine, ergonomics, engineering, and military sciences. The end users, military rotary-winged aviators, also need to be included in the development of an improved seat design. Finally, any knowledge gained and lessons learned will also have direct transition to the civilian sector.

The United States Armed Forces spends millions of dollars each year treating the injuries associated with the helicopter seat system. Improved seat design will not only improve mission

efficacy, but also save the Armed Forces tens of millions of dollars through reduced injury, training time lost, and disability while also improving mission efficacy.

Works Cited

1. Cohen D. An objective measure of seat comfort. *Aviat Space Environ Med.* Apr 1998;69(4):410-414.

2. Shackel B, Chidsey KD, Shipley P. The assessment of chair comfort. *Ergonomics.* Mar 1969;12(2):269-306.

3. Pellettiere JA, Parakkat J, Reynolds D, Sasidharan M, El-Zoghbi M, Oudenhuijzen A. The effects of eject seat cushion design on physical fatigue and cognitive performance. In: Force A, ed. Wright-Patterson AFB, OH2006:1-39.

4. Sheard SC, Pethybridge RJ, Wright JM, McMillan GHG. Back pain in aircrew - An initial survey. *Aviation Space and Environmental Medicine.* May 1996;67(5):474-477.

5. Simon-Arndt CM, Yuan H, Hourani LL. Aircraft type and diagnosed back disorders in US Navy pilots and aircrew. *Aviation Space and Environmental Medicine.* Nov 1997;68(11):1012-1018.

6. Taneja N, Pinto LJ. Diagnostic categories among 232 military aircrew with musculoskeletal disabilities. *Aviation Space and Environmental Medicine.* Jun 2005;76(6):581-585.

7. Army US. U.S. Army Fact Files: Black Hawk. http://www.army.mil/factfiles/equipment/aircraft/blackhawk.html. Accessed April 06, 2012, 2012.

8. MH-60 Black Hawk. 2012; http://www.soc.mil/160th/Black%20Hawk.html. Accessed May 23, 2012.

9. Pellettiere JA, Gallagher HL. Time based subjective evaluations of seating cushion comfort. In: Force A, ed. Wright-Patterson AFB, OH2007:1-24.

10. Little B. Forward arming and refueling team keeps aircraft in U.S. Army Europe-Led Task Force in flight. 2008:1. http://www.army.mil/article/7268/Forward_arming_and_refueling_team_keeps_aircraft_in_U_S__Army_Europe_Led_Task_Force_in_the_fight/. Accessed April 06, 2012.

11. Butler BP, Alem NM. Apache Helicopter Seat Cushion Evaluation. In: Defense Do, ed. Fort Rucker, AL: Army Aeromedical Research Laboratory; 1994:61.

12. Chen Y, Wickramasinghe V, Zimcik D. Development of Adaptive Seat Mounts for Helicopter Aircrew Body Vibration Reduction. *Journal of Vibration and Control.* Dec 2009;15(12):1809-1825.

13. Chen Y, Wickramasinghe V, Zimcik DG. Development of Adaptive Helicopter Seat for Aircrew Vibration Reduction. *Journal of Intelligent Material Systems and Structures.* Mar 2011;22(5):489-502.

14. Chen Y, Wickramasinghe V, Zimcik DG. Investigation of Helicopter Seat Structural Dynamics for Aircrew Vibration Mitigation. *Journal of the American Helicopter Society.* Jan 2011;56(1).

15. Jackson C, Emck AJ, Hunston MJ, Jarvis PC. Pressure Measurements and Comfort of Foam Safety Cushions for Confined Seating. *Aviation Space and Environmental Medicine.* Jun 2009;80(6):565-569.

16. Aydog ST, Turbedar E, Demirel AH, Tetik O, Akin A, Doral MN. Cervical and lumbar spinal changes diagnosed in four-view radiographs of 732 military pilots. *Aviation Space and Environmental Medicine.* Feb 2004;75(2):154-157.

17. Studying the nervous system. In: Purves D, Augustine GJ, Fitzpatrick D, et al., eds. *Neuroscience*. 4th ed. Sunderland, MA: Sinauer Associates; 2008:1-9.

18. Hall JE. Organization of the nervous system, basic functions of synapses, and neurotransmitters. *Guyton and Hall Textbook of Medical Physiology*. Philadelphia: Saunders Elsevier; 2011:543-558.

19. Silverthorn DU. Neurons: Cellular and network properties. *Human Physiology: An Integrated Approach*. 4 ed. San Francisco: Pearson Benjamin Cummings; 2007:243-290.

20. Edstrom A, Mattsson H. Fast axonal transport in vitro in the sciatic system of the frog. *Journal of neurochemistry.* Jan 1972;19(1):205-221.

21. Powers SK, Howley ET. *Exercise physiology: Theory and application to fitness and performance*. 8th ed. New York: McGraw-Hill Inc.; 2012.

22. Synaptic transmission. In: Purves D, Augustine GJ, Fitzpatrick D, et al., eds. *Neuroscience*. 4 ed. Sunderland, MA: Sinauer Associates; 2008:85-117.

23. Hodgkin AL, Huxley AF. Propagation of electrical signals along giant nerve fibers. *Proc R Soc Lond B Biol Sci.* Oct 16 1952;140(899):177-183.

24. Hodgkin AL, Huxley AF. Currents carried by sodium and potassium ions through the membrane of the giant axon of Loligo. *J Physiol.* Apr 1952;116(4):449-472.

25. Hodgkin AL, Huxley AF. The components of membrane conductance in the giant axon of Loligo. *J Physiol.* Apr 1952;116(4):473-496.

26. Hodgkin AL, Huxley AF, Katz B. Measurement of current-voltage relations in the membrane of the giant axon of Loligo. *J Physiol.* Apr 1952;116(4):424-448.

27. Armstrong CM, Bezanilla F. Charge movement associated with the opening and closing of the activation gates of the Na channels. *The Journal of general physiology.* May 1974;63(5):533-552.

28. Bezanilla F, Rojas E, Taylor RE. Sodium and potassium conductance changes during a membrane action potential. *J Physiol.* Dec 1970;211(3):729-751.

29. Noble D, Stein RB. The threshold conditions for initiation of action potentials by excitable cells. *J Physiol.* Nov 1966;187(1):129-162.

30. Laporte Y. Continuous conduction of impulses in peripheral myelinated nerve fibers. *The Journal of general physiology.* Nov 1951;35(2):343-360.

31. Gray H. *Gray's Anatomy*. Raleigh, NC: Sweetwater Press; 2007.

32. Martini FH, Bartholomew EF. *Essentials of anatomy and physiology*. 4th ed. San Francisco: Pearson; 2006.

33. Hall JE. Vascular distensibility and functions of the arterial and venous systems. *Guyton and Hall Textbook of Medical Physiology*. 12 ed. Philadelphia: Saunders Elsevier; 2011:167-176.

34. Silverthorn DU. Blood flow and the control of blood pressure. *Human Physiology: An Integrated Approach*. 4 ed. San Francisco: Pearson Benjamin Cummings; 2007:501-534.

35. Burton AC. Relation of structure to function of the tissues of the wall of blood vessels. *Physiological reviews.* Oct 1954;34(4):619-642.

36. Hall JE. Local and humoral control of tissue blood flow. *Guyton and Hall Textbook of Medical Phsyiology*. 12 ed. Philadelphia: Saunders Elsevier; 2011:191-200.

37. Hall JE. Nervous regulation of the circulation, and rapid control of arterial pressure. *Guyton and Hall Textbook of Medical Physiology*. 12 ed. Philadelphia: Saunders Elsevier; 2011:201-211.

38. Casey DP, Joyner MJ. Local control of skeletal muscle blood flow during exercise: influence of available oxygen. *J Appl Physiol.* Dec 2011;111(6):1527-1538.

39. Casey DP, Madery BD, Curry TB, Eisenach JH, Wilkins BW, Joyner MJ. Nitric oxide contributes to the augmented vasodilatation during hypoxic exercise. *J Physiol.* Jan 15 2010;588(Pt 2):373-385.

40. Leuenberger UA, Johnson D, Loomis J, Gray KS, MacLean DA. Venous but not skeletal muscle interstitial nitric oxide is increased during hypobaric hypoxia. *European journal of applied physiology.* Mar 2008;102(4):457-461.

41. Pohl U, Busse R. Hypoxia stimulates release of endothelium-derived relaxant factor. *The American journal of physiology.* Jun 1989;256(6 Pt 2):H1595-1600.

42. Singel DJ, Stamler JS. Chemical physiology of blood flow regulation by red blood cells: the role of nitric oxide and S-nitrosohemoglobin. *Annual review of physiology.* 2005;67:99-145.

43. Stamler JS, Jia L, Eu JP, et al. Blood flow regulation by S-nitrosohemoglobin in the physiological oxygen gradient. *Science.* Jun 27 1997;276(5321):2034-2037.

44. Casey DP, Madery BD, Pike TL, et al. Adenosine receptor antagonist and augmented vasodilation during hypoxic exercise. *J Appl Physiol.* Oct 2009;107(4):1128-1137.

45. Metting PJ, Weldy DL, Ronau TF, Britton SL. Effect of aminophylline on hindlimb blood flow autoregulation during increased metabolism in dogs. *J Appl Physiol.* Jun 1986;60(6):1857-1864.

46. Persson MG, Ohlen A, Lindbom L, Hedqvist P, Gustafsson LE. Role of adenosine in functional hyperemia in skeletal muscle as indicated by pharmacological tools. *Naunyn-Schmiedeberg's archives of pharmacology.* Jan 1991;343(1):52-57.

47. Poucher SM. The role of the A(2A) adenosine receptor subtype in functional hyperaemia in the hindlimb of anaesthetized cats. *J Physiol.* Apr 15 1996;492 (Pt 2):495-503.

48. Poucher SM, Nowell CG, Collis MG. The role of adenosine in exercise hyperaemia of the gracilis muscle in anaesthetized cats. *J Physiol.* Aug 1990;427:19-29.

49. Silverberg AB, Shah SD, Haymond MW, Cryer PE. Norepinephrine: hormone and neurotransmitter in man. *The American journal of physiology.* Mar 1978;234(3):E252-256.

50. Rush JW, Aultman CD. Vascular biology of angiotensin and the impact of physical activity. *Applied physiology, nutrition, and metabolism = Physiologie appliquee, nutrition et metabolisme.* Feb 2008;33(1):162-172.

51. Spier SA, Laughlin MH, Delp MD. Effects of acute and chronic exercise on vasoconstrictor responsiveness of rat abdominal aorta. *J Appl Physiol.* Nov 1999;87(5):1752-1757.

52. Laughlin MH, Rubin LJ, Rush JW, Price EM, Schrage WG, Woodman CR. Short-term training enhances endothelium-dependent dilation of coronary arteries, not arterioles. *J Appl Physiol.* Jan 2003;94(1):234-244.

53. Carroll PR, Neering IR. Relationship between vasoconstriction and histamine induced vasodilation. *The Australian journal of experimental biology and medical science.* Apr 1976;54(2):197-202.

54. Thomas GD, Segal SS. Neural control of muscle blood flow during exercise. *J Appl Physiol.* Aug 2004;97(2):731-738.

55. Uflacker R. *Atlas of vascular anatomy: An angiographic approach*. 2nd ed. Philadelphia: Lippincott Williams & Wilkins; 2006.

56. Cacchione B, Janszen G, Nettuno PG. Numerical investigation on carbon foam-based dampers for helicopter seats. *International Journal of Crashworthiness.* 2011;16(5):511-522.

57. Akins JS, Karg PE, Brienza DM. Interface shear and pressure characteristics of wheelchair seat cushions. *J Rehabil Res Dev.* 2011;48(3):225-234.

58. Brienza DM, Karg PE, Brubaker CE. Seat cushion design for elderly wheelchair users based on minimization of soft tissue deformation using stiffness and pressure measurements. *IEEE Trans Rehabil Eng.* Dec 1996;4(4):320-327.

59. Crawford SA, Stinson MD, Walsh DM, Porter-Armstrong AP. Impact of sitting time on seat-interface pressure and on pressure mapping with multiple sclerosis patients. *Arch Phys Med Rehabil.* Jun 2005;86(6):1221-1225.

60. Dabnichki P, Taktak D. Pressure variation under the ischial tuberosity during a push cycle. *Med Eng Phys.* Jun 1998;20(4):242-256.

61. Geyer MJ, Brienza DM, Karg P, Trefler E, Kelsey S. A randomized control trial to evaluate pressure-reducing seat cushions for elderly wheelchair users. *Adv Skin Wound Care.* May-Jun 2001;14(3):120-129; quiz 131-122.

62. Gil-Agudo A, De la Pena-Gonzalez A, Del Ama-Espinosa A, Perez-Rizo E, Diaz-Dominguez E, Sanchez-Ramos A. Comparative study of pressure distribution at the user-

cushion interface with different cushions in a population with spinal cord injury. *Clin Biomech (Bristol, Avon).* Aug 2009;24(7):558-563.

63. Hobson DA. Comparative effects of posture on pressure and shear at the body-seat interface. *J Rehabil Res Dev.* Fall 1992;29(4):21-31.

64. Kernozek TW, Wilder PA, Amundson A, Hummer J. The effects of body mass index on peak seat-interface pressure of institutionalized elderly. *Arch Phys Med Rehabil.* Jun 2002;83(6):868-871.

65. Jackson C, Emck AJ, Hunston MJ, Jarvis PC. Pressure measurements and comfort of foam safety cushions for confined seating. *Aviat Space Environ Med.* Jun 2009;80(6):565-569.

66. Hamaoka T, McCully KK, Niwayama M, Chance B. The use of muscle near-infrared spectroscopy in sport, health and medical sciences: recent developments. *Philos Transact A Math Phys Eng Sci.* Nov 28 2011;369(1955):4591-4604.

67. Brienza DM, Karg PE, Geyer MJ, Kelsey S, Trefler E. The relationship between pressure ulcer incidence and buttock-seat cushion interface pressure in at-risk elderly wheelchair users. *Arch Phys Med Rehabil.* Apr 2001;82(4):529-533.

68. Rosenthal MJ, Felton RM, Hileman DL, Lee M, Friedman M, Navach JH. A wheelchair cushion designed to redistribute sites of sitting pressure. *Arch Phys Med Rehabil.* Mar 1996;77(3):278-282.

69. Stockton L, Gebhardt KS, Clark M. Seating and pressure ulcers: clinical practice guideline. *J Tissue Viability.* Nov 2009;18(4):98-108.

70. Bennett L, Kavner D, Lee BY, Trainor FS, Lewis JM. Skin blood flow in seated geriatric patients. *Arch Phys Med Rehabil.* Aug 1981;62(8):392-398.

71. Bennett L, Kavner D, Lee BY, Trainor FS, Lewis JM. Skin stress and blood flow in sitting paraplegic patients. *Arch Phys Med Rehabil.* Apr 1984;65(4):186-190.

72. Allen J. Photoplethysmography and its application in clinical physiological measurement. *Physiol Meas.* Mar 2007;28(3):R1-39.

73. Goossens RH, Zegers R, Hoek van Dijke GA, Snijders CJ. Influence of shear on skin oxygen tension. *Clin Physiol.* Jan 1994;14(1):111-118.

74. Seiler WO, Stahelin HB. Skin oxygen tension as a function of imposed skin pressure: implication for decubitus ulcer formation. *Journal of the American Geriatrics Society.* Jul 1979;27(7):298-301.

75. Ogrin R, Woodward M, Sussman G, Khalil Z. Oxygen tension assessment: an overlooked tool for prediction of delayed healing in a clinical setting. *Int Wound J.* Oct 2011;8(5):437-445.

76. Dahlin LB, Shyu BC, Danielsen N, Andersson SA. Effects of nerve compression or ischaemia on conduction properties of myelinated and non-myelinated nerve fibres. An experimental study in the rabbit common peroneal nerve. *Acta Physiol Scand.* May 1989;136(1):97-105.

77. Fern R, Harrison PJ. The effects of compression upon conduction in myelinated axons of the isolated frog sciatic nerve. *J Physiol.* Jan 1991;432:111-122.

78. Hargens AR, Botte MJ, Swenson MR, Gelberman RH, Rhoades CE, Akeson WH. Effects of local compression on peroneal nerve function in humans. *J Orthop Res.* Nov 1993;11(6):818-827.

79. Rainer WG, Mayer J, Sadler TR, Jr., Dirks D. Effect of graded compression on nerve conduction velocity. An experimental study. *Arch Surg.* Nov 1973;107(5):719-721.

80. Gupta R, Steward O. Chronic nerve compression induces concurrent apoptosis and proliferation of Schwann cells. *J Comp Neurol.* Jun 23 2003;461(2):174-186.

81. Mozaffar T, Strandberg E, Abe K, Hilgenberg LG, Smith MA, Gupta R. Neuromuscular junction integrity after chronic nerve compression injury. *J Orthop Res.* Jan 2009;27(1):114-119.

82. Pelletier J, Fromy B, Morel G, Roquelaure Y, Saumet JL, Sigaudo-Roussel D. Chronic sciatic nerve injury impairs the local cutaneous neurovascular interaction in rats. *Pain.* Jan 2012;153(1):149-157.

83. Marchini C, Zambito Marsala S, Fabris F, Fornasier A, Ferracci F. Peroneal nerve orthodromic sensory conduction technique: normative data. *Neurol Sci.* Jun 2009;30(3):201-205.

84. Han SE, Lin CS, Boland RA, Kiernan MC. Nerve compression, membrane excitability, and symptoms of carpal tunnel syndrome. *Muscle Nerve.* Sep 2011;44(3):402-409.

85. St. Onge PM. *Effects of tissue compression on the Hoffmann reflex: Comparison between ischial tuberosity and posterior thigh* [Dissertation]. Auburn, AL: Kinesiology, Auburn University; 2007.

86. Palmieri RM, Ingersoll CD, Hoffman MA. The hoffmann reflex: methodologic considerations and applications for use in sports medicine and athletic training research. *J Athl Train.* Jul 2004;39(3):268-277.

87. Brienza DM, Chung KC, Brubaker CE, Wang J, Karg TE, Lin CT. A system for the analysis of seat support surfaces using surface shape control and simultaneous measurement of applied pressures. *IEEE Trans Rehabil Eng.* Jun 1996;4(2):103-113.

88. Brienza DM, Karg PE. Seat cushion optimization: a comparison of interface pressure and tissue stiffness characteristics for spinal cord injured and elderly patients. *Arch Phys Med Rehabil.* Apr 1998;79(4):388-394.

89. Gyi DE, Porter JM. Interface pressure and the prediction of car seat discomfort. *Appl Ergon.* Apr 1999;30(2):99-107.

90. Stinson MD, Porter-Armstrong A, Eakin P. Seat-interface pressure: a pilot study of the relationship to gender, body mass index, and seating position. *Arch Phys Med Rehabil.* Mar 2003;84(3):405-409.

91. Vos GA, Congleton JJ, Moore JS, Amendola AA, Ringer L. Postural versus chair design impacts upon interface pressure. *Appl Ergon.* Sep 2006;37(5):619-628.

92. Hitosugi M, Niwa M, Takatsu A. Rheologic changes in venous blood during prolonged sitting. *Thromb Res.* Dec 1 2000;100(5):409-412.

93. Goossens RH, Snijders CJ, Holscher TG, Heerens WC, Holman AE. Shear stress measured on beds and wheelchairs. *Scand J Rehabil Med.* Sep 1997;29(3):131-136.

94. DiGiovine MM, Cooper RA, Boninger ML, Lawrence BM, VanSickle DP, Rentschler AJ. User assessment of manual wheelchair ride comfort and ergonomics. *Archives of Physical Medicine and Rehabilitation.* Apr 2000;81(4):490-494.

95. Sondergaard KH, Olesen CG, Sondergaard EK, de Zee M, Madeleine P. The variability and complexity of sitting postural control are associated with discomfort. *J Biomech.* Jul 20 2010;43(10):1997-2001.

96. de Oliveira CG, Nadal J. Back muscle EMG of helicopter pilots in flight: effects of fatigue, vibration, and posture. *Aviat Space Environ Med.* Apr 2004;75(4):317-322.

97. Makhsous M, Lin F, Bankard J, Hendrix RW, Hepler M, Press J. Biomechanical effects of sitting with adjustable ischial and lumbar support on occupational low back pain: evaluation of sitting load and back muscle activity. *BMC Musculoskelet Disord.* 2009;10:17.

98. Goossens RH, Snijders CJ, Fransen T. Biomechanical analysis of the dimensions of pilot seats in civil aircraft. *Appl Ergon.* Feb 2000;31(1):9-14.

99. Bennett L, Kavner D, Lee BK, Trainor FA. Shear vs pressure as causative factors in skin blood flow occlusion. *Arch Phys Med Rehabil.* Jul 1979;60(7):309-314.

100. Gyi DE, Porter JM, Robertson NK. Seat pressure measurement technologies: considerations for their evaluation. *Appl Ergon.* Apr 1998;29(2):85-91.

101. Dinsdale SM. Decubitus ulcers: role of pressure and friction in causation. *Arch Phys Med Rehabil.* Apr 1974;55(4):147-152.

102. Bouten CV, Oomens CW, Baaijens FP, Bader DL. The etiology of pressure ulcers: skin deep or muscle bound? *Arch Phys Med Rehabil.* Apr 2003;84(4):616-619.

103. Hall RC, Nyland J, Nitz AJ, Pinerola J, Johnson DL. Relationship between ankle invertor H-reflexes and acute swelling induced by inversion ankle sprain. *J Orthop Sports Phys Ther.* Jun 1999;29(6):339-344.

104. Hopkins JT, Ingersoll CD, Edwards JE, Cordova ML. Changes in soleus motoneuron pool excitability after artificial knee joint effusion. *Arch Phys Med Rehabil.* Sep 2000;81(9):1199-1203.

105. Hopkins JT, Ingersoll CD, Krause BA, Edwards JE, Cordova ML. Effect of knee joint effusion on quadriceps and soleus motoneuron pool excitability. *Med Sci Sports Exerc.* Jan 2001;33(1):123-126.

106. McVey ED, Palmieri RM, Docherty CL, Zinder SM, Ingersoll CD. Arthrogenic muscle inhibition in the leg muscles of subjects exhibiting functional ankle instability. *Foot Ankle Int.* Dec 2005;26(12):1055-1061.

107. Palmieri RM, Ingersoll CD, Edwards JE, et al. Arthrogenic muscle inhibition is not present in the limb contralateral to a simulated knee joint effusion. *Am J Phys Med Rehabil.* Dec 2003;82(12):910-916.

108. Palmieri RM, Ingersoll CD, Hoffman MA, et al. Arthrogenic muscle response to a simulated ankle joint effusion. *Br J Sports Med.* Feb 2004;38(1):26-30.

109. Palmieri RM, Tom JA, Edwards JE, et al. Arthrogenic muscle response induced by an experimental knee joint effusion is mediated by pre- and post-synaptic spinal mechanisms. *J Electromyogr Kinesiol.* Dec 2004;14(6):631-640.

110. Palmieri RM, Weltman A, Edwards JE, et al. Pre-synaptic modulation of quadriceps arthrogenic muscle inhibition. *Knee Surg Sports Traumatol Arthrosc.* Jul 2005;13(5):370-376.

111. Palmieri-Smith RM, Hopkins JT, Brown TN. Peroneal activation deficits in persons with functional ankle instability. *Am J Sports Med.* May 2009;37(5):982-988.

112. Sefton JM, Hicks-Little CA, Hubbard TJ, et al. Segmental spinal reflex adaptations associated with chronic ankle instability. *Arch Phys Med Rehabil.* Oct 2008;89(10):1991-1995.

113. Sefton JM, Hicks-Little CA, Hubbard TJ, et al. Sensorimotor function as a predictor of chronic ankle instability. *Clin Biomech (Bristol, Avon).* Jun 2009;24(5):451-458.

114. Spencer JD, Hayes KC, Alexander IJ. Knee joint effusion and quadriceps reflex inhibition in man. *Arch Phys Med Rehabil.* Apr 1984;65(4):171-177.

115. Leroux A, Belanger M, Boucher JP. Pain effect on monosynaptic and polysynaptic reflex inhibition. *Arch Phys Med Rehabil.* Jun 1995;76(6):576-582.

116. Garland SJ, McComas AJ. Reflex inhibition of human soleus muscle during fatigue. *J Physiol.* Oct 1990;429:17-27.

117. Kuchinad RA, Ivanova TD, Garland SJ. Modulation of motor unit discharge rate and H-reflex amplitude during submaximal fatigue of the human soleus muscle. *Exp Brain Res.* Oct 2004;158(3):345-355.

118. Dishman JD, Dougherty PE, Burke JR. Evaluation of the effect of postural perturbation on motoneuronal activity following various methods of lumbar spinal manipulation. *Spine J.* Nov-Dec 2005;5(6):650-659.

119. Etnyre BR, Abraham LD. H-reflex changes during static stretching and two variations of proprioceptive neuromuscular facilitation techniques. *Electroencephalogr Clin Neurophysiol.* Feb 1986;63(2):174-179.

120. Games KE, Sefton JM. Whole-body vibration influences lower extremity circulatory and neurological function. *Scand J Med Sci Sports.* Nov 23 2011.

121. Guissard N, Duchateau J. Effect of static stretch training on neural and mechanical properties of the human plantar-flexor muscles. *Muscle Nerve.* Feb 2004;29(2):248-255.

122. Guissard N, Duchateau J, Hainaut K. Muscle stretching and motoneuron excitability. *Eur J Appl Physiol Occup Physiol.* 1988;58(1-2):47-52.

123. Guissard N, Duchateau J, Hainaut K. Mechanisms of decreased motoneurone excitation during passive muscle stretching. *Exp Brain Res.* Mar 2001;137(2):163-169.

124. Haruna Y, Styf JR, Kahan N, Hargens AR. Hoffmann-reflex is delayed during 6 degree head-down tilt with balanced traction. *Aviat Space Environ Med.* Mar 1999;70(3 Pt 1):220-224.

125. Sefton JM, Yarar C, Hicks-Little CA, Berry JW, Cordova ML. Six weeks of balance training improves sensorimotor function in individuals with chronic ankle instability. *J Orthop Sports Phys Ther.* Feb 2011;41(2):81-89.

126. Dragert K, Zehr EP. Rhythmic arm cycling modulates Hoffmann reflex excitability differentially in the ankle flexor and extensor muscles. *Neurosci Lett.* Feb 6 2009;450(3):235-238.

127. Klass M, Guissard N, Duchateau J. Limiting mechanisms of force production after repetitive dynamic contractions in human triceps surae. *J Appl Physiol.* Apr 2004;96(4):1516-1521; discussion.

128. Ogawa T, Kim GH, Sekiguchi H, Akai M, Suzuki S, Nakazawa K. Enhanced stretch reflex excitability of the soleus muscle in experienced swimmers. *European journal of applied physiology.* Jan 2009;105(2):199-205.

129. Perrey S, Racinais S, Saimouaa K, Girard O. Neural and muscular adjustments following repeated running sprints. *European journal of applied physiology.* Aug 2010;109(6):1027-1036.

130. Roll JP, Martin B, Gauthier GM, Mussa Ivaldi F. Effects of whole-body vibration on spinal reflexes in man. *Aviat Space Environ Med.* Nov 1980;51(11):1227-1233.

131. Schubert M, Beck S, Taube W, Amtage F, Faist M, Gruber M. Balance training and ballistic strength training are associated with task-specific corticospinal adaptations. *Eur J Neurosci.* Apr 2008;27(8):2007-2018.

132. Knikou M. The H-reflex as a probe: pathways and pitfalls. *J Neurosci Methods.* Jun 15 2008;171(1):1-12.

133. Sefton JM, Hicks-Little CA, Koceja DM, Cordova ML. Modulation of soleus H-reflex by presynaptic spinal mechanisms during varying surface and ankle brace conditions. *Neurophysiol Clin.* Jan-Mar 2007;37(1):15-21.

134. Cordova ML, Bernard LW, Au KK, Demchak TJ, Stone MB, Sefton JM. Cryotherapy and ankle bracing effects on peroneus longus response during sudden inversion. *J Electromyogr Kinesiol.* Apr 2010;20(2):348-353.

135. Sefton JM, Hicks-Little CA, Koceja DM, Cordova ML. Effect of inversion and ankle bracing on peroneus longus Hoffmann reflex. *Scand J Med Sci Sports.* Oct 2007;17(5):539-546.

136. Alrowayeh HN, Sabbahi MA, Etnyre B. Flexor carpi radialis H-reflex modulation during spinal loading and unloading with varied forearm postures. *J Clin Neurophysiol.* Apr 2010;27(2):116-119.

137. Baudry S, Enoka RM. Influence of load type on presynaptic modulation of Ia afferent input onto two synergist muscles. *Exp Brain Res.* Oct 2009;199(1):83-88.

138. Lamy JC, Russmann H, Shamim EA, Meunier S, Hallett M. Paired associative stimulation induces change in presynaptic inhibition of Ia terminals in wrist flexors in humans. *J Neurophysiol.* Aug 2010;104(2):755-764.

139. Lee HM, Wu SK, You JY. Quantitative application of transverse friction massage and its neurological effects on flexor carpi radialis. *Man Ther.* Oct 2009;14(5):501-507.

140. Lin KH, Chen YC, Luh JJ, Wang CH, Chang YJ. H-reflex, muscle voluntary activation level, and fatigue index of flexor carpi radialis in individuals with incomplete cervical cord injury. *Neurorehabil Neural Repair.* Jan 2012;26(1):68-75.

141. Phadke CP, Robertson CT, Condliffe EG, Patten C. Upper-extremity H-reflex measurement post-stroke: Reliability and inter-limb differences. *Clin Neurophysiol.* Jan 23 2012.

142. Uysal H, Kizilay F, Inel SE, Ozen H, Pek G. Medium-latency reflex response elicited from the flexor carpi radialis by radial nerve stimulation. *Exp Brain Res.* Mar 2012;217(2):223-235.

143. Zehr EP. Considerations for use of the Hoffmann reflex in exercise studies. *European journal of applied physiology.* Apr 2002;86(6):455-468.

144. Schieppati M. The Hoffmann reflex: a means of assessing spinal reflex excitability and its descending control in man. *Prog Neurobiol.* 1987;28(4):345-376.

145. Panizza M, Nilsson J, Roth BJ, Basser PJ, Hallett M. Relevance of stimulus duration for activation of motor and sensory fibers: implications for the study of H-reflexes and magnetic stimulation. *Electroencephalogr Clin Neurophysiol.* Feb 1992;85(1):22-29.

146. Capaday C. Neurophysiological methods for studies of the motor system in freely moving human subjects. *J Neurosci Methods.* Jun 27 1997;74(2):201-218.

147. Christie A, Lester S, LaPierre D, Gabriel DA. Reliability of a new measure of H-reflex excitability. *Clin Neurophysiol.* Jan 2004;115(1):116-123.

148. Earles DR, Dierking JT, Robertson CT, Koceja DM. Pre- and post-synaptic control of motoneuron excitability in athletes. *Med Sci Sports Exerc.* Nov 2002;34(11):1766-1772.

149. Hayes BT, Hicks-Little CA, Harter RA, Widrick JJ, Hoffman MA. Intersession reliability of Hoffmann reflex gain and presynaptic inhibition in the human soleus muscle. *Arch Phys Med Rehabil.* Dec 2009;90(12):2131-2134.

150. Hoch MC, Krause BA. Intersession reliability of H:M ratio is greater than the H-reflex at a percentage of M-max. *Int J Neurosci.* 2009;119(3):345-352.

151. Hopkins JT, Ingersoll CD, Cordova ML, Edwards JE. Intrasession and intersession reliability of the soleus H-reflex in supine and standing positions. *Electromyogr Clin Neurophysiol.* Mar 2000;40(2):89-94.

152. Hopkins JT, Wagie NC. Intrasession and intersession reliability of the quadriceps Hoffmann reflex. *Electromyogr Clin Neurophysiol.* Mar 2003;43(2):85-89.

153. McIlroy WE, Brooke JD. Within-subject reliability of the Hoffmann reflex in man. *Electromyogr Clin Neurophysiol.* Oct-Nov 1987;27(6-7):401-404.

154. Hwang IS, Tsai IY. Inter-trial variation of soleus H reflex in humans: implication for supraspinal influence. *Electromyogr Clin Neurophysiol.* Dec 2002;42(8):507-512.

155. Lee DH, Claussen GC, Oh S. Clinical nerve conduction and needle electromyography studies. *J Am Acad Orthop Surg.* Jul-Aug 2004;12(4):276-287.

156. Clark BC, Cook SB, Ploutz-Snyder LL. Reliability of techniques to assess human neuromuscular function in vivo. *J Electromyogr Kinesiol.* Feb 2007;17(1):90-101.

157. Lo YL, Xu LQ, Leoh TH, et al. Superficial peroneal sensory and sural nerve conduction studies in peripheral neuropathy. *J Clin Neurosci.* Jun 2006;13(5):547-549.

158. Joynt RL. Calculated nerve conduction velocity dependence upon the method of testing. *Arch Phys Med Rehabil.* May 1983;64(5):212-216.

159. Drenthen J, Blok JH, van Heel EB, Visser GH. Limb temperature and nerve conduction velocity during warming with hot water blankets. *J Clin Neurophysiol.* Apr 2008;25(2):104-110.

160. Emad MR, Najafi SH, Sepehrian MH. The effect of provocative tests on electrodiagnosis criteria in clinical carpal tunnel syndrome. *Electromyogr Clin Neurophysiol.* Sep-Oct 2010;50(6):265-268.

161. Gazioglu S, Boz C, Cakmak VA. Electrodiagnosis of carpal tunnel syndrome in patients with diabetic polyneuropathy. *Clin Neurophysiol.* Jul 2011;122(7):1463-1469.

162. Kommalage M, Pathirana KD. Influence of age and the severity of median nerve compression on forearm median motor conduction velocity in carpal tunnel syndrome. *J Clin Neurophysiol.* Dec 2011;28(6):642-646.

163. Koszewicz M, Gosk-Bierska I, Jerzy G, et al. Peripheral nerve changes assessed by conduction velocity distribution in patients with primary Raynaud's phenomenon and dysautonomia. *Int Angiol.* Aug 2011;30(4):375-379.

164. Moghtaderi AR, Moghtaderi N, Loghmani A. Evaluating the effectiveness of local dexamethasone injection in pregnant women with carpal tunnel syndrome. *J Res Med Sci.* May 2011;16(5):687-690.

165. Rajabally YA, Narasimhan M. Electrophysiological entrapment syndromes in chronic inflammatory demyelinating polyneuropathy. *Muscle Nerve.* Sep 2011;44(3):444-447.

166. Rha DW, Im SH, Kim SK, Chang WH, Kim KJ, Lee SC. Median nerve conduction study through the carpal tunnel using segmental nerve length measured by ultrasonographic and conventional tape methods. *Arch Phys Med Rehabil.* Jan 2011;92(1):1-6.

167. Watson J, Zhao M, Ring D. Predictors of normal electrodiagnostic testing in the evaluation of suspected carpal tunnel syndrome. *J Hand Microsurg.* Dec 2010;2(2):47-50.

168. Werner RA, Franzblau A, D'Arcy HJ, Evanoff BA, Tong HC. Differential aging of median and ulnar sensory nerve parameters. *Muscle Nerve.* Jan 2012;45(1):60-64.

169. Won SJ, Yoon JS, Kim JY, Kim SJ, Jeong JS. Avoiding false-negative nerve conduction study in ulnar neuropathy at the elbow. *Muscle Nerve.* Oct 2011;44(4):583-586.

170. Zhong W, Zhang W, Zheng X, Li S, Shi J. Comparative study of different surgical transposition methods for ulnar nerve entrapment at the elbow. *J Int Med Res.* 2011;39(5):1766-1772.

171. Evans NS, Liu K, Criqui MH, et al. Associations of calf skeletal muscle characteristics and peripheral nerve function with self-perceived physical functioning and walking ability in persons with peripheral artery disease. *Vasc Med.* Feb 2011;16(1):3-11.

172. Garg PK, Liu K, Ferrucci L, et al. Lower extremity nerve function, calf skeletal muscle characteristics, and functional performance in peripheral arterial disease. *Journal of the American Geriatrics Society.* Oct 2011;59(10):1855-1863.

173. Harbo T, Andersen H, Jakobsen J. Length-dependent weakness and electrophysiological signs of secondary axonal loss in chronic inflammatory demyelinating polyradiculoneuropathy. *Muscle Nerve.* Aug 2008;38(2):1036-1045.

174. Plastaras CT, Marciniak CM, Sipple DP, D'Amore KG, Garvan C, Zaman SM. Effect of interelectrode distance on sural nerve action potential parameters. *Am J Phys Med Rehabil.* Mar 2008;87(3):183-188.

175. Rayegani SM, Daneshtalab E, Bahrami MH, et al. Prevalence of accessory deep peroneal nerve in referred patients to an electrodiagnostic medicine clinic. *J Brachial Plex Peripher Nerve Inj.* 2011;6(1):3.

176. Thometz J, Sathoff L, Liu XC, Jacobson R, Tassone JC. Electromyography nerve conduction velocity evaluation of children with clubfeet. *Am J Orthop (Belle Mead NJ).* Feb 2011;40(2):84-86.

177. Oh SJ, Hatanaka Y, Ohira M, Kurokawa K, Claussen GC. Clinical utility of sensory nerve conduction of medial femoral cutaneous nerve. *Muscle Nerve.* Feb 2012;45(2):195-199.

178. Bales J, Bales K, Baugh L, Tokish J. Evaluation for ulnar neuropathy at the elbow in ironman triathletes: physical examination and electrodiagnostic evidence. *Clin J Sport Med.* Mar 2012;22(2):126-131.

179. Watson J, DiBenedetto M, Gale SD. Mixed median nerve forearm conduction velocity in the presence of focal compression neuropathy at the wrist versus peripheral neuropathy. *Arch Phys Med Rehabil.* Mar 2002;83(3):302-307.

180. Oh SJ, Demirci M, Dajani B, Melo AC, Claussen GC. Distal sensory nerve conduction of the superficial peroneal nerve: new method and its clinical application. *Muscle Nerve.* May 2001;24(5):689-694.

181. Rivner MH, Swift TR, Crout BO, Rhodes KP. Toward more rational nerve conduction interpretations: the effect of height. *Muscle Nerve.* Mar 1990;13(3):232-239.

182. Oh SJ. *Clinical electromyography: Nerve conduction studies*. Philadelphia: Lippincott, Williams, & Wilkins; 2003.

183. Leandri M, Leandri S, Lunardi G. Effect of temperature on sensory and motor conduction of the rat tail nerves. *Neurophysiol Clin.* Oct 2008;38(5):297-304.

184. Herrera E, Camargo DM, Delgado DC, Salvini TF. Reliability of superficial peroneal, sural, and medial plantar nerve conduction studies: analysis of statistical methods. *J Clin Neurophysiol.* Oct 2009;26(5):372-379.

185. Izzo KL, Sridhara CR, Rosenholtz H, Lemont H. Sensory conduction studies of the branches of the superficial peroneal nerve. *Arch Phys Med Rehabil.* Jan 1981;62(1):24-27.

186. Bleasel AF, Tuck RR. Variability of repeated nerve conduction studies. *Electroencephalogr Clin Neurophysiol.* Dec 1991;81(6):417-420.

187. Chaudhry V, Cornblath DR, Mellits ED, et al. Inter- and intra-examiner reliability of nerve conduction measurements in normal subjects. *Ann Neurol.* Dec 1991;30(6):841-843.

188. Chaudhry V, Corse AM, Freimer ML, et al. Inter- and intraexaminer reliability of nerve conduction measurements in patients with diabetic neuropathy. *Neurology.* Aug 1994;44(8):1459-1462.

189. Andersen H, Stalberg E, Falck B. F-wave latency, the most sensitive nerve conduction parameter in patients with diabetes mellitus. *Muscle Nerve.* Oct 1997;20(10):1296-1302.

190. Dyck PJ, Kratz KM, Lehman KA, et al. The Rochester Diabetic Neuropathy Study: design, criteria for types of neuropathy, selection bias, and reproducibility of neuropathic tests. *Neurology.* Jun 1991;41(6):799-807.

191. Valensi P, Attali JR, Gagant S. Reproducibility of parameters for assessment of diabetic neuropathy. The French Group for Research and Study of Diabetic Neuropathy. *Diabet Med.* Dec 1993;10(10):933-939.

192. Fuchs JL, Brown PB. Two-point discriminability: relation to properties of the somatosensory system. *Somatosens Res.* 1984;2(2):163-169.

193. Rozental TD, Beredjiklian PK, Guyette TM, Weiland AJ. Intra- and interobserver reliability of sensibility testing in asymptomatic individuals. *Ann Plast Surg.* Jun 2000;44(6):605-609.

194. Bell-Krotoski J, Weinstein S, Weinstein C. Testing sensibility, including touch-pressure, two-point discrimination, point localization, and vibration. *J Hand Ther.* Apr-Jun 1993;6(2):114-123.

195. Dellon ES, Mourey R, Dellon AL. Human pressure perception values for constant and moving one- and two-point discrimination. *Plast Reconstr Surg.* Jul 1992;90(1):112-117.

196. Wolf SL, Nahai F, Brown DM, Jordan N, Kutner M. Objective determinations of sensibility in the upper extremity. Part II. Application of cutaneous stimuli in control subjects. *Phys Ther.* Oct 1977;57(10):1126-1131.

197. Chu NS. Recovery of finger sensibility and somatosensory evoked potentials following digit-to-digit replantation in man. *Scand J Rehabil Med.* Sep 1996;28(3):125-131.

198. Henry FP, Farkhad RI, Butt FS, O'Shaughnessy M, O'Sullivan ST. A comparison between complete immobilisation and protected active mobilisation in sensory nerve recovery following isolated digital nerve injury. *J Hand Surg Eur Vol.* Dec 6 2011.

199. Ingersoll CD, Knight KL, Merrick MA. Sensory perception of the foot and ankle following therapeutic applications of heat and cold. *J Athl Train.* 1992;27(3):231-234.

200. Rubley MD, Denegar CR, Buckley WE, Newell KM. Cryotherapy, Sensation, and Isometric-Force Variability. *J Athl Train.* Jun 2003;38(2):113-119.

201. Kowalzik R, Hermann B, Biedermann H, Peiper U. Two-point discrimination of vibratory perception on the sole of the human foot. *Foot Ankle Int.* Oct 1996;17(10):629-634.

202. Bullock-Saxton JE. Sensory changes associated with severe ankle sprain. *Scand J Rehabil Med.* Sep 1995;27(3):161-167.

203. Braun RM. Two-point discrimination tester. *J Hand Surg Am.* Sep 1986;11(5):770-771.

204. Cope EB, Antony JH. Normal values for the two-point discrimination test. *Pediatr Neurol.* Jul-Aug 1992;8(4):251-254.

205. Nolan MF. Two-point discrimination assessment in the upper limb in young adult men and women. *Phys Ther.* Jul 1982;62(7):965-969.

206. Nolan MF. Limits of two-point discrimination ability in the lower limb in young adult men and women. *Phys Ther.* Sep 1983;63(9):1424-1428.

207. Guyot GW, Johnson FD, Weaver C. Two-point tactual discrimination: a signal detection approach. *Percept Mot Skills.* Apr 1981;52(2):433-434.

208. Halar EM, Hammond MC, LaCava EC, Camann C, Ward J. Sensory perception threshold measurement: an evaluation of semiobjective testing devices. *Arch Phys Med Rehabil.* Aug 1987;68(8):499-507.

209. Feng Y, Schlosser FJ, Sumpio BE. The Semmes Weinstein monofilament examination as a screening tool for diabetic peripheral neuropathy. *J Vasc Surg.* Sep 2009;50(3):675-682, 682 e671.

210. Collins S, Visscher P, De Vet HC, Zuurmond WW, Perez RS. Reliability of the Semmes Weinstein Monofilaments to measure coetaneous sensibility in the feet of healthy subjects. *Disabil Rehabil.* 2010;32(24):2019-2027.

211. McGill M, Molyneaux L, Yue DK. Use of the Semmes-Weinstein 5.07/10 gram monofilament: the long and the short of it. *Diabet Med.* Jul 1998;15(7):615-617.

212. Medical NC. Touch-Test Sensory Evaluator instructions. In: Medical NC, ed. *North Coast Medical Inc.* Morgan Hill, CA2002:1-2.

213. Imai H, Tajima T, Natsuma Y. Interpretation of cutaneous pressure threshold (Semmes-Weinstein monofilament measurement) following median nerve repair and sensory reeducation in the adult. *Microsurgery.* 1989;10(2):142-144.

214. Polatkan S, Orhun E, Polatkan O, Nuzumlali E, Bayri O. Evaluation of the improvement of sensibility after primary median nerve repair at the wrist. *Microsurgery.* 1998;18(3):192-196.

215. Jeng C, Michelson J, Mizel M. Sensory thresholds of normal human feet. *Foot Ankle Int.* Jun 2000;21(6):501-504.

216. McGill M, Molyneaux L, Spencer R, Heng LF, Yue DK. Possible sources of discrepancies in the use of the Semmes-Weinstein monofilament. Impact on prevalence of insensate foot and workload requirements. *Diabetes Care.* Apr 1999;22(4):598-602.

217. Modawal A, Fley J, Shukla R, Rudawsky D, Welge J, Yang J. Use of monofilament in the detection of foot lesions in older adults. *J Foot Ankle Surg.* Mar-Apr 2006;45(2):76-81.

218. Peeters GG, Aufdemkampe G, Oostendorp RA. Sensibility testing in patients with a lumbosacral radicular syndrome. *J Manipulative Physiol Ther.* Feb 1998;21(2):81-88.

219. Ring EF, Ammer K. Infrared thermal imaging in medicine. *Physiol Meas.* 2012;33:R33-R46.

220. Wright CI, Kroner CI, Draijer R. Non-invasive methods and stimuli for evaluating the skin's microcirculation. *J Pharmacol Toxicol Methods.* Jul-Aug 2006;54(1):1-25.

221. Alderson JK, Ring EF. 'Sprite' high resolution thermal imaging system. *Thermology.* 1995;1:110-114.

222. Ring EF, Dicks JM. Spatial resolution of new thermal imaging systems. *Thermol Int.* 1999;19:7-14.

223. Spalding SJ, Kwoh CK, Boudreau R, et al. Three-dimensional and thermal surface imaging produces reliable measures of joint shape and temperature: a potential tool for quantifying arthritis. *Arthritis Res Ther.* 2008;10(1):R10.

224. Varju G, Pieper CF, Renner JB, Kraus VB. Assessment of hand osteoarthritis: correlation between thermographic and radiographic methods. *Rheumatology (Oxford).* Jul 2004;43(7):915-919.

225. Rich PB, Dulabon GR, Douillet CD, et al. Infrared thermography: a rapid, portable, and accurate technique to detect experimental pneumothorax. *J Surg Res.* Aug 2004;120(2):163-170.

226. Vardasca R. *The effect of work related mechanical stress on the peripheral temperature of the hand*. Glamorgan, University of Glamorgan; 2010.

227. Bonnett P, Hare DB, Jones CD, Ring EF, Hare CJ. Some preliminary observations of the effects of sports massage on heat distribution of lower limb muscles during a graded exercise test. *Thermol Int.* 2006;16:143-149.

228. Sefton JM, Yarar C, Berry JW, Pascoe DD. Therapeutic Massage of the Neck and Shoulders Produces Changes in Peripheral Blood Flow When Assessed with Dynamic Infrared Thermography. *Journal of Alternative and Complementary Medicine.* Jul 2010;16(7):723-732.

229. Wu CL, Yu KL, Chuang HY, Huang MH, Chen TW, Chen CH. The application of infrared thermography in the assessment of patients with coccygodynia before and after manual therapy combined with diathermy. *J Manipulative Physiol Ther.* May 2009;32(4):287-293.

230. Yarar C, Pascoe DD, Sefton JM. Therapeutic Massage Effects on Skin and Muscle Blood Flow. *Medicine and Science in Sports and Exercise.* May 2010;42(5):244-244.

231. Ferreira JJ, Mendonca LC, Nunes LA, Andrade Filho AC, Rebelatto JR, Salvini TF. Exercise-associated thermographic changes in young and elderly subjects. *Ann Biomed Eng.* Aug 2008;36(8):1420-1427.

232. Merla A, Mattei PA, Di Donato L, Romani GL. Thermal imaging of cutaneous temperature modifications in runners during graded exercise. *Ann Biomed Eng.* Jan 2010;38(1):158-163.

233. Zontak A, Sideman S, Verbitsky O, Beyar R. Dynamic thermography: analysis of hand temperature during exercise. *Ann Biomed Eng.* Nov-Dec 1998;26(6):988-993.

234. Cholewka A, Stanek A, Sieron A, Drzazga Z. Thermography study of skin response due to whole-body cryotherapy. *Skin Res Technol.* Apr 21 2011.

235. Selfe J, Hardaker N, Whitaker J, Hayes C. An investigation into the effect on skin surface temperature of three cryotherapy modalities. *Thermol Int.* 2009;19:119-124.

236. Hildebrandt C, Raschner C. An intra-examiner reliability study of knee temperature patterns with medical infrared thermal imaging. *Thermol Int.* 2009;19:73-76.

237. Pauling JD, Shipley JA, Raper S, et al. Comparison of infrared thermography and laser speckle contrast imaging for the dynamic assessment of digital microvascular function. *Microvascular Research.* Mar 2012;83(2):162-167.

238. Denoble AE, Hall N, Pieper CF, Kraus VB. Patellar skin surface temperature by thermography reflects knee osteoarthritis severity. *Clin Med Insights Arthritis Musculoskelet Disord.* 2010;3:69-75.

239. Ammer K. The Glamorgan Protocol for recording and evaluation of thermal images of the human body. *Thermol Int.* 2008;18:125-144.

240. Jiang LJ, Ng EY, Yeo AC, et al. A perspective on medical infrared imaging. *J Med Eng Technol.* Nov-Dec 2005;29(6):257-267.

241. Alexander CM, Teller LE, Gross JB. Principles of pulse oximetry: theoretical and practical considerations. *Anesth Analg.* Mar 1989;68(3):368-376.

242. Sinex JE. Pulse oximetry: Principles and limitations. *The American Journal of Emergency Medicine.* 1999;17(1):59-66.

243. Hinkelbein J. Pulse oximetry: Basic principles and applications in aerospace medicine. *Aviation Space and Environmental Medicine.* Apr 2008;79(4):444-444.

244. Li G, Li SY, Lin L, Wang Y, Li XX, Lu ZY. Accuracy analysis of pulse oximetry based on dynamic spectroscopy. *Spectroscopy and Spectral Analysis.* Oct 2006;26(10):1821-1824.

245. Valdez-Lowe C, Ghareeb SA, Artinian NT. Pulse Oximetry in Adults. *AJN The American Journal of Nursing.* 2009;109(6):52-59 10.1097/1001.NAJ.0000352474.0000355746.0000352481.

246. Vegfors M, Tryggvason B, Sjöberg F, Lennmarken C. Assessment of peripheral blood flow using a pulse oximeter. *Journal of Clinical Monitoring and Computing.* 1990;6(1):1-4.

247. Harper RC. The role of pulse oximetry in athletic health care. *Athletic Therapy Today.* Sep 2000;5(5):44-46.

248. Kuniyoshi S, Endoh Y, Kobayashi M, Endoh H. Arterial oxygen desaturation response to repeated bouts of sprint exercise in healthy young women. *Advances in experimental medicine and biology.* 2010;662:335-340.

249. Wood RJ, Gore CJ, Hahn AG, et al. Accuracy of two pulse oximeters during maximal cycling exercise. *Australian journal of science and medicine in sport.* Jun 1997;29(2):47-50.

250. Spanoudaki SS, Maridaki MD, Myrianthefs PM, Baltopoulos PJ. Exercise induced arterial hypoxemia in swimmers. *The Journal of sports medicine and physical fitness.* Dec 2004;44(4):342-348.

251. Severinghaus JW, Naifeh KH. Accuracy of response of six pulse oximeters to profound hypoxia. *Anesthesiology.* Oct 1987;67(4):551-558.

252. Barker SJ, Tremper KK. The effect of carbon monoxide inhalation on pulse oximetry and transcutaneous PO2. *Anesthesiology.* May 1987;66(5):677-679.

253. Scheller MS, Unger RJ, Kelner MJ. Effects of intravenously administered dyes on pulse oximetry readings. *Anesthesiology.* Nov 1986;65(5):550-552.

254. Cote CJ, Goldstein EA, Fuchsman WH, Hoaglin DC. The effect of nail polish on pulse oximetry. *Anesth Analg.* Jul 1988;67(7):683-686.

255. Petterson MT, Begnoche VL, Graybeal JM. The effect of motion on pulse oximetry and its clinical significance. *Anesth Analg.* Dec 2007;105(6 Suppl):S78-84.

256. Ellermeier W, Westphal W, Heidenfelder M. On the "absoluteness" of category and magnitude scales of pain. *Percept Psychophys.* Feb 1991;49(2):159-166.

257. Shen WQ, Parsons KC. Validity and reliability of rating scales for seated pressure discomfort. *International Journal of Industrial Ergonomics.* Dec 1997;20(6):441-461.

258. Telfer S, Spence WD, Solomonidis SE. The Potential for Actigraphy to Be Used as an Indicator of Sitting Discomfort. *Hum. Factors.* Oct 2009;51(5):694-704.

259. Melzack R. The McGill Pain Questionnaire: major properties and scoring methods. *Pain.* Sep 1975;1(3):277-299.

260. Melzack R. The short-form McGill Pain Questionnaire. *Pain.* Aug 1987;30(2):191-197.

261. Frost S, Grossfeld S, Kirkley A, Litchfield B, Fowler P, Amendola A. The efficacy of femoral nerve block in pain reduction for outpatient hamstring anterior cruciate ligament reconstruction: a double-blind, prospective, randomized trial. *Arthroscopy : the journal of arthroscopic & related surgery : official publication of the Arthroscopy Association of North America and the International Arthroscopy Association.* Apr 2000;16(3):243-248.

262. Pellow JE, Brantingham JW. The efficacy of adjusting the ankle in the treatment of subacute and chronic grade I and grade II ankle inversion sprains. *J Manipulative Physiol Ther.* Jan 2001;24(1):17-24.

263. Kim ED, Seo JT. Minimally invasive technique for sural nerve harvesting: technical description and follow-up. *Urology.* May 2001;57(5):921-924.

264. Schiller L. Effectiveness of spinal manipulative therapy in the treatment of mechanical thoracic spine pain: a pilot randomized clinical trial. *J Manipulative Physiol Ther.* Jul-Aug 2001;24(6):394-401.

265. van den Dolder PA, Roberts DL. A trial into the effectiveness of soft tissue massage in the treatment of shoulder pain. *The Australian journal of physiotherapy.* 2003;49(3):183-188.

266. Grafton KV, Foster NE, Wright CC. Test-retest reliability of the Short-Form McGill Pain Questionnaire: assessment of intraclass correlation coefficients and limits of agreement in patients with osteoarthritis. *The Clinical journal of pain.* Jan-Feb 2005;21(1):73-82.

267. Crone C, Hultborn H, Mazieres L, Morin C, Nielsen J, Pierrot-Deseilligny E. Sensitivity of monosynaptic test reflexes to facilitation and inhibition as a function of the test reflex size: a study in man and the cat. *Exp Brain Res.* 1990;81(1):35-45.

268. Ammer K. The Glamorgan Protocol for recording and evaluation of thermal images of the human body. *Thermol Int.* 2008;18(4):125-144.

269. Hoffman M, Schrader J, Applegate T, Koceja D. Unilateral postural control of the functionally dominant and nondominant extremities of healthy subjects. *J Athl Train.* Oct 1998;33(4):319-322.

270. Hoffman M, Schrader J, Koceja D. An investigation of postural control in postoperative anterior cruciate ligament reconstruction patients. *J Athl Train.* Apr 1999;34(2):130-136.

271. Hislop HJ, Montgomery J. *Daniels and Worthingham's Muscle Testing: Techniques of Manual Examination*. 8th ed. St. Louis: Saunders Elsevier; 2007.

272. Hoppenfeld S. *Physical Examination of the Spine and Extremity*. Upper Saddle River, NJ: Prentice Hall; 1976.

273. Kendall FP, McCreary EK, Provance PG, Rodgers MM, Romani WA. *Muscles: Testing and Function with Posture and Pain*. 5 ed. Philadelphia, PA: Lippincott Williams & Wilksins; 2005.

274. Army Dot. FM 3-04.203-Fundamentals of Flight. In: Army Dot, ed. Washington DC: Department of Defense; 2007:1-392.

275. Ashruf CMA. Thin flexible pressure sensors. *Sensor Review*. 2002;22(4):6.

276. Johansson AG, Forslund A, Sjodin A, Mallmin H, Hambraeus L, Ljunghall S. Determination of body composition--a comparison of dual-energy x-ray absorptiometry and hydrodensitometry. *Am J Clin Nutr*. Mar 1993;57(3):323-326.

277. Laskey MA. Dual-energy X-ray absorptiometry and body composition. *Nutrition.* Jan 1996;12(1):45-51.

278. Thompson M. Painful chopper rides: Maintaining your "Optimal Buttocks Reference Point" can kill your back - failure to do so can kill you. *Time*. New York: Time Inc.; 2011.

279. Caldwell J, Crowley J, Caldwell L, et al. Sustaining female UH-60 helicopter performance with dexedrine during sustained operations: A simulator study. In: Army Dot, ed. Fort Rucker, AL1995:68.

280. Chen Y, Wickramasinghe V, Zimcik DG. Development of adaptive helicopter seat systems for aircrew vibration mitigation. 2008:69280N-69280N.

281. Castelo Branco NA, Rodriguez E. The vibroacoustic disease--an emerging pathology. *Aviat Space Environ Med.* Mar 1999;70(3 Pt 2):A1-6.

282. Smith SD. Characterizing the effects of airborne vibration on human body vibration response. *Aviat Space Environ Med.* Jan 2002;73(1):36-45.

283. Strand LI, Ljunggren AE, Bogen B, Ask T, Johnsen TB. The Short-Form McGill Pain Questionnaire as an outcome measure: test-retest reliability and responsiveness to change. *Eur J Pain.* Oct 2008;12(7):917-925.

284. Bell-Krotoski JA, Fess EE, Figarola JH, Hiltz D. Threshold Detection and Semmes-Weinstein Monofilaments. *Journal of Hand Therapy.* 1995;8(2):155-162.

285. FAA. ALC-105: Helicopter - Controls, systems, and limitations. 2013; https://www.faasafety.gov/gslac/ALC/course_content.aspx?cID=105&sID=456. Accessed February 15, 2013, 2013.

286. Pascoe DD, Mercer JB, de Weerd L. Physiology of thermal signals. In: Bronzino JD, ed. *Medical devices and systems*. Boca Raton, FL: CRC Press; 2006.

287. Phillips A, S. *The scope of back pain in Navy helicopter pilots*. Monteray, CA: Department of Operations Research, Naval Postgraduate School; 2011.

288. Magill RA. *Motor learning: Concepts and application*. 6th ed. Boston: McGraw Hill; 2001.

289. Schmidt RA, Lee TD. *Motor control and learning: A behavioral emphasis*. 4th ed. Champagne, IL: Human Kinetics; 2005.

290. Systems K. Business case analysis for the improved Navy helicopter seat system. Arlington, VA2010.

291. Sargent P, Bachmann A. Back pain in the Naval rotary wing community2005:7.

292. Games KE. *Physiological effects of prolonged sitting and local pressure application in the UH-60 Black Hawk helicopter*. Auburn, AL: Kinesiology, Auburn University; 2013.

293. Cordova ML. Giving clinicians more to work with: let's incorporate confidence intervals into our data. *J Athl Train.* Oct-Dec 2007;42(4):445.

294. Fronek HS. *The fundamentals of phlebology: Venous disease for clinicians*. 2 ed. London: Royal Society of Medicine Press Ltd; 2007.

295. Bastani A, Hadian MR, Talebian S, Bagheri H, Olyaie GR. Modulation of the ipsilateral and contralateral H reflexes following ipsilateral mechanical pressure of the foot in normal subjects. *Electromyogr Clin Neurophysiol.* Jul-Aug 2010;50(5):251-256.

296. Sayenko DG, Vette AH, Obata H, Alekhina MI, Akai M, Nakazawa K. Differential effects of plantar cutaneous afferent excitation on soleus stretch and H-reflex. *Muscle Nerve.* Jun 2009;39(6):761-769.

Appendix A

Means, Standard Deviations, and 95% Confidence Intervals for Project One

Table A- 1. Participant demographic data. y: year; cm: centimeter; kg: kilogram; °: degree.

	Mean	Standard Deviation
Age, y	23.47	3.11
Height, cm	177.17	5.32
Weight, kg	79.09	12.15
Arm Reach, cm	184.73	8.8
Crotch Height, cm	94.07	3.9
Sitting Height, cm	93.03	3.36
Design Eye Point Knee Angle, °	76.33	4.7

Table A- 2. Category Partitioning Scale means, standard deviations, and 95% confidence intervals. min: minutes; CP-50: Category Partitioning Scale; pts: points.

Time, min	Mean CP-50 Score, pts	Standard Deviation	95% Confidence Interval	
			Lower Bound	Upper Bound
0	1.2	1.57	0.33	2.07
30	6.33	4.32	3.94	8.73
60	10.67	6.53	7.05	14.28
90	14.6	8.84	9.71	19.49
120	20.53	10.06	14.96	26.11
150	25.4	11.48	19.04	31.76
180	29.27	13.6	21.73	36.8
210	29.93	13.42	22.5	37.36
240	31.47	13.15	24.19	38.75

Table A- 3. McGill Pain Questionnaire descriptor score means, standard deviations, and 95% confidence intervals. min: minutes; MPQ: McGill Pain Questionnaire; pts: points.

Time, min	Mean MPQ Descriptor Score, pts	Standard Deviation	95% Confidence Interval	
			Lower Bound	Upper Bound
0	0.33	0.82	-0.12	0.79
30	1.2	1.15	0.57	1.84
60	2	1.51	1.16	2.84
90	3.2	2.24	1.96	4.44
120	4.87	2.88	3.27	6.46
150	6.33	4.2	4.01	8.66
180	7.53	4.85	4.85	10.22
210	7.6	4.69	5	10.2
240	8.87	5.91	5.59	12.14

Table A- 4. Visual Analog Scale means, standard deviations, and 95% confidence intervals. min: minutes; VAS: Visual Analog Scale; cm: centimeters.

Time, min	Mean VAS Score, cm	Standard Deviation	95% Confidence Interval	
			Lower Bound	Upper Bound
0	0.23	0.25	0.09	0.37
30	0.64	0.51	0.36	0.92
60	1.2	0.66	0.84	1.56
90	1.89	1.25	1.2	2.59
120	3.05	2.22	1.82	4.28
150	3.67	2.57	2.25	5.1
180	4.47	3.04	2.79	6.16
210	4.6	3.37	2.73	6.47
240	5.06	3.56	3.09	7.03

Table A- 5. Present Pain Intensity score means, standard deviations, and 95% confidence intervals. min: minutes; PPI: Present Pain Intensity; cm: centimeters.

Time, min	Mean PPI Score, cm	Standard Deviation	95% Confidence Interval	
			Lower Bound	Upper Bound
0	0.13	0.35	-0.06	0.33
30	0.73	0.46	0.48	0.99
60	1.07	0.59	0.74	1.4
90	1.47	0.64	1.11	1.82
120	1.73	0.59	1.41	2.06
150	1.93	0.7	1.54	2.32
180	2.13	0.92	1.63	2.64
210	2.33	0.98	1.79	2.87
240	2.47	0.99	1.92	3.02

Table A- 6. Great toe monofilament test score means, standard deviations, and 95% confidence intervals. min: minute; GTMFT; great toe monofilament test.

Time, min	Mean GTMFT Score, size	Standard Deviation	95% Confidence Interval	
			Lower Bound	Upper Bound
0	3.99	0.46	3.73	4.24
30	3.95	0.56	3.64	4.26
60	4.06	0.56	3.75	4.37
90	4.17	0.4	3.95	4.4
120	4.16	0.42	3.93	4.39
150	4.29	0.49	4.02	4.56
180	4.24	0.47	3.98	4.5
210	4.2	0.5	3.92	4.47
240	4.38	0.76	3.96	4.8

Table A- 7. Third metatarsal monofilament test score means, standard deviations, and 95% confidence intervals. min: minutes; 3MMFT: third metatarsal monofilament test.

Time, min	Mean 3MMFT Score, size	Standard Deviation	95% Confidence Interval	
			Lower Bound	Upper Bound
0	3.83	0.38	3.62	4.04
30	3.99	0.43	3.75	4.22
60	3.92	0.57	3.61	4.24
90	3.95	0.56	3.64	4.26
120	3.97	0.41	3.75	4.2
150	4.07	0.56	3.76	4.38
180	4.16	0.53	3.82	4.46
210	4.06	0.55	3.75	4.36
240	4.14	0.55	3.83	4.44

Table A- 8. Fifth metatarsal monofilament test score means, standard deviations, and 95% confidence intervals. min: minutes; 5MMFT: fifth metatarsal monofilament test.

Time, min	Mean 5MMFT Score, size	Standard Deviation	95% Confidence Interval	
			Lower Bound	Upper Bound
0	4.02	0.49	3.75	4.29
30	4.12	0.54	3.82	4.42
60	4.1	0.45	3.85	4.35
90	4.18	0.43	3.94	4.41
120	4.13	0.56	3.82	4.44
150	4.35	0.79	3.91	4.79
180	4.26	0.48	3.99	4.52
210	4.39	0.52	4.1	4.68
240	4.49	0.84	4.02	4.95

Table A- 9. Great toe two-point discrimination test means, standard deviations, and 95% confidence intervals. min: minutes; GT: great toe; mm: millimeters.

Time, min	Mean GT Interpoint Distance, mm	Standard Deviation	95% Confidence Interval	
			Lower Bound	Upper Bound
0	11.33	2.44	9.92	12.63
30	10.67	2.5	9.28	12.05
60	9.53	2.39	8.21	10.86
90	10.73	3.08	9.03	12.44
120	10.73	2.37	9.42	12.05
150	11.67	2.64	10.21	13.13
180	10.87	2.23	9.63	12.1
210	11.73	2.37	10.42	13.05
240	10.33	2.53	8.93	11.73

Table A- 10. Medial malleolus two-point discrimination test means, standard deviations, and 95% confidence intervals. min: minutes; MM: medial malleolus; mm: millimeters.

Time, min	Mean MM Interpoint Distance, mm	Standard Deviation	95% Confidence Interval	
			Lower Bound	Upper Bound
0	14.67	0.82	14.22	15.12
30	14.73	1.03	14.16	15.31
60	14.87	0.52	14.58	15.13
90	14.87	0.52	14.58	15.13
120	14.93	0.26	14.79	15.08
150	14.93	0.26	14.79	15.08
180	14.8	0.56	14.49	15.11
210	14.73	1.03	14.16	15.31
240	14.8	0.41	14.57	15.03

Table A- 11. Lateral malleolus two-point discrimination test means, standard deviations, and 95% confidence intervals. min: minutes; LM: lateral malleolus; mm: millimeters.

Time, min	Mean LM Interpoint Distance, mm	Standard Deviation	95% Confidence Interval	
			Lower Bound	Upper Bound
0	14.73	1.03	14.16	15.31
30	14.73	0.59	14.47	15.06
60	14.27	2.15	13.07	15.46
90	14.73	0.7	14.34	15.21
120	14.8	0.41	14.57	15.03
150	14.73	0.59	14.41	15.06
180	14.8	0.41	14.57	15.03
210	14.73	0.59	14.41	15.06
240	14.73	0.59	14.41	15.06

Table A- 12. Arterial oxygen saturation means, standard deviations, and 95% confidence intervals. min: minutes.

Time, min	Mean Arterial Oxygen Saturation, %	Standard Deviation	95% Confidence Interval	
			Lower Bound	Upper Bound
0	99.2	1.27	98.5	99.9
30	99	1.6	98.11	99.89
60	99.13	1.06	98.55	99.72
90	99.2	1.15	98.57	99.84
120	99.27	0.88	98.78	99.76
150	99.27	0.88	98.78	99.76
180	99.6	0.63	99.25	99.95
210	99.6	0.63	99.25	99.95
240	99.47	0.74	99.06	99.88

Table A- 13. Anterior ankle superficial skin temperature means, standard deviations, and 95% confidence intervals. min: minutes; C: Celsius.

Time, min	Mean Anterior Ankle Temperature, °C	Standard Deviation	95% Confidence Interval	
			Lower Bound	Upper Bound
0	29.66	1.73	28.7	30.62
30	28.88	1.68	27.95	29.81
60	28.34	1.64	27.43	29.25
90	27.99	1.71	27.05	28.94
120	27.67	1.66	26.75	28.59
150	27.42	1.47	26.61	28.23
180	27.31	1.6	26.42	28.19
210	27.01	1.52	26.17	27.85
240	26.88	1.43	26.09	27.67

Table A- 14. Lateral ankle superficial skin temperature means, standard deviations, and 95% confidence intervals. min: minutes; C: Celsius.

Time, min	Mean Lateral Ankle Temperature, °C	Standard Deviation	95% Confidence Interval	
			Lower Bound	Upper Bound
0	29.44	1.49	28.61	30.27
30	28.55	1.4	27.78	29.33
60	28.13	1.37	27.37	28.88
90	27.53	1.2	26.93	28.26
120	27.26	1.29	26.55	27.97
150	27.03	1.21	26.36	27.7
180	26.9	1.14	26.27	27.53
210	26.71	1.1	26.1	27.32
240	26.59	1.14	25.96	27.22

Appendix B

Means, Standard Deviations, and 95% Confidence Intervals for Project Two

Table B- 1. Participant demographic data. y: year; cm: centimeters; kg: kilograms; °: degrees.

	Mean	Standard Deviation
Age, y	23.47	3.11
Height, cm	177.17	5.32
Weight, kg	79.09	12.15
Arm Reach, cm	184.73	8.8
Crotch Height, cm	94.07	3.9
Sitting Height, cm	93.03	3.36
Design Eye Point Knee Angle, °	76.33	4.7

Table B- 2. Category Partitioning Scale score means, standard deviations, and 95% confidence intervals. CP-50: Category Partitioning Scale; pts: points.

Time Point	Mean CP-50 Score, pts	Standard Deviation	95% Confidence Interval	
			Lower Bound	Upper Bound
36 kP Posterior Thigh Pre	2.2	4.46	-0.27	4.67
36 kP Posterior Thigh Post	8.67	7.08	4.75	12.59
36 kP Ischial Tuberosity Pre	1.2	1.9	0.15	2.25
36 kP Ischial Tuberosity Post	4.67	4.27	2.3	7.03
44 kP Posterior Thigh Pre	2.07	3.67	0.03	4.1
44 kP Posterior Thigh Post	13.93	6.08	10.57	17.3
44 kP Ischial Tuberosity Pre	1.8	2.78	0.26	3.34
44 kP Ischial Tuberosity Post	7.33	4.03	5.1	9.56

Table B- 3. McGill Pain Questionnaire descriptor score means, standard deviations, and 95% confidence intervals. MPQ: McGill Pain Questionnaire; pts: points.

Time Point	Mean MPQ Descriptor Score, pts	Standard Deviation	95% Confidence Interval	
			Lower Bound	Upper Bound
36 kP Posterior Thigh Pre	0.2	0.56	-0.11	0.51
36 kP Posterior Thigh Post	1.33	1.5	0.5	2.16
36 kP Ischial Tuberosity Pre	0.13	0.35	-0.06	0.33
36 kP Ischial Tuberosity Post	0.87	1.13	0.24	1.49
44 kP Posterior Thigh Pre	0.27	0.46	0.01	0.52
44 kP Posterior Thigh Post	2.07	1.16	1.42	2.71
44 kP Ischial Tuberosity Pre	0.2	0.41	-0.03	0.43
44 kP Ischial Tuberosity Post	1.13	0.74	0.72	1.54

Table B- 4. Visual Analog Scale means, standard deviations, and 95% confidence intervals. VAS: Visual Analog Scale; cm: centimeters.

Time Point	Mean VAS Score, cm	Standard Deviation	95% Confidence Interval	
			Lower Bound	Upper Bound
36 kP Posterior Thigh Pre	0.27	0.53	-0.02	0.57
36 kP Posterior Thigh Post	0.92	0.78	0.48	1.35
36 kP Ischial Tuberosity Pre	0.13	0.19	0.02	0.23
36 kP Ischial Tuberosity Post	0.46	0.55	0.16	0.76
44 kP Posterior Thigh Pre	0.15	0.23	0.02	0.28
44 kP Posterior Thigh Post	1.43	1.1	0.82	2.04
44 kP Ischial Tuberosity Pre	0.16	0.24	0.02	0.3
44 kP Ischial Tuberosity Post	0.77	0.67	0.4	1.14

Table B- 5. Present Pain Intensity score means, standard deviations, and 95% confidence intervals. PPI: Present Pain Intensity; pts: points.

Time Point	Mean PPI Score, pts	Standard Deviation	95% Confidence Interval	
			Lower Bound	Upper Bound
36 kP Posterior Thigh Pre	0.2	0.56	-0.11	0.51
36 kP Posterior Thigh Post	0.67	0.72	0.27	1.07
36 kP Ischial Tuberosity Pre	0.07	0.26	-0.08	0.21
36 kP Ischial Tuberosity Post	0.4	0.51	0.12	0.68
44 kP Posterior Thigh Pre	0.13	0.35	-0.06	0.32
44 kP Posterior Thigh Post	1.13	0.74	0.72	1.54
44 kP Ischial Tuberosity Pre	0.2	0.56	-0.11	0.51
44 kP Ischial Tuberosity Post	0.73	0.59	0.4	1.06

Table B- 6. Great toe monofilament test score means, standard deviations, and 95% confidence intervals. GTMFT: great toe monofilament test.

Time Point	Mean GTMFT Score, size	Standard Deviation	95% Confidence Interval	
			Lower Bound	Upper Bound
36 kP Posterior Thigh Pre	3.97	0.49	3.7	4.25
36 kP Posterior Thigh Post	4.1	0.53	3.81	4.4
36 kP Ischial Tuberosity Pre	4.02	0.49	3.75	4.3
36 kP Ischial Tuberosity Post	4.18	0.84	3.71	4.64
44 kP Posterior Thigh Pre	4.08	0.41	3.85	4.31
44 kP Posterior Thigh Post	4.18	0.46	3.92	4.43
44 kP Ischial Tuberosity Pre	4.05	0.47	3.79	4.31
44 kP Ischial Tuberosity Post	4.15	0.49	3.88	3.42

Table B- 7. Third metatarsal monofilament test score means, standard deviations, and 95% confidence intervals. 3MMFT: third metatarsal monofilament test.

Time Point	Mean 3MMFT Score, size	Standard Deviation	95% Confidence Interval	
			Lower Bound	Upper Bound
36 kP Posterior Thigh Pre	4.19	0.87	3.7	4.67
36 kP Posterior Thigh Post	4.13	0.85	3.66	4.6
36 kP Ischial Tuberosity Pre	4.03	0.82	3.58	4.5
36 kP Ischial Tuberosity Post	4.32	1.05	3.73	4.9
44 kP Posterior Thigh Pre	4.1	0.53	3.81	4.4
44 kP Posterior Thigh Post	4.05	0.55	3.75	4.36
44 kP Ischial Tuberosity Pre	4.05	0.52	3.77	4.34
44 kP Ischial Tuberosity Post	4.07	0.56	3.76	4.38

Table B- 8. Fifth metatarsal monofilament test score means, standard deviations, and 95% confidence intervals. 5MMFT: fifth metatarsal monofilament test.

Time Point	Mean 5MMFT Score, size	Standard Deviation	95% Confidence Interval	
			Lower Bound	Upper Bound
36 kP Posterior Thigh Pre	4.24	0.78	3.8	4.67
36 kP Posterior Thigh Post	4.33	1.05	3.75	4.92
36 kP Ischial Tuberosity Pre	4.01	0.62	3.67	4.35
36 kP Ischial Tuberosity Post	4.25	1.09	3.64	4.85
44 kP Posterior Thigh Pre	4.11	0.55	3.81	4.42
44 kP Posterior Thigh Post	4.28	0.51	3.99	4.56
44 kP Ischial Tuberosity Pre	4.08	0.57	3.76	4.4
44 kP Ischial Tuberosity Post	4.33	0.79	3.9	4.77

Table B- 9. Great toe two-point discrimination test means, standard deviations, and 95% confidence intervals. GT: great toe; mm: millimeters.

Time Point	Mean GT Interpoint Distance, mm	Standard Deviation	95% Confidence Interval	
			Lower Bound	Upper Bound
36 kP Posterior Thigh Pre	10.33	2.19	9.12	11.55
36 kP Posterior Thigh Post	11.27	2.22	10.04	12.5
36 kP Ischial Tuberosity Pre	11.27	2.09	10.11	12.42
36 kP Ischial Tuberosity Post	10.87	1.92	9.8	11.93
44 kP Posterior Thigh Pre	11.2	1.82	10.19	12.21
44 kP Posterior Thigh Post	11.13	2.26	9.88	12.39
44 kP Ischial Tuberosity Pre	10.47	2.7	8.97	11.96
44 kP Ischial Tuberosity Post	11.2	2.27	9.94	12.46

Table B- 10. Medial malleolus two-point discrimination test means, standard deviations, and 95% confidence intervals. MM: medial malleolus; mm: millimeters.

Time Point	Mean MM Interpoint Distance, mm	Standard Deviation	95% Confidence Interval	
			Lower Bound	Upper Bound
36 kP Posterior Thigh Pre	14.93	0.26	14.79	15.08
36 kP Posterior Thigh Post	14.67	0.82	14.21	15.12
36 kP Ischial Tuberosity Pre	14.93	0.26	14.79	15.07
36 kP Ischial Tuberosity Post	14.8	0.56	14.49	15.11
44 kP Posterior Thigh Pre	14.73	0.8	14.29	15.18
44 kP Posterior Thigh Post	14.8	0.41	14.57	15.03
44 kP Ischial Tuberosity Pre	14.87	0.35	14.67	15.06
44 kP Ischial Tuberosity Post	14.87	0.52	14.58	15.15

Table B- 11. Lateral malleolus two-point discrimination test means, standard deviations, and 95% confidence intervals. LM: lateral malleolus; mm: millimeters.

Time Point	Mean LM Interpoint Distance, mm	Standard Deviation	95% Confidence Interval	
			Lower Bound	Upper Bound
36 kP Posterior Thigh Pre	14.53	1.13	13.91	15.16
36 kP Posterior Thigh Post	15	0	15	15
36 kP Ischial Tuberosity Pre	14.67	0.72	14.27	15.07
36 kP Ischial Tuberosity Post	14.73	1.03	14.16	14.31
44 kP Posterior Thigh Pre	14.67	0.82	14.21	15.12
44 kP Posterior Thigh Post	14.87	0.35	14.67	15.06
44 kP Ischial Tuberosity Pre	14.73	0.8	14.92	15.17
44 kP Ischial Tuberosity Post	14.8	0.77	14.37	15.23

Table B- 12. Arterial oxygen saturation means, standard deviations, and 95% confidence intervals.

Time Point	Mean Arterial Oxygen Saturation, %	Standard Deviation	95% Confidence Interval	
			Lower Bound	Upper Bound
36 kP Posterior Thigh Pre	98.8	1.21	98.13	99.47
36 kP Posterior Thigh Post	99	1.07	98.41	99.59
36 kP Ischial Tuberosity Pre	98.2	1.97	97.11	99.29
36 kP Ischial Tuberosity Post	97.13	7.08	93.21	101.05
44 kP Posterior Thigh Pre	98.93	1.16	98.29	99.58
44 kP Posterior Thigh Post	98.4	2.82	96.84	99.96
44 kP Ischial Tuberosity Pre	98.8	1.37	98.04	99.56
44 kP Ischial Tuberosity Post	99.14	1.13	98.51	99.76

Table B- 13. Anterior ankle superficial skin temperature means, standard deviations, and 95% confidence intervals. C: Celsius.

Time Point	Mean Anterior Ankle Temperature, °C	Standard Deviation	95% Confidence Interval	
			Lower Bound	Upper Bound
36 kP Posterior Thigh Pre	30.33	1.79	29.34	31.33
36 kP Posterior Thigh Post	30.95	1.63	30.05	31.85
36 kP Ischial Tuberosity Pre	30.38	1.49	29.56	31.2
36 kP Ischial Tuberosity Post	31.08	1.63	30.18	31.98
44 kP Posterior Thigh Pre	30.13	1.57	29.26	30.99
44 kP Posterior Thigh Post	30.74	1.45	29.94	31.54
44 kP Ischial Tuberosity Pre	30.25	1.62	29.35	31.15
44 kP Ischial Tuberosity Post	30.78	1.67	29.86	31.7

Table B- 14. Lateral ankle superficial skin temperature means, standard deviations, and 95% confidence intervals. C: Celsius.

Time Point	Mean Lateral Ankle Temperature, °C	Standard Deviation	95% Confidence Interval	
			Lower Bound	Upper Bound
36 kP Posterior Thigh Pre	30.09	1.48	29.27	30.91
36 kP Posterior Thigh Post	29.9	2.1	28.23	31.56
36 kP Ischial Tuberosity Pre	30.09	1.18	29.44	30.75
36 kP Ischial Tuberosity Post	30.65	1.22	29.98	31.33
44 kP Posterior Thigh Pre	29.99	1.14	29.36	30.62
44 kP Posterior Thigh Post	30.51	1.29	29.79	31.22
44 kP Ischial Tuberosity Pre	30.09	1.4	29.32	30.87
44 kP Ischial Tuberosity Post	30.45	1.41	29.67	31.23

Appendix C

Means, Standard Deviations, and 95% Confidence Intervals for Project Three

Table C- 1. Participant demographic data. y: year; cm: centimeters; kg: kilograms; %: percent; °: degrees.

	Mean	Standard Deviation
Age, y	21.73	2.24
Height, cm	179.24	4.58
Weight, kg	80.64	12.02
Body Fat, %	20.09	9.19
Arm Reach, cm	185.05	5.16
Crotch Height, cm	94.63	2.91
Sitting Height, cm	95.1	2.6
Design Eye Point Knee Angle, °	76.13	3.19

Table C- 2. Category Partitioning Scale score means, standard deviations, and 95% confidence intervals. CP-50: Category Partitioning Scale; pts: points.

Time Point	Mean CP-50 Score, pts	Standard Deviation	95% Confidence Interval	
			Lower Bound	Upper Bound
Posterior thigh pre	3.17	3.99	1.68	4.66
Posterior thigh 5 min into-pressure	9.9	7.67	7.04	12.76
Posterior thigh 10 min into-pressure	12.53	7.58	9.7	15.36
Posterior thigh 5 min post-pressure	11.47	9.46	7.93	14.99
Posterior thigh 10 min post-pressure	12.67	10.51	8.74	16.59
Ischial tuberosity pre	2.77	3.29	1.54	3.99
Ischial tuberosity 5 min into-pressure	7.83	5.31	5.85	9.81
Ischial tuberosity 10 min into-pressure	9.9	7.4	7.14	12.66
Ischial tuberosity 5 min post-pressure	10.63	8.39	7.49	13.77
Ischial tuberosity 10 min post-pressure	11.7	9.47	8.16	15.24
Control pre	3.17	4.65	1.43	4.9
Control 5 min into-pressure	5.43	6.13	3.14	7.72
Control 10 min into-pressure	6.73	6.7	4.23	9.24
Control 5 min post-pressure	8.83	7.69	5.96	11.71
Control 10 min post-pressure	10.27	9.67	6.66	13.88

Table C- 3. McGill Pain Questionnaire descriptor score means, standard deviations, and 95% confidence intervals. MPQ: McGill Pain Questionnaire; pts: points.

Time Point	Mean MPQ Descriptor Score, pts	Standard Deviation	95% Confidence Interval	
			Lower Bound	Upper Bound
Posterior thigh pre	0.87	1.25	0.4	1.33
Posterior thigh 5 min into-pressure	2.1	2.09	1.32	2.88
Posterior thigh 10 min into-pressure	2.23	2.11	1.44	3.02
Posterior thigh 5 min post-pressure	2.6	3.18	1.41	3.79
Posterior thigh 10 min post-pressure	2.97	3.65	1.6	4.33
Ischial tuberosity pre	0.8	0.89	0.47	1.13
Ischial tuberosity 5 min into-pressure	1.67	1.32	1.17	2.16
Ischial tuberosity 10 min into-pressure	2	1.72	1.36	2.64
Ischial tuberosity 5 min post-pressure	2.6	2.82	1.54	3.65
Ischial tuberosity 10 min post-pressure	2.9	3.36	1.65	4.15
Control pre	0.53	0.73	0.26	0.81
Control 5 min into-pressure	1.07	1.34	0.57	1.57
Control 10 min into-pressure	1.4	1.87	0.7	2.09
Control 5 min post-pressure	2.03	2.5	1.1	2.97
Control 10 min post-pressure	2.57	3.33	1.32	3.81

Table C- 4. Visual Analog Scale score means, standard deviations, and 95% confidence intervals. cm: centimeters.

Time Point	Mean Visual Analog Score, cm	Standard Deviation	95% Confidence Interval	
			Lower Bound	Upper Bound
Posterior thigh pre	0.41	0.72	0.14	0.68
Posterior thigh 5 min into-pressure	1.09	0.95	0.74	1.45
Posterior thigh 10 min into-pressure	1.31	1.24	0.84	1.77
Posterior thigh 5 min post-pressure	1.35	1.4	0.82	1.87
Posterior thigh 10 min post-pressure	1.54	1.57	0.96	2.13
Ischial tuberosity pre	0.31	0.38	0.17	0.45
Ischial tuberosity 5 min into-pressure	0.73	0.7	0.47	0.99
Ischial tuberosity 10 min into-pressure	0.92	0.98	0.56	1.29
Ischial tuberosity 5 min post-pressure	1.07	1.18	0.63	1.51
Ischial tuberosity 10 min post-pressure	1.33	1.59	0.73	1.93
Control pre	0.25	0.32	0.13	0.37
Control 5 min into-pressure	0.59	0.78	0.29	0.88
Control 10 min into-pressure	0.71	0.72	0.44	0.98
Control 5 min post-pressure	1	1.07	0.6	1.4
Control 10 min post-pressure	1.06	1.17	0.63	1.5

Table C- 5. Present Pain Intensity score means, standard deviations, and 95% confidence intervals. PPI: Present Pain Intensity; pts: points.

Time Point	Mean PPI Score, pts	Standard Deviation	95% Confidence Interval	
			Lower Bound	Upper Bound
Posterior thigh pre	0.43	0.5	0.24	0.62
Posterior thigh 5 min into-pressure	1	0.64	0.76	1.24
Posterior thigh 10 min into-pressure	1	0.64	0.76	1.24
Posterior thigh 5 min post-pressure	0.93	0.73	0.66	1.21
Posterior thigh 10 min post-pressure	1.07	0.78	0.77	1.36
Ischial tuberosity pre	0.4	0.5	0.21	0.59
Ischial tuberosity 5 min into-pressure	0.77	0.57	0.55	0.98
Ischial tuberosity 10 min into-pressure	0.8	0.55	0.59	1.01
Ischial tuberosity 5 min post-pressure	0.97	0.67	0.71	1.21
Ischial tuberosity 10 min post-pressure	1.03	0.72	0.77	1.3
Control pre	0.23	0.43	0.07	0.39
Control 5 min into-pressure	0.57	0.63	0.33	0.8
Control 10 min into-pressure	0.67	0.71	0.4	0.93
Control 5 min post-pressure	0.83	0.79	0.54	1.13
Control 10 min post-pressure	0.9	0.8	0.6	1.19

Table C- 6. Great toe monofilament test score means, standard deviations, and 95% confidence intervals. GTMFT: great toe monofilament test.

Time Point	Mean GTMFT Score, size	Standard Deviation	95% Confidence Interval	
			Lower Bound	Upper Bound
Posterior thigh pre	4.06	0.67	3.81	4.31
Posterior thigh 5 min into-pressure	4.19	0.63	3.96	4.43
Posterior thigh 10 min into-pressure	4.24	0.78	3.94	4.53
Posterior thigh 5 min post-pressure	4.26	0.64	4.02	4.5
Posterior thigh 10 min post-pressure	4.29	0.82	3.98	4.59
Ischial tuberosity pre	4.09	0.8	3.79	4.39
Ischial tuberosity 5 min into-pressure	4.17	0.66	3.92	4.42
Ischial tuberosity 10 min into-pressure	4.17	0.69	3.91	4.42
Ischial tuberosity 5 min post-pressure	4.24	0.63	4	4.48
Ischial tuberosity 10 min post-pressure	4.29	0.67	4.04	4.54
Control pre	4.22	0.79	3.93	4.52
Control 5 min into-pressure	4.14	0.72	3.87	4.41
Control 10 min into-pressure	4.32	0.77	4.03	4.6
Control 5 min post-pressure	4.33	0.71	4.06	4.59
Control 10 min post-pressure	4.3	0.67	4.05	4.55

Table C- 7. Third metatarsal monofilament test score means, standard deviations, and 95% confidence intervals. 3MMFT: third metatarsal monofilament test.

Time Point	Mean 3MMFT Score, size	Standard Deviation	95% Confidence Interval	
			Lower Bound	Upper Bound
Posterior thigh pre	4.15	0.65	3.91	4.39
Posterior thigh 5 min into-pressure	4.15	0.68	3.9	4.41
Posterior thigh 10 min into-pressure	4.17	0.68	3.91	4.42
Posterior thigh 5 min post-pressure	4.32	0.79	4.03	4.62
Posterior thigh 10 min post-pressure	4.21	0.69	3.95	4.47
Ischial tuberosity pre	4.07	0.54	3.87	4.27
Ischial tuberosity 5 min into-pressure	4.12	0.69	3.86	4.37
Ischial tuberosity 10 min into-pressure	4.06	0.68	3.81	4.32
Ischial tuberosity 5 min post-pressure	4.15	0.7	3.89	4.41
Ischial tuberosity 10 min post-pressure	4.14	0.72	3.87	4.41
Control pre	4.17	0.64	3.93	4.41
Control 5 min into-pressure	4.12	0.67	3.87	4.37
Control 10 min into-pressure	4.2	0.81	3.9	4.51
Control 5 min post-pressure	4.36	0.75	4.08	4.64
Control 10 min post-pressure	4.18	0.81	3.88	4.48

Table C- 8. Fifth metatarsal monofilament test score means, standard deviations, and 95% confidence intervals. 5MMFT: fifth metatarsal monofilament test.

Time Point	Mean 5MMFT Score, size	Standard Deviation	95% Confidence Interval	
			Lower Bound	Upper Bound
Posterior thigh pre	4.26	0.7	3.4	4.52
Posterior thigh 5 min into-pressure	4.5	0.61	4.27	4.72
Posterior thigh 10 min into-pressure	4.44	0.76	4.15	4.72
Posterior thigh 5 min post-pressure	4.46	0.77	4.17	4.75
Posterior thigh 10 min post-pressure	4.37	0.83	4.06	4.68
Ischial tuberosity pre	4.15	0.66	3.91	4.4
Ischial tuberosity 5 min into-pressure	4.3	0.6	4.08	4.53
Ischial tuberosity 10 min into-pressure	4.36	0.76	4.07	4.64
Ischial tuberosity 5 min post-pressure	4.35	0.78	4.06	4.64
Ischial tuberosity 10 min post-pressure	4.35	0.78	4.06	4.64
Control pre	4.32	0.87	3.4	4.65
Control 5 min into-pressure	4.25	0.66	4	4.5
Control 10 min into-pressure	4.38	0.89	4.05	4.71
Control 5 min post-pressure	4.4	0.73	4.12	4.67
Control 10 min post-pressure	4.33	0.79	4.03	4.62

Table C- 9. Great toe two-point discrimination test means, standard deviations, and 95% confidence intervals. GT: great toe; mm: millimeters.

Time Point	Mean GT Interpoint Distance, mm	Standard Deviation	95% Confidence Interval	
			Lower Bound	Upper Bound
Posterior thigh pre	10.17	2.31	9.31	11.03
Posterior thigh 5 min into-pressure	10.87	2.53	9.92	11.81
Posterior thigh 10 min into-pressure	11.13	2.64	10.15	12.12
Posterior thigh 5 min post-pressure	10.97	2.89	10.14	11.78
Posterior thigh 10 min post-pressure	10.87	2.67	9.88	11.86
Ischial tuberosity pre	10.7	2.19	9.88	11.52
Ischial tuberosity 5 min into-pressure	10.96	2.41	10.07	11.87
Ischial tuberosity 10 min into-pressure	10.97	2.17	10.51	10.78
Ischial tuberosity 5 min post-pressure	11.07	2.77	10.03	12.1
Ischial tuberosity 10 min post-pressure	11.33	2.81	10.28	12.38
Control pre	10.56	2.33	9.7	11.44
Control 5 min into-pressure	10.13	2.39	9.24	11.02
Control 10 min into-pressure	10.77	2.58	9.8	11.73
Control 5 min post-pressure	10.67	2.52	9.72	11.61
Control 10 min post-pressure	10.7	2.89	9.62	11.78

Table C- 10. Medial malleolus two-point discrimination test means, standard deviations, and 95% confidence intervals. MM: medial malleolus; mm: millimeters.

Time Point	Mean MM Interpoint Distance, mm	Standard Deviation	95% Confidence Interval	
			Lower Bound	Upper Bound
Posterior thigh pre	14.87	0.57	14.65	15.08
Posterior thigh 5 min into-pressure	14.77	0.94	14.42	15.12
Posterior thigh 10 min into-pressure	15	0	15	15
Posterior thigh 5 min post-pressure	14.93	0.37	14.79	15.07
Posterior thigh 10 min post-pressure	14.9	0.55	14.69	15.1
Ischial tuberosity pre	14.83	0.59	14.61	15.05
Ischial tuberosity 5 min into-pressure	14.97	0.18	14.9	15.03
Ischial tuberosity 10 min into-pressure	15	0	15	15
Ischial tuberosity 5 min post-pressure	14.93	0.37	14.8	15.07
Ischial tuberosity 10 min post-pressure	14.93	0.25	14.84	15.03
Control pre	14.6	1.48	14.05	15.15
Control 5 min into-pressure	14.67	1.49	14.11	15.22
Control 10 min into-pressure	14.87	0.43	14.7	15.03
Control 5 min post-pressure	14.87	0.57	14.65	15.08
Control 10 min post-pressure	14.9	0.31	14.79	15.01

Table C- 11. Lateral malleolus two-point discrimination test means, standard deviations, and 95% confidence intervals. LM: lateral malleolus; mm: millimeters.

Time Point	Mean LM Interpoint Distance, mm	Standard Deviation	95% Confidence Interval	
			Lower Bound	Upper Bound
Posterior thigh pre	14.8	0.76	14.52	15.08
Posterior thigh 5 min into-pressure	14.87	0.57	14.65	15.08
Posterior thigh 10 min into-pressure	14.6	1.52	14.03	15.17
Posterior thigh 5 min post-pressure	14.6	1.33	14.1	15.1
Posterior thigh 10 min post-pressure	14.5	2.39	13.61	15.39
Ischial tuberosity pre	14.97	0.18	14.9	15.03
Ischial tuberosity 5 min into-pressure	14.87	0.43	14.7	15.03
Ischial tuberosity 10 min into-pressure	14.93	0.37	14.8	15.07
Ischial tuberosity 5 min post-pressure	14.77	0.57	14.55	14.98
Ischial tuberosity 10 min post-pressure	14.67	0.8	14.37	14.97
Control pre	14.73	1.28	14.25	15.21
Control 5 min into-pressure	14.8	0.48	14.62	14.98
Control 10 min into-pressure	14.77	0.57	14.55	14.98
Control 5 min post-pressure	14.83	0.59	14.61	15.05
Control 10 min post-pressure	14.73	0.83	14.42	15.04

Table C- 12. Arterial oxygen saturation means, standard deviations, and 95% confidence intervals.

Time Point	Mean Arterial Oxygen Saturation, %	Standard Deviation	95% Confidence Interval	
			Lower Bound	Upper Bound
Posterior thigh pre	98.83	1.44	98.3	99.37
Posterior thigh 5 min into-pressure	98.63	2.95	97.53	99.74
Posterior thigh 10 min into-pressure	98.6	1.9	98.89	99.31
Posterior thigh 5 min post-pressure	98.8	1.75	98.15	99.45
Posterior thigh 10 min post-pressure	98.17	2.09	97.39	98.95
Ischial tuberosity pre	99.17	1.02	98.79	99.55
Ischial tuberosity 5 min into-pressure	98.8	1.19	98.36	99.23
Ischial tuberosity 10 min into-pressure	97.93	2.61	96.96	98.91
Ischial tuberosity 5 min post-pressure	98.73	1.23	99.27	99.19
Ischial tuberosity 10 min post-pressure	98.93	1.39	98.42	99.45
Control pre	98.93	1.26	98.46	99.4
Control 5 min into-pressure	99	1.2	98.55	99.45
Control 10 min into-pressure	98.67	1.71	98.03	99.3
Control 5 min post-pressure	98.93	1.17	98.5	99.37
Control 10 min post-pressure	99.27	0.94	98.91	99.62

Table C- 13. Anterior ankle superficial skin temperature. C: Celsius.

Time Point	Mean Anterior Ankle Temperature, ˚C	Standard Deviation	95% Confidence Interval	
			Lower Bound	Upper Bound
Posterior thigh pre	29.69	1.61	29.09	30.29
Posterior thigh 5 min into-pressure	29.53	1.75	28.88	30.18
Posterior thigh 10 min into-pressure	29.47	1.85	28.78	30.16
Posterior thigh 5 min post-pressure	29.43	1.89	28.73	30.14
Posterior thigh 10 min post-pressure	29.4	1.4	28.72	30.13
Ischial tuberosity pre	29.46	1.59	28.86	30.06
Ischial tuberosity 5 min into-pressure	29.72	1.73	29.07	30.36
Ischial tuberosity 10 min into-pressure	29.55	1.65	28.93	30.17
Ischial tuberosity 5 min post-pressure	29.84	2.56	28.89	30.79
Ischial tuberosity 10 min post-pressure	29.43	1.69	28.79	30.06
Control pre	29.19	1.38	28.68	29.71
Control 5 min into-pressure	29.71	1.56	29.13	30.3
Control 10 min into-pressure	29.49	1.59	28.9	30.08
Control 5 min post-pressure	29.33	1.66	28.71	29.97
Control 10 min post-pressure	29.39	1.7	29.76	30.03

Table C- 14. Lateral ankle superficial skin temperature. C: Celsius.

Time Point	Mean Lateral Ankle Temperature, °C	Standard Deviation	95% Confidence Interval	
			Lower Bound	Upper Bound
Posterior thigh pre	29.56	1.3	29.08	30.05
Posterior thigh 5 min into-pressure	29.31	1.47	28.76	29.86
Posterior thigh 10 min into-pressure	29.21	1.54	28.63	29.78
Posterior thigh 5 min post-pressure	29.18	1.64	28.56	28.79
Posterior thigh 10 min post-pressure	29.17	1.49	28.56	29.79
Ischial tuberosity pre	29.24	1.41	28.72	29.77
Ischial tuberosity 5 min into-pressure	29.64	1.55	29.06	30.21
Ischial tuberosity 10 min into-pressure	29.49	1.5	28.93	30.05
Ischial tuberosity 5 min post-pressure	29.39	1.52	28.82	29.96
Ischial tuberosity 10 min post-pressure	29.22	1.58	28.63	29.81
Control pre	28.97	1.32	28.48	29.46
Control 5 min into-pressure	29.38	1.25	28.91	29.85
Control 10 min into-pressure	29.27	1.27	28.8	29.74
Control 5 min post-pressure	29.11	1.36	28.67	29.62
Control 10 min post-pressure	29.09	1.4	28.56	29.61

Table C- 15. Soleus Hoffmann reflex peak-to-peak amplitude means, standard deviations, and 95% confidence intervals. H-reflex: Hoffmann reflex; V: volts.

Time Point	Mean H-reflex Amplitude, V	Standard Deviation	95% Confidence Interval	
			Lower Bound	Upper Bound
Posterior thigh pre	2.99	1.49	2.43	3.54
Posterior thigh 5 min into-pressure	3.02	1.9	2.31	3.72
Posterior thigh 10 min into-pressure	2.87	1.78	2.2	3.58
Posterior thigh 5 min post-pressure	2.34	1.5	1.78	2.89
Posterior thigh 10 min post-pressure	2.28	1.48	1.73	2.84
Ischial tuberosity pre	3.59	1.64	2.97	4.19
Ischial tuberosity 5 min into-pressure	3.54	1.68	2.91	4.17
Ischial tuberosity 10 min into-pressure	3.54	1.67	2.92	4.17
Ischial tuberosity 5 min post-pressure	3.46	1.74	2.81	4.11
Ischial tuberosity 10 min post-pressure	3.69	1.93	2.97	4.41
Control pre	3.24	1.56	2.66	3.82
Control 5 min into-pressure	3.32	1.88	2.61	4.02
Control 10 min into-pressure	3.17	1.72	2.53	3.81
Control 5 min post-pressure	3.14	1.74	2.49	3.78
Control 10 min post-pressure	3.21	1.93	2.49	3.93

Table C- 16. Sural sensory nerve conduction velocity means, standard deviations, and 95% confidence intervals. NCV: nerve conduction velocity; $m \cdot s^{-1}$: meters per second.

Time Point	Mean NCV, $m \cdot s^{-1}$	Standard Deviation	95% Confidence Interval	
			Lower Bound	Upper Bound
Posterior thigh pre	31.9	3.96	30.42	33.38
Posterior thigh 5 min into-pressure	32.09	4.01	30.59	33.59
Posterior thigh 10 min into-pressure	32.13	4.28	30.53	33.73
Posterior thigh 5 min post-pressure	32.45	3.86	31.03	33.89
Posterior thigh 10 min post-pressure	32.26	3.89	30.8	33.71
Ischial tuberosity pre	31.75	2.84	30.69	32.82
Ischial tuberosity 5 min into-pressure	32.24	3.33	30.99	33.48
Ischial tuberosity 10 min into-pressure	31.79	3.32	30.55	33.03
Ischial tuberosity 5 min post-pressure	31.72	2.96	30.62	32.83
Ischial tuberosity 10 min post-pressure	31.91	2.78	30.88	32.95
Control pre	32.44	4.04	30.93	33.95
Control 5 min into-pressure	32.18	3.1	30.67	33.67
Control 10 min into-pressure	32.81	4.04	31.3	34.32
Control 5 min post-pressure	32.73	3.38	31.47	33.1
Control 10 min post-pressure	32.9	4.11	31.37	34.44